This is to certify that the
thesis entitled

EFFECT OF SELF CONSOLIDATING CONCRETE
MIX PROPORTIONING ON
TRANSFER AND DEVELOPMENT LENGTH

presented by

MAHMOODUL HAQ

has been accepted towards fulfillment
of the requirements for the

MASTER OF SCIENCE degree in CIVIL ENGINEERING

Major Professor's Signature

5/13/05

Date

MSU is an Affirmative Action/Equal Opportunity Institution

EFFECT OF SELF CONSOLIDATING CONCRETE (SCC) MIX PROPORTIONING ON TRANSFER AND DEVELOPMENT LENGTH OF PRESTRESSINGSTRANDS

By

Mahmoodul Haq

A THESIS

Submitted to
Michigan State University
in partial fulfillment of the requirements
for the degree of

MASTER OF SCIENCE

Department of Civil and Environmental Engineering

2005

ABSTRACT

EFFECT OF SELF CONSOLIDATING CONCRETE (SCC) MIX PROPORTIONING ON TRANSFER AND DEVELOPMENT LENGTH OF PRESTRESSINGSTRANDS

By

Mahmoodul Haq

Self-consolidating concrete (SCC), a special concrete tailored for high deformability and stability, has recently gained much interest from the precast/prestressed industry. In spite of many developments on SCC material technology, knowledge on the performance of elements built using SCC is limited. Of particular relevance in prestressed concrete is the issue of strand bond. The research objective was thus to study the effect of SCC mix proportioning on the bond of prestressing strands as it relates to transfer and development lengths in prescast/prestressed girders. The study focused on 13mm (0.5 in.) diameter strands on laboratory-scale T-beams. Three SCC mix designs were strategically designed to bound the accepted proportioning methods. Comparison was made with a conventionally vibrated concrete mix (NCC). Transfer lengths were determined by strand draw-in and concrete strain measurements and development lengths were obtained through flexural beam tests. Transfer length results were within the current ACI-318/AASHTO code recommendations. Experimentally determined development lengths were longer than the ACI-318/AASHTO values. The source for this discrepancy solely on the concrete mix is questionable and the quality of the strand is being further evaluated to fully justify this findings. In spite of these doubts, the effect of SCC mix proportioning was found to distinctly affect the different mechanisms of strand bond performance influencing transfer and development length.

To my parents
for their continuous prayers, sacrifices and
guidance throughout my life

ACKNOWLEDGEMENTS

Praise be to the LORD, The Most Beneficent, The Most Merciful

It is difficult to overstate my gratitude to my advisor, Dr. Rigoberto Burgueño. With his enthusiasm, his inspiration, and his great efforts to explain things clearly and simply, he helped to make research fun for me. Throughout my thesis, he provided encouragement, sound advice, good teaching, good company, and lots of good ideas. I would have been lost without him.

I wish to thank the members of my master's committee, Dr. Ronald Harichandran and Dr. Parviz Soroushian for their valuable time and constructive comments.

I am grateful to Mr. Siavosh Ravanbakhsh for all the help in the laboratory. His valuable time, friendship and support helped me through the difficult times in this research. I also thank James "JC" Brenton for his help in preparing test-setup accessories.

I would like to thank Dana Katherine Nuffer and David A Bendert for their friendship and help in laborious tasks. I would also like to thank my colleagues who helped me during the casting of concrete.

Lastly, and most importantly, I wish to thank my parents, Dr. Abdul Haq and Jowhara; they bore me, raised me, supported me, taught me, and loved me. To them I dedicate this thesis.

This study was possible thanks to the financial support of the Precast/Prestressed Concrete Institute (PCI), through a 2003-2004 Daniel P. Jenny Research Fellowship, and the Department of Civil and Environmental Engineering at MSU. The in-kind financial and technical support from our industry partners Premarc Corporation (Grand Rapids, MI) and Degussa Admixtures Inc. (Cleveland, OH) is also thankfully acknowledged.

TABLE OF CONTENTS

LIST OF TABLES

LIST OF FIGURES

Appendix 2

Appendix 4

CHAPTER 1 INTRODUCTION AND BACKGROUND

1.1 Background and Problem Definition

First introduced in Japan in the early 1980s (Okamura, 1999), self-consolidating, or self-compacting concrete (SCC) has been gaining increased attention due its unique behavior to fill formwork and flow around obstructions without blocking or segregating. This behavior, obtained by tailoring the selection of materials and mix proportioning has allowed it to be classified as a kind of high-performance concrete, offering the possibility of designing for both the fresh and hardened properties of concrete to specific project needs.

Much work has been done since the development of SCC, particularly in the development of mix designs, characterization of its rheology and mechanical properties, and evaluation its in-situ properties. The underlying principles governing the development of SCC-type behavior, i.e., a stable highly flowable concrete mix, are now generally well accepted and a great variety of SCC mixes have been developed using different materials and optimized for different purposes. In spite of all the progress made on the material characterization of SCC, very limited information exists on construction and design specifications to guide industry, designers, and highway transportation authorities. If this trend continues, it is likely that even the most extensive and detailed material characterization efforts on SCC will not address the concerns of the state DOT's, whose ultimate interest lies on the structural performance and durability of the built structure.

The underlying principles governing the development of SCC-type behavior, i.e., a stable highly flowable concrete mix, are now generally well accepted and a great

variety of SCC mixes have been developed using different materials and optimized for different purposes (Khayat, 1999). However, the special mix designs that give SCC its unique fresh-property advantages significantly deviate from what is currently considered as ideal and developed through many years of experience and research. This has raised concerns regarding material and structural performance issues. Among them are material properties such as creep and shrinkage; structural issues such as prestress losses and bond; and durability issues such as freeze-thaw behavior. These concerns have limited the acceptance of SCC in the United States, despite of its increased use in Japan, Canada and Europe.

Self-consolidating concrete (SCC) has become of high interest to the precast concrete industry due to the benefits it offers in enhancing construction productivity. In spite of this interest and rapid developments on SCC technology, its acceptance in the U.S. is lagging due to material and structural performance concerns; among these is the issue of bond. The issue of bond for prestressed concrete members has been debated from the past six decades. Considerable work has been done regarding the development of a better understanding of bond and its relationship with transfer and development length for conventionally consolidated concrete. Consequently, several theories for transfer and development length have been formulated. In spite of the multiple efforts, current provisions by the ACI Code (318-02) [3] and AASHTO [2] are primarily based on the work of Hanson and Kaar [17]. However, in general, it has been found that these guidelines underestimate the actual transfer and flexural bond lengths, and their validity has been questioned for over 25 years [8][10][18][24][31][33][35][41]. Thus, even for conventional concrete, which is well developed and ideal shows large deviation on results

related to bond issues. In such a scenario, with the absence of specific design codes and guidelines for SCC, the study of bond in SCC has become inevitable

1.2 Objectives

The design of a concrete mix for SCC-type behavior for specific project needs grants SCC its quality as a high-performance material. However, this advantage can also limit the development of all-inclusive guidelines. It is now generally agreed that SCC can be obtained by two general approaches or the combination thereof: (a) mixtures with high fines content and high-range-water-reducing admixtures, and (b) mixtures with high-range-water-reducing admixtures and viscosity-modifying admixtures.

The current study thus focuses on bounding the parameters that allow the development of SCC-type behavior and on investigating the bond performance of SCC in precast/pretensioned bridge elements with the objective of providing guidance on the construction and design of these elements when using self-consolidating concrete.

The specific aims will be:

- To investigate the material properties of three types of SCC mixes through small-scale tests.
- To experimentally investigate the development and transfer lengths for ½" prestressing strands in SCC through small-scale tests.

Also, the constitutive hardened concrete properties including the compressive strength, split tensile strength and modulus of elasticity were evaluated at various ages of concrete. The results from SCC mixes are compared with a normally consolidated concrete (NCC) mix.

1.3 Self Compacting Concrete (SCC) Vs. Normally Consolidated Concrete (NCC)

The unique self-consolidation behavior of SCC and its tailorable nature to suit specific project needs has allowed it to be classified as a kind of high-performance concrete. SCC offers many advantages for the precast/prestressed industry, among them are:

a) It can be placed with no mechanical vibration, resulting in savings in placement costs.

b) Improved and more uniform architectural surface finish with little to no remedial surface work

c) Ease of filling restricted sections and hard to reach areas

d) Opportunities to create structural and architectural shapes and finished not achievable with conventional concrete.

e) Improved consolidation around reinforcement and bond with reinforcement.

f) Improved Pumpability

g) Improved uniformity of in-place concrete by eliminating variable operator – related effort of consolidation,

h) Labor Savings,

i) Shorter construction periods and resulting cost savings and

j) Quicker concrete turn – around times enabling the producer to service the project more efficiently.

In order to completely utilize the advantages SCC offers, specifically to the precast/prestressed industry, bond parameters need to be carefully evaluated. Considering the extensive mix designs of SCC available, the current work focuses on bounding the hardened properties by proper mix proportions.

1.4 Thesis Organization

This thesis has been organized into 7 chapters. Chapter 2 includes a brief review of the existing literature on both SCC and bond issues. Definitions of important parameters related to this project have also been included. Chapter 3 includes: (a) study of the mix designs used in the project and their fresh and hardened properties and (b)test Specimen details and fabrication. Chapter 4 gives details about the pull-out testing program. Transfer length, measurement, methods and results are discussed in Chapter 5. Development length testing, measurement and discussion of results are presented in Chapter6. Chapter 7 gives a brief summary of the entire project and the conclusions drawn from this research

CHAPTER 2 LITERATURE REVIEW

In order to gain the perspective on the use of Self Consolidating Concrete (SCC) around the world and to understand the different issues related to bond performance of prestressing strands, a literature review was carried out. This chapter provides a brief overview of pertinent work related to this research. This chapter has been subdivided into five sections: (1) SCC material technology (2) importance of bond in prestressed concrete, (3) Concept of transfer and development length, (4) studies on transfer and development length of prestressing strands and (5) concluding remarks. The sections are explained briefly below:

2.1 SCC Material Technology

Self-consolidating concrete (SCC), or "vibration-free" concrete, was developed in Japan in the 1980's in response to the gradual reduction in the numbers of skilled workers required for quality construction work [27]. The unique self-consolidation behavior of SCC has allowed it to be classified as a kind of high-performance concrete [1][27]. The design of SCC involves tailoring the selection of materials and mix proportioning to ensure high deformability and adequate resistance to segregation, to achieve high filling capability and flow around obstructions without blocking [20]. Such requirements require different opposing measures, such as reduction in coarse aggregate volume and reduction of free water content to limit inter-particle friction among coarse aggregate, sand and cement. Although there is no common definition for SCC, a common understanding is that a self consolidating concrete is a one that:

a) has the fluidity that allows self-consolidation without external vibration,

b) remains homogeneous during and after placement, and

c) flows easily through reinforcement

Thus, the most important criteria that differentiates SCC from conventional concrete are those that are related to the properties of fresh concrete. These requirements are [19] :

- Self-placing and self-consolidation
- Retention of deformability throughout transportation and placement
- High stability during transportation and placement
- Resistance to segregation, bleeding, and surface settlement (i.e., stability) after casting
- Limited bleeding and settlement
- Uniform surface quality
- Homogeneous distribution of in-situ properties.

Achieving all of the above performance requirements is not easy and it requires a compromise between the many parameters influencing the mixture proportioning [20] . In order to understand SCC material technology, this study has been subdivided into the following: (1) SCC mix behavior and parameters (2) SCC fresh property evaluation and quality control (3) Hardened properties, and(4) structural performance Each of these topics is discussed as follows:

2.1.1 SCC Mix Behavior and Parameters

In rheological terms, SCC is often described as a Bingham fluid (viscoelastic) where the linear relation between the stress and the shear rate ratio is characterized by two constants – viscosity and yield stress. The yield stress primarily governs the self-consolidation behavior, while the viscosity affects the homogeneity (stability) and flowability [20]. While the viscosity may be modified depending on the application

(flowability requirements), the yield stress must remain much lower than conventional concrete mixes in order to achieve self-consolidation [38].It is clear that the fresh properties of SCC are particularly important for its ability ***to flow*** under its own weight ***without segregation*** and ***to fill congested structural sections***. Thus it is very important to ensure the following three main parameters:

- Fluidity / Deformability
- Easy Flow / Low Blockage, and
- Homogeneity / Stability.

The above primary parameters need to be properly adjusted to satisfy all the requirements of SCC. These three primary parameters can be adjusted (as shown in Figure 2-1 [20]) and achieved by varying the mix proportions of SCC. Thus, the mix design factors that affect these three basic parameters are as follows:

- Water to cement ratio (w/c)
- Amount of high-range-water-reducers (HRWR)
- Use of viscosity modifying admixtures (VMA)
- Coarse aggregate content (CAC)
- Sand to paste content (S/Pt)
- Entrained air (EA).

Proper proportioning of these parameters is essential to achieve SCC and to obtain the required primary parameters of deformability, passing ability and stability. The effects of

the various mix proportioning on the basic parameters of SCC are explained in detail below:

The ***deformability*** of concrete is closely dependent on the quantity of cement paste, which can be increased with the use of **high-range water reducers (HRWR)** that allow lowering of the yield value with only moderate drops in viscosity. Thus, highly flowable concrete can be obtained without significant reduction in cohesiveness. Deformability can also be increased by increasing the **water to cement (w/c) ratio**, which controls the deformability of the cement paste. However, high w/c ratios reduce the cohesiveness of the paste and mortar and lead to fine and coarse aggregate segregation. This means that care must be taken when lowering w/c ratios to ensure that, it does not lead to large reductions in cohesiveness. Another factor affecting deformability is the **friction between** the various **solid particles** (sand, gravel, cement, and mineral additives). The inter-particle friction increases the internal resistance to flow thus reducing the deformability and rate of flow of the concrete. This effect can be reduced with the use of **HRWR**, which, by dispersing cement grains, enable water content reduction with limited drops in viscosity. Reducing the **coarse aggregate and sand volumes** and increasing the **paste volume** also enhances deformability. In addition, the use of continuously graded cementitious materials and fillers can also help reduce inter-particle friction.

The second main parameter necessary for SCC properties is that this highly flowable concrete has proper ***stability*** during transportation, placement, and after casting. As shown in Figure 2-1 [20], enhanced stability requires reduction in **coarse aggregate content** and reduction of the **maximum aggregate size**. Cohesion must also be improved by enhancing bond between the mortar paste and the coarse aggregate. This can be

achieved by reducing the **w/c ratio** and the use of **viscosity modifier admixtures (VMA)**. Stability must also be ensured after concrete placement to avoid water migration (bleeding) that can lead to weak interface between the aggregate and the cement paste, accumulation of cement paste in the bottom half of horizontal reinforcement, and segregation of suspended solid particles. Decrease in bleeding can be achieved by reducing the **w/c ratio**, addition of **HRWR**, and the use of **VMA** and/or increased volume of cementitious and filler materials (i.e., low w/c ratio) to bind some of the excess water [20].

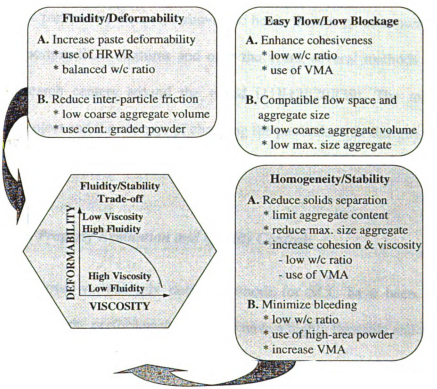

Figure 2-1 SCC Parameters and Behavior [20]

The third essential property for a successful SCC mix is its ability to easily **flow through reinforcement** or reduction of the risk of blockage when flowing through

narrow spaces. Such risk can be minimized by providing adequate viscosity, to ensure good suspension of the solid particles during flow and reducing inter-particle friction. However, increase in viscosity reduces deformability [20]. Thus, to allow SCC to easily flow through reinforcement it should have appropriate cohesiveness by reducing the w/c ratio and/or using VMA. In addition, as the free space between obstacles and reinforcement reduces, the **coarse aggregate volume** and the **maximum size aggregate** should be reduced.

As discussed earlier, successful SCC mixes can be achieved by varying the achieving the three parameters discussed above and hence there is no commonly accepted procedure to proportion SCC mixtures and over the years, several methods have been developed in research centers around the world [11][12][20][39]. The mix designs selected for this project and the concept of choosing the particular mix designs is given in Chapter 3.

2.1.2 SCC Fresh Property Evaluation and Quality Control:

As stated above, various mix design methods for SCC have been proposed. However, it is clear that the performance criteria to have a highly flowable and stable mix remains the same. This indicates that quality control and acceptance criteria for SCC should be based on a performance-based approach. Performance requirements for the hardened concrete are well established for use of precast/prestressed bridge elements. However, the performance requirements for the ***fresh SCC mix*** can only be evaluated at the time of placement.

Considerable work has been done around the world in developing and evaluating the self-compactability of SCC, including deformability, stability, and filling capacity. The most commonly used tests are [29][30][38]:

- Concrete Rheometer. A device applies a range of shear rates and monitors the force needed to maintain these shear rates in a plastic material; later converting the force into stress. However, only a few concrete and mortar rheometers are available since this type of equipment is very expensive and not easy to use in the job site. Thus, these devices have been limited for use in large research centers.

- Spread Test. The slump spread test also called as Slump flow test is used to asses the horizontal free flow of SCC in absence of obstructions [30]. This procedure uses the conventional Abram's cone (Figure 2-2). The cone is filled in one layer without rodding and the diameter, instead of the slump, of the concrete sample is measured after the cone is lifted. The test evaluates self-compactibility as it mainly relates to yield stress. An evaluation of viscosity can be made by monitoring the time it takes for the concrete to reach a spread of 50 mm (2 in.). This test was performed in this study and the results are discussed in Chapter 3.

Figure 2-2 Slump Spread Test and VSI

- J-Ring. This apparatus is used to force the SCC flow through reinforcement in conjunction with an Abrams cone or the Orimet setup. The size and the spacing between the bars can be adjusted to simulate any reinforcement configuration. J-Ring value is obtained from the differences between the spread; with and without the ring or the height difference between the concrete inside and outside the ring are measured. The J-Ring value is calculated as follows (Figure 2-3) [30]:

    a) Measure the values d_1 (Figure 2-3)in the center of the J-Ring and also 4 values of d_a and d_b just inside and outside the ring (measurements in mm)

    b) Calculate h_1=125-d_1 and all h values h_{ax}=125-d_{ax} (x=1 to 4)

    c) Calculate 4 values h_1-h_{ax}; calculate median value h_{1m}-h_{am}.

    d) Calculate 4 values h_{ax}-h_{bx}; calculate median value h_{am}-h_{bm}.

    e) Calculate 2(h_{am}-h_{bm})-(h_{1m}-h_{am}). This is J-Ring value.

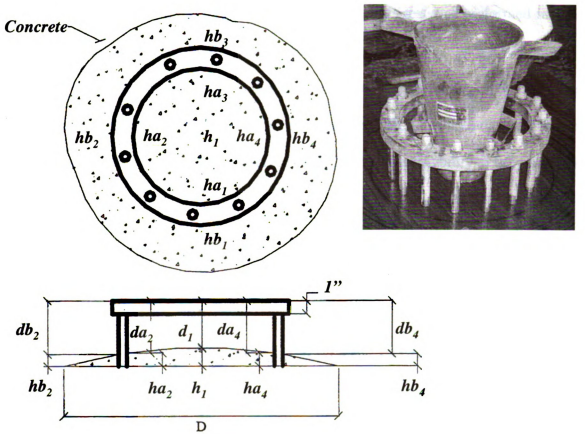

Figure 2-3 J-Ring Value [30]

In general, greater J-ring spread flow results in greater passing ability. Satisfactory passing ability without blockage is attained when the value $2(h_{am}-h_{bm})-(h_{1m}-h_{am})$ is less than 15mm (0.59 in.). Generally acceptable passing ability is achieved when this value is around 10 mm (0.39 in.). This test was performed in this study and the results are discussed in Chapter3.

Visual Stability Index. This method involves the visual evaluation of the SCC patty resulting from observation of the SCC just prior to placement and after the performance of the spread (slump flow) test. It is used to evaluate the relative stability of batches of the same or similar SCC mixes. The test requires the development of

considerable judgment and may thus be subjective. This test was performed in this study and the results are discussed in Chapter3.

- L-Box and U-Box. These tests simulate the casting process by forcing an SCC sample to flow through obstacles under a static pressure. They provide and indication on the static and dynamic segregation resistance of SCC as well as its ability to flow through reinforcement.

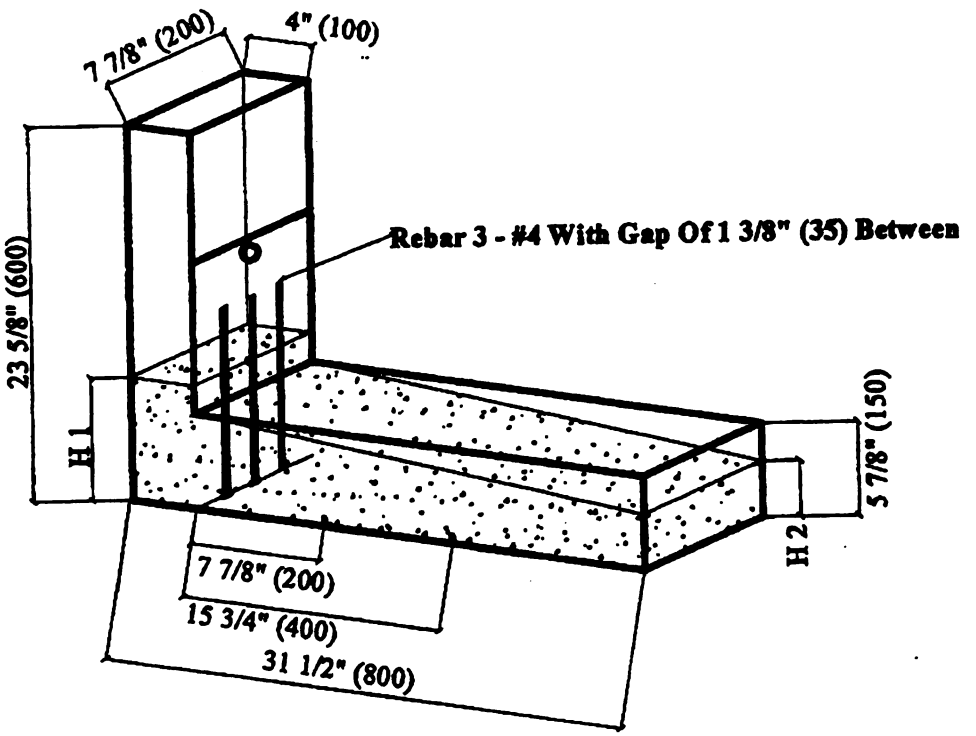

Figure 2-4 Schematic of L- Box Test [30]

L-Box test (Figure 2-4) assesses the flow of SCC and also the extent to which it is subjected to blocking by reinforcement [30]. The test apparatus comprises of a rectangular cavity in with reinforcement. The level of reinforcement can be changed to enforce severe or light restraints depending on the actual reinforcement blocking of the structure. This opening is controlled by a gate. The SCC is placed in the vertical

cavity without any vibration and held there for a minute. The gate is then opened for the SCC to flow into the horizontal cavity. After the flow is complete the heights of SCC in the vertical chamber (H1) and the horizontal chamber (H2) are measured. The ratio of H2/H1 is termed as the blocking ratio. If the SCC flows as freely as water, at rest, it will be horizontal, so H2/H1=1 Thus closer the blocking ratio is to unity, the better is the passing ability. The segregation of aggregates, if any can easily noted in the vertical chamber. This test was performed in this study and the results are discussed in Chapter 3.

This test was performed in this study and the results are discussed in Chapter 3.

- V-Funnel and Orimet. These tests measure the time it takes for the SCC concrete to flow through an orifice under its own weight, these tests give an indication of its viscosity.

- Sieve Stability. This test is used to evaluate the resistance of SCC to static segregation. It consists of pouring a concrete sample over a 5-mm sieve and measuring the amount of mortar passing through the sieve in a two-minute period.

The above methods are not exclusive and while different research groups around the world have evaluated these concepts, dimensions and measurement specifications have not been standardized and/or commonly accepted [30].

2.1.3 SCC Hardened Property and Structural Performance

Since the target engineering properties of hardened SCC should be the same as those for conventional concrete, the same test and procedures that are used for conventional concrete are used for SCC. Most of the research work to-date on SCC has been focused on three fronts: (1) development of self-compacting mix designs

[11][12][26][39], (2) comparison of mechanical properties of SCC against well compacted regular concrete [1][28], and (3) evaluation of in- situ properties of SCC in full-scale structural elements [21][40]. The above-mentioned efforts have shown (a) the feasibility of mix designs with self-compacting behavior and the development of simple and optimized combinations and (b) that, overall, the uniformity and value of the mechanical properties of SCC do not vary significantly from that of normal well-compacted concrete [5].

In spite of the above-mentioned research developments, much less is known on the performance of structural elements cast using SCC. While similar performance might be expected based on the similitude of mechanical properties between SCC and normal concrete, the studies performed thus far have mainly focused on compressive strength, elastic modulus, and to a lesser extent on creep and shrinkage [28]. While, as mentioned above, these properties were found to be similar to those corresponding to traditionally vibrated samples, SCC has been found to exhibit higher early age creep coefficients [28], and not much has been reported on fracture strength.

Researchers from University of Sherbrooke, Canada [21][22] evaluated the uniformity of in-situ mechanical properties of wall elements using eight different mixes of SCC. Cores were obtained at various heights of the wall and normal hardened properties like compressive strength and elastic modulus were evaluated. The results from this study show very slight or no variation in the compressive strength and modulus of elasticity values obtained from the top and bottom portions of the wall.

These researchers [21][22] also compared the mechanical performance of highly confined columns cast using normally consolidated concrete (NCC) and self compacting

concrete (SCC) with stirrup configurations representing different degrees of confinement. The cores were cut at various heights of the column. Results from these cores were compared with those of normally cast specimens. The test results showed that the SCC columns developed similar stiffness but approximately 7% lower load carrying capacity. Also the SCC showed 10% lower cylinder compressive strength relative to NCC. Depending on the reinforcement configuration SCC columns exhibited 62% to 23% more ductility than corresponding NCC columns. The distribution of in-place properties was found to be more homogeneous in SCC than in NCC.

As previously mentioned, the nature of SCC proportioning is to deviate from well-understood mix designs developed over many years of experience. This implies that compromises must be made with respect to performance. Highly fluid mixes, or high-rate discharge, can compromise the stability of the concrete mix, which can lead to bleeding and segregation around reinforcement that can adversely affect the bond characteristics of conventional and prestressed reinforcement such as transfer and development length. Another potential adverse effect of SCC on structural performance is that related to the ability to transfer shear stresses across cracks, or the so-called "aggregate interlock." Thus, it is foreseen that bond and aggregate interlock are two types of hardened behavioral mechanisms that can affect the design and performance of precast/prestressed bridge elements using SCC. The nature and importance only the only bond type of behavioral mechanism is discussed next.

2.2 Importance of Bond in Prestressed Concrete

The importance of bond between prestressing steel and concrete has been studied considerably during the development of prestressed concrete [23]. The concept behind

prestressing and reinforced concrete clearly relies on the ability to transfer tensile forces from the strands into the hardened concrete both during service as well as at ultimate. This parameter (bond) thus forms part of the design considerations of precast/prestressed members through semi-empirical formulations of development length to ensure proper anchorage of the prestressing strand when relying only on the interaction between the strand and the surrounding concrete. The behavioral mechanism and importance of bond for both (transfer and ultimate) should be understood if a suitable measure of this parameter (bond) is to be performed.

2.2.1 Bond Stresses and Mechanisms

The transfer of stresses from the strand to the concrete by bond can be classified into three distinct mechanisms: (1) adhesion, (2) Poisson's (Hoyer's) effect and (3) mechanical interlock. Each of these mechanisms is explained briefly explained in the following:

1. ***Adhesion:*** This refers to the chemical bond resisting mechanism by which the concrete bonds to the strands. Adhesion helps in the bond transfer only when there is no relative slip of the strand with concrete. This mechanism is relatively small and hence often neglected [16].
2. ***Hoyer's Effect:*** When the strand is prestressed there is a lateral contraction in the strand diameter due to the steel's Poisson's ratio. When the strand is released, this lateral contraction is recovered and the strand swells. This swelling is prevented by the surrounding hardened concrete preventing the strand to return to its original diameter. This restraint is in the form of a radial normal force on the strand inducing frictional force along the axis of the strand (Figure 2-5). At the

end of the beam, where the surrounding concrete does not exist, the strand is free to expand, and hence the strand at the end has a relatively larger diameter than the portion embedded in concrete. This produces a wedge action. This anchorage mechanism was first described by Hoyer in 1939 [36] and thus is commonly referred to as Hoyer's effect. The concrete resists this wedging effect transferring part of the stress from the strand to concrete.

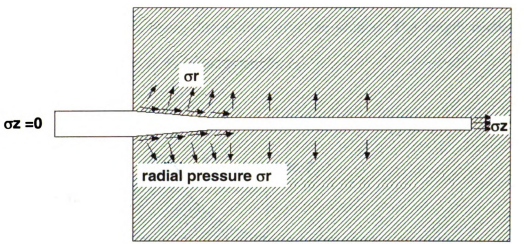

Figure 2-5 Hoyer's Effect [34]

3. ***Mechanical Interlock:*** Seven wire prestressing strands consist of six wires wound in a helical shape around a single wire. When concrete is cast around the strands the hardened concrete shape matches that of the stressed strands. Due to the match casting between the concrete and strand, the concrete resists the unwinding of the strand providing slip resistance. Mechanical interlock is the main contributor to bond when the stresses are increased beyond the initial transfer stresses [36].

2.2.2 Transfer Bond Stresses (at release of prestress)

The approximate distribution of the bond stress τ at transfer due to all the mechanisms cited above is shown in Figure 2-6 [23], where τ becomes zero, the stress in the strand becomes equal to the stress due to prestressing ($\sigma_z = \sigma_{zv}$ = constant). The length associated with this is termed the bond length, u. It will depend on the quality of the bond and on the transverse pressure determined by the member geometry and transverse reinforcement. The prestressing force is introduced into the member until the concrete stresses exhibit a linear distribution over the section. The length needed for achieving this is referred to as the transfer length, L_t.

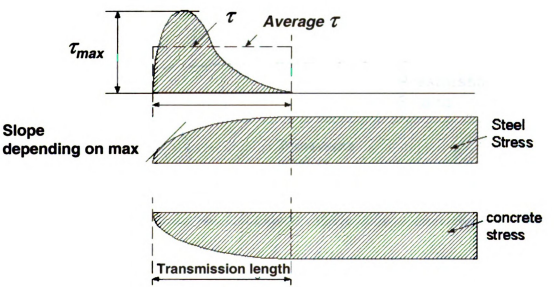

Figure 2-6. Bond Stress Distribution at Strand End [23]

At the face of the concrete unit, the steel and concrete stresses are zero. The shear, or bond stress between the strand and the concrete increases rapidly until it reaches its maximum value, beyond which it decreases approximately according to a parabolic

curve. Due to the bond effect, compressive stresses radiate from the wire into the concrete causing warping at the member end (Figure 2-7) [23]. As a consequence of this, a zone of compressive stresses develops acting radially towards the strand. This further enhances the Hoyer effect. However, this deformation also introduces tensile stresses that require the provision of transverse reinforcement.

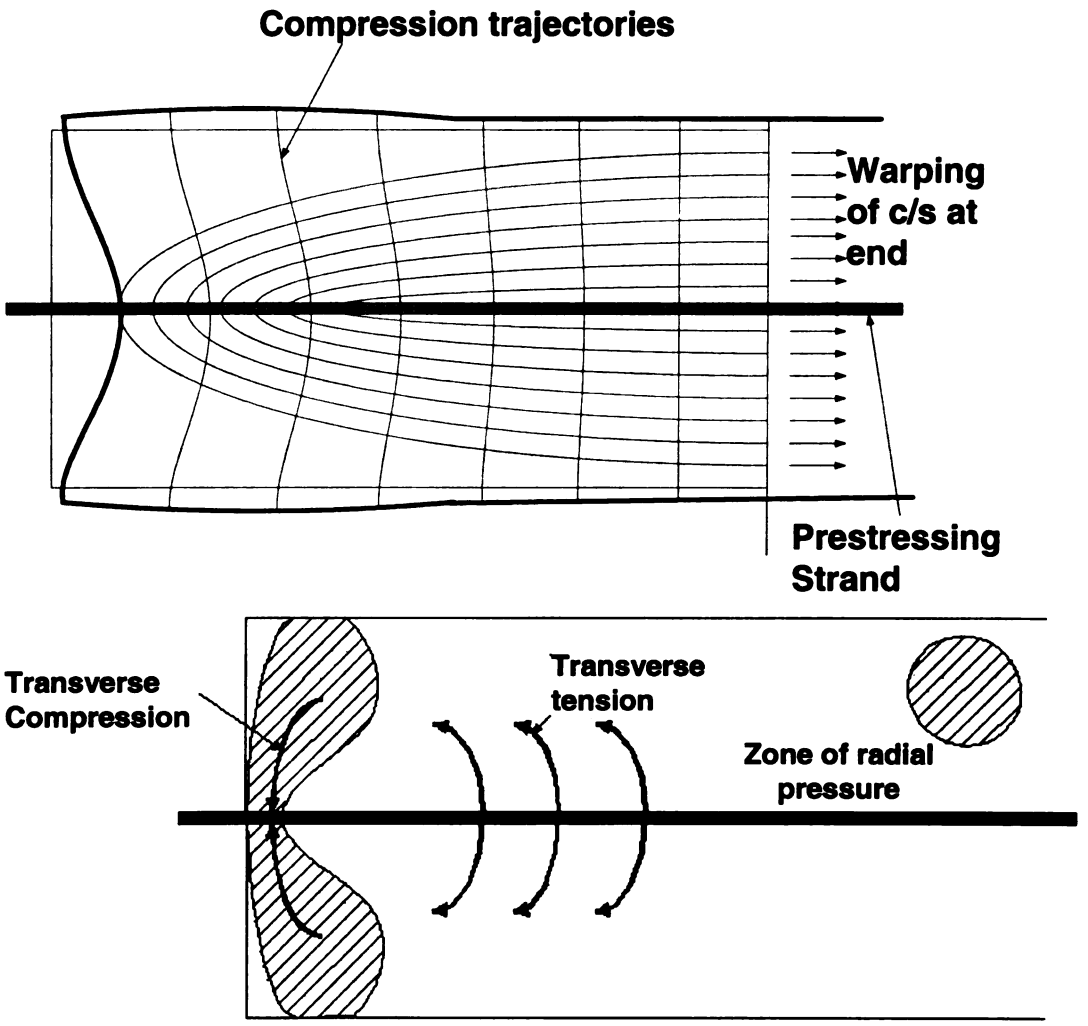

Figure 2-7. Section Warping and Forces at End [23]

Of all of the above-mentioned mechanisms, the Hoyer effect is the greatest contributing mechanism to "bond" upon prestress release. Mechanical interlock is the main contributor to "bond" when the stress in the strand is increased above the initial transfer stresses, i.e., when the concrete cracks and the strand stress levels are increased over their initial state. The adhesion mechanism is the smallest contributor to developing bond stresses between strand and the concrete [23][36].

2.2.3 Flexural Bond Stresses at Ultimate Strength

In most cases, full prestressing is provided in the design of prestressed concrete members, which implies that there will be no cracks under working load. It can be shown that the demands placed upon bond action before the appearance of cracks is very limited since the transmission of shear takes place just as in a section made from a homogeneous material. For this reason, prestressed concrete beams can adequately carry working loads even without the presence of bond [23]. If bond does exist, then only a very slight shear stress occurs between the tendon and the concrete due to the connection between the small area of steel (times the material modular ratio) and the rest of the total cross-section. Thus, only when the working load is exceeded and cracks occur in the tensile zone of the concrete does bond become necessary [23].

The importance of bond on ultimate strength is better understood by considering the failure behavior with and without bond. Upon loading and appearance of the first crack at the location of highest tensile stress, there will be a sudden increase of tensile stress in the strand due to the abrupt disappearance of the concrete tensile force contribution. If there is no bond, this increase will extend over the entire length of the tendon. This will lead to considerable deformations and wide crack spacing. In addition,

new flexural cracks will be widely spaced, which will tend to decrease the depth of the compression zone and eventually lead to early failure of the compression flange. Thus, in the absence of bond the ultimate capacity is reduced and the strength of the steel strand cannot be fully utilized.

Early failure is thus avoided by establishing a shear-resisting mechanism, i.e., bond, between the steel and the concrete. The bond stresses between the tendon and the surrounding concrete, τ_1, have the effect of immediately reducing the increased stress that develops in the steel at the crack location a short distance next to it (Figure 2-8) [23]. Depending on the bond quality, the increased steel stress σ_z is thus limited to a short length, which will lead to only slight local elongation of the strand and narrow crack spacing.

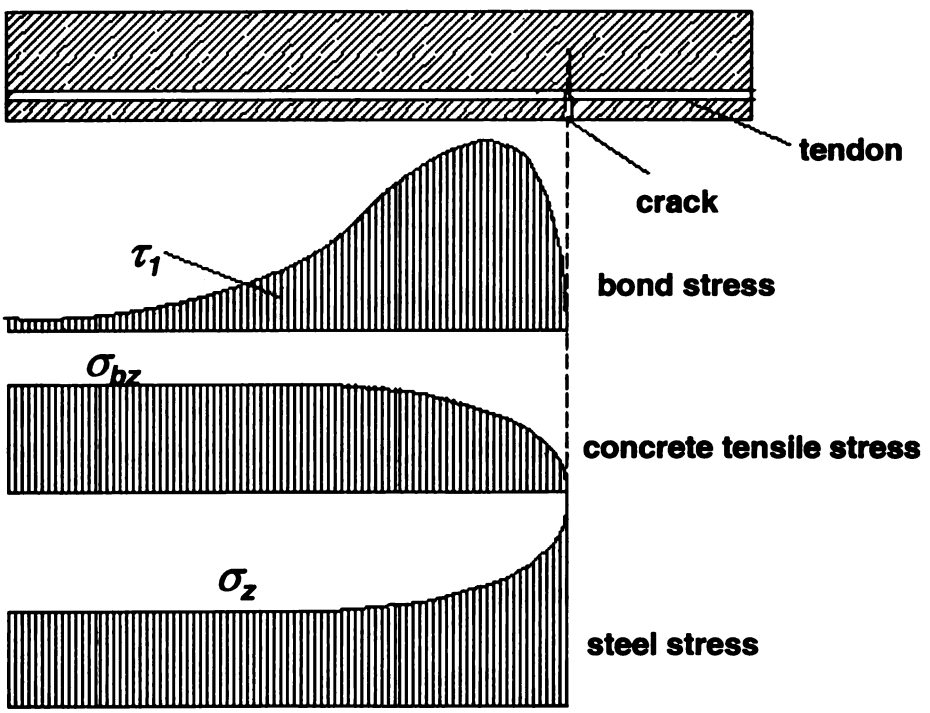

Figure 2-8. Stress Distributions at a Crack Front [23]

The presence of bond will permit the tensile concrete stresses σ_{bz} to continue to exist besides the crack location, which can increase further upon further loading. This will lead to closely spaced cracks and a failure pattern with a large number of cracks that slowly move upwards. The neutral axis depth is thus slowly reduced, allowing development of large steel stresses. Consequently, bond allows for a safe failure mode and better use of the steel reinforcement [23].

As pointed out above, a series of thin cracks are expected to be developed in route to the ultimate flexural capacity of a prestressed concrete member. Thus, in addition of addressing the mechanism of bond at a single crack, the distribution of bond stresses along the member length is now of importance. First, it must be understood that bond stresses in the cracked region cannot be determined by the approach followed in reinforced concrete. At flexural cracks the bond stress beside it will locally increase up to the bond strength as shown in Figure 2-8 and

Figure 2-9 [23]. Beyond this peak, the bond stress quickly decreases and in some cases it even changes into a stress of opposite sign. If there are a number of cracks in succession, the distribution of bond stresses follows a "saw-tooth" pattern [23]. Although not described in this manner, this same phenomenon was identified by Hanson and Kaar [17] (Upon whose work the current ACI recommendations [3] for strand development length are based) as a "bond stress wave." Calculation of these bond stresses, however, is not possible without an accurate knowledge of the bond strength and bond strains.

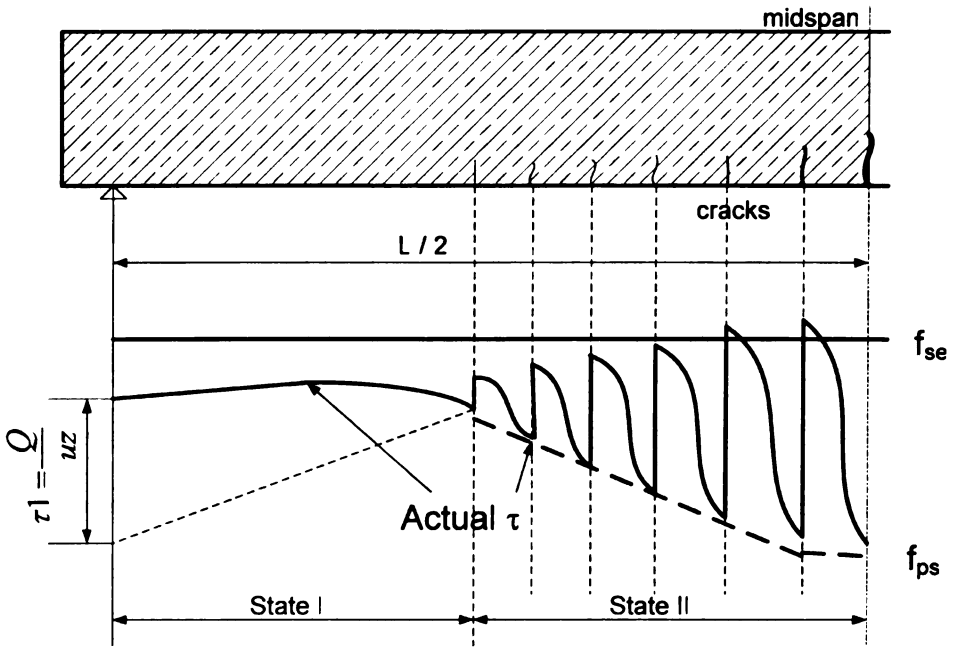

Figure 2-9. Bond Stresses at Flexural Cracks [23]

The development of new flexural cracks towards the end of the member will continue with increasing load demands due to load redistribution. As seen in

Figure 2-9, the bond stress demands will follow along with localized high steel stress demands at the crack [23]. Increased tensile stresses in the strand will cause a reduction of cross sectional area due to Poisson's effect. Thus, if cracking extends into the transfer zone region, the reduced cross-section tendon area will compromise the Hoyer effect, which is the main mechanism for bond in the transfer region. Relative slip of the strand can then occur leading to a reduction in prestressing force and thus limiting the attainment of the section full flexural capacity. In addition, the reduced compression stress state at the beam end will decrease the section shear capacity. Bond failures and shear failures at end supports are thus clearly related, an issue that has been identified for

some time but yet continues to be topic of debate as to the precedence of each effect [8][33][35].

2.3 The Concept of Transfer and Development Length

Bond is of importance to the design of prestressed members for both initial, or service, as well as ultimate, or overload conditions. The bond strength between prestressing strands and concrete depends on the concrete's ability to transfer shear forces along the material interface. The distance over which the effective prestress f_{se} is developed in the strand has been traditionally called the transfer length, L_t. An additional bond length is required so that the stress f_{ps} may be developed in the strand at ultimate flexural strength of the member. This additional length is termed the flexural bond length, L_f. The sum of these two lengths is commonly referred to as the development length, L_d, of the strand (Figure 2-10).

Considerable work has been done regarding the development of a better understanding of bond and its relationship with transfer and development length for conventionally consolidated concrete. Consequently, several theories for transfer and development length have been formulated. In spite of the multiple efforts, current provisions by the ACI-318 Code (318-02) [3] and AASHTO [2] (see Figure 2-10) are primarily based on the work of Hanson and Kaar [17]. However, in general, it has been found that these guidelines underestimate the actual transfer and flexural bond lengths, and their validity has been questioned for over 25 years [8][10][18][24][31][32] [33][35][41]. In this time several approaches have been developed. In the following, a brief account of these efforts is given and then the proposed approach is described in detail.

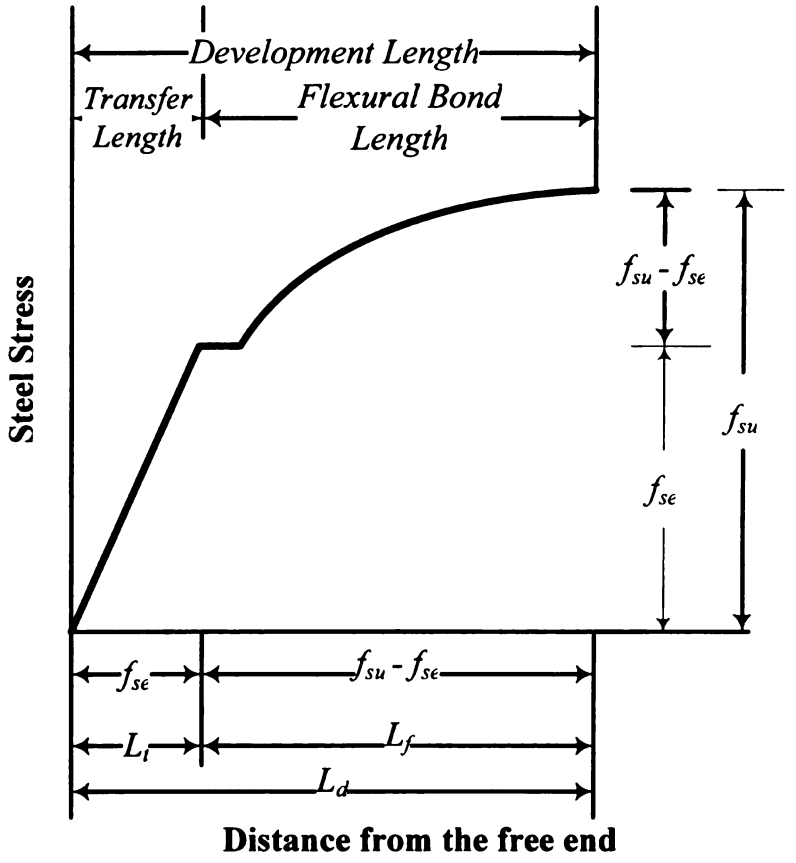

Figure 2-10 Variation of stresses – ACI-318 equation representation [3][2]

Although strand development seldom governs the design of prestressed concrete members, with the exception of cantilevers and short span members, several bond-related failures have been reported with members using conventionally consolidated concrete and the current criteria [8]. In addition, the relationship between development length and shear failures at beam supports has been clearly documented and has become a recent concern, particularly as it relates to the response of prestressed beams due to earthquake-induced vertical loading. It is then clear that the issues related to bond between hardened SCC and prestressing strand will be reflected in design practice through these parameters

2.3.1 Definitions

Some of the basic definitions that describe the behavior of bond in the prestressing strand are described below:

Transfer Length (L_t):

Transfer length is defined as the bonded length of the strand required to fully transfer the effective prestress (f_{se}) from the strand to concrete. In other words, transfer length is the length from the end of the beam to the point where the prestressing force is fully effective [34].

Flexural Bond Length (L_f):

Flexural bond length is defined as the distance, in addition to the transfer length over which the tendon must be bonded to the concrete to develop the full design strength of the tendons (f_{ps}) to resist flexural stresses at nominal resistance of the member.

Development Length (L_d):

Development length is defined as the total length of bond required to develop the steel stress f_{ps} at the ultimate strength of the member. Development length is the sum of the transfer and flexural bond lengths. In other words, Development length can be defined as the shortest bonded length of tendon along which the tendon stress can increase from zero to the stress required for achievement of the full nominal strength at the section under consideration.

Embedment Length (L_e):

Embedment length is defined as the length of bond from the critical section to the beginning of bond. Critical section can be defined as the section closest to the end of the member that develops full strength when subjected to external loading. It should be noted that embedment length is related to development length. If the embedment length is

greater than the development length then a general bond failure would occur, else the strand slip will occur and the nominal stresses will not be developed in the strand.

2.3.2 ACI-318 [3] / AASHTO- LRFD [2] Code Recommendations

The current provisions by the ACI Code (318-02) [3] and AASHTO Design Guidelines (Figure 2-10) are primarily based on the work of Hanson and Kaar [17][18]. The current ACI 318 / AASHTO provisions are as follows:

$$L_d = \frac{1}{6.895}(f_{ps} - \frac{2}{3} f_{se})d_b \qquad [f_{ps}, f_{se} \text{in MPa}; d_b, L_d \text{ in m}]$$

$$L_d = (f_{ps} - \frac{2}{3} f_{se})d_b \qquad [f_{ps}, f_{se} \text{in ksi \& } d_b, L_d \text{ in in.}] \tag{2-1}$$

Equation 2-1 can be re-written as:

$$L_d = \frac{1}{6.895}\left[\frac{f_{se}}{3} d_b - (f_{ps} - f_{se})d_b\right], \qquad [f_{ps}, f_{se} \text{in MPa}; d_b, L_d \text{ in m}]$$

$$L_d = \left[\frac{f_{se}}{3} d_b - (f_{ps} - f_{se})d_b\right], \qquad [f_{ps}, f_{se} \text{in ksi \& } d_b, L_d \text{ in in.}] \tag{2-2}$$

where, d_b is the diameter of the strand, f_{se} and f_{ps} are the effective and nominal stresses in the tendon respectively.

The first term of the Equation 2-2 represents the transfer length and the second term represents the flexural bond length. In Figure 2-10, the steel stress is shown to vary linearly along the transfer length. Along the flexural bond length, the slope of this curve decreases. AASHTO-LRFD specifications state that the flexural bond may be assumed to vary parabolically [7][3]. The ACI code also states that the transfer length may be taken as 60 strand diameters.

2.4 Studies on Transfer and Development length of Prestressing strand.

The previous discussions have presented the mechanisms and the importance of bond between prestressing strands and concrete for the design and performance of prestressed concrete beams. Determining the bond strength, or *slip resistance*, is however, not a straightforward task. The reason is that the "bond" phenomena that have been described for both transfer and ultimate strength rely on different mechanisms to transfer the shear stresses between concrete and strand. It was explained how the bond shear stresses follow complex distributions at the member ends and at flexural cracks. Thus, appropriate determination of bond strength must replicate actual conditions as close as possible.

It has been found that bond mechanisms are affected by many parameters [41]. Among them are:

- The type of Steel
- The diameter of the strands
- The level of stress in the strand
- The surface condition of the strand
- The concrete strength
- The type of loading (static, repeated, impact)
- The type of prestress release (sudden, gradual)
- Confinement reinforcement
- Time–dependent effects (losses due to creep, shrinkage etc.,)
- Concrete cover and spacing of strands
- Amount of shear reinforcement in the critical zone.

2.4.1 Studies on Bond Performance

In order to determine values of the slip resistance of a prestressing strand through experimental methods, care must be taken to consider the mechanisms affecting bond response [23]:

1. The bond stress (slip resistance), typically assumed as uniformly distributed, is higher for shorter embedment lengths in a pull-out test specimen. This is shown in Figure 2-11. This maximum stress value has a decisive part in the shear stress vs. slip response.

2. The slip resistance increases with the quality, the compaction, and the degree of hardening of the concrete, thus the relevance of evaluating this mechanical behavior parameter for SCC.

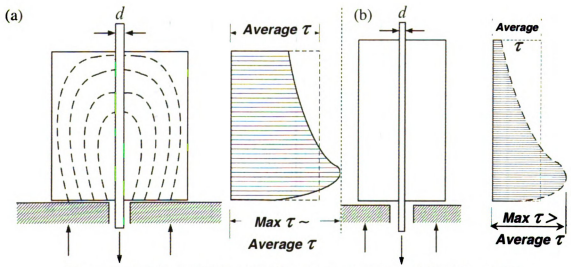

Figure 2-11 Effect of Embedded Length in Normal Pull-Out Tests [23]

3. The slip resistance is significantly dependent on whether a transverse compressive stress acts on the strand. This effect can be reproduced through normal pull-out tests (see Figure 2-11a).

4. Additional transverse pressure is created by the Hoyer effect.

Because of all of these influencing factors, it is difficult to determine bond lengths by means of simple pull-out tests. Tests on strand bond confirmation by means of the "Moustafa test" (Figure 2-12) have been recommended by the PCI Interim Guidelines for SCC [30].

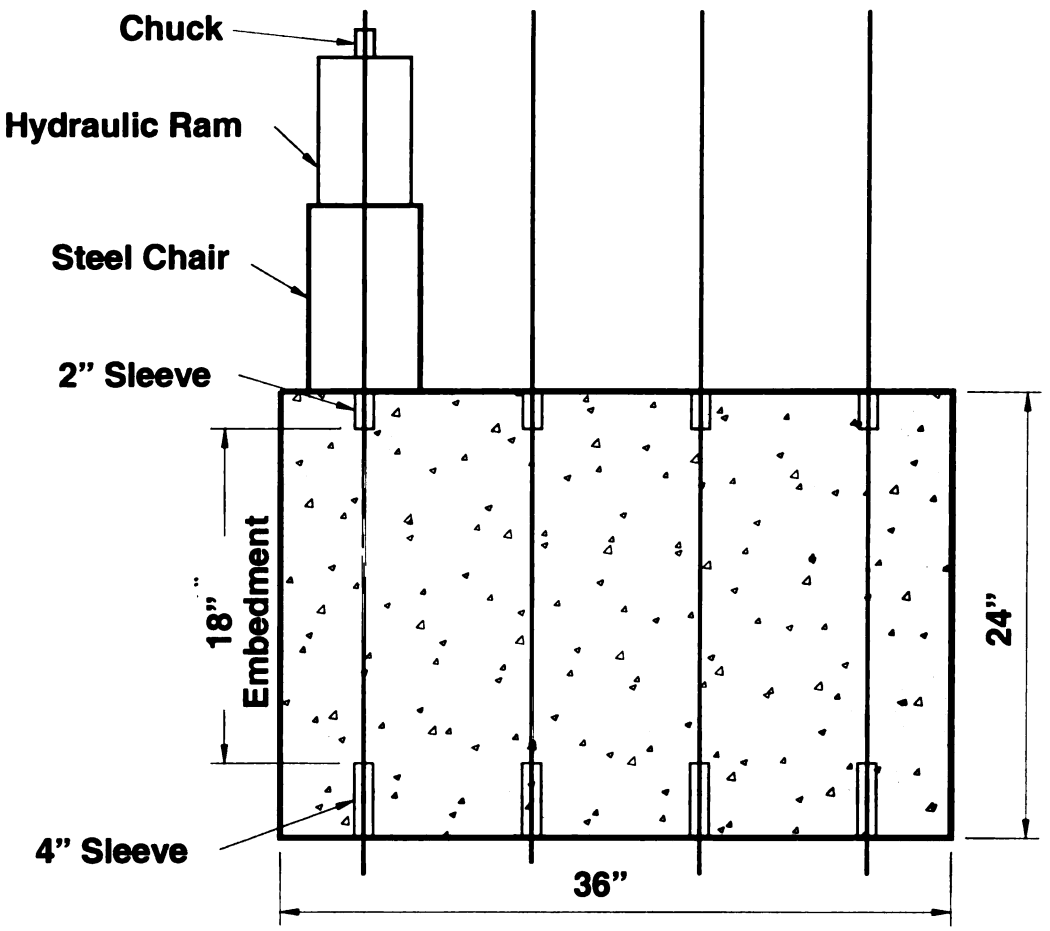

Figure 2-12. Details of Moustafa Test

It should be noted that the bond performance is related to the bond mechanisms and complex phenomena. The results of these simple pullout tests depend on the bond resistance created by friction and mechanical interlock. The Hoyer's mechanism which is the main contributor for transfer length [7] is not represented in these tests. The

correspondence between the results obtained from this test and structural design parameters such as transfer length and development length have been questioned for conventional concrete [7][27][33][32] and seem to be of continued debate now for SCC. In order to qualify the strand for adequate bond performance, the test has to be performed in a specific manner on a specific mix design of concrete. The following are the guidelines and test procedure as prescribed by Logan [25]:

1) The hydraulic jack shall be a pull-jack with a center hole assembly at the end of the ram (similar to those normally used for single-strand stressing). It shall be tested and calibrated to permit loading upto 50 kips (222 kN), and shall have a travel of at least 12 in. (305 mm)
2) A specific bridging device should be used [25].
3) On the day of casting the test blocks (with heat curing), the cylinbdrs shall be tested and the concrete strength recorded. Based on results of past testing, the concrete strength can range from 24.1 to 40.7 MPa (3500 to 5900 psi) without affecting the pull-out strengths.
4) The bridge is slipped over each strand to be tested and placed against the concrete surface. The strand chucks are slipped over the strand to the top of the bridge and light pressure is applied to the jack to seat the jaws of the chuck into the strand.
5) The jacking load shall be applied in a single increasing application of load at the rate of approximately 20 kips per minute (89kip per minute) until the maximum load is reached and the load gauge indicator can no longer sustain maximum load. Do not stop the test at the sign of movement of the strand sample

or for any other reason. The strand samples can pullout as much as 203 mm to 254 mm (8 to 10 in.) before maximum load is reached with a poor strand, and 25.5 to 51 mm (1 to 2 in.) with good bonding strand.

6) The pull-out capacity of the strand sample shall be recorded as the maximum load attained by the strand sample before the load drops off on the gage and cannot be further increased.

7) The following data shall be recorded for each strand sample:

(a) Maximum capacity

(b) Approximate load at first load movement

(c) Approximate distance the strand pulls out at maximum load

(d) General description of failure

8) Record data and compute average failure load and standard deviation for eah strand group tested. Compare results with minimum requirements for acceptance for pretensioning applications.

As discussed earlier, tests on strand bond confirmation by means of the "Moustafa test" (Figure 2-12) have been recommended by the PCI Interim Guidelines for SCC [30]. However, the correspondence between the results obtained from this test and structural design parameters such as transfer length and development length have been questioned for conventional concrete [7][27][33][32] and seem to be of continued debate now for SCC. While the response evaluated through the Moustafa test is clearly related to bond performance, its correlation to the complex phenomena occurring in the transfer zone region and during development of strand capacity under flexural actions, as previously discussed, is questionable.

The pull-out tests and the Moustafa test are excellent methods to provide a baseline to qualify the strand bonding characteristics, which may be affected by rust or manufacturing residues. Thus, bond length evaluation needs to be conducted in a manner consistent with the stress state in both transfer and flexural regions.

2.4.2 Studies on Transfer and Development Length

Significant research has been done in the past to investigate the bond mechanisms of prestressing strand in concrete as it relates to transfer and development length. Existing code provisions for the development length of fully bonded strands are based on the results of two studies conducted in the Research and Development Laboratories of Portland Cement Association (PCA) [7]. The results of these studies were reported in papers by Hanson and Kaar [17] and Kaar, LaFraugh and Mass [18]. An overview of the research including the work conducted at PCA is described in brief in the following:

a) Paul H. Kaar, Robert W. LaFraugh and Mark A. Mass [18]

This study was presented at the Ninth Annual Convention of the Prestressed Concrete Institute in 1959. This study investigated the influence of concrete strength on the stress transfer length of seven–wire strand at the time of prestress transfer. Strands of 6.35mm (¼), 9.53 mm (3/8), 12.7 mm (½), and 15.24 mm (0.6 in.) diameter strands were used to prestress rectangular prisms having various concrete strengths. For all strands except the 15.24 mm (0.6 in.) diameter strands, smooth, unrusted strands were used. The length of the prisms was 2.44 m (8 ft) for all specimens except 6/10 diameter which had a length of 3.05 m (10 ft). The cross section of the prisms varied with the size of the strand.

The researchers concluded that the concrete strength has little influence on the transfer length for strands up to 12.7 mm. (½ in.) diameter. The 15.24 mm (0.6 in.)

strands had a smaller transfer length for concrete with higher compressive strength and vice-versa. The influence of strand diameter was also studied in this research. The researchers found that transfer length varied linearly with respect to strand diameter. They also found that the average increase in transfer length over a period of one year following prestress transfer was 6% for all strand sizes and that the increase in transfer length was independent of the concrete strength at transfer.

The method of measurement of transfer length used in this project was by means of the DEMEC (DEtachable MEChanical) gauge method which has also been used in many other research programs to measure transfer length of prestressing strands.

b) Norman W. Hanson., and Paul H. Kaar. [17]

This study was performed at the Portland Cement Association (PCA) laboratories in 1959 and is considered to be the backbone for the current approaches to development length testing and code provisions. The test program involved 47 beam tests, with varying diameter of the strands were tested in a series of flexural tests. The main variable in the study was the strand diameter. Secondary variables included the percentage of steel reinforcement, the concrete strength, the strand surface condition and the use of embedded end anchorages on pretensioned strands. The authors propose a hypothetical shape of the bond wave from the flexural test results before slip.

The researchers found that strand size and embedment length have a considerable influence on the value of average bond stress at which general bond slip occurs. From the test results, the researchers determined curves that could be used for design such that general bond slip could be avoided. They also found out that the increase in percentage of reinforcement or a reduction in concrete strength reduces the possibility of general bond

slip, since the steel stress at flexural failure, and the corresponding bond stresses are reduced. The results of this research are the basis for the current ACI-318 recommendations (Equation 2-1 and 2-2) for development length of prestressing strands.

c) Paul Zia and Talat Mostafa [41]

This study was performed at the University of North Carolina, Raleigh, United States. The authors proposed a new equation for transfer length of prestressing strands that accounts for the effects of strand size, initial prestress and concrete strength at transfer. This equation is applicable to concrete strengths ranging from 13.8 MPa (2000 psi) to 55.2 MPa (8000 psi.). The researchers also studied the various parameters affecting the transfer and development length and reviewed the experimental results of the previous researchers.

The researchers found that the use of reinforcement to resist the bursting stress near the end of prestressing steel slightly reduced the transfer length, although the effect was not significant. Based on the review of the then available research information, the researchers proposed the following new equations for the transfer (L_t) (Equation 2-3) and development length (L_d) (Equation 2-4), which is applicable for concrete strengths varying from 13.8 MPa (2000 psi) to 55.16 MPa (8000 psi):

$$L_t = 1.5\frac{f_{si}}{f_{ci}}d_b - 4.6, \qquad f_{si}, f_{ci}(\text{ksi}) \;\&\; d_b \text{ (in.)} \tag{2-3}$$

$$L_d = 1.5\frac{f_{si}}{f_{ci}}d_b - 4.6 + 1.25(f_{ps} - f_{se})d_b, \qquad f_{si}, f_{ci}, f_{ps} \text{ (ksi)} \;\&\; d_b \text{ (in.)} \tag{2-4}$$

where, f_{si} is the initial prestress force, f_{ci} is the concrete strength at transfer, d_b is the nominal diameter of the strand, f_{su} is the ultimate stress in the strand and f_{se} is the effective stress in the strand after transfer.

d) Byung Hwan Oh., and Eui Sung Kim. [9]

This study was performed at the Seoul University, Korea. The main objective of the research was to study the effects of various important parameters on the transfer length on pretensioned, prestressed concrete girders. The principal test variables were strand diameter, concrete strength, concrete cover and strand spacing.

Results of this research showed that the current ACI-318 code equation for transfer length overestimates the actual measured transfer length. This overestimation is more significant in high strength concrete with larger concrete cover, which is not considered in the current equation.

The experimental program included testing of 36 pretensioned, prestressed concrete beams. The transfer length was measured by the concrete strain profiles measured using the DEMEC system and end-slip measurements. Results from the research can be summarized as follows:

- *Strand diameter:* The transfer length for 15.2 mm strand was found to be 25% longer than the 12.7 mm strand. Using the ACI code equation (Equation 2-1), the 15.2 mm strand was found to have a 20% longer transfer length than the 12.7 mm strand.
- *Concrete Strength:* The measured transfer lengths for high strength concrete were shorter than the lower strength concrete. Transfer length of prestressed members with a compressive strength of 45 MPa (6500 psi) was found to be approximately 12% shorter relative to similar members with a compressive strength of 35 MPa (5075psi) for 12.7 mm (0.5 in.) diameter strands. Similarly, for 15.2 mm (0.6 in.) diameter strands, this decrease was found to be approximately 15%.

- *Cut End Vs. Dead End Effect:* The cut end refers to the end of the specimen where the ends are cut and the dead end refers to the undisturbed end where the stresses are relieved by the cutting of the strands in the other end. The transfer lengths at the cut end were found to be consistently longer than the dead end due to the sudden release of the prestress. On average, the researchers found 16% and 13% increase in transfer lengths at cut ends for 12.7 mm (0.5 in.) and 15.2 mm (0.6 in.) strands respectively
- *Strand spacing:* The strand spacing studied was $2d_b$, $3d_b$ and $4d_b$, where d_b is the nominal diameter of the prestressing strands. The spacing was varied and the transfer lengths were measured for both the 12.7 mm (0.5 in.) and 15.2 mm (0.6 in.) strands. Reduction of clear strand spacing from $3d_b$ to $4d_b$ resulted in a remarkable increase in transfer length. The increase in strand spacing from $3d_b$ to $4d_b$, showed a very little reduction in transfer length.
- *Concrete Cover:* The side cover was kept constant at 5cm and the clear cover was varied. The beams contained only one strand and the clear bottom cover values tested were: 3,4 and 5 cm. The researchers found that the transfer length increased with reduction in clear bottom cover.
- *Time dependent effect:* The transfer length was measured at release, 7 days, and periodically up to 90 days. The authors found a shift in the transfer length profiles but not significant increase in transfer length values, this was due to the increase in axial concrete strains due to creep and shrinkage. The increase in transfer length at 90 days was found to be 5%.

- *Prediction from End Slip:* The researchers predicted the transfer length from end-slip measurements at the cut and dead ends. They found that theoretically calculated transfer lengths from end-slip measurements correlated well with the test data.

e) Mohsen Sahawy [35]

In this work the author performed a critical evaluation of the existing proposals of calculating the development length of prestressing strands. He also discusses on the extensive test programs on variety of prestressed concrete members and the modifications to the existing equation made by various researchers over the past 10 years (since 2001) are discussed. The objectives of this research were to compare and contrast the development length equations given by AASHTO specifications (Equations 2-1 and 2-2) and the equations proposed by other researchers, compare the federal highway agency (FHWA) results with findings of florida department of transportation structures research center (FSRC) and to present a rational method for calculating development length of prestressing strands. Based on the study, the author proposes two equations for development length, depending on the depth of the girder:

(a) For members with depth equal to or less than 610 mm (24 in.)

$$L_d = (\frac{f_{si}}{3})D + \frac{(f_{su} - f_{se})D}{1.2},\ (f_{si}, f_{su}, f_{se})\ \text{(ksi)}\ \&\ d_b\ \text{(in.)} \quad (2\text{-}5)$$

(b) For members with depth greater than 610 mm (24 in.)

$$L_d = (\frac{f_{si}}{3})D + \frac{(f_{su} - f_{se})D}{1.2} + 1.47h,\quad f_{si}, f_{su}, f_{se}\ \text{(ksi) and}\ D, h\ \text{(in.)} \quad (2\text{-}6)$$

where, D is the nominal diameter of the strand, f_{su} is the stress in the strand (in ksi) at nominal strength of the critical section, f_{si} is the stress in the strand at time of initial prestress (ksi) and h is the overall depth (in.) of the member.

The brief features and results from this investigation are as follows:

- Shear – flexural interaction affects the development length of prestressing strands and that it should be included in the design recommendations.
- The effects of shear are more pronounced in deeper members and the author proposes his new equation taking this effect into consideration
- For prestressed concrete members with depth equal or greater than 610 mm (24 in.), the existing AASHTO [2] equation and the proposed equation (Equation 2-3) yields the closest prediction, while FHWA [35] and Buckner predictions [8] (increase in development length by a factor of 1.6) are extremely conservative.
- For prestressed concrete members with a depth greater than 24 in., the AASHTO equation [2] yields unacceptable low values for most cases and the new proposed equation (Equation 2-6) gives conservative values.

f) Deatherage, J.H., Burdette, E.G., and Chew, C.K., [14]

This study was performed at the University of Tennessee, Knoxville.. Twenty full scale AASHTO Type-I girders with large strand diameters: 12.7 mm (1/2 in.), 14.3 mm (9/16 in.) and 15.2 mm (0.6 in.) were statically tested to failure. Transfer and development lengths were measured and factors affecting both transfer and development length are discussed and evaluated. Based on the test data, new equations are proposed. From the existing equation, the authors proposed replacing the initial stress instead of the

effective stress in the transfer length term and introduce a conservative factor of 1.5 in the flexural bond length term. The proposed equation is given as follows:

$$L_d = (\frac{f_{si}}{3})D + 1.5(f_{ps} - f_{se})D \quad (2\text{-}5)$$

Based on the study, the authors concluded that the 15.2 mm (0.6 in.) strand should be accepted as a common practice. The authors found that 15.2 mm (0.6 in.) strands have much shorter transfer lengths relative to any other strand diameter used in their research. Also, the measured development lengths from 15.2 mm (0.6 in.) strand were comparable with those of other diameter strands used. The ultimate capacity of members with 15.2 mm (0.6 in.) were substantially higher relative to all other strands used in the study

2.4.3 Oustanding issues

With the exception of cantilevers and short span members, strand development seldom governs the design of pretensioned concrete members. Nevertheless, several bond-related failures of pretensioned members have been reported since the adoption of the current criteria.

Diameter of the strand

In current practice, Grade 1860 MPa (270 ksi) strand with a higher tensile strength, 1.860 MPa (270 ksi) and larger cross sectional are is used. Low-relaxation strand with higher yield stress has replaced stress relieved strand. The current ACI-318 / AASHTO LRFD expression for transfer length was derived using a bond stress of 2.76 MPa (400 psi), which represents the average values form the tests conducted by Hanson and Kaar [17]. This stress applies to the actual perimeter of the seven wire perimeter of the strand. For Grade 270strand, this constant is about 6% larger. Despite wide variations

in measured values, several researchers have concluded that the transfer length increases directly with strand diameters ranging up to 15.7 mm (0.6 in.).

Shear – Bond interaction

The issue of web-shear cracking and bond of prestressing strands has been discussed and debated for a long time. The interaction between shear and bond has been considered to be cause for slip failures[17][7][8] It has been found that the initial slip occurred coincident with the web shear cracking[7][8]. However, there is a doubt on whether web-shear cracking initiates strand slip or vice versa. Researchers from University of Texas at Austin [7][8] found that the results indicate a direct interaction between shear and bond with the initial slip occurring immediately or shortly after the appearance of first shear crack. The best documented evidence found to explain interaction between shear and bond gives a strong indication that general bond slip occurred prior to the sudden shear failure [7][8].

Shahawy [35] proposed two different equations (Equations 2-5 and 2-6) for development length depending on the depth of the member. He found that the effects of shear on development length cannot be neglected on members greater than 610 mm (24 in.) as there exists interaction between shear and flexure and the slippage of the strand is most likely to occur before the flexural capacity of the member is achieved.

The wide variations and the confusion in the validation of the current code provisions may also be due to the inconsistency in the amount of shear reinforcement used in the various research studies performed. Researchers have used different amounts of shear reinforcements in their studies on transfer and development lengths. Taking into account the shear-bond interaction, researchers who have had relatively higher shear

reinforcement are more likely to have lower transfer and development lengths and vice versa. This may also be a reason for the wide variation in the results in past studies. Shear-bond interaction must be taken into consideration to properly correlate the variations in transfer and development length results available.

Failure strains in test specimens

The wide variation in the results of development lengths have also been attributed to the level of strand strains at section failure. Apparently to simplify testing, most development specimens have been proportioned to fail at relatively low strains. The exceptions have been girders with cast–in place composite slabs [8]. Experimental results from most test programs suggest that average bond strength is lower in specimens with large strand strains at failure (eg. strains near the guaranteed ultimate minimum elongation of 0.0350) as compared to specimens that failed with strains near the yield strain. Studies indicate that the studies on non-composite sections with failure strains much lower than the guaranteed ultimate minimum elongation showed that the ACI-318/AASHTO LRFD recommendations were conservative. At the same time, composite sections with failure strains near the guaranteed minimum elongation showed 1.7 times longer development length than the ACI-318/AASHTO LRFD recommendations [8][35]. A possible reason for this discrepancy has been attributed to the relative difference in strain levels at failure. Members with composite sections represent the actual bridge applications and hence it has been recommended that development length studies should be made with cross sections that would develop strand strains near the minimum guaranteed ultimate elongation.

2.5 Concluding Remarks

From the above-mentioned studies, it is clear that SCC is of high interest due to the many advantages it provides to the precast industry for improved construction efficiency and quality. However, it becomes obvious that most efforts to date have focused on the material aspect of SCC and only limited efforts have validated its structural performance. For precast/prestressed concrete construction, the bond between concrete and prestressing strands is of primary importance. Given the complex nature of bond stresses and the mechanisms controlling them; along with the varied results and continuous debate over the existing code recommendations for conventional concrete, it becomes essential to evaluate the bond performance of prestressing strand in members built using SCC. The evaluation of bond performance on SCC is not an easy task taking into account that there is no commonly accepted procedure to proportion SCC mixes. Proper evaluation of the bond performance and evaluation of the respective bond parameters (transfer and development lengths) is essential to take the advantages SCC offers into safe implementation in precast/prestressed concrete construction.

CHAPTER 3 MIX DESIGN DEVELOPMENT AND EVALUATION

Due to the many options available for obtaining SCC, the goal of this research was to bound the effects of SCC mix proportioning by considering extreme conditions for its proportioning. This chapter describes the philosophy behind the selected mix designs for this project and provides the specific proportioning used. Also included herein is the evaluation of the fresh and hardened properties of the experimental mix design matrix. SCC mix development and test results are compared with a reference normally consolidated concrete (NCC) mix.

3.1.1 SCC Mix Design Approaches

As previously discussed in Chapter2, SCC achieves its fresh property advantages through specially proportioned mix designs that significantly deviate from what is considered ideal and developed through many years of research and development. The tailorable design of SCC mixes for fresh and hardened properties gives infinite possibilities to obtain SCC. While there is no commonly accepted procedure to proportion SCC mixes, over the years several methods have been developed in research centers around the world [20][11][12][27]. In spite of the different methods of achieving SCC, it is commonly agreed that all methods are **bounded** by two main approaches [20] :

- ***Approach 1:*** Proportioning concrete with moderate w/c ratios (e.g., 0.45), and use of HRWR and VMA to provide fluidity and increase stability, respectively. The VMA increases both the yield value and viscosity, while the HRWR reduces the yield value. The resulting combination provides a mix with relatively low yield and moderate viscosity.

- ***Approach 2:*** Mixes without any viscosity-enhancing admixture, but with lower w/c ratios (e.g., 0.33) to reduce free water content and provide stability and use of a relatively high content of HRWR to provide high-fluidity.

Due to the wide variety of mix designs that have been proposed, and that can be developed to create SCC, this research focused on bounding the proportioning techniques for SCC. Hence an approach was adopted in which the mix design characteristics of SCC and their effect on material and structural properties were bounded, to provide designers with knowledge on the compromises made through optimization of an SCC mix for fresh-concrete behavior. This will allow design freedom to tailor the proportioning of SCC to match fresh performance objectives while giving guidance to design engineers on the compromises that the mix design will have on short term and long term hardened properties as well as the structural response of structural elements.

In this research, an SCC mix was selected from each of the above mentioned approaches. The first SCC mix (SCC1) with low w/c ratios (0.35) was designed after Approach 1, the second SCC mix (SCC3) with high w/c ratios (0.45) followed Approach 2 and the third SCC mix (SCC2) with moderate w/c ratio (0.40) was obtained from the combination of these two approaches. Also a normally consolidated concrete (NCC) mix (w/c ratio = 0.40) was used as a reference. These mix designs and the controlling parameters are described in the following section. The SCC2 and NCC mixes had to be repeated due to poor performance of the mix and testing equipment. The first and second attempts are designated by the letters "A" and "B," respectively.

3.2 Project Mix Design Matrix

Based on the parameters governing the proportioning of a SCC mix and implementing the idea of bounding the performance of all SCC mixes, the mix design matrix for the test program is shown conceptually in Table 3-1.

Table 3-1 Mix Design Matrix - Binding of Performance by w/c ratio

Mix Design	w/c	HRWR	VMA	CAC	S/Pt	EA
SCC1	**0.35**	+	–	Less	more	+
SCC2	**0.40**	+	–			+
SCC3	**0.45**	+	+	More	less	+
NCC	**0.40**	–	–	0.50	0.50	+

All mixes used Type III cement with a design compressive strength of 48.3 MPa (7,000 psi). Local natural aggregates in agreement with the Michigan Department of Transportation specifications for use in bridge elements were used, namely 6AA coarse aggregates and 2NS sand. The level of entrained air for all mixes was 6%. The high range water reducer, viscosity modifying admixture, air entraining admixture and set-retarding admixture were provided by Degussa Admixtures Inc. The set retardants were used to delay the initial setting time of concrete since it had to be delivered to the laboratory via a ready mix delivery truck. In addition the casting process was long as it included multiple test units and material testing samples. Thus it should be noted that since these requirements of ready mix concrete delivery, these mix designs may vary slightly from those used in situ in the precast/prestressed plants.

The mix designs with respect to the approaches, were obtained from consultation with Degussa Admixtures Inc. The mix designs in Table 3-2 were used as target to be

achieved to cast the test specimens at MSU's Civil Infrastructure Laboratory. However, during the actual casting of the specimens, some of the mix designs had to be modified on site due to variations in delivery time, moisture and temperature.The mix design proportions used in this research for all the mixes are given in. Table 3-2 The in-situ admixtures and w/c ratio which slightly varied from the target mix design (Table 3-2) for the various mix designs used in this research are expressed in terms of percentage change from the original (Table 3-3) for all the mixes. The negative values indicate that less quantity of particular admixture has been added in the mix relative to the target mix. There was no change in any other mix proportion component of the mix design. Table 3-4 gives the final mix designs used in the test beams.

Table 3-2 Mix Designs used in the project – Target mixes

COMPONENT	MIX TYPE			
	SSD weights (lbs / cyd)			
	NCCA & NCCB	SCC1	SCC2A & SCC2B	SCC3
Cement - Type III	700	700	700	700
Fine Aggregates.	1216	1519	1426	1275
Coarse Aggregates.	1580	1380	1380	1435
Water	280	245	280	315
Air	6%	6%	6%	6%
w / c ratio - Target	0.40	0.35	0.40	0.45
ADMIXTURES	fl.oz./cwt			
Air Entraining Admixture	1	0.5	0.5	0.5
High Range Water Reducer	6	6	7	8
Viscosity Modifying Admixture	0	0	1	2
Set Retardant	6	6	6	6
$1 lb/yd^3 = 0.593 kg/m^3$ 1 fl oz./cwt = 65 mL/100 kg				

Table 3-3 Changes in Admixtures for Actual Project Mix Designs

ADMIXTURES	MIX TYPE Changes in Admixtures relative to target mix (%)					
	NCCA	NCCB	SCC1	SCC2A	SCC2B	SCC3
Air Entraining Admixture	0.00	0.00	0.00	-57.14	0.00	81.63
High Range Water Reducer	-33.33	-66.67	33.65	21.28	0.00	0.00
Viscosity Modifying Admixture	0.00	0.00	0.00	293.88	0.00	350.00
Set Retardant	-100.00	0.00	16.67	-100.00	11.56	0.00
w / c Ratio	0.00	0.00	0.00	5.00	0.00	0.00

Table 3-4 Actual Project Mix Designs

	NCCA	NCCB	SCC1	SCC2A	SCC2B	SCC3
COMPONENT	SSD WTS (lbs./cyd)					
Cement - Type III	700	700	750	700	700	700
Fine Aggregates.	1216	1216	1627.5	1426	1426	1275
Coarse Aggregates.	1580	1580	1478.57	1380	1380	1435
Water	280	280	262.5	280	280	315
Air	6%	6%	6%	6%	6%	6%
w / c ratio - Target	**0.4**	**0.4**	**0.35**	**0.42**	**0.4**	**0.45**
ADMIXTURES	oz./cwt					
Air Entraining Admixture	3.50	3.50	1.75	0.75	1.75	3.18
High Range Water Reducer	8.06	4.03	12.93	14.59	12.03	15.37
Viscosity Modifying Admixture	0.00	0.00	0.00	6.99	1.78	15.37
Set Retardant	0.00	52.50	70.00	0.00	58.57	46.67
1 lb/yd^3=0.593 kg/m^3 1 fl oz./cwt = 65 mL/100 kg 1 in. = 25.4 mm						

3.3 Fresh Property Evaluation:

As previously discussed in Chapter 2, The acceptability of the SCC mix resides on the ability for the mix design to satisfy performance criteria that defines a concrete as self-consolidating, namely to have a highly flowable and stable mix. A brief discussion and results of the tests performed in this research is given as follows:

3.3.1 Slump Spread and Visual Stability Index (VSI)

The Slump spread was the first test performed. If the concrete performance was satisfactory then the next tests were performed. A flat base plate was kept on a level ground and was slightly moist with water. All tests were consistently performed with an inverted cone, by the same person. The concrete was filled in the cone with a scoop; no tamping was done. Any excess concrete was removed and the cone was lifted vertically allowing the SCC to flow freely. The diameter of the spread was measured in perpendicular directions. The average of the two measured diameters was calculated. The stability of the mixture was rated by visual examination of the spread concrete. The results of the slump spread values before cast for all the SCC mixes and their VSI ratings are shown in Table 3-5.

Table 3-5 Slump Spread and VSI rating of SCC mixes.

MIX	AverageSlump Spread (in.)	VSI Rating
SCC1	27.0	0.0
SCC2A	25.0	0.5
SCC2B	24.5	0.0
SCC3	27.0	1.0
1 in. = 25.4 mm		

a) Slump Spread test apparatus

b) Step1 - Cone Filled with SCC

c) Step 3 - Cone lifted vertically

d) Step 4 - Measurement of spread

Figure 3-1 – Slump Spread test

3.3.2 J Ring Test

The J Ring test is used to determine the passing ability of SCC. For this test, J Ring is used in conjunction with the slump flow test procedure. The combination of these two tests enables to study the flowing ability and the passing ability of SCC. The procedure is essentially the same as for the slump spread test with the exception that a J ring is placed concentrically around the slump cone. (Figure 3-2). The cone is lifted and the SCC is allowed to pass through the J-Ring. The spread in perpendicular directions was measured as before. Visual examination of any segregation or bleeding was also

carried out. The values of concrete spread with J – Ring were compared with the values of slump spread without the J-Ring. The smaller these differences showed the better passing ability of concrete. Table 3-6 shows the results obtained from the slump spread in conjunction with the J-Ring. The J-Ring measurements were not taken for SCC2B mix as the mix was stiffening rapidly. Table 3-6 also shows the J-Ring value calculated as explained in Chapter2.

a) J – Ring test apparatus

b) J – Ring test in Progress

Figure 3-2 J – Ring Test

Table 3-6 and J – Ring Slump Spread and J-Ring Values

MIX	Average Slump Spread (in.)	J- Ring Value (mm)
SCC1	25.0	6.35
SCC2A	20.5	9.53
SCC2B	-	-
SCC3	23.5	0
1 in. = 25.4 mm		

3.3.3 L – Box Test

L-Box test assesses the flow of SCC and also the extent to which it is subjected to blocking by reinforcement [30]. The test apparatus comprises of a rectangular cavity in with reinforcement. The level of reinforcement can be changed to enforce severe or light restraints depending on the actual reinforcement blocking of the structure. The L-Box used in this test had the same level of reinforcement as given in PCI guidelines [30] (Figure 2-4). This opening is controlled by a gate.

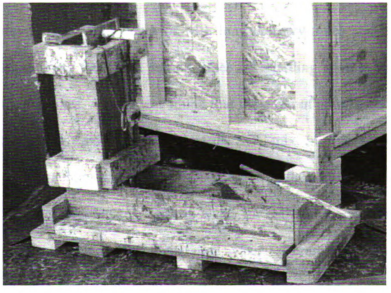

Figure 3-3 L- Box Test

The L-Box results obtained for the various SCC mixes are reported in Table 3-7

Table 3-7 L- Box Blocking Ratio

MIX	Blocking Ratio (H2/H1)
SCC1	0.80
SCC2A	0.86
SCC2B	0.77
SCC3	0.69

3.4 Challenges in SCC Quality Control and Quality Assurance

Ready Mix Concrete was used for the SCC in this project. The travel time for the concrete mixer to reach to MSU's Civil Infrastructure Laboratory was approximately 30 to 45 minutes. In the first SCC mix (SCC2A), all the admixtures were added in the plant and by the time SCC reached the lab, its behavior was not of typical of SCC (low fluidity). This mix did not have any set-retarding agents (stabilizers). Substantial addition of HRWR's was needed to achieve SCC behavior. It was thus determined that it was difficult to achieve proper SCC behavior with long delivery times and use of Type III cement. In order to delay the initial setting time, set retarding agents (stabilizers) were used in all the future mixes. Also, it was found that the order of admixtures addition plays a vital role in the setting time and behavior of the SCC mix. In order to avoid the issues of rapid setting and to achieve the target SCC mixes, all of the admixtures were not added at the Ready Mix Plant. Aggregates, cement, water, air entraining agent and set retarding agent were added in the plant. The high range water reducers (HRWR) and viscosity modifying admixtures (VMA) were added at the laboratory, and in that order. These admixtures were added individually and mixed in the truck drum for approximately 5-10 minutes before the next admixture was added. The fresh behavior of SCC was studied

after all the admixtures were added. In some cases it was found that proper fluidity of the SCC mix was not achieved or not satisfactory. Hence additional quantities of admixtures were added to achieve the desired SCC behavior. As a result, the actual SCC mixes deviated from the target mix design (see Table 3-3). This deviation was mainly in the content of admixtures.

The desired target properties for the NCC mix were achieved without any problem. This reflects the significant experience with the conventional concrete (NCC) mix designs. Conversely, even though SCC was first introduced in 1980, it is still relatively new to the industry. In spite of much research work done in fresh concrete properties and mix designs of SCC, achieving the same target mix is not easy in the field, as climate conditions and aggregate properties may vary significantly. More research on various practical difficulties needs to be performed in collaboration with industry and admixtures experts to make SCC achievable, controllable and available to industry as easily as NCC.

3.5 Hardened Concrete Property Evaluation

Since the target engineering properties of hardened SCC should be the same as those for conventional concrete, the same test and procedures that are used for conventional concrete were used for SCC. Tests were performed on concrete cylinders of following dimensions: 101.6 mm x 203.2 mm (4"x8"). The compressive strength tests, modulus of elasticity tests and split tensile strengths were performed in accordance with ASTM C39, ASTM C469 and ASTM C496 standards, respectively. Compressive and Split tensile strength tests were performed at 1, 3 (day of release of prestress), 7, 14, and 28 days. Tests were also performed at the day of flexural testing, where in the average

age of concrete was approximately 110-130 days Elastic modulus tests were performed only at the day of release (3 days) and at 28 days of age.

3.5.1 Compressive Strength (f'_c)

The target compressive strength for all mix designs used in this project was 48.26 MPa (7000 psi) at 28 days. The compressive strength tests were performed in accordance with the ASTM C39 standards. Three concrete cylinders were tested for each test.

Table 3-8 shows the average compressive strength values and their standard deviation for concrete ages varying from 1 to 28 days for all the mixes. Table 3-9 shows the compressive strength and the standard deviation for all mixes the day of flexural testing (~110-130 days). Figure 3-4 the variation of compressive strength with the age of concrete. Due to improper functioning of the equipment, 14 day test results are not available for SCC1.

Table 3-8 Compressive Strength (f'_c) Test Results – 1 to 28 days

MIX	NCCB		SCC1		SCC2A	
Age Of Concrete (Days)	Average f'c (psi)	Standard Deviation (psi)	Average f'c (psi)	Standard Deviation (psi)	Average f'c (psi)	Standard Deviation (psi)
1	4899.2	191.1	7003.6	194.37	N/A	N/A
3	5545.1	93.41	7685.0	129.42	7693.25	607.29
7	6478.2	146.9	8500.7	350.76	7778.93	1307.9
14	6535.8	232.9	-	-	8161.18	323.00
28	6864.6	1131.6	8686.9	374.77	8646.88	392.77
MIX	SCC2B		SCC3			
Age Of Concrete (Days)	Average f'c (psi)	Standard Deviation (psi)	Average f'c (psi)	Standard Deviation (psi)		
1	6132.4	124.9	6132.4	124.9		
3	6703.8	344.2	6703.8	344.2	1 MPa = 145.04 psi	
7	7065.1	603.2	7665.4	157.3		
14	7671.9	29.8	7671.9	29.8		
28	8038.4	1388.8	7810.0	924.0		

Table 3-9 Compressive Strength at Day of Test

MIX	Age of Concrete at Day of Test (days)	Compressive Strength (psi)	Standard Deviation (psi)
NCCB	133	7018.28	302.69
SCC1	124	8973.29	322.27
SCC2A	118	9208.98	1121.69
SCC2B	109	9378.28	1131.81
SCC3	120	7971.25	199.62

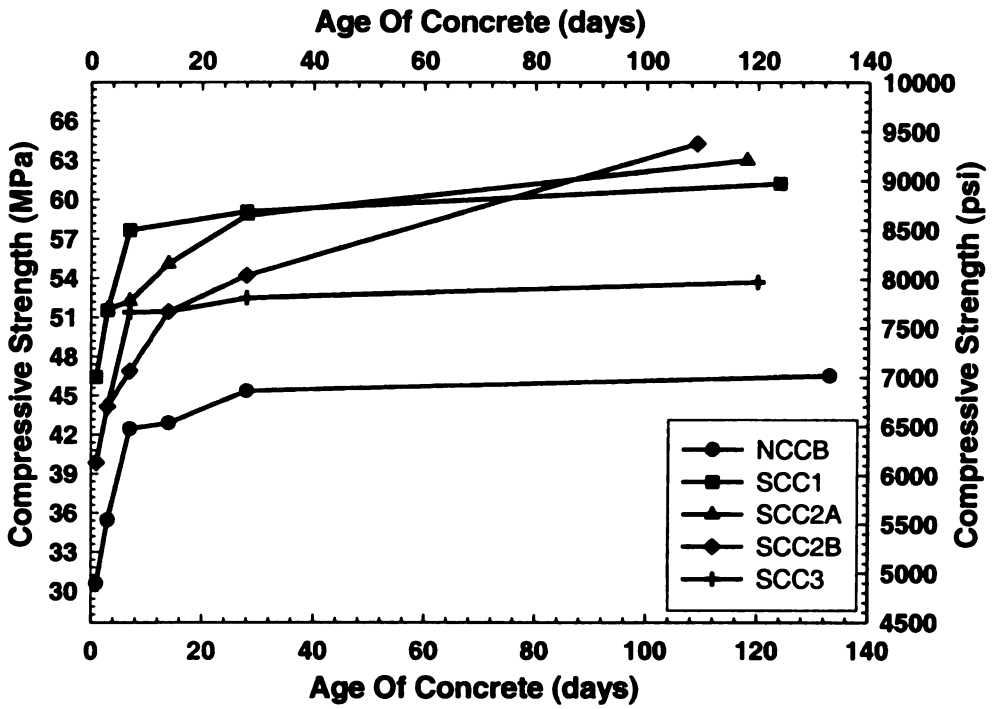

Figure 3-4 Compressive Strength variation with time – All Mixes

3.5.2 Elastic Modulus Test

The average Elastic modulus *(E_c)* was calculated as per the ASTM C469 standards and was compared with the equation recommended by the ACI code $E_{c,code} = 57000\sqrt{f'_c}$ (psi). Table 3-10 and Table 3-11 show the values of the modulus of elasticity obtained both experimentally and from the ACI code expression and their relative comparison for 3 days and 28 days respectively. Due to improper functioning of testing equipment, reliable values of E_c could not be obtained for SCC1 and SCC2A mixes at 3 days and for SCC2B mix at 28 days. A sample plot of the compressive stress–strain response (28 days) for each of the mix designs showing the calculation of the modulus of elasticity are given in Figure 3-5 to Figure 3-8. Detailed individual plots are shown in Appendix 1.

Table 3-10 Elastic Modulus Tests at 3days – all mixes.

MIX	$E_{c,meas}$ (ksi)		$E_{c,code}$ (ksi)		$E_{c.meas} / E_{c,code}$
	Average	Standard Deviation	Average	Standard Deviation	
NCCB	4,053.20	24.81	4,244.46	35.75	0.95
SCC1	-	-	4,996.86	648.46	-
SCC2A	-	-	4,999.54	1,404.67	-
SCC2B	4,333.26	313.59	4,912.91	341.70	0.88
SCC3	4,090.24	494.76	4,611.07	104.08	0.89

Table 3-11 Elastic Modulus Tests at 28 days

MIX	$E_{c,meas}$ (ksi)		$E_{c,code}$ (ksi)		$E_{c.meas} / E_{c,code}$
	Average	Standard Deviation	Average	Standard Deviation	
NCCB	4,383.35	0.00	4,693.45	391.68	0.93
SCC1	4,624.80	530.86	5,311.99	114.61	0.87
SCC2A	5,312.35	221.35	5,299.69	102.23	1.00
SCC2B	-	-	4,992.59	311.28	-
SCC3	4,463.93	130.92	5,032.90	298.24	0.89

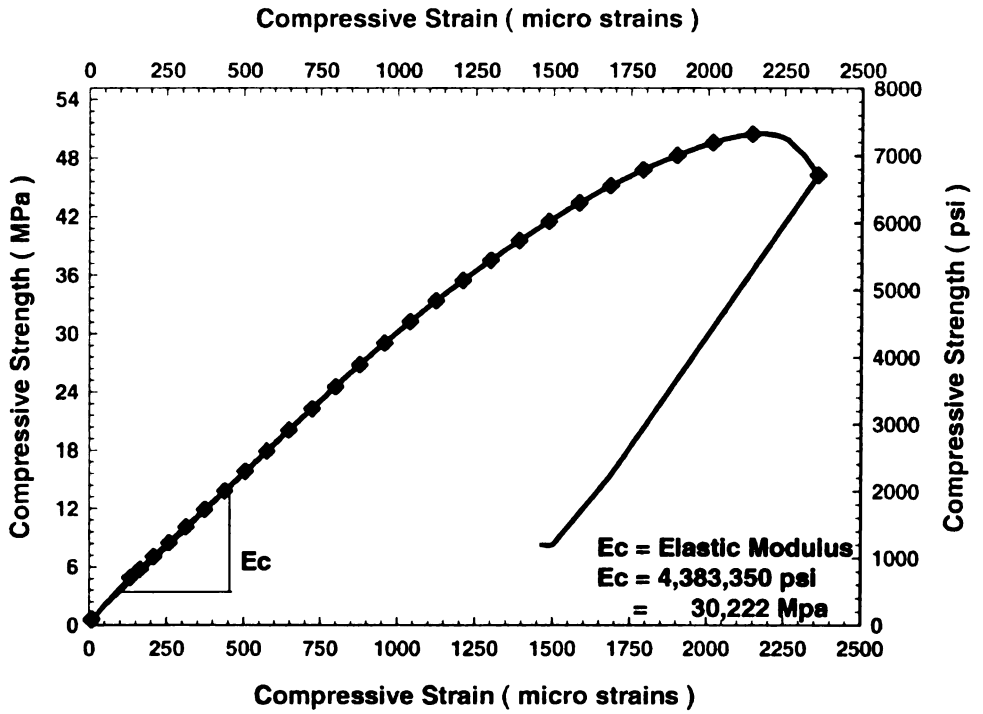

Figure 3-5 Typical Stress–Strain Response – NCCB – 28 days

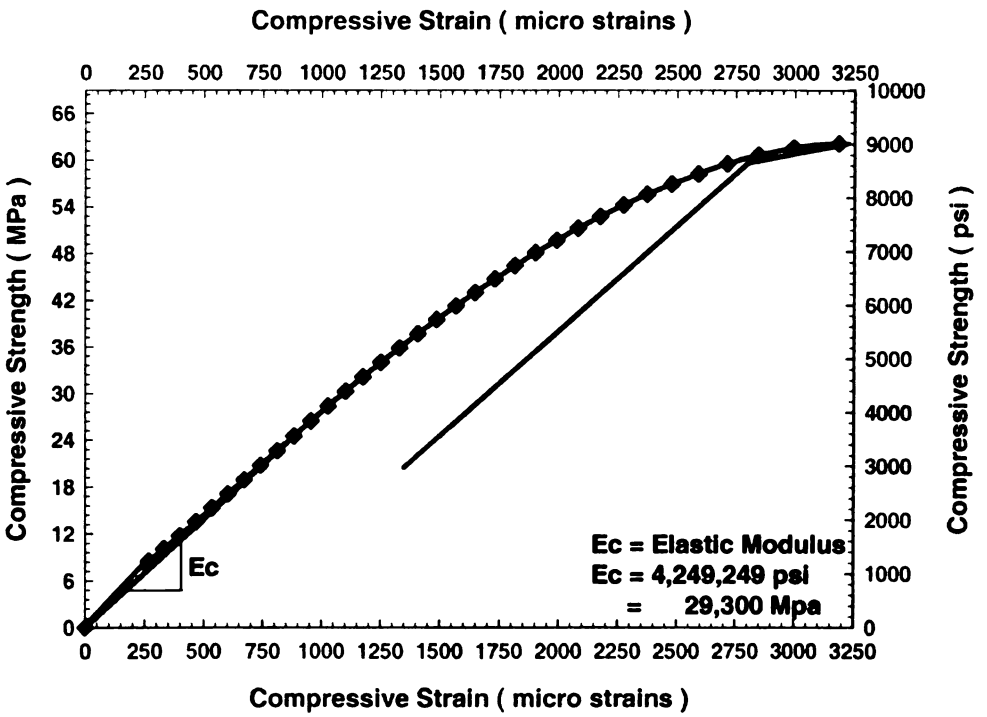

Figure 3-6 Typical Stress–Strain Response – SCC1 – 28 days

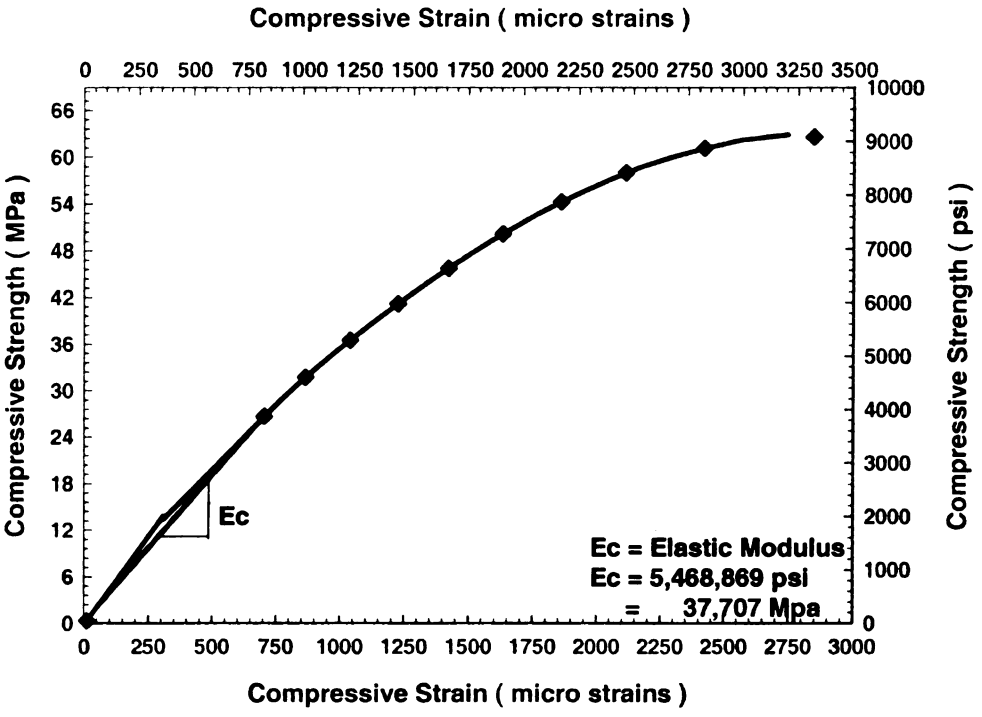

Figure 3-7 Typical Stress–Strain Response – SCC2A – 28 days

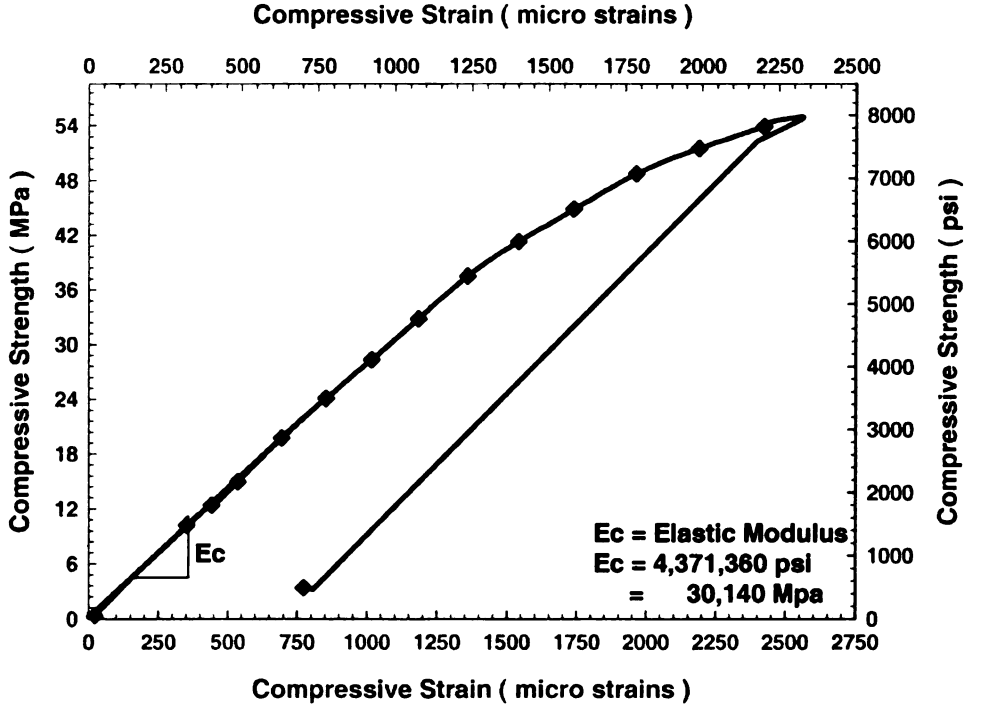

Figure 3-8 Typical Stress–Strain Response – SCC3 – 28 days

3.5.3 Split Tensile Test.

As previously mentioned, split tensile strength (f'_t) tests were performed in accordance with the ASTM C469 standards for all mixes. Table 3-12 shows the average split tensile strength values and their standard deviation for concrete ages varying from 1 to 28 days. Table 3-13 shows the split tensile strength and the standard deviation for all mixes at their respective days of flexural test. Figure 3-4 shows the variation of split tensile strength with the age of concrete. Due to large variation and improper functioning of testing equipment, some data was considered unreliable and not included in the results given here. Thus, Table 3-12 and Table 3-13 below have some blank spaces.

Table 3-12 Split Tensile Strength – 1 to 28 Days

MIX	NCCB		SCC1		SCC2A	
Age Of Concrete (Days)	Average Split Tensile Strength (psi)	Standard Deviation (psi)	Average Split Tensile Strength (psi)	Standard Deviation (psi)	Average Split Tensile Strength (psi)	Standard Deviation (psi)
1	434.43	65	514.97	73	-	-
3	-	-	519.94	0	574.95	68
7	424.28	120	571.96	58	574.95	68
14	540.63	33	540.63	33	583.57	8
28	-	-	581.11	33	596.33	88

MIX	SCC2B		SCC3		
Age Of Concrete (Days)	Average Split Tensile Strength (psi)	Standard Deviation (psi)	Average Split Tensile Strength (psi)	Standard Deviation (psi)	
1	528.46	64	509.01	73	1 MPa = 145.04 psi
3	-	-	532.20	121	
7	534.26	11	569.09	82	
14	572.89	111	569.33	36	
28	589.47	40	-	-	

Table 3-13 Split Tensile Strength - Day of Test

MIX	Age at Day of Test (days)	Average Split Tensile Strength (psi)	Standard Deviation (psi)
NCCB	133	544.54	113
SCC1	124	615.73	117
SCC2A	118	623.76	218
SCC2B	109	629.47	219
SCC3	120	580.33	92

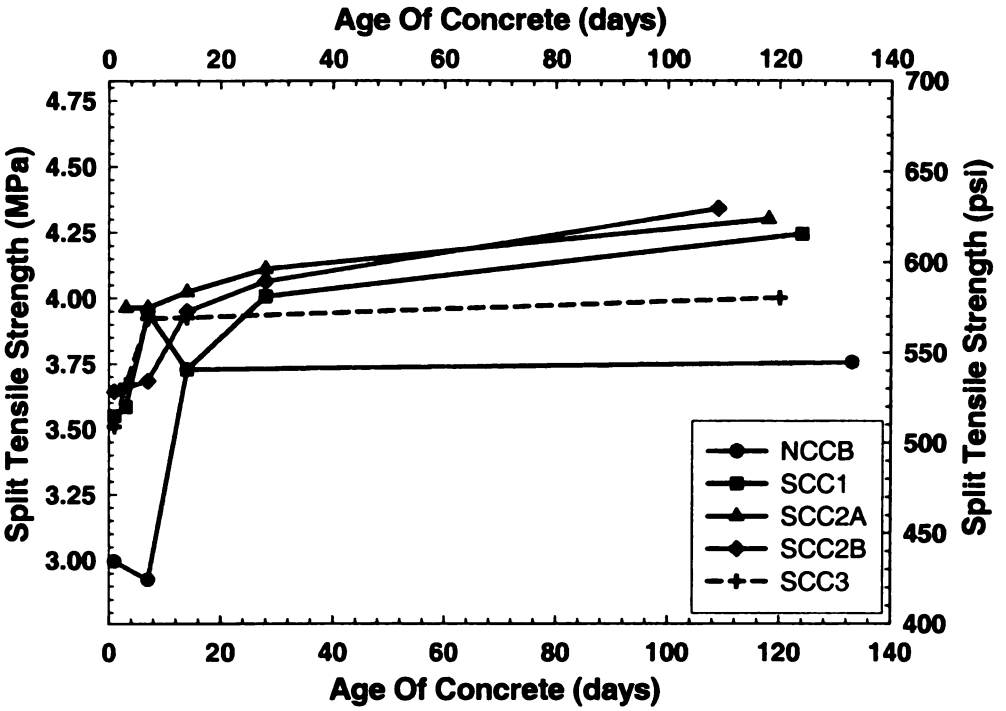

Figure 3-9 Split Tensile Strength variation with Time

3.5.4 Discussion of Results - Hardened Test properties

The target compressive strength at 28 days for all mixes was 48.3 MPa (7000 psi). It was found that all the mixes had compressive strengths much beyond this target value at 28 days. Figure 3-10 shows the variation of the compressive strengths at 28 days. The results show that the compressive strength at 28 days was approximately 2% lower than the designed target for NCCB and was greater than the design target by 11% – 25% for the SCC mixes. Considerable research in all aspects and extensive use of NCC has made it possible to control the hardened properties of NCC with more confidence. The same amount of control and confidence has not been achieved with SCC. From the elastic modulus (Table 3-11) at 28 days of concrete age it was observed that the measured value of NCCB was 7% lower than that predicted by the ACI code, whereas SCC1 and SCC3

had lower measured modulus by 13% and 11%, respectively, relative to the code predicted values. Figure 3-11 shows the relative comparison of the elastic modulus for the various mixes Due to technical problems with the testing equipment, SCC2B modulus tests at 28 days could not be performed. SCC2A showed no variation with the code predicted values. It should be noted that SCC2A was a very stiff mix and the performance of the mix was poor and hence the data reliability is questionable.

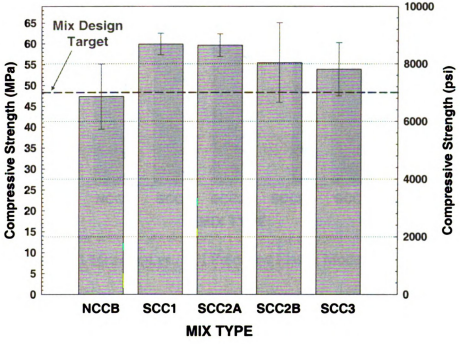

Figure 3-10 Comparison of Compressive Strength at 28 days

Overall, the SCC mixes showed a larger variation in elastic modulus compared to the code predicted values than the NCC mix. The results reiterate the fact that much control in hardened properties has not yet been gained in SCC mix proportioning relative to NCC mix design. It should also be noted that the variations in SCC hardened properties may also be due to the various mix proportions used. Infact, SCC1 and SCC3

are mixes obtained from two different approaches and the variation is expected. SCC2B is the only mix relatively similar to NCCB mix.

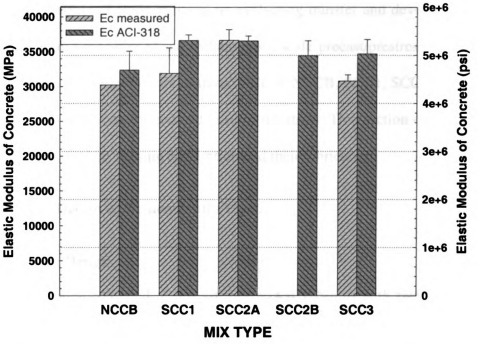

Figure 3-11 Measured vs. ACI Predicted Elastic Modulus at 28 days

CHAPTER 4 TEST PROGRAM – INTRODUCTION

The effect of bond on transfer and development length of precast/prestressed girders built using SCC was evaluated through a structural testing program described herein. The experimental study is based on evaluating transfer and development lengths for 13 mm (0.5 in.) diameter strand in laboratory scale precast/prestressed beams. Two beams for each of the program mix designs (NCCA, NCCB, SCC1, SCC2A, SCC2B and SCC3 Table 3-4) were constructed and used in the study. This section discusses the test unit (beams) design, their naming convention and their fabrication.

4.1 Specimen Design & Nomenclature Used.

4.1.1 Specimen Design

The test units consisted of precast/prestressed T-beams with two 13mm (0.5 in.) diameter prestressing stands and nominal compression and shear reinforcement (Figure 4-1). The cross-section and reinforcement amounts were chosen so that the strand strain at the section nominal capacity was close to the guaranteed ultimate strain of the strand, taken to be 0.0035. The strands with a nominal diameter of 13mm (0.5 in.), Seven wire low relaxation 1860 MPa (270 ksi) Grade strands with a nominal diameter of 13 mm (0.5 in.) were used. The beam length was 11.58 m (38 ft) with the goal of being able to perform two flexural tests per beam (one for each end). The prestressing strands were completely bonded. Nominal shear reinforcement was provided with 6mm (0.25 in.) diameter smooth stirrups. The U-shaped stirrups were placed at 305 mm (12 in.) spacing through out the length of the beam except at the ends where they were spaced at 152 mm

(6 in.) for a length of 610 mm (24in.) An elevation drawing is showing the reinforcement details is given in Figure 4-2.

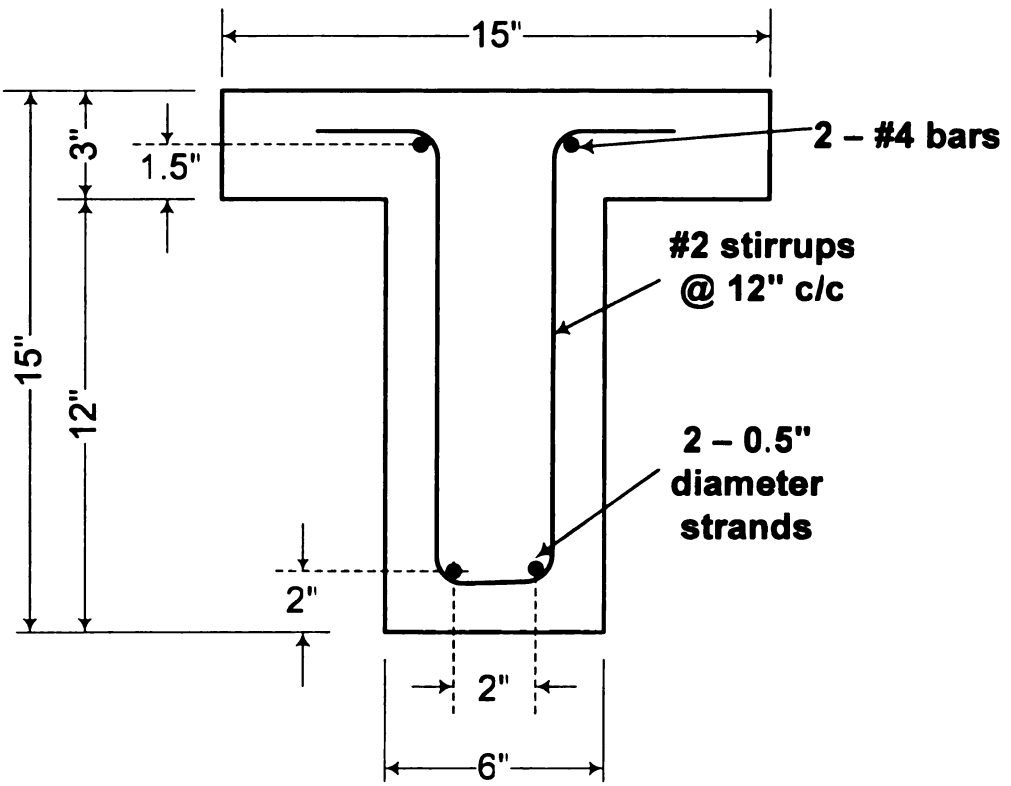

Figure 4-1 Test Specimen - Cross Section Details

1 in. = 25.4 mm

The strain level in the prestressing strand has been identified to be an important parameter in the discrepancy of experimentally obtained values for development length [8]. Experimental values from most test programs suggest that the average bond strength is lower in test units with large strand strains at failure (e.g., near the guaranteed ultimate elongation) as compared to specimens that failed with strains near the yield strain (0.010) [8].Therefore, the beams for this study were designed such that the strain demand on the strands was closer to the guaranteed ultimate strength.

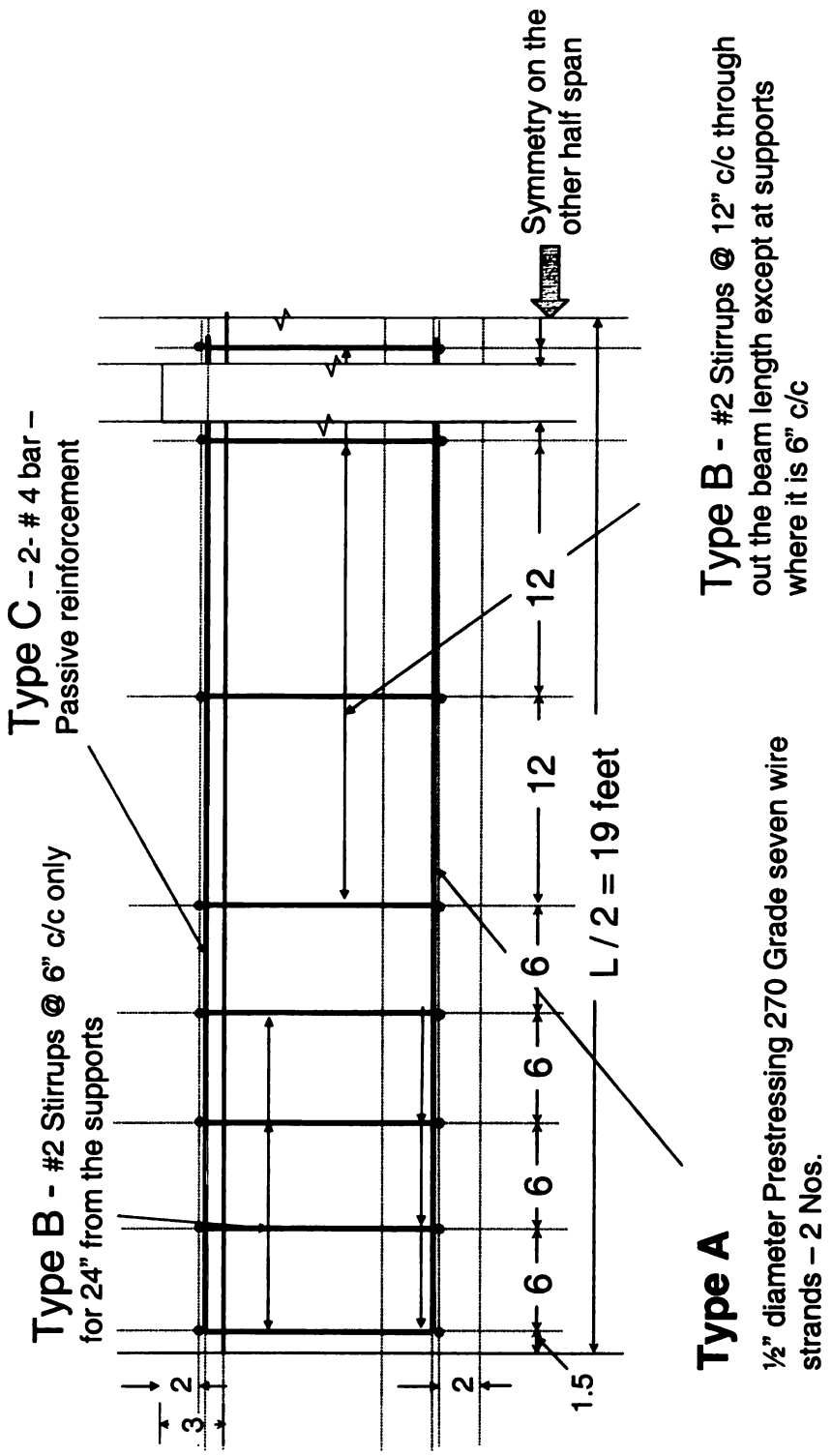

Figure 4-2 Reinforcement Details of the test specimens

4.1.2 Nomenclature

Two test specimens were cast at a time for each mix. For transfer length measurements, strains on both sides of the beam web were measured. The specimen identification nomenclature used through out this project for transfer length studies is summarized in Figure 4-3.

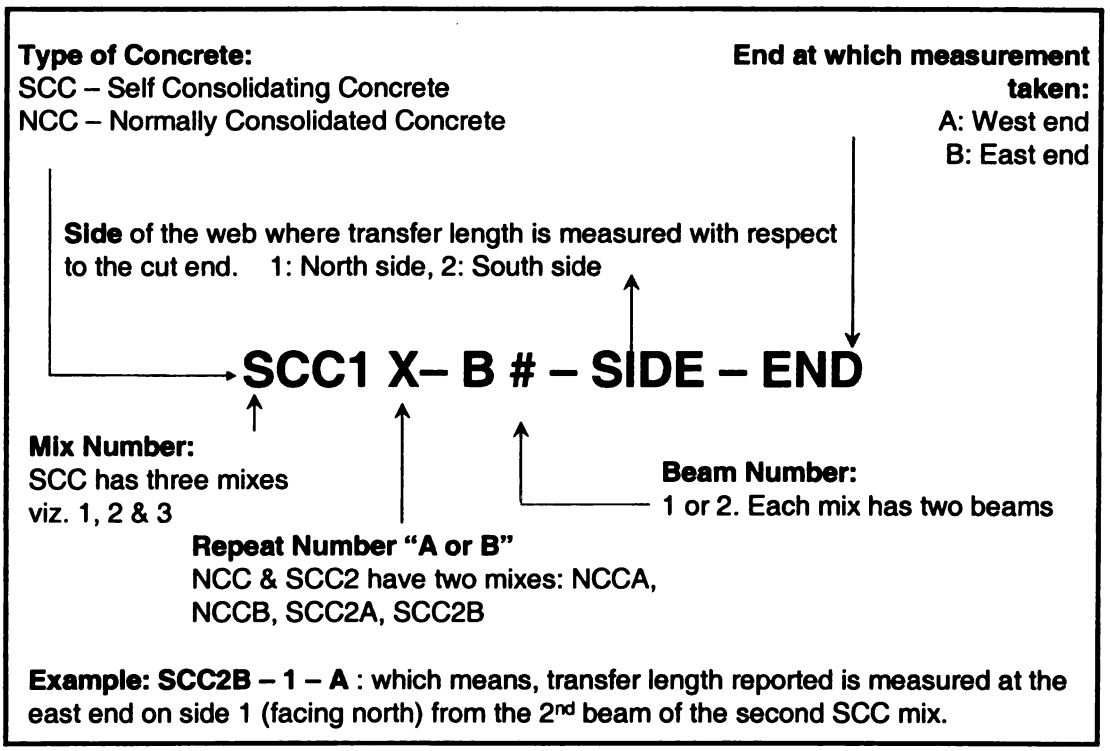

Figure 4-3 Nomenclature for Transfer Length

The nomenclature used for the development length tests was similar to the transfer length nomenclature. The flexural tests to determine the development length were performed on both the ends of the beams. The only difference in the nomenclature for development length is the removal of the "side" term from the nomenclature for

transfer length. Thus, "SCC2B–1–A" refers to the development length test of the first beam of SCC2B mix and the test being performed at beam end A..

4.2 Material Properties

4.2.1 Concrete

Fresh property tests on concrete were performed for every mix before acceptance for use in the beam units. Results on the fresh concrete properties of the SCC mixes are described in Section 3.3. The hardened concrete material properties were determined at various ages of concrete. The target f'_c at 28 days for all mix designs was 48.3 MPa (7000 psi) and was achieved or exceeded by all the mixes. Results of the hardened concrete properties are given in Section 3.5

4.2.2 Prestressing Steel

The pretensioning reinforcement used in the test specimens was 13 mm (0.5 in.) diameter Grade 1860 MPa (270 ksi) low–relaxation seven wire strand. The nominal cross sectional area was 97.870 mm^2 (0.152 in^2). The modulus of elasticity and guaranteed minimum elongation provided by the manufacturer was 196 GPa (28400 ksi) and 0.035 in./in. (3.5%) respectively.

Same strands were to be used for all test beam specimens for all the mix designs. But, due to the bad performance of the first SCC2 mix (SCC2A), the mix design was repeated. Hence, a new set of strands from the same pool, but two months later were obtained. This new set of strand pieces had slight rust on its surface. The rust condition was minor and could be removed if wiped off with a cloth. Nonetheless, in order to avoid disturbing the relative performance of SCC mixes, clean non- rusted strands (Figure 4-4a)

were used for all SCC mix designs and the slightly pitted strand (Figure 4-4b) was used for NCCB beam specimens.

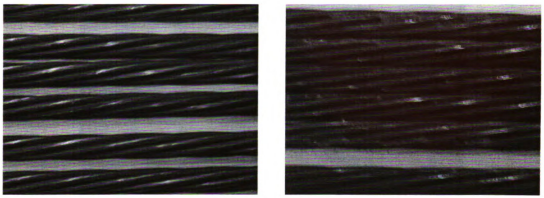

(a) Clean Strand (b) Slightly pitted Strand

Figure 4-4 Strand Condition

4.3 Specimen Fabrication

The beam units were fabricated at Michigan State University's Civil Infrastructure Laboratory. The fabrication process can be grouped into four steps: a) Assembly of formwork, b) prestressing operation, c) placement and curing of concrete, and d) release of prestress. A brief description of the fabrication process is explained as follows:

The formwork assembly with the reinforcement and prestressing tendons placed is shown in Figure 4-5. The strands were then pretensioned by anchoring them to reaction concrete blocks post tensioned to the laboratory strong floor. The strands were pretensioned individually using a hydraulic jack to a level of approximately 75% of the ultimate after anchor-set losses. Electrical resistance strain gages were attached to the strands to monitor the prestress operation and to measure the forces before and after

release of the strands. Figure 4-6 shows the schematic layout of the casting bed and Figure 4-7 shows the prestressing operation carried out for one of the strands.

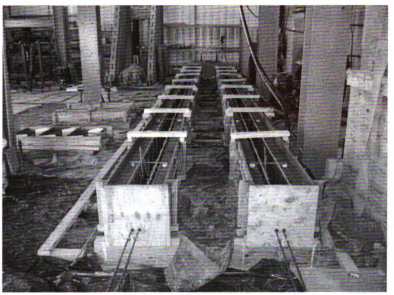

Figure 4-5 Layout of Formwork

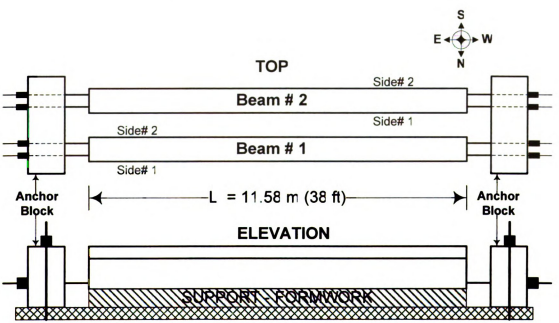

Figure 4-6 Schematic Layout of the casting bed

The concrete was mixed at a ready mix plant and brought to MSU's Civil Infrastructure Laboratory. As discussed in Section 3.4 , the admixtures were added on site

in order to achieve proper SCC behavior. After appropriate fresh property tests and approval from the research team, the concrete was poured into the test specimens. Pull out blocks cast and material testing cylinders were cast in the same operation. After casting the beams were left to cure at room temperature and humidity conditions. The formwork was removed the next day to place instrumentation for transfer length measurements.

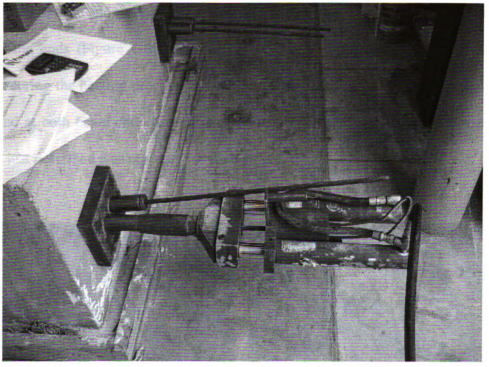

Figure 4-7 Pretensioning of strands

After instrumentation of the test specimens had been completed for the transfer length measurements and the initial measurements taken, the release of prestress was carried out. Prestress release was done by flame cutting on both the ends simultaneously. However, the strands were first gradually heated with a broad flame, until most of the prestressing force was completely transferred by thermal elongation of the strands. The strands were heated over a distance of 305 mm (12 in.) by slowly moving the flame

above and below the strand in gradual strokes. This process was done simultaneously on both ends and was coordinated by a team member. The annealing process was performed for approximately 5 minutes to release as much of the prestress as possible. The release of prestress was also monitored by resistance strain gages attached to one of the wires of the strands. These strain gages were installed during the loading of tendons to measure the amount of stress in the strands. During the heating process, the strain in the strands was verified to drop and reach near zero values. The strands were then cut simultaneously on both the ends (Figure 4-8). In some cases, one of the wires of the strands would fracture during the heating process. In such cases the heating process was terminated and the strand at both beam ends was cut simultaneously immediately after such event. The process just described was repeated for each strand.

Figure 4-8 Release of Prestress – Both ends of the beam being cut simultaneously

CHAPTER 5 STRAND BOND PERFORMANCE EVALUATION

5.1 Introduction

This Chapter deals with the evaluation of strand bond performance with the different concrete mixes in the test program. This evaluation was done by means of simple pull-out tests on unstressed strands. The test description, procedure and results are presented in detail. These tests were performed in series with the transfer length study. Pull out tests were performed at the day of transfer (mostly 3 days) and at 7 days. Results for the SCC mixes are compared to those obtained for the NCC mix.

5.2 Background

The need to have a standardized test to measure the bond performance of prestressing strands lead to the development of various tests such as simple Pull-out tests, and tensioned Pull-out tests. Tests on strand bond confirmation by means of the "Moustafa test" have been recommended by the PCI Interim Guidelines for SCC [30]. Previous research has shown that the bond quality of strands from different manufacturers varied significantly. Hence, a modified version of the Moustafa test, the large block pull out test (LBPT) has been recommended by Logan [25] to qualify strand for prestressing use.

As discussed in Section 2.4.1, the test recommended by the PCI Interim Guidelines for SCC [30], has to be performed in a specific manner to qualify the strand for use in pretensioning purposes. In this research, the pullout test is being performed to study the relative bond performances on different SCC mixes.

5.3 Specimen Preparation

The test procedure used for the pull-out tests was similar to that proposed by Moustafa [41] and Logan [24], 1974. The pull-out block details are shown in Figure 5-1. Each pull-out block contained six non-tensioned prestressing strands, except for the NCCA mix, for which the pull-out block was made with 12 strands. A block was cast for each concrete mix. The prestressing strands used were of the same type as that used in the test beam specimens. The total depth of the block was 610 mm (24 in.). Plastic sleeves of 50 mm (2in.) and 101 mm (4 in.) were provided in the top and bottom of the strands respectively. The prestressing strands had an embedment length of 457mm (18 in.) The strands had a side cover of 115 mm (4.5 in.) and a center to center spacing of 229 mm (9 in.). The total strand length was 1.83 m (6 ft), with approximately 300mm (1 ft) extending below the block and 915 mm (3 ft) extending above the block. The longer end was used as the jacking end to attach the pull-out equipment and instrumentation was done on both the ends of the strands while performing the pull-out test. Nominal reinforcement was provided to the block to prevent any temperature or shrinkage effects on the block. The casting procedure and the concrete used were the same as that used in the test beam specimens. Formwork for the block was removed at the same time as the formwork for the test beams. Figure 5-2 shows the casting of the Pull-out block and Figure 5-3 shows the finished pull-out block with a test in progress. No vibration was used for the SCC mixes, while the NCC mix was conventionally vibrated.

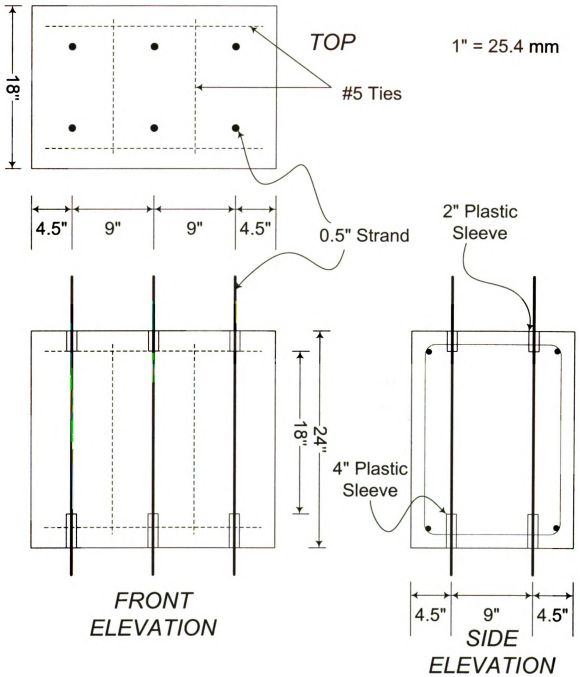

Figure 5-1 Pull-out Block Geometry and Reinforcement

Figure 5-2 Casting of Pull-out Test Block

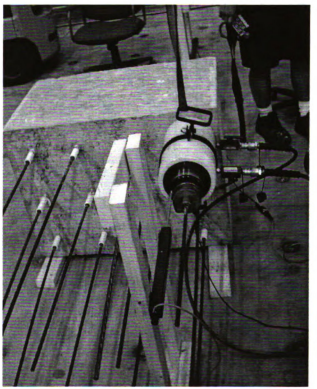

Figure 5-3 Pull-out Test Setup Overview

5.4 Test Procedure

The Pull-out tests were performed at the Civil Infrastructure Laboratory in Michigan State University. The pull-out test were performed after the release of prestress in the test beam specimens. This was done so that the bond strength at the time of transfer in the actual beam specimens could be correlated with the pull-out test data obtained. The test procedure slightly differed from that proposed by Logan [25] (See Section 2.4.1.) The schematic pull-out test setup is shown in Figure 5-4. The actual Pull-out test setup is also shown in Figure 5-5

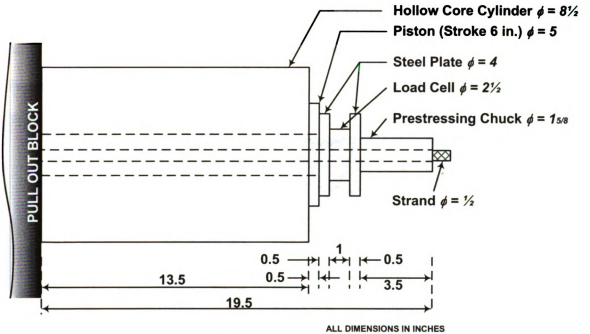

Figure 5-4 Schematic of Pull Out Test Setup

After removal of forms the pull-out block was turned on its side so that both the free and jacking (end from which the strand is pulled) ends of the strand could be easily accessed and instrumented. A hollow core hydraulic cylinder with a capacity of 100 ton

(220 kips) and a ram stroke of 150 mm (6 in.) was used to pull-out the strands. The pull-out test setup was assembled as described next: A hollow core cylinder's piston was brought to zero position (completely intruded), the strand was inserted and the cylinder was attached to the face of the block. A load cell assembly consisting of a center-hole load cell [capacity = 334 kN (75 kips.)] sandwiched between two center-hole steel plates was then placed next to the cylinder ram. A prestressing chuck was then placed over the load cell assembly to anchor the strand against the cylinder piston. During the loading process the piston of the cylinder would extrude thereby pushing the load cell assembly against the chuck. The chuck, in turn would pull the strand out and the corresponding load was measured by the load cell. Two linear potentiometers placed in line with the stand were used to measure the strand movements at both the free and jacking ends (Figure 5-5).

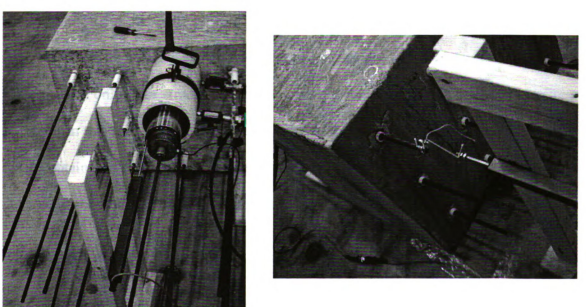

Front Displacement **Back Displacement**

Figure 5-5 Measurement of Displacements – Pull-out Test

The Pull-out rate was calculated from the peak load and the total time taken to complete the test. The loading rate of 90 kN (20 kip) per minute as proposed by Logan [25] could not be achieved with the hydraulic jack used. An average pull-out rate varying from 13 kN (3 kip) to 27 kN (6 kip) per minute was obtained with this jack. As expected, past researchers have noted that slower jacking rates will result in loer pull-out force measurements [31]The time taken to complete the test varied from 3 to 6 minutes. The test was stopped after the peak load was recorded and when there was no significant increase in load corresponding to the increase in the displacements, in other words when excessive slip was observed.

A total of 12 trial tests were performed on strands embedded in the NCCA mix at different concrete ages. As expected, there was an increase in the measured peak pull-out force measured with the increase in age of concrete. Also, there was very little variation observed in the peak pull-out forces of multiple strands tested at the same age of concrete. From the insights gained from these trial tests, the following pull-out-tests were performed on only three strands at concrete ages corresponding to the release of prestress in the beam test specimens. The remaining three strands were tested at 7 days. Also, the results obtained from the individual set of three tests showed very little variation. A detail discussion about the results is presented in the next section.

5.5 Results and Discussion

Peak pull-out forces were recorded for all mix designs from the tests performed at 3 and 7 days. Table 5-1 shows the peak pull-out forces and the standard deviation for all mixes at 3 days. Table 5-2 shows the peak pull-out forces and its standard deviation for all the mixes at 7 days. In the pullout tests performed by Rose and Russell [13] the onset

of general bond slip is defined as the load at a free end slip of 0.005 in. In this project the loads at first slip were determined by examining the measured test force–displacement response data. It was observed that the first slip was noticeable by a pronounced drop in load and increase rate of deformation at both the free and jacking ends. Table 5-3 shows the pull-out forces and the coefficients of variation for all the mixes corresponding to the first slip at 3 days. Table 5-4 shows the pull-out forces and the coefficients of variation for all the mixes corresponding to the first slip at 7 days. The values of the pull-out forces that deviated significantly from the average were neglected and such values are reported as "n/a" in the following tables.

Table 5-1 Maximum (Peak) Pull-out Force – Release (3 days)

Mix	**Maximum Pull-out Force (kips)** 1 kip = 4.448 kN				
Strand #	**1**	**2**	**3**	**Average**	**Deviation**
NCCB	28.66	32.81	29.73	30.40	2.15
SCC1	17.61	14.91	17.30	16.61	1.48
SCC2A	27.06	n/a	24.95	26.01	1.49
SCC2B	18.28	20.92	18.98	19.39	1.37
SCC3	16.30	20.25	23.80	20.12	3.75

Table 5-2 Maximum (Peak) Pull-out Force - 7 days.

Mix	**Maximum Pull-out Force (kips.)** 1 kip = 4.448 kN				
Strand #	**4**	**5**	**6**	**Average**	**SD**
NCCB	n/a	32.23	33.05	32.64	0.58
SCC1	18.03	16.75	n/a	17.39	0.91
SCC2A	37.69	29.45	26.94	31.36	5.62
SCC2B	27.28	25.03	21.60	24.64	2.86
SCC3	28.74	31.85	28.78	29.79	1.78

Table 5-3 Pull Out Forces at First Slip - Release (3 days)

Mix	Pull-out Force (kips.) @ First Slip kN				1 kip = 4.448
Strand #	1	2	3	Average	SD
NCCB	18.83	20.68	19.49	19.67	0.94
SCC1	10.30	7.62	8.74	8.89	1.35
SCC2A	6.46	n/a	6.96	6.71	0.35
SCC2B	7.50	6.94	6.94	7.13	0.32
SCC3	5.35	6.87	8.01	6.74	1.34

Table 5-4 Pull Out forces at first Slip - 7 days.

Mix	Pull-out Force (kips.) @ First Slip kN				1 kip = 4.448
Strand #	1	2	3	Average	SD
NCCB	14.11	15.68	15.01	14.93	0.47
SCC1	9.86	8.85	n/a	9.36	0.71
SCC2A	8.52	7.42	6.04	7.33	1.24
SCC2B	9.05	6.19	6.13	7.12	1.67
SCC3	6.72	6.55	6.57	6.61	0.09

All the pull-out tests displayed a gradual load-slip behavior and no fracture of strand was achieved. It took approximately 4 to7 minutes to complete each test. A typical load-slip response for all the mixes at release and 7 days is shown in Figure 5-6 and Figure 5-7, respectively. A "close-up" of the response at first movement for all the mixes at release and 7 days are shown in Figure 5-8 and Figure 5-9 respectively. The Individual Pull-out Plots for all the strands are given in Appendix 2. The average peak pull-out forces obtained at 7 days were compared with those obtained at release (3 days), and as expected, it was found that the 7 day pull-out forces were slightly higher The smallest increase of approximately around 6% was found for the SCC1 and NCCB mixes, a moderate increase of around 24% was found for the SCC2 mixes and a large increase of around 48% was observed for SCC3 mixes. Figure 5-10 shows the comparison of the peak pull-out forces at release (3days) and 7 days for all mixes.

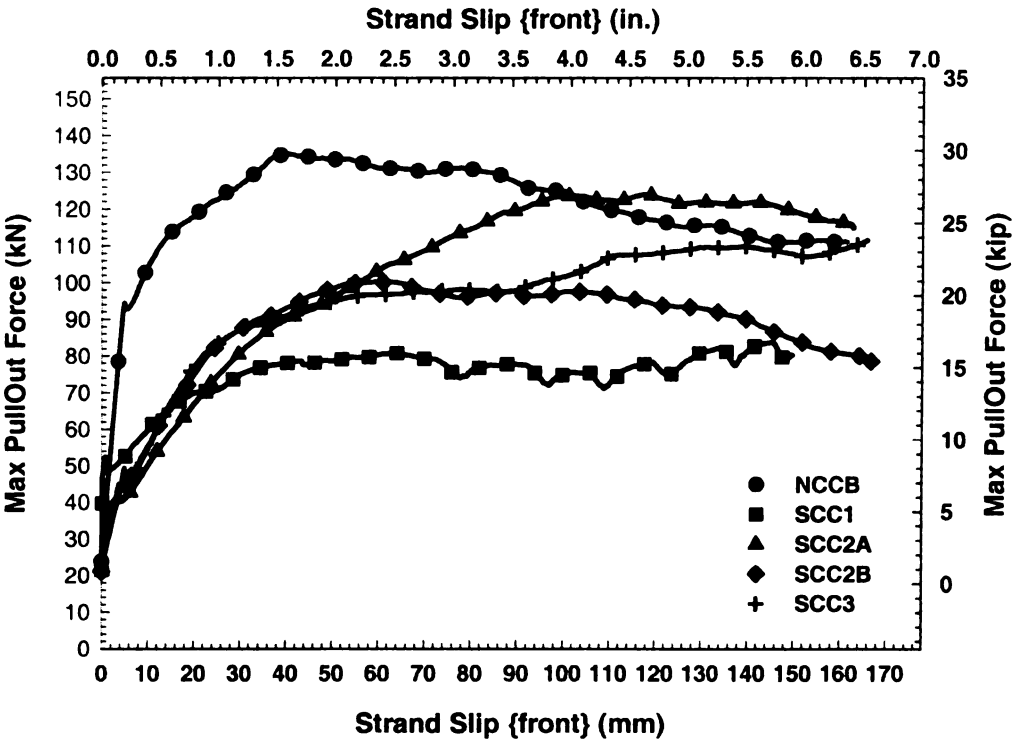

Figure 5-6 Typical Pull-out Test Response - Release

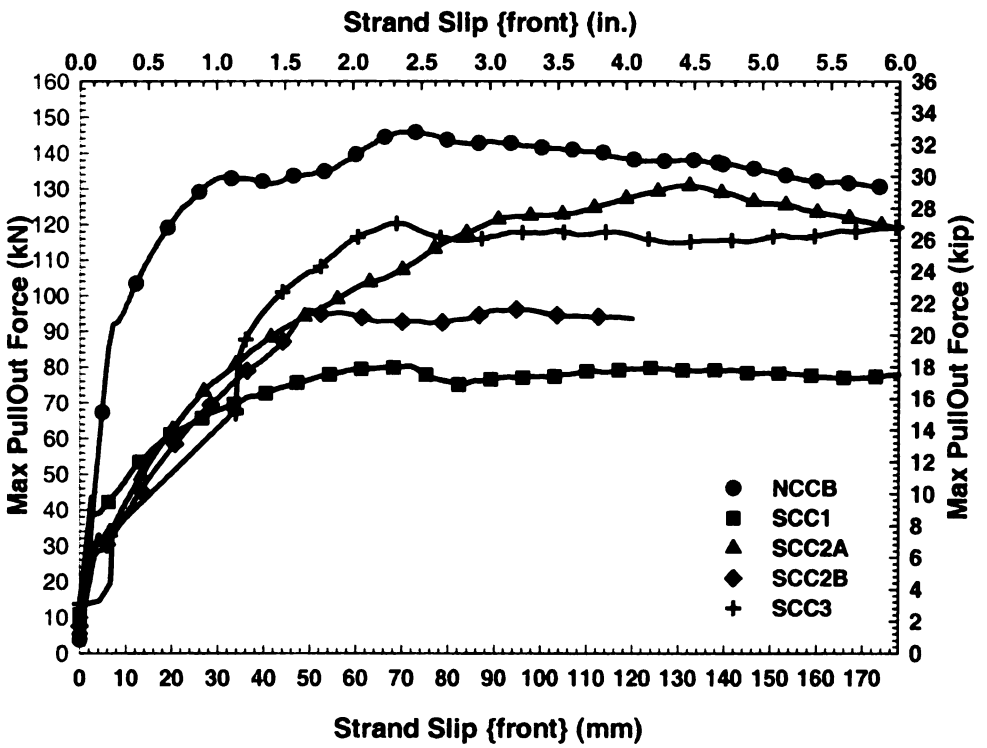

Figure 5-7 Typical Pull-out Test Response at 7 days

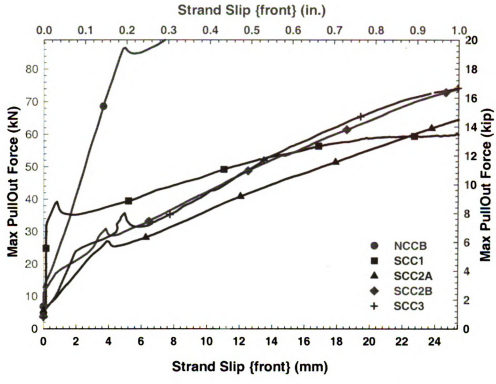

Figure 5-8 "Close-Up" of First slip occurrence - Release (3 days)

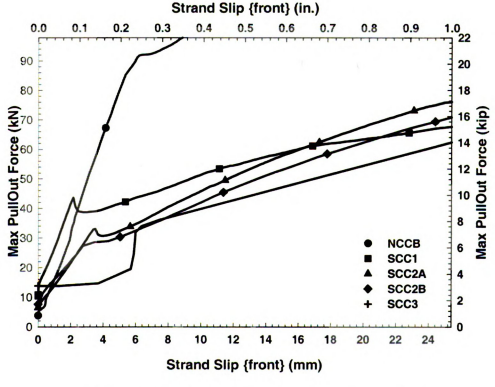

Figure 5-9 "Close-Up" of First slip occurrence 7 days

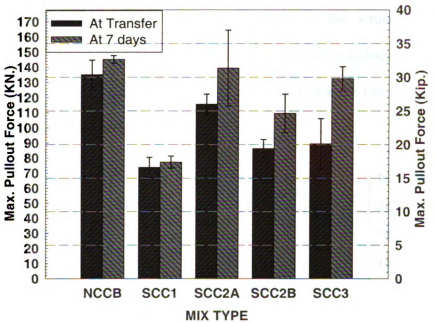

Figure 5-10 Comparison of Peak Pull-out forces

The results of the peak pull-out forces both at release and at 7 days follow the same trend (Figure 5-10). The NCCB mix had the highest average peak pull-out force while SCC1 (high-paste SCC mix), had the lowest. Of the SCC mixes, the highest pull-out force was for SCC3 (high aggregate content mix). SCC2A was a stiff concrete that had to be repeated and its performance was closer to the NCCB mix. Thus, the results support the concept of bounding the response of SCC behavior with the selected mix designs.

As expected, an increase in peak pull-out forces was observed for all mixes for 7 days relative to those at transfer. The same trend was not observed for the first peak loads (Figure 5-11). The first peak loads at 7 days were smaller than the first peak loads at 3 days for the NCCB and SCC3 mixes. This could be due to a variety of reasons as the

bond phenomena is quite complex. The surface conditions of the concrete at 3 days and 7 days could vary and may affect the bond properties of the strand. These surface conditions depend on various factors including the age of concrete, the mix design, admixtures added etc. However, in general, it was found that the first peak load for all SCC mixes was relatively the same.

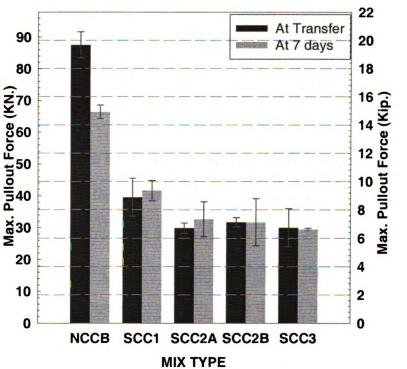

Figure 5-11 Comparison of Pull-out forces at first Slip

The average pull-out forces corresponding to the first slip for all the SCC mixes were found to be relatively the same at both release and at 7 days. Of all the SCC mixes, SCC1 had the highest average first slip pull-out force, approximately 40 kN (8.9 kips) while all others had an average first slip pull-out force of around 30 kN (6.75 kips). The NCCB mix block yielded the highest average first slip loads for both release and 7 days of 67 kN (14.93 kips.) and 88 kN (19.67 kips) respectively.

The average maximum bond strength (U) for all the mixes was obtained from the average peak pull-out forces, given the embedment length, and the surface area of the strand. The following Equation 5-1 shows the calculation of this average maximum bond strength

$$U = \frac{P_{max}}{D_n . L_b} \tag{5-1}$$

where, D_n is the nominal Circumference $= \frac{4}{3} * \pi * d_b$, d_b is the diameter of the prestressing strands [17], and L_b is the embedment length, distance of the strand contributing to bond = 457 mm (18 in.).

The average maximum bond strength was calculated only from the peak pull-out force and not the first slip force. The bond strength calculated from the peak pull-out forces at release for each mix type is reported in Table 5-5. In order to effectively correlate the bond strength for all mix designs, the bond strength value was normalized with respect to concrete compressive strength at the time of test. The variation of bond strength of SCC mixes with respect to the NCC mix was evaluated by observing the relative ratios of the normalized bond strength of the SCC mixes against the NCC mix.

Table 5-5 Average Maximum Bond Strengths from Peak Pull-out Forces

	Peak Load *(kip)*	***Bond strength (U)*** *(psi)*	***Compressive strength (f'c)*** *(psi)*	$U' = \frac{U}{\sqrt{f'_c}}$ $\sqrt{(\text{psi})}$	$\frac{U'_{SCC}}{U'_{NCC}}$
NCCB	30.40	806.39	5545.12	10.83	1.00
SCC1	16.61	440.51	7685.02	5.02	0.46
SCC2A	26.01	689.80	7693.25	7.86	0.73
SCC2B	19.39	514.42	6703.80	6.28	0.58
SCC3	20.12	533.61	6703.80	6.52	0.60

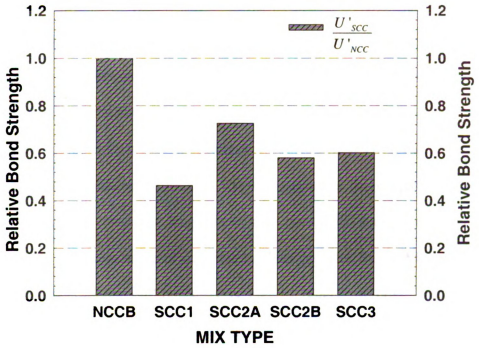

Figure 5-12 Comparison of Relative Bond Strengths

Comparison of the normalized maximum bond strength (Figure 5-12) shows that all SCC mixes had less bond resistance than the NCC mix. The SCC1 mix (high fines) showed the least average bond strength, with approximately 54% less bond resistance than the NCC mix. The SCC3 (high coarse aggregates) mix showed the best performance of all the SCC mixes with a 40% reduction in bond strength relative to NCC. The SCC2A mix being a stiff mix, showed only 27% reduction in bond relative to NCC. However, this test is not being considered as the reliability of the SCC2A mix is in question. A the same time the SCC2B showed a reduction of 42% in bond strength relative to NCC, Hence, the results support the concept of bounnding the response of the SCC mixes with selective mix designs.

5.6 Summary and Conclusions

As discussed earlier bond phenomena depends on different mechanism to transfer the shear stresses between concrete and strand. Bond shear stresses follow complex distributions at member ends and at flexural cracks. Because of all these factors influencing the slip resistance of a prestressing strand in concrete, it is difficult to determine bond lengths by means of simple pull-out tests [23]. Thus, the correspondence between the results obtained from this test and structural design parameters such as transfer length and development length have been questioned for conventional concrete [8][24][31][32] and seem to be of continued debate now for SCC. While the response evaluated through simple pull-out tests is clearly related to bond performance, its correlation to the complex phenomena occurring in the transfer zone region and during development of strand capacity under flexural actions, as previously discussed, is questionable. Nonetheless, pull-out tests are good methods to provide a baseline to qualify the strand bonding characteristics and can serve as a relative performance measure between normally consolidated concrete and the different SCC mixes under evaluation (Figure 5-12).

As presented in Section 2.4.1, simple pullout tests can also serve as a good index tests to qualify strand bond performance. According to Logan's [24] LBPT guidelines, the peak pull-out strength and the first slip load for 13mm (0.5 in.) daimeter strands must be over 160 kN (36 kip) and 71 kN (16 kip), respectively for the strand to be qualified for the desired bond performance. It should be emphasized, however, that these values have been proposed based on precise recommendations for concrete age, mix, and test procedure[24] . As noted earlier with the pull-out tests performed in this research (Figure 5-10 and Figure 5-11), the peak and first slip pull-outs were considerably lower than

these values for both the smooth and slightly rusted strand for all mixes. The lower pull-out forces are attributed to the different concrete mixes (both NCC and SCC) and modifications in the test setup and test procedure.

In order to check the qualification of the strand based on the pull-out tests, the strand samples used in this research were independently tested by Logan [24]. Table 5-6 and shows the results of the pull-out tests on strand specimens used in this research as performed by Logan [24] in full accordance to his LBPT protocol. The "B-control" strand is the benchmark strand used by Logan to compare to other strands. The slightly rusted strand (used in NCCB mix) met the peak pull-out force requirement of 160 kN (36 kip), but did not reach the first slip requirement. The new (i.e clean and shiny) strand (used in all SCC mixes) did not meet the pull-out force requirements prescribed by Logan [24].

Table 5-6 Pull Out Tests Results - Performed by Logan

Strand Type	First Slip Load (kips)	Standard Deviation (kips)	Peak Pull-out Force (kips)	Standard Deviation (kips)
B-Control	22.8	3.37	40.5	2.31
New/Clean	7.9	0.83	31.3	2.91
SR – Slightly rusted	12.9	1.23	37.7	1.43
1 kip= 4.448 kN				

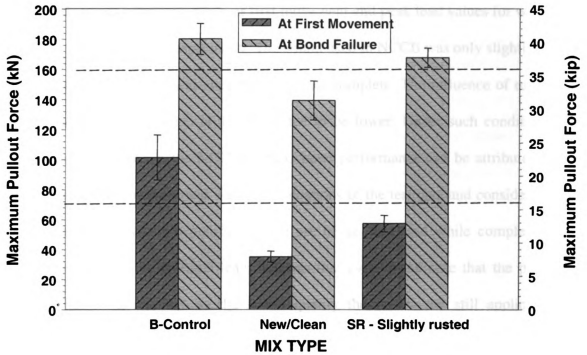

Figure 5-13 Results from LBPT performed by Logan according to [24]

As seen in the results of figure 5-13, the strand used in this research does not seem to qualify the bond quality requirements with respect to the criteria prescribed by Logan [24]. Unfortunately, the LBPT evaluation by Mr.Logan came as an afterthought to the research team upon noticing the low pull-out values and longer development lengths (Chapter 7) observed in this research. The research team did not pursue this qualification tests earlier as they ad no reason to doubt the quality of the strand being used. This new information has obviously raised concerns regarding the validity of the results from this research program as discussed in this chapter and results presented in Chapters 6 and 7 on transfer and development length studies, respectively.

Another factor influencing interpretation of the presented results is the effect of rust in the strand used for the NCCB mix. The surface condition has been recognized as an

important parameter to bond performance. Pull-out tests performed on clean and weathered strands have shown higher first movement and peak load values for weathered strand by 100% and 24% respectively. The strand used in NCCB was only slightly rusted, whereby most of the rust was superficial and not complete. The influence of rust in the testes strand in this program is thus expected to be lower. Under such conditions, the large difference between the NCC and SCC bond performance can be attributed to the concrete mix and not the strand. Further evaluations of the test data and consideration of further testing using a pre-qualified strand are being discussed while completing this work. Nonetheless, the research team believes that even in the case that the presented research has been affected by the strand quality the results are still applicable for assessment of the relative effect of SCC mix proportioning on bond behavior and its relationship to transfer and development length parameters.

Thus, from the results of the pull-out tests it was found that all SCC mixes have less bond strengths relative to NCC. Among the SCC mixes, SCC1 had the least bond strength followed by SCC2 and SCC3 mixes, thereby the behavior of SCC mixes was bound by the concept of selective mix design.

CHAPTER 6 TRANSFER LENGTH EVALUATION

6.1 Introduction

This chapter deals with the evaluation of bond performance of strands in terms of transfer length in precast/prestressed beams. Two different techniques were used to experimentally determine transfer length: (i) measurement of concrete strains along the length of the beam, and (ii) measurement of strand draw-in. Results, observations and discussion are also included in this chapter.

6.2 Test Procedure – Concrete Strains

As previously defined in Section 2.3.1, transfer length is the distance from the end of the beam to the point in the concrete member where the entire stress from the strands is transferred to the concrete member. As discussed before, steel stresses along the beam length increase rapidly from the beam end until becoming constant once equilibrium between concrete and steel stresses is achieved. The strain in the concrete can be thus measured as a means to locate where the strain becomes constant, and hence can be used to measure the transfer length. This section describes the procedure of instrumentation and measurement of transfer length using concrete strains.

6.2.1 Specimen Preparation

The DEMEC (DEtachable MEChanical) strain measurement system (Figure 6-1) was used to measure the strains on the surface of concrete. The DEMEC system consists of a mechanical gauge used in conjunction with small stainless discs (ϕ = 6.3 mm), each with a small hole (ϕ = 1.0 mm) in the center designated to fit the mechanical gage (Figure 6-2.). The stainless discs are glued to the surface of interest at a given spacing over which

the strain needs to be measured. These discs thus define strain measuring points or target points obtained from the change in length between target points (gage length) measured by the mechanical gage.

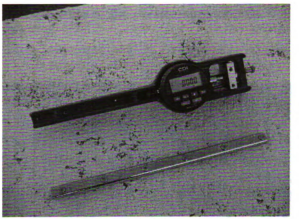

Figure 6-1 Actual Picture of the DEMEC Instrument

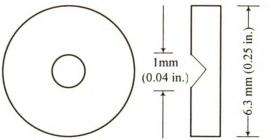

Figure 6-2 Schematic Representation of Target point

For placement of the DEMEC target points the forms were removed after a day (18-24 hours) and the specimen was allowed to dry at ambient conditions to obtain surface dry condition. The strain profile strand centerline was marked. The strand centerline is to be measured along the strand centroid and thus this defines the placements of the target points. The strand centerline was 51mm (2 in.) from the base of the beam (Figure 4-1). The concrete surface was grinded and then cleaned along the prestressing centerline to prepare the surface for bonding of the target points. The target points were attached using a rapid setting adhesive on both sides of the beam. Since the variation of stresses is more pronounced in the transfer zone (end of the beam), the spacing of the target points was 51 mm (2 in) along the expected transfer zone of 1.52 m (60 in.). For the rest of the beam excluding the transfer zones the spacing of the target points was increased to 203 mm (8 in.). In order to measure the strains in the target points close to

the face of the beam, extension brackets were attached as shown in Figure 6-4. The target points were attached to both sides of the beam in order to capture any unbalanced effects from the pair of prestressing tendons. Initial strain readings were taken (Figure 6-3) prior to the release of the prestressing strands.

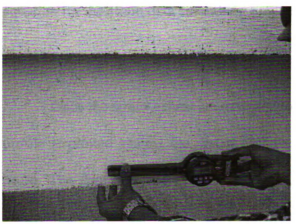

Figure 6-3 Performing measurement with a DEMEC gauge

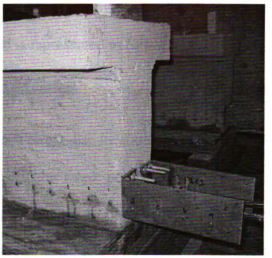

Figure 6-4 Extension Brackets to measure the strains at the ends

6.2.2 Concrete Surface Strain Measurements

Concrete surface strain measurements were taken approximately 4 hours after the release of prestress. Two sets of readings were recorded for each side to increase confidence in the readings. Readings were taken by the same person and care was taken to maintain the same amount of pressure and posture while taking the measurements.

6.2.3 Construction of Surface Compressive Strain Profile

The first step to determine transfer length from concrete strains involves the construction of a concrete surface profile for each end for each side of the beam. The compressive strain for each measured gauge length of 203 mm (8in.) was obtained by dividing the gauge length with the difference in the recorded values of the measurements

taken prior and after the release of prestress. The value obtained from the measurement of two DEMEC points is assigned to the middle of these two points. In the transfer zone, where the spacing of the target points is reduced, these middle values overlap. Hence an average is taken of three consecutive readings and this value is applied to the middle of these three points. This procedure has been termed "smoothing the data" [34]. A general equation for the strain data smoothing procedure is represented as follows:

$$\varepsilon_{i,smooth} = \frac{\varepsilon_{i-1} + \varepsilon_i + \varepsilon_{i+1}}{3} \tag{6-1}$$

Once the strain values are assigned to each target disc location, the concrete strain profile is plotted against the distance of the particular target point from the end of the beam. The data obtained from the DEMEC points tends to have considerable scatter. Smoothing techniques (Figure 6-5) has been shown to lessen the scatter and reduce the effect of data points that have values higher or lower than the average. By smoothing the data it is easier to define the plateau at which the constant strain in the beam is established [36]. A plot comparison of the smoothed and non- smoothed (raw data) is shown in Figure 6-6.

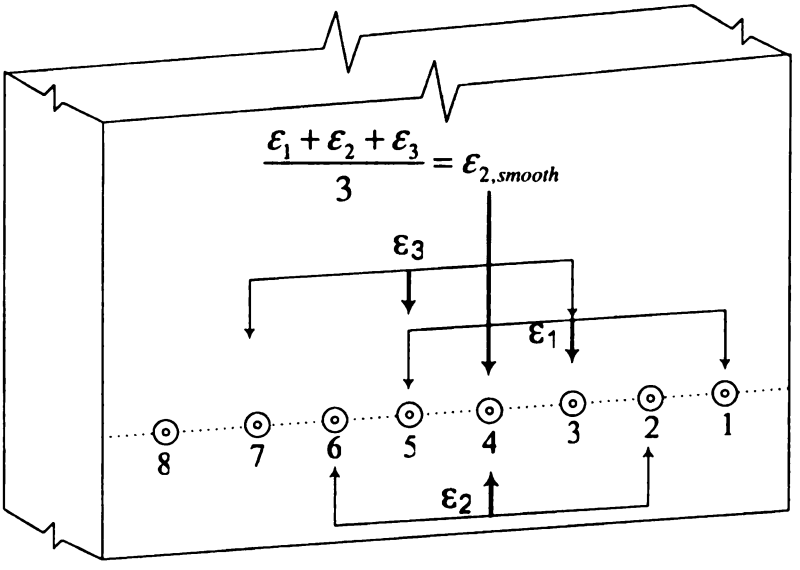

Figure 6-5 Smoothening Of Strain Profile

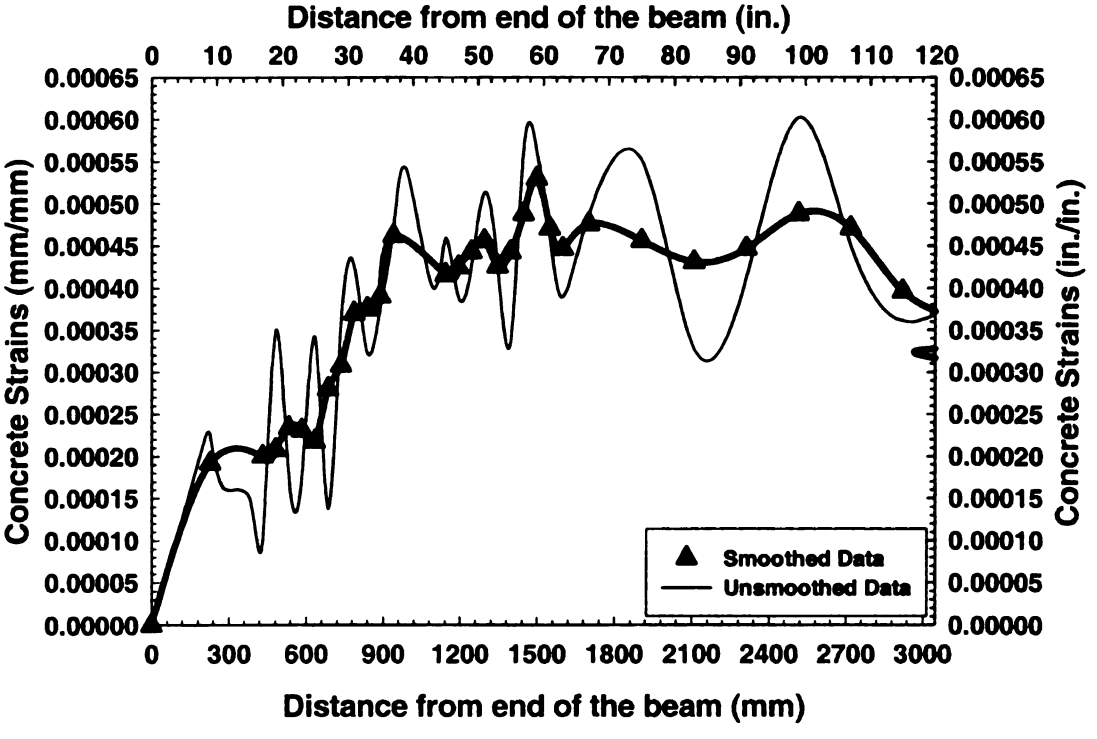

Figure 6-6 Comparison of Smooth and Non- Smooth (RAW) data

6.2.4 Determination of Average Maximum Strain (AMS)

Due to the scatter in the concrete strain profile, a uniform constant strain value in the concrete is difficult to define. Thus a representative value, given by 95% of the average maximum strain (AMS), is commonly used as the effective transfer prestress level. To determine the AMS, strain values in the likely plateau region were visually inspected and then the arithmetic mean of these values was calculated. This method is subjective as it requires visual definition of the plateau region. Care was taken to be consistent in this approach for all the transfer zones.

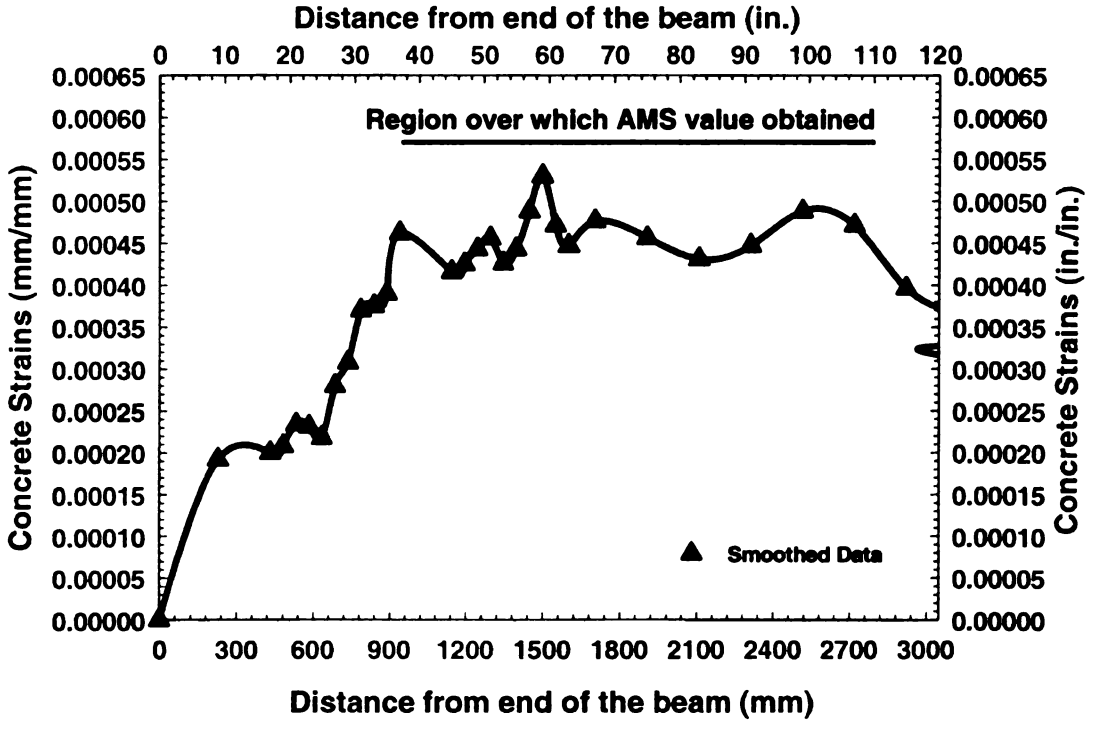

Figure 6-7 Location of AMS values

In this project, the 95% AMS method was used to obtain the transfer length from the concrete strain profiles. This method defines the transfer length as the distance at

which the measured strain profile crosses a horizontal line representing 95% of the AMS value. For this, the smoothed concrete strain profiles were plotted along the length of the beam and a horizontal line representing the 95% AMS value for that particular transfer zone was also plotted. The transfer length was obtained as the value of the distance along the length of the beam where the 95% AMS line intersected the concrete strain profile.

With two beams for each mix and concrete strains measurements taken on both sides of the beam, four transfer zones were evaluated for each beam. Moreover, two trials of readings were taken for each side of the beam. Hence, a total of 8 transfer length values were obtained for each beam. A total of 16 values of transfer lengths were obtained for each mix design. A single plot of concrete strains was obtained for each beam by averaging 8 sets of concrete strains. Also, a single plot of concrete strains was obtained by averaging all the 16 sets of concrete strain measurements, thereby obtaining a single transfer length value for each concrete mix. In this section, plots for each mix (average of 16 values) are shown as follows: (NCCB (Figure 6-8), SCC1 (Figure 6-9), SCC2A (Figure 6-10), SCC2B (Figure 6-11), SCC3 (Figure 6-12)). The plots for each beam (averages of 8 plots) are given in Appendix 3. In order to obtain a single value of transfer length for each mix, selective numerical average of the transfer length values obtained from individual concrete strain profiles of the 16 sets of plots was used. The single concrete strain profile for each mix obtained from the averages of the concrete strains does not represent the actual transfer length for that particular mix, since it may include bad data points which may skew the overall plot. As a result, individual transfer

length values were obtained from the 16 concrete strain plots and the outlier[1] values were not considered in the determination of a single value of the transfer length for a particular mix. Figure 6-8 compares the transfer length values for each mix obtained from the numerical averages of all the 16 set of values and the selective numerical average. Removal of outlier values in the selective averages reduced the standard deviation. It should be noted that for all the mixes, out of the 16 values only 2 to 3 values were outlying the average transfer length values, thereby increasing confidence in the data. Figure 6-13 summarizes the transfer length value for each mix by the method of concrete strain measurements. It can be noted that the obtained transfer length values show a trend, where in the transfer length values of the SCC2 mix seems to be bounded by the results of SCC1 and SCC3 mixes.

[1] An outlier is a data point that is located far from the rest of the data. Given a mean and standard deviation, a statistical distribution expects data points to fall within a specific range. Those values that do not fall in the specific range are called outliers and should be investigated

Table 6-1 Average value of Transfer Length per Mix Type – Concrete Strains

	Transfer Length (inches)		1 in. = 25.4 mm	
	Non – Selective Numerical Averages		Selective Numerical Averages	
Mix Type	Average	Standard Deviation	Average	Standard Deviation
NCCB	20.53	4.25	**19.65**	**2.56**
SCC1	28.82	3.64	**29.81**	**3.25**
SCC2A	30.88	4.07	**27.00**	**4.07**
SCC2B	31.56	5.15	**29.81**	**3.85**
SCC3	30.02	5.54	**30.13**	**3.78**

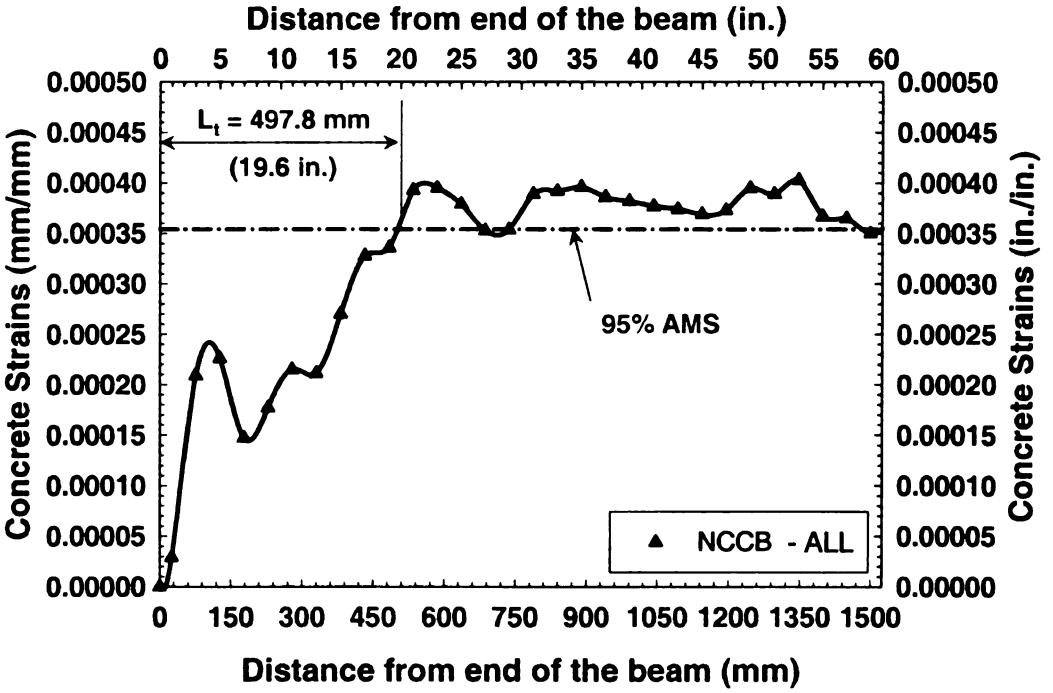

Figure 6-8 Determination of Transfer length from Concrete Strain Profiles – NCCB (Average of all 16 transfer zones)

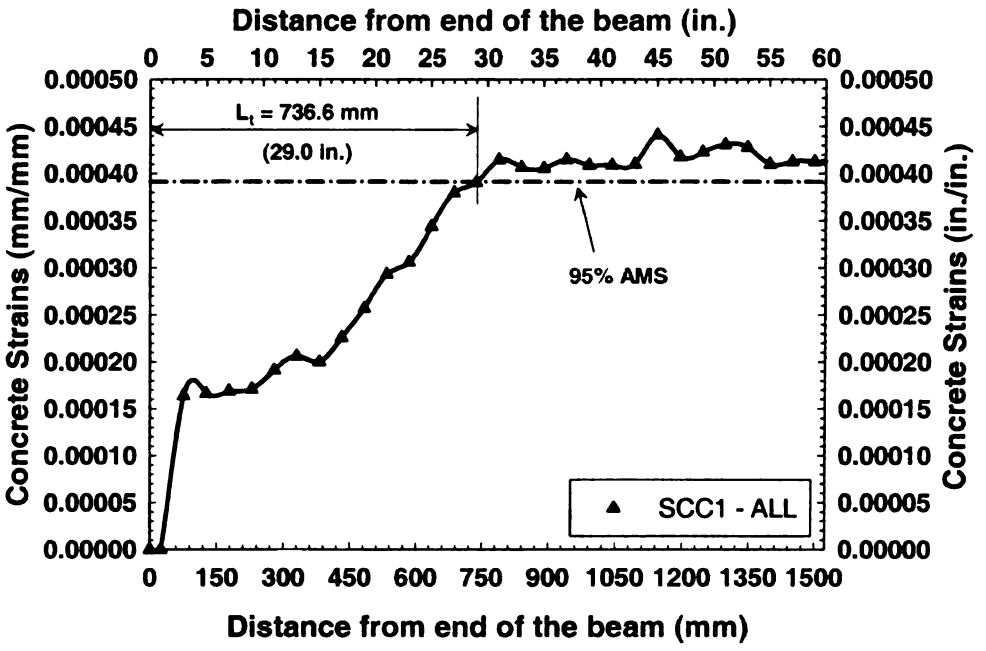

Figure 6-9 Determination of Transfer length from Concrete Strain Profiles – SCC1 (Average of all 16 transfer zones)

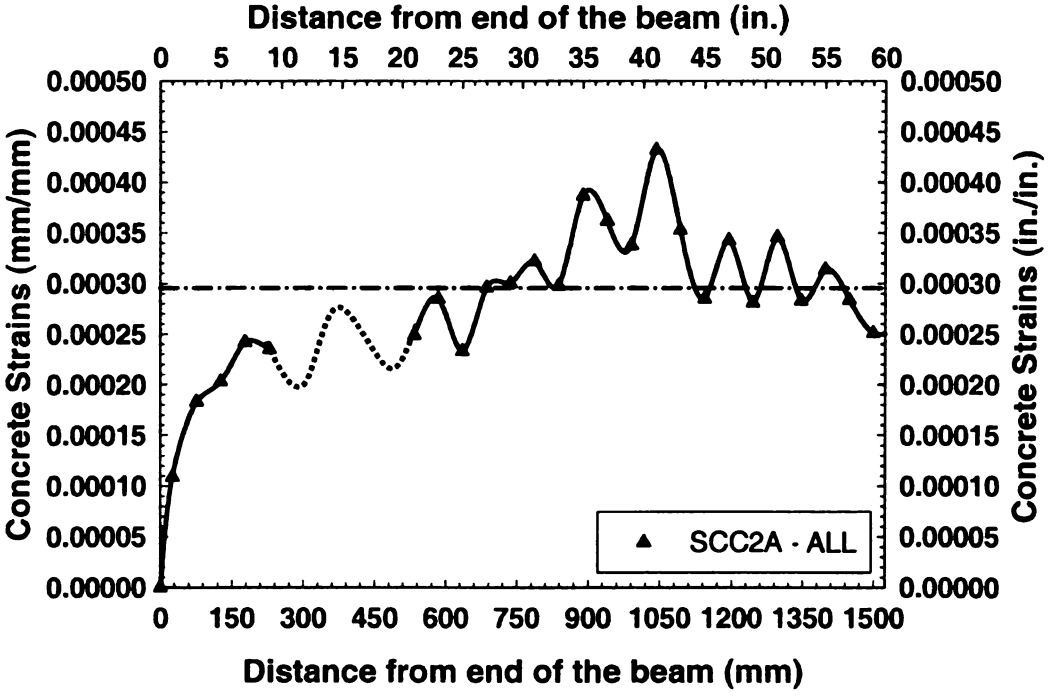

Figure 6-10 Determination of Transfer length from Concrete Strain Profiles – SCC2A (Average of all 16 transfer zones)

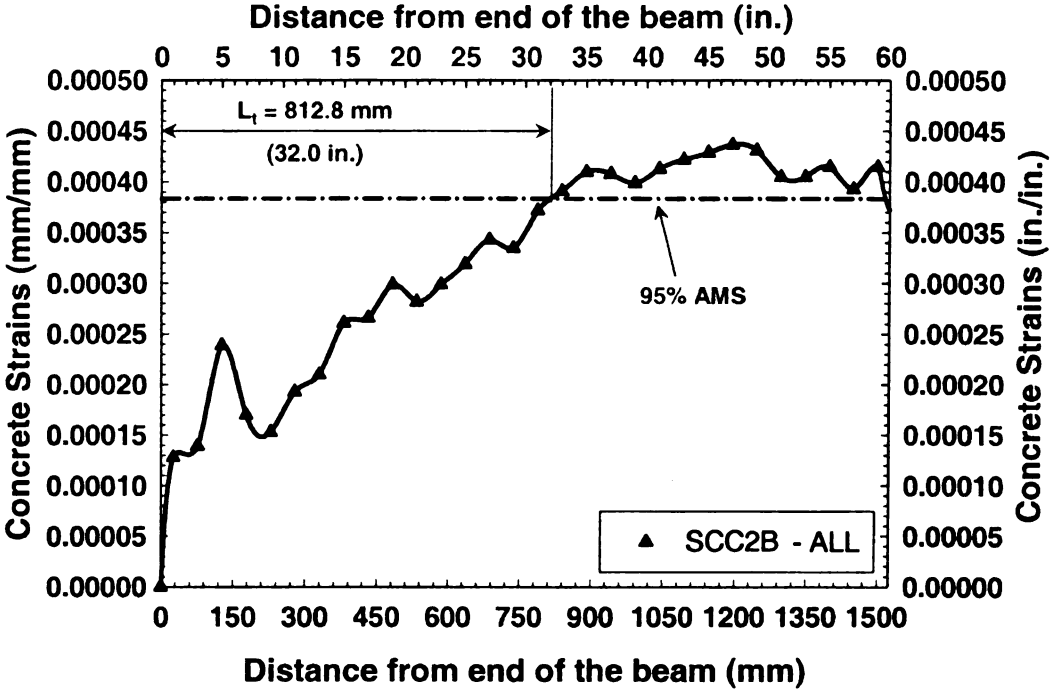

Figure 6-11 Determination of Transfer length from Concrete Strain Profiles – SCC2B (Average of all 16 transfer zones)

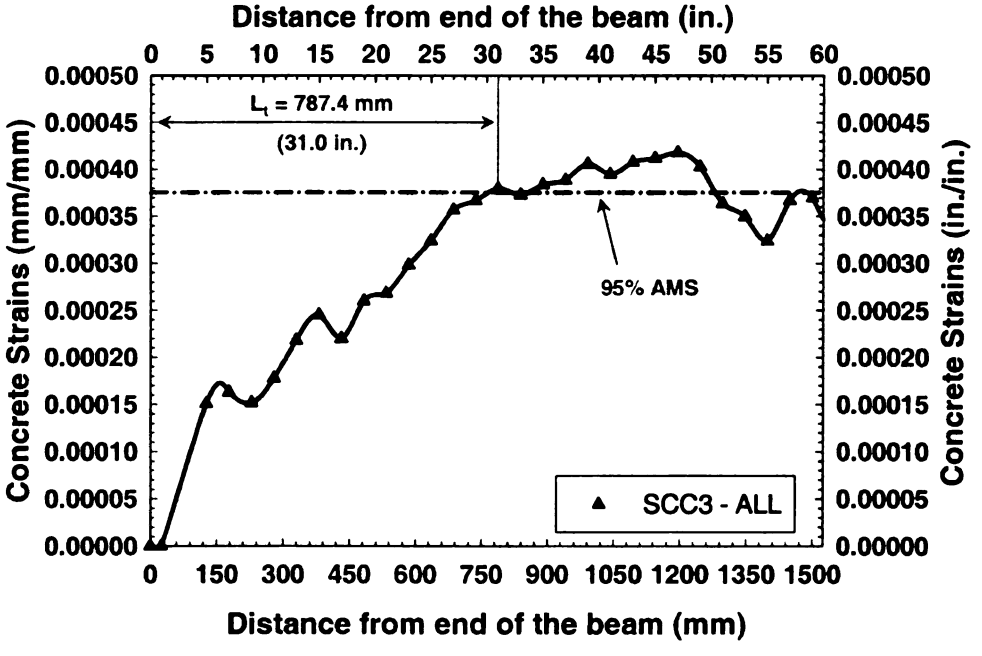

Figure 6-12 Determination of Transfer length from Concrete Strain Profiles – SCC3 (Average of all 16 transfer zones)

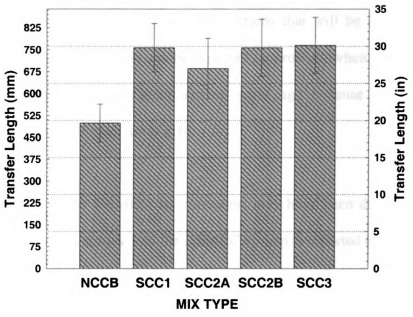

Figure 6-13 Comparison of Transfer Length Values Obtained from Concrete Strains

6.2.5 Precision of Reported Results

The degree of accuracy of the transfer length values obtained by the concrete strain measurement method depends on various factors as follows:

- *Spacing of DEMEC points:* The minimum spacing of the target points was 51mm (2in.), thus assigning a precision less than that value would completely rely on the smoothening process and interpolation.
- *Strain measurements*: The DEMEC readings needed to be taken in hard-to-reach places, which compromised the quality and consistency of the readings.
- *Temperature:* Almost all the DEMEC measurements were made consistently at approximately same ambient temperature, since the casting

of the test specimen and measurements were all done indoors. But it should be noted that temperature fluctuations of the concrete surface between readings will introduce strains that will be incorporated in the measurements. This can be especially a problem when instrumenting high strength concrete specimens at early age because of the very high hydration temperatures [16].

The accuracy of the DEMEC measurements may have been decreased by any of these factors. The overall accuracy of the DEMEC system is reported to be approximately 16 micro strains. [16].

6.3 Strand Draw-In Method

The second method used to determine transfer length of the 13 mm (0.5 in.) prestressing strands was the draw-in method. This method follows from the premise that when prestress is released, the strand at the face of the member is pulled into the concrete member. Draw-in is the measurement of this pulling-in phenomena, hence it is also referred to as "suck-in" or 'free end slip" [7]. In this thesis the term "draw-in" is used to refer to this phenomenon and the term "end slip" is used to refer the strand slip due to external loads. The draw in measurement can be correlated with transfer length as they both involve the bonding of the strand with concrete [36] .

6.3.1 Theoretical Background

The relationship of strand draw-in with the transfer length (L_t) was proposed by Guyon (1953) A simple account of its derivation is provided next. Since there is no

displacement between the steel and the concrete at the end of the transfer length, then the strand draw-in may be calculated as:

$$\Delta_d = \delta_s - \delta_c \qquad (6\text{-}2),$$

where:

Δ_d = Strand Draw in measured at the face of concrete

δ_s = Contraction of steel tendon in the transfer length zone

δ_c = Contraction of concrete in the transfer length zone.

The contractions of the tendon and the concrete resulting from the release of prestress can be obtained by integrating the strains over the transfer length.

$$\delta_s = \int_{L_t} \Delta\varepsilon_s dx$$
$$\delta_c = \int_{L_t} \Delta\varepsilon_c dx \qquad (6\text{-}3)$$

where:

$\Delta\varepsilon_t$ = Change in steel strains resulting from prestress release

$\Delta\varepsilon_t$ = Change in concrete strains resulting from prestress release.

Equation (6-3) can be re-written in the following form:

$$\Delta_d = \int_{L_t} \left(\Delta\varepsilon_s - \Delta\varepsilon_c\right) dx \qquad (6\text{-}4)$$

At the beginning of the transfer zone (in this case, at the face of the beam where bonding of the tendon with the concrete begins.), the change in concrete strains is zero. Hence, the change in steel strain may be calculated as:

$$\Delta\varepsilon_s = \frac{\delta f_s}{E_s} = \frac{f_{si}}{E_s} \qquad (6\text{-}5)$$

where:

δf_s = Change in steel stress resulting from prestress release

f_{si} = Intial Stress in the strand – Jacking strain minus relaxation of Steel

E_s = Modulus of Elasticity of Steel.

At the end of the transfer zone the steel and concrete strains are compatible to each other. The strain remaining in the section after the transfer zone is the effective stress (f_{se}), which is related to the concrete and steel by:

$$\Delta_s = \Delta_c = \frac{\delta f_s}{E_s} = \frac{f_{si} - f_{se}}{E_s} \qquad (6\text{-}6),$$

where:

f_{se} = effective stress immediately after transfer

If the variation of both concrete and steel strains is assumed to be linear along the length of the transfer zone, then equation varies from f_{si} at the initiation of the transfer zone to zero at the termination of the transfer zone. Then, a relationship between the jacking stress, strand draw–in and transfer length can thus be obtained from Equation (6-4) as:

$$\Delta_d = \frac{f_{si}}{\alpha.E_p} L_t \qquad (6\text{-}7).$$

The above equation can be rearranged to obtain transfer lengths from measured strand draw–in as:

$$L_t = \frac{\alpha . E_{ps}}{f_{si}} \Delta_d \qquad (6\text{-}8)$$

where:

α = constant that depends on the load stress distribution ($\alpha = 2$ for constant load stress distribution and $\alpha = 3$ for linear load stress distribution [6]) and

E_{ps} = Modulus of Elasticity of the strand.

In this report, the variation of strains from the beam end is assumed to be lkinear. With this assumption, the value of α is taken as 2 for the determination of transfer length. Equation 5-2 can be written in terms of stress as:

$$L_t = \frac{2 . E_{ps} . \Delta_d}{f_{si}} \qquad (6\text{-}9)$$

6.3.2 Test Procedure

Draw-in measurement involves determining the relative movement of the strand into the concrete member at the end of the beam. In order to avoid irregularities in the concrete surface, a glass target plate was attached with rapid setting glue on the place where the draw-in measurements were to be taken. The draw-in measurements were made using a digital vernier with a precision of 0.00254 mm (0.0001 in.). The draw-in measurements were made possible by mounting reference brackets on to the strands approximately 50 mm (2in.) from the face of the beam. These brackets (U-channels) were attached to the strands with metal clamps. The metal clamps were tightened such that there was no relative motion of the clamp, U channel and the strand. The channel webs

had a cavity in them through which the movable end of the vernier was inserted such that the vernier came in contact with the target glass plate. Since the vernier had to pass through the two cavities in the channel webs, it made it possible for the readings to be taken from approximately the same point of consideration, thus making the measurements more consistent and accurate.

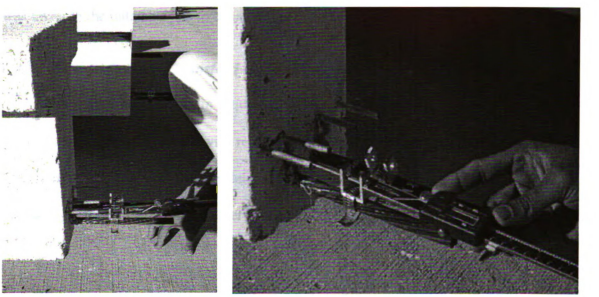

Figure 6-14 Strand Draw-in – Instrumentation and Measurement

It should be noted the strands were flame cut after annealing. However, in some cases, the strands unwound or splayed violently thereby affecting the U–channel mounting. This problem was overcome by tightly attaching three or more metal clamps before the measurement device. In such cases, these metal clamps prevented the effect of the strand unwinding from reaching the measurement device. For most of the test specimens, prestress release was gradual, and without any disturbance to the reference U channels.

The draw–in measurements were taken prior and after release (~4 hours later), and then at 7, 14, 28 days and finally at the day of flexural test (Chapter7). The beams had to

be moved from the casting bed to the storage yard and brought back from the yard to the test setup for flexural test (Chapter7). In some cases, during this process, the glass target plates for draw-in measurements were damaged. In such cases, new glass target plates were attached at the same location in the best possible way and draw-in measurements were carried out. Effect on accuracy from these instances is difficult to estimate but care was taken in the data analysis to consider the possibility of error sources such as this one.

6.3.3 Determination Of Transfer Length - Draw-In Value

The draw-in value (Δ_d in Equation 6-7) was obtained as the difference of the readings taken prior to release with respect to all future readings. This value was used in Equation 5-3 to obtain the transfer length at various ages of concrete. Figure 6-15 shows the average draw-in values at transfer for each of the mix types.

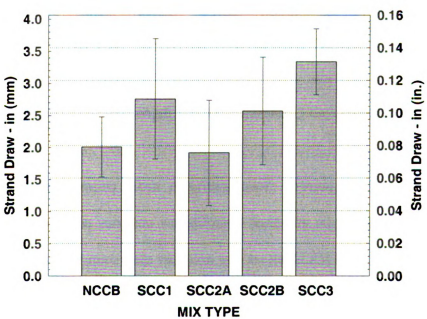

Figure 6-15 Average Draw–in Values at Transfer (3 days) for all mixes

Although the stress in the strands was almost the same for all strands and for all of test mix designs, the stress values for each of the test specimens was used to obtain the transfer length for each mix. Figure 6-16 shows the average transfer length values obtained at transfer for each of the mixes from the draw–in values.

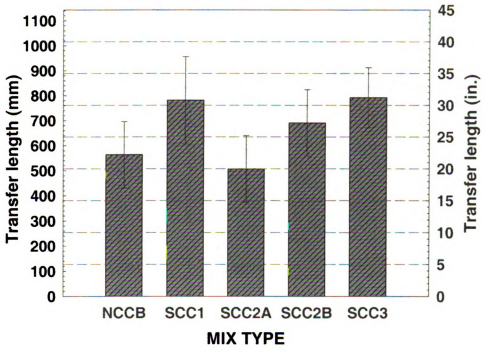

Figure 6-16 Average Transfer Length Values at transfer (3 days) obtained from Draw-in

Draw-in measurements taken at several times showed that the draw-in values increased with time. This variation was different for every mix. The least variation was for the NCC mix and the maximum variation was for the SCC1 (high fines) mix.

Table 6-2 shows the variation of draw–in and the corresponding transfer length values for various mixes at different ages of concrete. The day of test (DOT) reading for

the SCC2A mix was not taken due to some miscommunication between the team members and hence the corresponding values in Table 5-2 is shown as "n/a."

Table 6-2 Draw–in and Transfer Length Values at Various Concrete Ages

Age of Concrete (days)	Strand Draw – in (inches)		Transfer Length (inches)	
	Average	Standard Deviation	Average	Standard Deviation
		NCCB		
At transfer *	**0.0791**	**0.0185**	**22.22**	**5.20**
7	0.0934	0.0244	26.22	6.85
14	0.1063	0.0187	29.85	5.24
28	0.1100	0.0186	30.90	5.23
134.5	0.1236	0.0169	34.72	4.74
		SCC1		
At transfer	**0.1086**	**0.0370**	**30.79**	**10.48**
7	0.1100	0.0342	31.18	9.70
14	0.1155	0.0477	32.76	13.53
28	0.1210	0.0441	34.32	12.51
126	0.1992	0.0572	56.49	16.22
		SCC2-A		
At transfer	**0.0754**	**0.0324**	**19.97**	**8.58**
7	0.1022	0.0198	27.06	5.24
14	0.1105	0.0226	29.26	5.97
28	0.1239	0.0296	32.80	7.85
DOT	n/a	n/a	n/a	n/a
		SCC2-B		
At transfer	**0.1012**	**0.0330**	**27.21**	**8.88**
7	0.1177	0.0212	31.66	5.69
14	0.1228	0.0068	33.02	1.83
28	0.1301	0.0034	35.01	0.90
126	0.1962	0.0166	52.78	4.47
		SCC3		
At transfer	**0.1314**	**0.0202**	**31.19**	**4.80**
7	0.1364	0.0171	32.37	4.05
14	0.1430	0.0102	33.93	2.43
28	0.1551	0.0156	36.79	3.70
129.5	0.2109	0.0479	50.04	11.36
* For all beams, release was 3 days after cast				1 in. = 25.4 mm

The variation of draw-in measurements with time is shown in Figure 6-17. The NCCB beams showed a very gradual and small variation with time, while all the SCC mixes showed significant increase. The NCCB beam showed an increase of 56% more transfer length relative to the value at release where as SCC1, SCC2B and SCC3 showed an increase of 83%, 94% and 60% respectively. Draw-in measurements for SCC2A were not taken at the day of test.

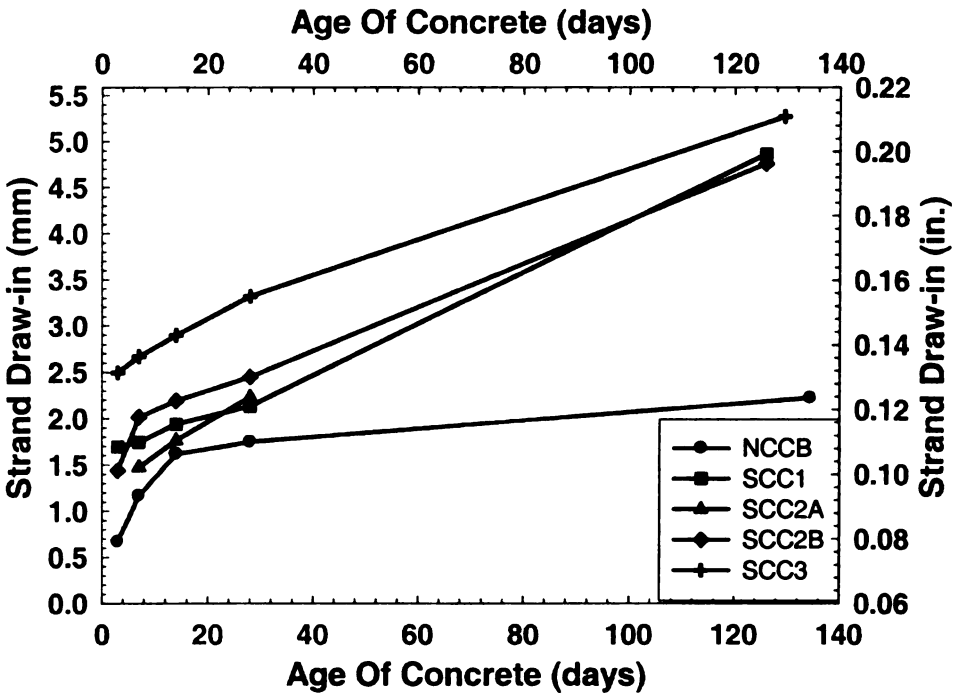

Figure 6-17 Variation of Strand Draw-in with time

6.4 Results and Discussion

Transfer length values obtained from the concrete strains and draw-in measurements are discussed in this section. Transfer length was also calculated from the ACI 318 / AASHTO recommendations [3] (Equation 2-6) and the results are compared in Table 6-3 .

Table 6-3 Transfer Length values from ACI 318 / AASHTO equation

Mix	Transfer length (f_{se} / 3)d_b (inches)
NCCB	28.74
SCC1	28.60
SCC2A	30.67
SCC2B	30.13
SCC3	34.09
	1 in. = 25.4 mm

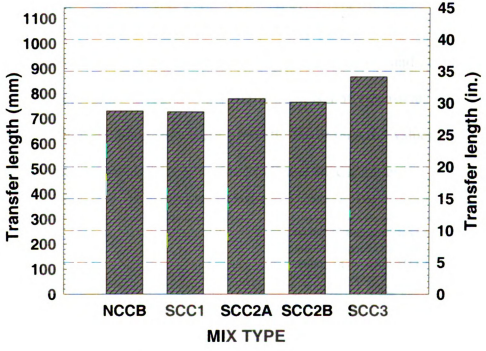

Figure 6-18 Transfer Length – ACI Code – All Mixes [3]

Figure 6-19 shows the overall comparison of the measured average transfer length values with the values obtained from the ACI code [3]. Both of the measurement methods (concrete strains and draw-in) show consistent trend in the obtained transfer length values. The transfer length value of the SCC2 mix is bounded by the SCC1 and SCC3 mixes. When compared with the predicted values from the ACI equation (Table 6-4), it

can be seen that all of the measured values are less than code estimate except for the SCC1 (high fines) mix. Thus the ACI equation appears to be applicable and conservative with respect to all transfer length for all mixes except SCC1 mix.

Table 6-4 Comparison of Measured and ACI transfer lengths

Mix	$(L_{t\,meas} / L_{t\text{-}ACI})$
NCCB	0.86
SCC1	1.02
SCC2A	0.82
SCC2B	0.90
SCC3	0.91

The transfer length values obtained from draw-in and concrete strain measurements had some variation. This variation was not consistent, transfer length values from draw-in measurements were generally lower than the values obtained from concrete strain measurements, except for the SCC1 and NCCB mixes.

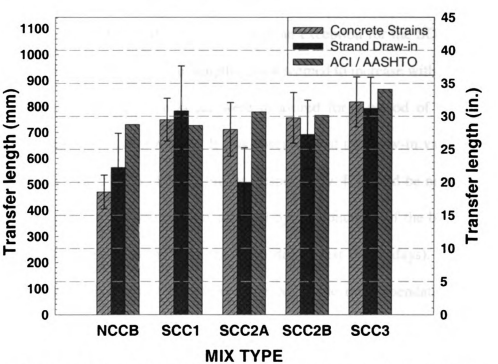

Figure 6-19 Comparison of Measured Transfer Length with ACI Equation

The average of transfer length values obtained form both the experimentally methods were compared with the ACI equation for all the mixes. A ratio of measured transfer length ($L_{t\ meas}$) with transfer length predicted by ACI equation ($L_{t\text{-}ACI}$) was found. Table 6-4 shows this ratio ($L_{t\ meas} / L_{t\text{-}ACI}$) for all the mixes. The table results show that the ACI code recommendation is conservative in determining the transfer lengths except for SCC1, which is under predicted by 2%.

6.5 Summary and Conclusions

Transfer lengths were experimentally found for a total of 12 beams (24 ends) of different concrete mixes. Initial transfer length was determined by concrete strain profiles and draw-in measurements. Long term transfer lengths were determined only with the draw- in values.

The overall average transfer length values at release were found to be less than those predicted by the ACI code provisions, with an exception for the SCC1 mix which was under predicted by 2%. Transfer length values seemed to increase with time based on draw-in measurements. Draw-in values were measured for a period of approximately 120-130 days from the date of release. It was observed that the draw-in values increased from 50% - 100% for NCCB to SCC1 mixes, respectively. It should be noted, however, that in many cases, the last reading was affected by the condition of the beam end. This decreases the confidences on the readings at the day of test (~130 days). In spite of the insight gained from this part of the project, the ACI code recommendations cannot be completely validated for SCC because of the limited scope of this project.

6.6 Recommendations

The determination of transfer length by draw-in measurement has been supported as well as questioned in previous research. Draw-in measurements give only the transfer length value directly and the stress variation along the length of the member cannot be obtained as in the case of concrete strain measurements. However, draw-in measurements are much simpler and less time consuming. In addition, the instrumentation is also quite simple thus cost efficient. This technique is also more practical for the prestress concrete industry as, it can be easily performed and tracked in the field. This is particularly advantageous when long term transfer length need to be determined since concrete strain profiles may not be practically feasible.

However, in order to make draw-in measurements acceptable to the prestress industry, a detailed statistical study should be performed considering as many factors like: type of release, strand condition, concrete type and concrete time dependent effects.

CHAPTER 7 DEVELOPMENT LENGTH TEST PROGRAM

Evaluation of strand bond on SCC precast/prestressed girders with respect to development length was made through flexural load tests on laboratory scale beams. The beam units are those described in Section 4.1 and shown diagramatically in Figure 4-1. As previously mentioned, two beams for each of the project concrete mix designs (see Table 3-2) were built. The beams were 11.58 m (38 ft) in length such that two tests (one per beam end) were conducted per beam unit. Thus, a total of 4 flexural tests for each concrete mix were performed. This chapter provides details on testing configuration, procedure, observations and results.

7.1 Test Approach

As discussed in section 2.4.2, development length is defined as the total length of bond required to develop the steel stress f_{ps} at the ultimate strength of the member. Development length consists of two components: transfer length and flexural bond length. Determination of transfer length is described in Chapter 6. It is not possible to evaluate flexural bond length separately and hence the total development length was determined from flexural tests. From these tests and the known transfer length values, the flexural bond length can hence be calculated.

By definition, the development length of a prestressing strand will depend on achievement of its design stress level at the section flexural capacity. Section capacity depends on several factors, which makes development length measurements, or estimates, difficult to determine in a single test. Thus, a trial and error or bounding approach has been typically used [14] and was hence also used in this project. The

distance from the end of the member to the critical section is defined as the embedment length (L_e). In this project, since the strands are completely bonded throughout the length of the beam, development length is the minimum embedment length required to develop nominal stresses at the critical section. The critical section can be defined as the section closest to the end of the member that develops full strength when subjected to external loading.

The testing approach thus consists in determining the minimum distance from the beam end that will allow attainment of the strand design stress level at the section nominal flexural capacity. The process is thus iterative, where the resulting failure mode (flexure, flexure–slip, or shear) defines whether the evaluated embedment length was sufficient. If the test response reveals that the ultimate moment at the critical section was equal or greater than the nominal capacity, then the next evaluated embedment length was reduced. Conversely, if the moment nominal capacity was not reached, then the embedment or development length to the critical section was increased. With beams long enough for two tests at each end and to beams per concrete mix, the current project could afford four trials. In this way, the range within which the actual development length may lie for the particular mix can be obtained.

7.2 Test Configuration

The flexural test setups consisted of a simple span beam loaded under a pair of concentrated loads at the critical section and a cantilever overhang that was unaffected by the test. A schematic of the test setup is shown in Figure 7-1. For most of the tests, the beam was supported over a span of 7.32 m (24 ft) leaving a cantilevered length of 4.27 m (14 ft). In the first few tests (NCCA and SCC2A), the span length was kept as a variable

and the support blocks were not moved. In all other tests (SCC1, SCC2B, SCC3 and NCCB), the span kept made constant at 24 feet. The beam was supported on two neoprene pads of dimensions 150 x 305 x 19 mm (6.125" x 12" x ¾") on each support. Loading was applied by means of a servo controlled hydraulic actuator mounted on a reaction frame. The actuator load was transferred to the girder through a loading beam with two contact points in order to create a constant moment demand region. Since the development length testing requires that the embedment length be varied from test to test, the support blocks were moved to get the required embedment length. Figure 7-2 shows the overall test setup at the MSU Civil Infrastructure laboratory with some of the components of the test setup labeled.

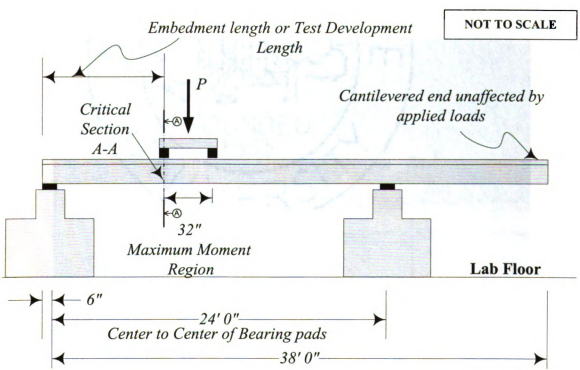

Figure 7-1 Schematic Representation of Flexural Test

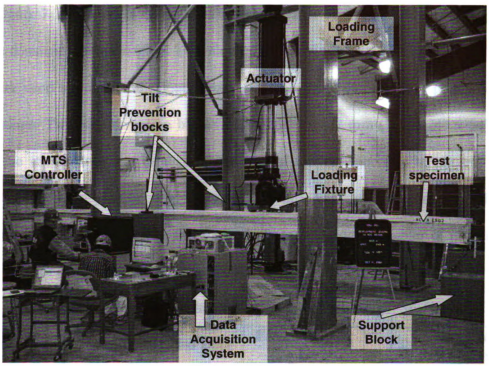

Figure 7-2 Overview of the Flexural Test Setup

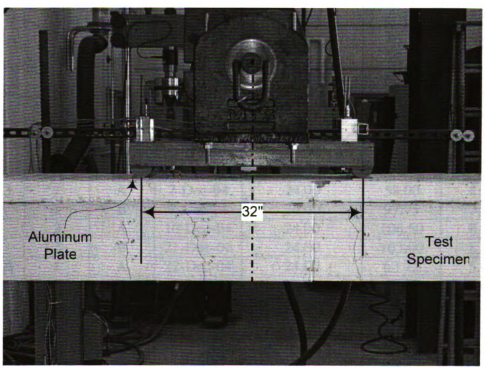

Figure 7-3 Test setup – View of Spreader Beam

Figure 7-3 shows a close-up view of the spreader beam attached to the actuator to create a constant moment region. Two aluminum plates of 305 x 76 x 6.4 mm (12" x 3"x ¼") were used to transfer the loads from the spreading beam loading points onto the beam flange. Two tilt prevention blocks 457 x 610 x 1372 mm (18" x 24" x 54") were tied to the strong floor and used on either side of the test specimen to prevent for the event that the beam may become unstable. The different test configurations: effective span, embedment length (L_{dtest}) , the shear span (considering the center of the support), the test date for all the mixes are given in Table 7-1 for the 24 tests performed.

Table 7-1 Test Configurations for Development Length Studies

Mix	Unit	End	Test Date	Effective span L	L_{dtest}	Shear Span, a
1 in. = 25.4 mm				(ft)	(in)	(ft)
NCCa	1	A	6-Oct-04	23.83	76.00	6.08
	1	B	11-Oct-04	27.67	122.70	9.98
	2	A	14-Oct-04	26.67	111.00	9.00
	2	B	20-Oct-04	24.25	60.00	4.75
SCC2A	1	A	30-Oct-04	23.50	70.50	5.63
	1	B	3-Nov-04	23.50	64.50	5.13
	2	A	9-Nov-04	23.50	80.00	6.42
	2	B	16-Nov-04	23.50	86.75	6.98
SCC2B	1	A	17-Nov-04	24.00	70.50	5.63
	1	B	19-Nov-04	24.00	102.75	8.31
	2	A	23-Nov-04	24.00	126.75	10.31
	2	B	30-Nov-04	24.00	124.50	10.13
SCC3	1	A	2-Dec-04	24.00	58.00	4.58
	1	B	7-Dec-04	24.00	97.75	7.90
	2	A	10-Dec-04	24.00	106.50	8.63
	2	B	21-Dec-04	24.00	103.00	8.33
NCCB	1	A	22-Dec-04	24.00	63.75	5.06
	1	B	25-Dec-04	24.00	64.00	5.08
	2	A	29-Dec-04	24.00	103.50	8.38
	2	B	30-Dec-04	24.00	93.50	7.54
SCC1	1	A	4-Jan-05	24.00	72.38	5.78
	1	B	5-Jan-05	24.00	133.75	10.90
	2	A	4-Jan-05	24.00	122.00	9.92
	2	B	4-Jan-05	24.00	118.50	9.63

7.3 Analysis of Section at Ultimate – Nominal Capacity

The analysis of the section for its ultimate strength is necessary to determine the nominal moment resisting capacity of the section. The cross-section dimensions, material properties, amount of reinforcement and the amount of prestress force in the strands must be known to calculate the moment at ultimate. The ultimate strength of the section is achieved outside the linear range of the behavior (load–deflection) of the prestressed section. Actual analysis of this response is quite cumbersome and may not be feasible in daily design practice. Simplifications have been made by most code provisions which allow a fast but sufficiently accurate evaluation of the nominal capacity of the section [4]. The following assumptions are made by the ACI code recommendations (Figure 7-4) [4]:

1. Plane sections remain plane before and after loading; strain distribution is linear
2. Perfect bond exists between steel and concrete
3. The limiting compressive strain of concrete is 0.003 for all cross-sections, types of concrete and amount of reinforcement.
4. Tensile strength of concrete is neglected.
5. The total force in the concrete compressive zone can be approximated by considering a uniform stress of magnitude $0.85f'_c$ over a rectangular block (Whitney's block) of width b and depth $a=\beta_1 c$, where c represents the depth of the neutral axis and β_1 (Equation 7-1) depends on the compressive strength of concrete as:

$$\begin{aligned} &\beta_1 = 0.85 \text{ for } f'c \le 4000 psi \\ &\beta_1 = 0.65 \text{ for } f'c \ge 8000 psi \\ &\beta_1 = 0.85 - 5x10^{-5}(f'c - 4000) \text{ for } f'c \le 4000 \le 8000 psi \end{aligned} \qquad (7\text{-}1)$$

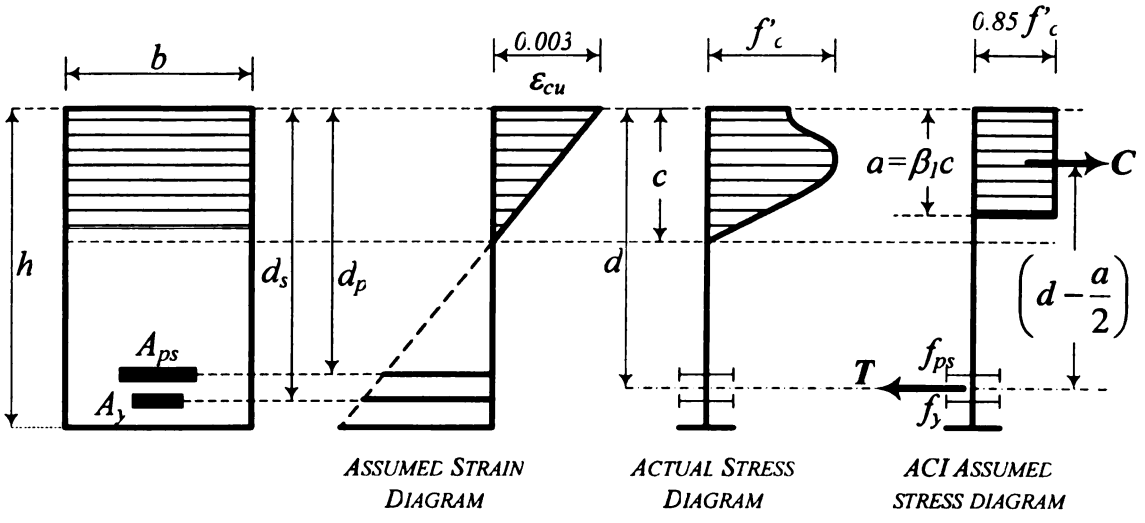

Figure 7-4 ACI-318 code Assumed Stress – Strain Distribution [4]

Calculation of the nominal capacity of a prestressed section according to the ACI method involves the assumption of the Whitney's rectangular stress block. In order to satisfy the horizontal equilibrium of the section, the resultant tensile (T) and compressive forces must balance each other. The nominal moment capacity (M_n) is obtained from the couple created by the resultant tensile (T) and compressive (C) forces, then thus giving:

$$M_n = 0.85 f'_c ba\left(d - \frac{a}{2}\right), \tag{7-2}$$

where, d is the distance from the extreme compression fiber to the centroid of the tensile force. If the section includes any passive compressive reinforcement, the contribution of such reinforcement must be included in the total compressive force. The centroid (d) of the tensile reinforcement can be estimated accurately from the locations, area and yield strengths of the prestressing tendons (d_p, A_{ps}) and passive reinforcement (d_s, A_s):

$$d = \frac{A_{ps} f_{ps} d_p + A_s f_y d_s}{A_{ps} f_{ps} + A_s f_y} \tag{7-3}$$

The ACI-318 code provides a simplified approach to determine the value of stress in the strand at the nominal capacity of the member (f_{ps}) if the effective stress (f_{se}) is not less than 0.5 times the ultimate strength of the tendon (f_{pu}) to be given by:

$$f_{ps} = f_{pu}\left[1-\frac{\gamma_p}{\beta_1}\left[\rho_p\frac{f_{pu}}{f'_c}+\frac{d}{d_p}(\omega-\omega')\right]\right], \qquad (7\text{-}4)$$

where:

γ_p = factor for type of prestressing steel
= 0.55 for f_{py}/f_{pu} not less than 0.80
= 0.40 for f_{py}/f_{pu} not less than 0.85
= 0.28 for f_{py}/f_{pu} not less than 0.90

f_{py} = specified yield strength of prestressing steel (psi).

ρ_p = ratio of prestressed reinforcement = A_{ps}/bd_p

d_p = distance from extreme compression fiber to centroid of prestressed reinforcement

ω, ω' = reinforcement indices, $\omega = \rho f_y / f_c'$ & $\omega' = \rho' f_y / f_c'$

ρ' = ratio of compression reinforcement = A_s/bd

Clearly, the nominal capacity can also be calculated from the resultant tensile forces:

$$M_n = \left(A_{ps}f_{ps} + A_s f_y\right)\left(d-\frac{a}{2}\right). \qquad (7\text{-}5)$$

Calculation of the nominal capacity by the ACI-318 code as discussed above is a simplified method. A more accurate analysis involves the use of the actual stress distributions in the section by considering strain compatibility and realistic material constitutive models. In this approach, the strain distribution in the section is still assumed to be linear. (plane sections remain plane). However, no assumptions for f_{ps} are made.

Rather, at every point of loading equilibrium between resultant compressive and tensile forces is checked and f_{ps} is calculated accordingly.

In this project, the nominal capacity was calculated by three methods: a) ACI-318 code equations, b) a custom program using a strain compatibility approach using Ramberg-Osgood constitutive model and c) a research software for analysis of concrete sections (RESPONSE 2000) [15], which also uses strain compatibility method and refined stress-strain models for both concrete and steel.

As discussed earlier, the ACI equations represent a simplified method of calculating the nominal section moment capacities. The custom program code used to find M_n by strain compatibility was validated by comparing its results to those from Response 2000 [15]. However, Response 2000[15] is a more powerful program that takes into account the detailed material constitutive models and can predict strain demands at various stages of loading. Taking these advantages to the best use, the moments developed during the test program (M_{test}) were compared with the nominal moment capacities obtained from both the ACI equations (M_{nACI}) and those of Response 2000 (M_{Res}).

7.4 Instrumentation

Instrumentation for the development length tests can be broadly classified into two types: (1) primary instrumentation – used to study the response of parameters essential to the development length study, and (2) secondary instrumentation – used for monitoring the overall test response and safety of the specimen and the crew during testing. All instrumentation readings were automatically recorded via a data acquisition system

The servo–controlled hydraulic actuator has in-built transducers that measure the load in the actuator and its displacement. The actuator has a capacity of 1450 kN (328 kips) with a stroke of 1016 mm (40 in.). The actuator load and displacement signals were recorded both at the controller computer and the data acquisition system.

Potentiometers were used to measure all the displacement responses of the test specimen. Two types of displacement transducers were used: (1) devices with a stroke of 305 mm (12 in.) were used to measure deformation under the points of application of the loads, and (2) devices with a stroke of 38 mm (1.5 in.) were used to measure support movements and strand end–slip. Figure 7-5 shows the three 305 mm (12 in.) devices that were used to measure the test unit displacements; two were used at the two points of application of the load and the third one at the center. A total of six 38 mm (1.5 in.) displacement transducers (38mm) were used: Two to measure the vertical deformation at the supports, two to measure the horizontal motion of the supports, and the last two were used to measure end-slip of the strands. The transducers used to measure strand end slip were attached to the strands with mounting of brackets and clamps. Figure 7-6 shows one of the supports with the instrumentation to measure these displacements.

Compressive strains at the top surface of the flange were monitored throughout the test with a 60 mm (2.36 in.) foil type strain gage placed at the top compression fiber of the section in the middle of the constant moment region.

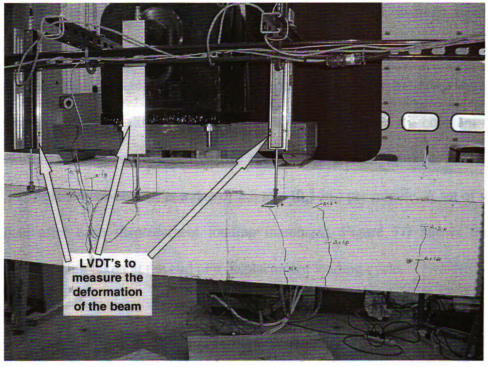

Figure 7-5 Instrumentation for Overall Unit Deformation

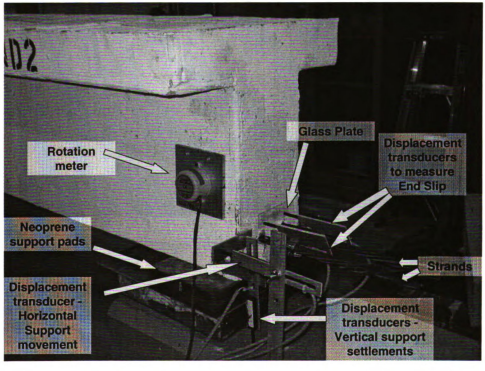

Figure 7-6 Instrumentation for Support Movement and strand End-Slip

In order to monitor the strains developed in the strand, average strains were measured on the concrete surface at the strand level on the constant moment region by means of a mechanical gage. DEMEC target points attached at strand level were spaced at 152.4 mm (6 in.) for a distance of 762 mm (30 in.) centered in the constant moment region. Initial readings were taken before the start of the experiment. Loading was applied in displacement-control at a rate of 2.5 mm (0.1 in.) per minute. A set of readings were taken after each displacement loading increment. Figure 7-7 shows the strain measurements being taken at the end of a displacement loading cycle.

Figure 7-7 Average Strain Measurement at Strand Level

7.5 Failure Modes and Analysis:

The failure mode and definition of the nominal moment capacity at the critical section performed play a vital role in determining the development length of the strands in test unit. The ultimate moment achieved at the critical section for a given test (M_{test}) was that obtained from the test response and the recorded data. Since all the beams tested in this project were of the same cross section, the nominal moment capacity (M_n) of the section for each test specimen depends on the amount of effective prestress in the strands and the concrete strength (Table 3-9) at the day of test. As discussed earlier in section 7.3, the nominal moment capacities were calculated by two methods: (1) ACI 318 method (Equation 7-2) [3], and (2) refined strain compatibility analysis (Response 2000) [15].

For a given embedment length, if the moment achieved in the critical section was greater than the calculated nominal capacity of the section, then the embedment length was considered equal to or greater than the actual development length and the embedment length for the next test was reduced. Conversely, if the moment achieved in the critical section was less than the calculated nominal capacity of the section, then the embedment length was considered to be insufficient relative to the actual development length and the embedment length for next test was increased. As a result, a range within which the actual development may occur for a particular mix was obtained. Three distinct failure modes were observed in the development length tests. 1) shear–slip failure, 2) flexural failure (no slip), and 3) flexure-slip failure. These failure modes are discussed as follows:

Shear–Slip failure:

This type of failure was initiated by large slip (or draw-in) at the free end of the beam. The nominal capacity of the section was not achieved under this type of failure. In this type of failure, the test behavior is as follows: Initially, as the loading was increased, flexural cracks symmetrical to the points of application of load were observed. The crack propagation ceased to remain symmetric after the first slip occurred. The crack closest to the end (support from which embedment length was measured), grew relatively much faster than the other cracks. Initiation of the strand end-slip is characterized by the formation of a horizontal crack at the strand level(Figure 7-8). This horizontal crack usually occurs at the crack closest to the support. As the load was increased, the strand end-slip increased rapidly until there was a compressive failure at the top flange. The strains in the strands were much lower (~ 0.220 strains for SCC3-1-A) than the ultimate strain capacity of the strand (0.035 strains) and the moment capacity of the section was not achieved. Figure 7-8 shows the initial stages of one of the shear-slip failure tests. Figure 7-9 shows the top flange compressive failure with the expansion of the crack close to the support. Figure 7-10 shows the test response corresponding to this type of failure.

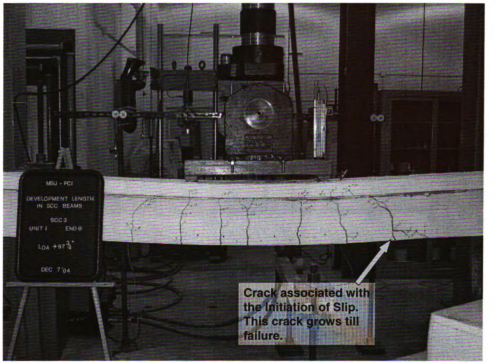

Figure 7-8 Shear- Slip Failure – Initial stage

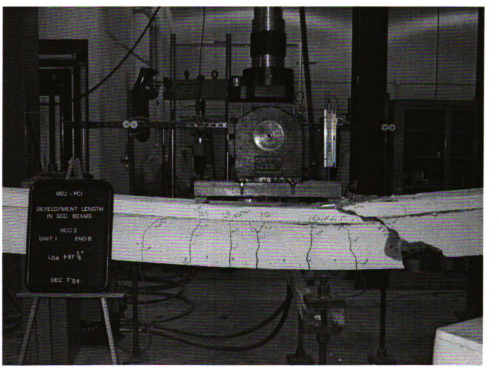

Figure 7-9 Typical Shear-Slip Failure

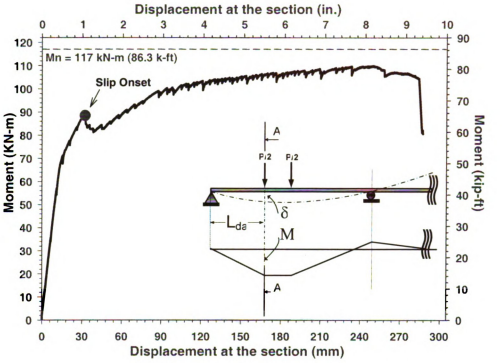

Figure 7-10 Test Response for a Typical Shear-Slip Failure

Flexural Failure:

This type of failure is basically a pure flexural failure wherein no end slip is observed. The nominal capacity of the section was mostly achieved in this type of failure. In this type of failure, the test behavior is as follows: Initially, as the loading was increased, flexural cracks symmetrical to the points of application of loads were observed (Figure 7-11). The cracks propagate symmetrically throughout the test and large crack openings and deformations were observed. As the load was increased, the crack pattern remained symmetric and the crack growth was proportional to the time of occurrence of the crack during the test. The failure, in most cases was reached first in the top compression flange. The compression flange failed within the maximum moment region (Figure 7-12) and not at the point of application of load as observed in test units

displaying shear–slip failures. In most cases, for this type of failure, the measured strain in the strand was beyond the guaranteed ultimate strain of 0.035 strains. Out of all the 24 development tests performed, the strands fractured in only two units. Figure 7-13 shows the flexural failure for one of the units failing with strand fracture. Figure 7-14 shows the moment-displacement response corresponding to this type of failure. In most cases, this type of failure occurred at long embedment lengths. Even though no strand slip is associated to this type of failure, this type of response does not guarantee that the nominal capacity of the section is achieved.

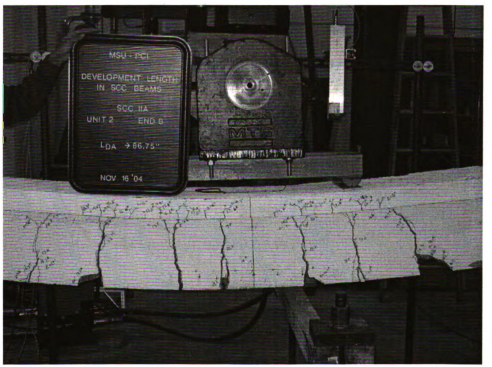

Figure 7-11 Flexural Failure – Symmetric crack pattern

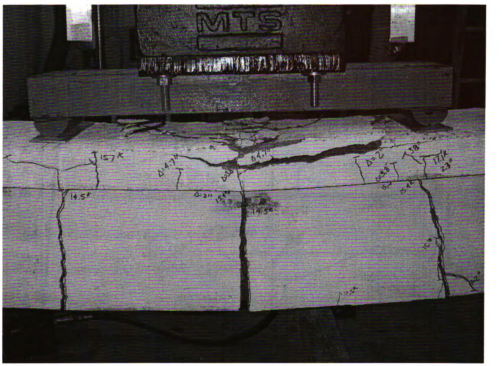

Figure 7-12 Flexural Failure – Final Condition (compression)

Figure 7-13 Flexural Failure – Final Condition (tension)

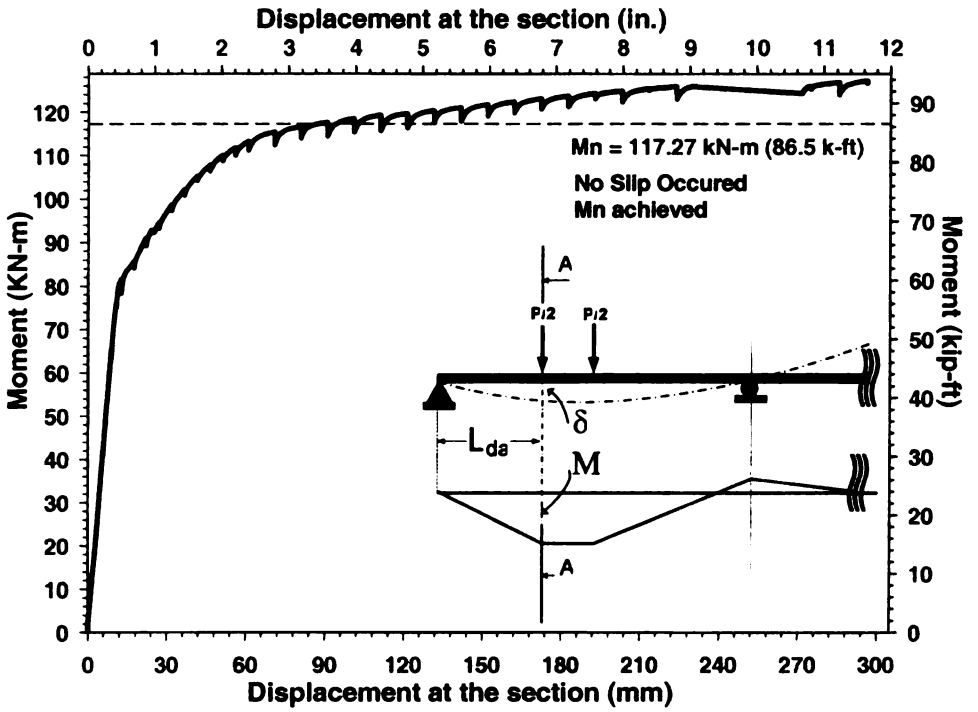

Figure 7-14 Test Response for a Typical Flexural Failure

Flexural–Slip Failure:

In this type of failure a combined effect of flexure and strand slip effects were observed. The nominal capacity was achieved at the critical section only in some cases, depending on the dominance of either the flexure or the strand slip contributions. If the test embedment length was slightly greater than the actual development length, then the bond component was dominant and the moment capacity at the critical section would be achieved with some amount of slip. Similarly if the test embedment length was slightly less than the actual development length then the strand–slip component would dominate and the moment capacity in the section would not be achieved. Only the cases in which the nominal capacity of the section was achieved are considered in this type of failure. If the nominal capacity was not achieved, such failure types were classified as shear-slip failures. In this type of failure, the test behavior was a combination of the first two cases.

Initially, as the loading was increased, flexural cracks symmetrical to the points of application of loads were observed (Figure 7-11). As the loading was increased, depending upon the dominance of the flexural bond or strand-slip contributions, the crack propagation varied slightly. The variation was mainly in the shear crack causing the strand slip. If the strand-slip component was larger than the flexural bond component, then this crack would grow relatively faster than the flexural cracks. If the flexural bond component dominated, then the flexural cracks would grow faster than the shear crack. It should be noted that strand-slip was recorded in all cases, irrespective of the dominance of the components.

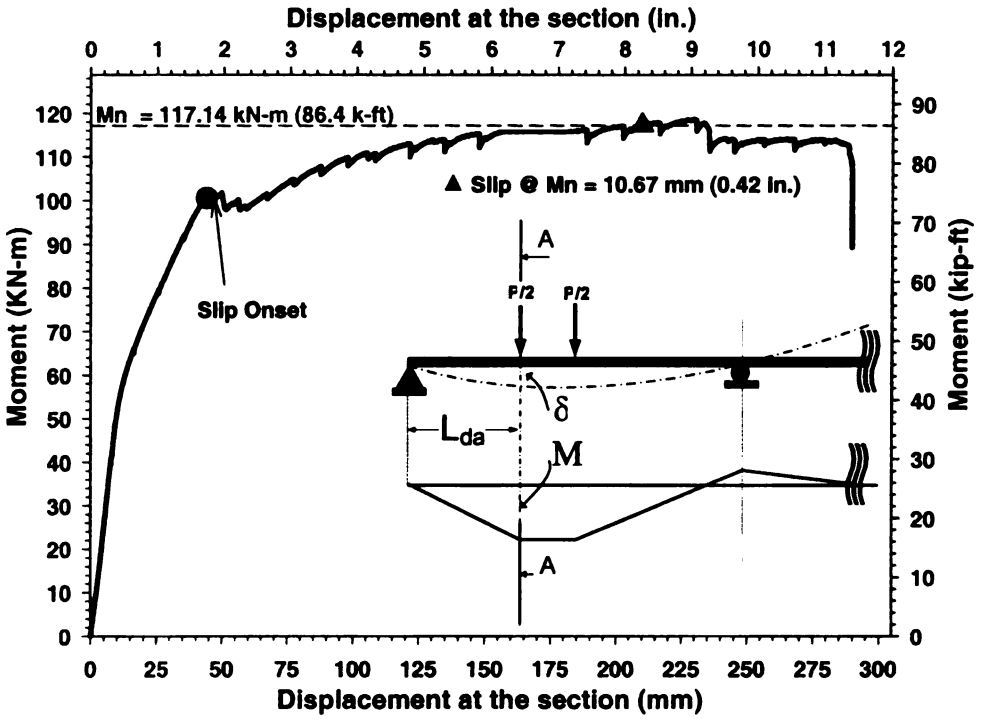

Figure 7-15 Test response for a typical Bond-Slip failure

In most cases, this type of failure was accompanied with the top flange failing in compression (Figure 7-12). The measured steel strains in this type of failure were very close to the strand guaranteed ultimate strain of 0.035 strains.

Figure 7-15 shows the test response for the case wherein the flexural response was dominant and the moment capacity was achieved. The test response for the case wherein the strand-slip component was dominant and moment capacity was not achieved is similar to a typical shear-slip failure as shown in Figure 7-10.

7.6 Presentation and Discussion of Test Results

A total of 24 development length tests were performed at MSU's Civil Infrastructure Laboratory. Four tests per concrete mix were performed. Excluding the NCCB test specimens, all other test specimens had unrusted clean strands The NCCB test specimens used a slightly rusted strand, since it was acquired a couple of months later due to the need to repeat the NCC mix. A clean cloth was used to wipe off the strands with one stroke before the cast of concrete. The NCC and SCC2 mixes were repeated due to the poor performance of the mix and the equipment, hence the first trial is represented by suffix "A" and the second trial is represented by the suffix "B." A brief description of the test results for individual concrete mixes are given in this section. The test results are tabulated in Table 7-2. The values of $L_{d\text{-}ACI}$, $M_{n\text{-}ACI}$ were obtained from the ACI-318 equations using a value for f_{ps} (nominal stress in the strand) as per the ACI 318 provisions (Equation 7-4) [3]. The value of $M_{n\text{-}SC}$ was obtained from the strain compatibility. The nominal strain at the nominal strength of the section (ε_{ps}) was obtained from strain compatibility analysis and the corresponding f_{ps} was evaluated from a constitutive model for prestressing steel (Ramberg Osgood model). Table 7-2 also shows the failure type of the test unit, where in "F" represents flexural failure, "S" represents the shear-slip failure and "FS" represents flexural slip failure. Results of the flexural tests for each mix design

are explained in detail in two cases: the ACI 318 method and the strain–compatibility method in the following:

Table 7-2 Development Length Test Results

Test ID	L_{dtest} (in.)	$M_n f_{ps}$ ACI-318		$M_n f_{ps}$ Strain Compatibilty (SC)		Failure Type
		$\frac{L_{d-test}}{L_{d-ACI}}$	$\frac{M_{test}}{M_{n-ACI}}$	$\frac{L_{d-test}}{L_{d-ACI(SC)}}$	$\frac{M_{test}}{M_{n-SC}}$	
SCC1-1-A	72.38	1.07	1.057	1.01	0.981	FS
SCC1-1-B	133.75	2.03	1.137	1.92	1.056	F
SCC1-2-A	122.00	1.79	1.121	1.70	1.039	F
SCC1-2-B	118.50	1.74	1.217	1.65	1.128	F
SCC2A-1-A	70.50	1.09	1.105	1.03	1.024	FS
SCC2A-1-B	64.50	1.00	0.966	0.94	0.896	S
SCC2A-2-A	80.00	1.27	1.127	1.19	1.045	FS
SCC2A-2-B	86.75	1.37	1.137	1.29	1.054	FS
SCC2B-1-A	70.50	1.21	1.007	1.13	0.934	FS
SCC2B-1-B	102.75	1.76	1.140	1.65	1.058	FS
SCC2B-2-A	126.75	1.78	1.101	1.69	1.021	F
SCC2B-2-B	124.50	1.75	1.187	1.66	1.100	F
SCC3-1-A	58.00	1.06	0.953	0.98	0.884	S
SCC3-1-B	97.75	1.79	1.090	1.66	1.010	FS
SCC3-2-A	106.50	1.80	1.100	1.67	0.994	FS
SCC3-2-B	103.00	1.74	1.132	1.61	1.050	FS
NCCA-1-A	76.00	1.06	0.952	1.03	0.910	FS
NCCA-1-B	122.70	1.71	1.158	1.67	1.107	FS
NCCA-2-A	111.00	1.55	1.201	1.51	1.149	FS
NCCA-2-B	60.00	0.84	0.907	0.82	0.867	S
NCCB-1-A	63.75	1.06	1.036	1.00	0.972	F
NCCB-1-B	64.00	1.07	1.049	1.00	0.983	F
NCCB-2-A	103.50	1.31	1.145	1.25	1.076	F
NCCB-2-B	93.50	1.22	1.137	1.16	1.068	F

TYPE OF FAILURE:
S - Shear Slip Failure
F – Flexural Failure
FS – Flexural Slip failure

1 in. = 25.4 mm

7.7 Development Length Test Results as per ACI-318 Method [3]

Results of the development length tests for each mix design with the nominal moment capacity (M_n) and the nominal stress in the strand at the nominal capacity of the section (f_{ps}) calculated as per the ACI-318 recommendations are explained next. Specific test details and failure type are given only for the test with the minimum embedment length that satisfied the moment requirements:

SCC1: All the four test beams achieved the nominal moment capacity. The least test embedment length that achieved the moment capacity had an L_{dtest}/L_{dACI} ratio of 1.07, corresponding to L_{dtest} of 1.83 m (72.38 in.). The maximum average value of strain in the steel at strand level measured on the concrete surface was 0.039. The corresponding $M_{test}/M_{n\text{-}ACI}$ ratio was evaluated to be 1.057. This test had a flexural-slip failure

SCC2A: Three out of the four test beams achieved the nominal moment capacity. The least test embedment length that achieved the moment capacity had an L_{dtest}/L_{dACI} ratio of 1.09, corresponding to L_{dtest} of 1.79 m (70.50 in.). The corresponding $M_{test}/M_{n\text{-}ACI}$ ratio was evaluated to be 1.105. This test had a flexure-slip failure

SCC2B: All the four test beams achieved the nominal moment capacity. The least test embedment length that achieved the moment capacity had an L_{dtest}/L_{dACI} ratio of 1.21, corresponding to a L_{dtest} of 1.79 m (70.50 in.). The average value of strain in the strand as measured on concrete surface was 0.0183 strains. The corresponding $M_{test}/M_{n\text{-}ACI}$ ratio was evaluated to be 1.007. This test had a flexure-slip failure

SCC3: Three of the four test beams achieved the nominal moment capacity. The least test embedment length that achieved the moment capacity had an L_{dtest}/L_{dACI} ratio of 1.79, corresponding to L_{dtest} of 2.48 m (97.75 in.). The maximum average strain value in the steel at strand level was 0.0371 strains. The corresponding $M_{test}/M_{n\text{-}ACI}$ ratio was evaluated to be 1.090. This test had a flexure-slip failure

NCCA: Two of four test beams achieved the nominal moment capacity. The least test embedment length that achieved the moment capacity had an L_{dtest}/L_{dACI} ratio of 1.55, corresponding to L_{dtest} of 2.82 m (111 in.). The corresponding $M_{test}/M_{n\text{-}ACI}$ ratio was evaluated to be 1.201. This test had a flexure-slip failure

NCCB: All the four test beams achieved the nominal moment capacity. The least test embedment length that achieved the moment capacity had an L_{dtest}/L_{dACI} ratio of 1.07, corresponding to a L_{dtest} of 1.63 m (64.00 in.). The maximum average value of strain in the strand was 0.0264. The corresponding $M_{test}/M_{n\text{-}ACI}$ ratio was evaluated to be 1.049. This test had a flexural failure

7.8 Development Length Test Results as per the Strain Compatibility (SC) Method.

Results of the development length tests for each mix design with the nominal moment capacity (M_n) and the nominal stress in the strand at the nominal capacity of the section (f_{ps}) calculated as per the strain compatibility (SC) method are explained as follows:

SCC1: Three of the four test beams achieved the nominal moment capacity. The least test embedment length that achieved the moment capacity had an $L_{dtest}/L_{dACI(SC)}$ ratio of 1.65, corresponding to a L_{dtest} of 3.01 m (118.50 in.). The maximum average value of strain in the strand was 0.039. The corresponding $M_{test}/M_{n\text{-}ACI}$ ratio was evaluated to be 1.128. This test had a flexural failure

SCC2A: Three out of the four test beams achieved the nominal moment capacity. The least test embedment length that achieved the moment capacity had an $L_{dtest}/L_{dACI(SC)}$ ratio of 1.03, corresponding to a L_{dtest} of 1.79 m (70.50 in.). The corresponding $M_{test}/M_{n\text{-}ACI(SC)}$ ratio was evaluated to be 1.024. This test had a flexural-slip failure

SCC2B: Three of the four test beams achieved the nominal moment capacity. The least test embedment length that achieved the moment capacity had an $L_{dtest}/L_{dACI(SC)}$ratio of 1.65, corresponding to a L_{dtest} of 2.61 m (102.75 in.). The maximum average value of strain in the strand was 0.0295 . The corresponding $M_{test}/M_{n\text{-}ACI(SC)}$ ratio was evaluated to be 1.058. This test had a flexure-slip failure

SCC3: Two of the four test beams achieved the nominal moment capacity. The smallest test embedment length that achieved the moment capacity had an $L_{dtest}/L_{dACI(SC)}$ ratio of 1.66, corresponding to L_{dtest} of 2.48 m (97.75 in.). The maximum average value of strain in the strand was 0.0371 strains. The

corresponding $M_{test}/M_{n\text{-}ACI(SC)}$ ratio was evaluated to be 1.010. This test had a flexure-slip failure

NCCA: Two of four test beams achieved the nominal moment capacity. The least test embedment length that achieved the moment capacity had an $L_{dtest}/L_{dACI(SC)}$ ratio of 1.51, corresponding to a L_{dtest} of 2.82 m (111 in.). The corresponding $M_{test}/M_{n\text{-}ACI(SC)}$ ratio was evaluated to be 1.149. This test had a flexure-slip failure

NCCB: Two of the four test beams achieved the nominal moment capacity. The least test embedment length that achieved the moment capacity had an $L_{dtest}/L_{dACI(SC)}$ ratio of 1.16, corresponding to L_{dtest} of 2.29 m (93.50 in.). The maximum average in strand was 0.0379. The corresponding $M_{test}/M_{n\text{-}ACI(SC)}$ ratio was evaluated to be 1.068. This test had a flexural failure

The refined method (strain compatibility method) of determining the nominal moment capacity gives higher moment capacities and longer development lengths relative to those based on the values taken from ACI-318 recommended equations. As a result, it was observed that in some cases that the nominal capacity as per the ACI-318 code was achieved in the development length tests but the same tests did not meet the nominal capacity as determined by strain compatibility approach. Out of the twenty four development length tests, twenty tests achieved the moment capacity requirements of the ACI-318 recommendations, but only fifteen of them met the refined analysis requirements. Although, the refined analysis methods may not be available or practically feasible for everyday design, these methods are more conservative.

The development length as discussed was found iteratively by bounding the failure modes. In order to obtain the relative performances of each mix type, the test development lengths need to be normalized. The test data (ratios of L_d and M_n) were fit to a third order polynomial and the value of L_d ratio corresponding to a value of unit ratio of nominal capacities (M_{test} / $M_{n\text{-}theory}$ = *1*) was found. Table 7-3 shows the values of normalized L_d ratios calculated from the ACI-318 and strain compatibility method.

Table 7-3 Comparision of Development Length Results

	ACI - 318			Strain Compatibility (SC)		
	$\frac{M_{test}}{M_{n-ACI}}$	$\frac{L_{d-test}}{L_{d-ACI}}$	$\frac{L_{d-expt.}}{L_{d-ACI}}$	$\frac{M_{test}}{M_{n-SC}}$	$\frac{L_{d-test}}{L_{d-ACI(SC)}}$	$\frac{L_{d-expt.}}{L_{d-ACI}}$
SCC1	**1.06**	1.07	**1.03**	1.128	1.650	1.2958
SCC2a	1.11	1.09	**1.04**	1.024	1.030	1.0300
SCC2b	1.01	1.21	**1.17**	1.058	1.650	1.6600
SCC3	1.09	1.79	**1.42**	1.010	1.660	1.6600
NCCb	1.04	1.06	**0.97**	1.076	1.160	1.0500

Results from the ACI-318 method show that the SCC beams required longer development lengths relative to the NCCB beams. The SCC1, SCC2B and SCC3 beams had 3%, 17% and 42% longer development lengths while NCCB beam had 3% shorter length than recommended by the ACI-318 code. Conversely, the results based on strain compatibility analyses showed that ACI-318 may be under-predicting the values of development length for all mixes. The SCC1, SCC2B, SCC3 and NCCB beams required 30%, 66%, 66% and 5% longer development lengths than that predicted by the ACI-318 recommendatons. Figure 7-16 shows the comparison of the experimental and ACI-318 predicted development lengths for all mix designs.

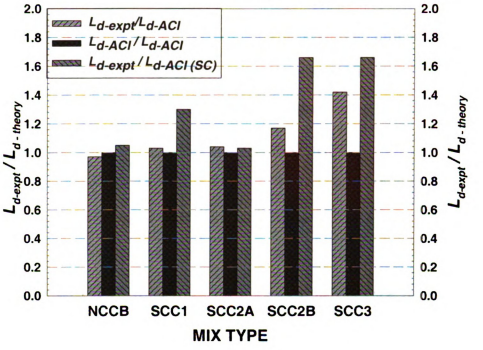

Figure 7-16 Comparison of Development Length Results

7.9 Flexural Bond Length:

As discussed earlier, a direct experimental method of determining only the flexural bond length is not possible. Hence, the total development length is obtained from flexural tests as as presented in this chapter and the flexural bond length is obtained as the difference of the development and length and the measured transfer lengths (Chapter 6). The development length was studied in two ways: (1) based on the ACI-318 equations and (2) based on strain compatibility analyses. The theoretical transfer length was obtained only by the ACI-318 recommendations. The experimental flexural bond length for each mix was obtained from the difference of the test development length ($L_{d\text{-}test}$) and the average experimental transfer length. The ratio of measured flexural bond lengths with that of ACI-318 predicted values for the test units corresponding to the least

development length for each of the mix design are given in Table 7-4. Similar to the development length, in order to compare the flexural bond lengths for different mixes, the test flexural bond lengths were normalized for unit nominal moment ratios.

Table 7-4 Flexural Bond lengths

	$L_{ftest}/L_{f\text{-}ACI}$	$L_{f\text{-}exp}/L_{fACI}$
SCC1	1.10	1.21
SCC2A	1.32	0.99
SCC2B	1.60	1.53
SCC3	3.53	2.29
NCCB	1.58	1.00

The experimental flexural bond lengths for NCCB and SCC2A (stiff mix) test units measured experimentally agree with the ACI-318 predictions. However, for all other SCC mixes the experimental flexural bond lengths are longer than the predictions of the ACI-318 code. It is observed that the SCC1, SCC2B and SCC3 test beam units had 21%, 53% and 229% longer flexural bond lengths respectively. It should also be noted that the values of flexural bond length discussed here were obtained from the transfer lengths measured at the release of prestress. The development length tests were performed approximately 120 days from the day of release. The transfer lengths in prestressed members increase slightly with time and creep [9]. The increase in transfer length with time was found experimentally with draw-in measurements. The draw-in measurements were taken at time of release, 7, 14, 28 days and the day of flexural testing. Measurements were not taken between 28 days and the day of flexural testing. As discussed earlier, the reliability of the draw-in measurements at the day of test are in question due to the damage of the glass target plate during the movement of the beam in the yard, hence were not used for the prediction of the transfer length.

7.10 Summary and Conclusions

Determining the development length of prestressing strand involves the study of complex bond phenomena between concrete and steel tendons. As discussed earlier, bond phenomena depend on various factors like material properties, industry practices, quality control etc. Hence a definite or accurate relationship of all the parameters cannot be obtained, but a relative study can be made.

The current ACI-318 equation (Equation7-2) [3] was studied, and in the previous chapter on transfer length it was found that the ACI equation applied conservatively for transfer length for all beams and the mixes in the study. The development length studies showed that the ACI equation was un-conservative for SCC mixes and thus the flexural bond length component of the ACI equation is underpredicted. The test flexural bond lengths (L_{ftest}) were obtained for all test units by calculating the difference of the test embedment length and the average measured transfer length values. As shown in Table 7-4, the experimental values of flexural bond lengths are longer than that predicted by the ACI-318 code.

The criteria for defining whether the development length for a particular beam depends on the determination of the ultimate moment capacity of the critical section. As discussed earlier, refined models tend to give larger moment capacities and the development length as per ACI-318 code recommendations may not be met in some cases. For NCCB, the ACI nominal capacity was reached with the recommended ACI development length. However, the SCC beams required slightly longer lengths: 3, 17, and 42% longer for the SCC1, SCC2B, and SCC3 test beams, respectively. The development lengths required to achieve the member capacity according to a strain compatibility analysis were longer: 30% longer for SCC1 beams and 66% longer for SCC2B and SCC3

beams. The NCCB beam achieved the higher nominal capacity with only a 5% increase in L_d.

An interesting observation was that mix designs that had relatively smaller transfer lengths had larger flexural bond lengths and vice versa. For example SCC1 test units, had a L_{tmeas} / L_{tACI} ratio of 1.02 (Table 6-4), where as it had the least L_{ftest} / L_{fACI} ratio (Table 7-4) for the SCC mix beams. The different bond transfer mechanisms contributing to the transfer and flexural bond components respectively seem to nullify each other producing approximately the same effect on development length for all SCC mixes. This indicates that the SCC mix proportioning has a distinct effect on the different bond mechanisms contributing to the development length of prestressing strands.

CHAPTER 8 SUMMARY AND CONCLUSIONS

8.1 Summary

Self compacting concrete has become of high interest specially to the precast/ prestressed industry because of the many advantages it offers. At the same time, not much work has been performed on the structural performance of members built using SCC. This study examined the bond of 13 mm (0.5 inch.) diameter strand in self consolidating concrete (SCC) in terms of transfer and development length in precast/prestressed beams. Three SCC mix designs were strategically selected to bound the different proportioning methods: (1) a design based on controlled coarse-to-fine aggregate ratios (2) a design based on the use of chemical admixtures and (3) an intermediate design. A baseline comparison is made with a conventionally vibrated concrete mix (NCC). Laboratory scale test beams with a T-cross section were designed in such a way that the prestressing strand experienced strains close to its guaranteed ultimate capacity during testing. The cross-section had a top flange width of 381 mm (15 in.) and the flange had a thickness of 76 mm (3 in.). The total depth of the section was 381 mm (15 in.) and the web was 152.4 mm (6 in.) thick. The section had two seven-wire low-relaxation 1860 MPa (270) Grade steel prestressing strands of 13mm (0.5 in.) nominal diameter. The strands were placed at a depth of 51 mm (2 in.) from the bottom of the beam. The effective stress for design was taken as 1100 Mpa (160ksi). For actual tests, the effective stress was calculated from the initial stressing loads (as determined from the strain gage readings) and estimated losses. Also a passive compressive reinforcement consisting of two 13 mm (#4) bars was provided at the top flange to control cracking at transfer. Nominal shear reinforcement, U stirrups of 6 mm diameter (#2 bars) at 305 mm (12 in.) center to center spacing, was provided. Concrete strengths at

release were greater than 28 MPa (4000 psi) for all test units. The strand condition was smooth and non-rusty for all mixes except for NCCB mix which used a strand that may be classified as slightly rusted.

Transfer length of the prestressing strand was assessed using two methods: (a) concrete strain profile and (b) draw-in measurements. The concrete strain profile measurements were taken using the DEMEC strain gage system. Small steel discs were affixed to the concrete surface on both sides of the beam test unit and measurements were taken using the mechanical gage before and after the release of prestress. The average strain was obtained from the changes in the locations of these discs. The transfer length was obtained using the 95% average maximum strain (AMS) method. The draw-in method involved the measurement of the strand movement at the end of the beam. A small U-channel was tightly clamped to the strand at the face of the beam and a glass target plate was fixed to the concrete face. The relative movement of the strand with respect to the face of the concrete was measured and the transfer length was calculated. The draw-in measurements were found to be less time consuming and required less-skill for the relatively same accuracy of the results. The strand profile method had been widely used and accepted as it gives the entire strand profile throughout the length of the beam. The results from both the methods compare favorably.

Strand bond was evaluated by means of simple pull-out tests on the used strands for the all concrete mixes. Six strands were pulled-out for each mix design, three at the time of release and the remaining were tested on 7 days. The pull-out tests were designed and conducted in a similar way to the test developed by Moustafa in 1974 and modified by Logan in 1997. The bonded length was 457 mm (18 in.). A hollow-core hydraulic jack

was used to pull the strands out of the block. Instrumentation to measure the movement of the strand was done at both the ends of the strands. The pull-out load and the strand movement at both the ends (free and jacking) were recorded.

Development length of the prestressing strand was determined through an iterative process of flexural tests. The beam units were loaded at various embedment lengths and the failure mode was recorded and observed. Loading was performed by a servo-controlled hydraulic actuator. The applied load, deflections at points of loading and at the resultant location of loading, strand-end slips, top fiber concrete compressive strains were measured continuously throughout the test.

Fabrication, instrumentation and testing for this test program was carried out at the Civil Infrastructure laboratory at Michigan State University, East Lansing, USA.

8.2 Conclusions

The following conclusions were drawn from this study:

- The designed concrete compressive strength at 28 days was 48.3 MPa (7000 psi). The compressive strength at 28 days achieved by the conventional concrete was exactly 48.3 MPa (7000) psi. At the same time, the compressive strengths of SCC mixes were much higher than design strength. The high strength of SCC may be advantageous, but at the same time, the same amount of confidence and control in designing the mixes may still not have achieved by SCC mix proportioning.
- The ACI 318/AASHTO code equations for transfer length were found to be conservative only for transfer length measurements for all the mix designs and only marginally (2%) under estimated the results for the SCC1 mix.

- The SCC1 mix had the largest transfer length with a (L_{tmeas} / $L_{t\text{-}ACI}$) ratio of the measured transfer length (L_{tmeas}) to the value predicted by the ACI code ($L_{t\text{-}ACI}$) of 1.02.
- The (L_{tmeas} / $L_{t\text{-}ACI}$) ratio for NCCB, SCC2A, SCC2B, SCC3 was found to be 0.86, 0.82, 0.90 and 0.91, respectively. The NCCB and SCC2A mixes were stiff and hence a significant reduction in transfer length was found.
- It was found that SCC mixes, had larger transfer length values relative to the NCC mixes.
- Results of transfer length studies supported the concept of bounding the hardened properties by proper mix selection. The transfer length values for the SCC2 mix (moderate w/c) was bounded by the SCC1 (high fines) and SCC3 (high aggregates) mixes.
- The high values of transfer length for SCC1 could be attributed to the presence of high paste content and large amount of admixtures.
- Draw-in values were found to increase significantly with time. Draw-in measurements at approximately 110 – 130 days after release showed an increase of approximately 50% for NCC mixes and about 80% - 100% for SCC mixes. Correspondence of the increase in draw-in measurements to increase transfer lengths with time can be inferred. However, further evaluation is needed in order to assess other factors influencing the increase in draw-in values such as concrete shrinkage and creep
- The peak pull-out test results at release show that SCC mixes had low pull-out strengths relative to the NCC mixes.

- The peak pull-out strengths at release are discussed as follows: The SCC1 (high fines) mix was found to have the least peak pull-out strength of 74. kN (16.61 kip.). The SCC3 (high aggregates) had the highest peak pull-out strength of all SCC mixes with a value of 89.53kN (20.12 kip.). The peakpull-out strength of the SCC2 mix was bounded between SCC1 and SCC3 and found to be 86.29 kN (19.39 kip)
- The development length values of SCC mixes were found to be significantly greater than the values predicted by the ACI-318/AASHTO recommendations.
- Development length test results were studied in two cases: based on nominal capacities according to the ACI-318 equations and based on capacities obtained from a refined strain-compatibility analysis.
- Conclusions regarding the development lengths required to achieve the member capacity according to the ACI-318 equations are: for NCCB, the ACI nominal capacity was reached with the recommended ACI development length. However, the SCC beams required slightly longer lengths: 3, 17, and 42% longer for SCC1, SCC2B, and SCC3, respectively.
- The development lengths required to achieve the member capacity according to a strain compatibility analysis were longer: 30% longer for SCC1 and 66% longer for SCC2B and SCC3. The NCCB beam achieved the higher nominal capacity with only 5% increase in L_d.
- All SCC mixes had longer development length than that predicted by the ACI-318 code. Thus the code was found to be unconservative with respect to the development length for members built using SCC.

- The strands used in this research did not meet the pull-out (bond qualification) requirements as proposed by Logan [25]. Hence, the under-performance of strands in SCC elements based on predictions of the ACI-318 code cannot be completely confirmed.
- Since the same strand and relatively the same parameters being maintained for all the SCC mixes, the relative performances of SCC mixes should remain the same.
- Thus, inspite of the inconclusive outcome set forth by the possibility of low quality strand, the relative bond performance of strand in different SCC mix designs is still valid.
- The concept of bounding the hardened bond behavioral properties (in this study, transfer and development length) by proper mix proportions was supported by the obtained experimental transfer lengths. In the transfer length study, the experimental values of transfer length for SCC2 mixes were bounded by the values of the SCC1 and SCC3 mixes.
- The end result for development length seems to be fairly uniform for all SCC mixes; however, the transfer and flexural bond length components were not. This indicates that SCC mix proportioning has clear and different effects on the bond mechanisms (hoyer's effect and mechanical interlock) contributing to the development length of prestressing strands. This supports the concept that bond performance of prestressing strand is influenced by the hardened behavioral properties defined by different mix proportioning.

APPENDICES

Appendix 1 - Stress – Strain Response – Elastic Modulus Tests

The elastic modulus of the different concrete mixes used in this project was evaluated in accordance with the ASTM C469 test method. The stress–strain responses measured for the different mixes are provided in this section

The elastic modulus tests were performed at the release of prestress (approximately 3 days of age) and at 28 days. Elastic modulus tests at release were not performed for all mixes due to technical and equipment problems. In this section the elastic modulus plots at release (approximately 3 days) are followed by the elastic modulus plots at 28 days. The plots for the various mixes are given in the following order: SCC1, SCC2A, SCC2B, SCC3 and NCCB for both transfer and 28 days of concrete age.

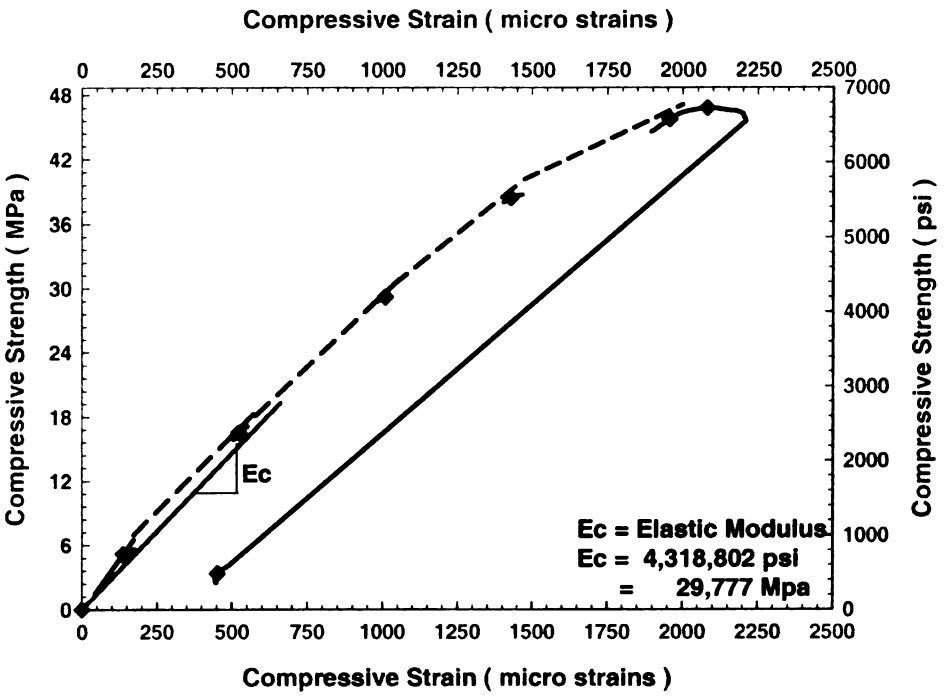

Figure A1- 1 Elastic Modulus Test – Transfer – SCC2B – Test1

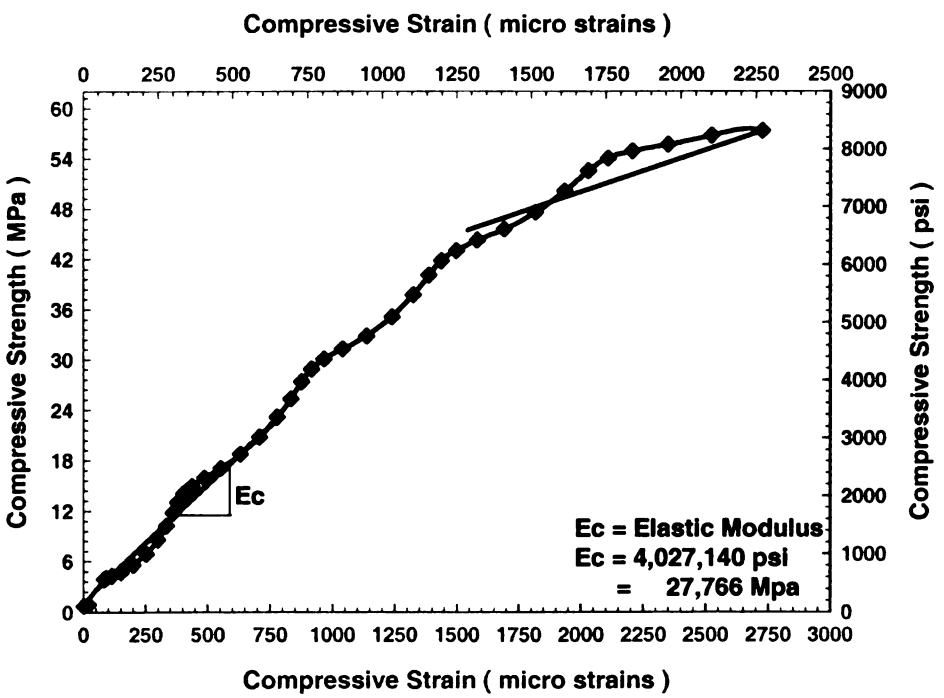

Figure A1- 2 Elastic Modulus Test – Transfer – SCC2B – Test2

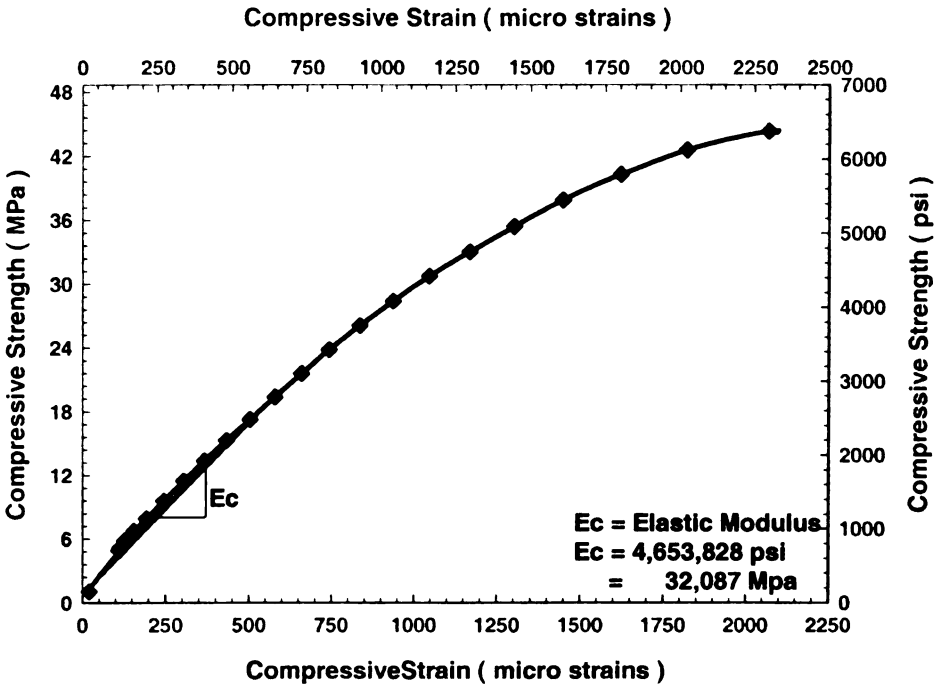

Figure A1- 3 Elastic Modulus Test – Transfer – SCC2B – Test3

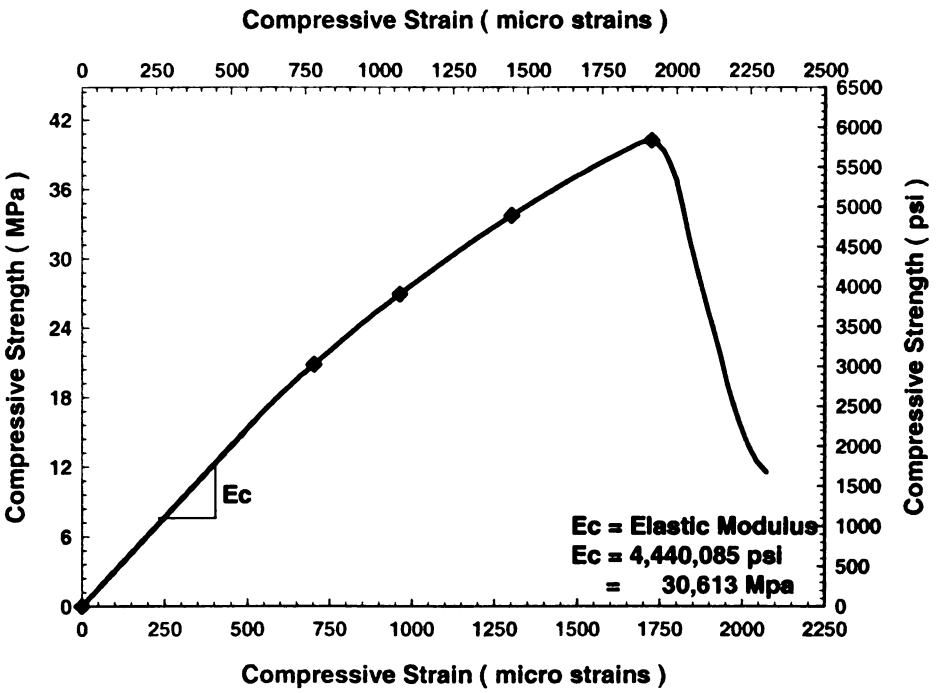

Figure A1- 4 Elastic Modulus Test – Transfer – SCC3 – Test1

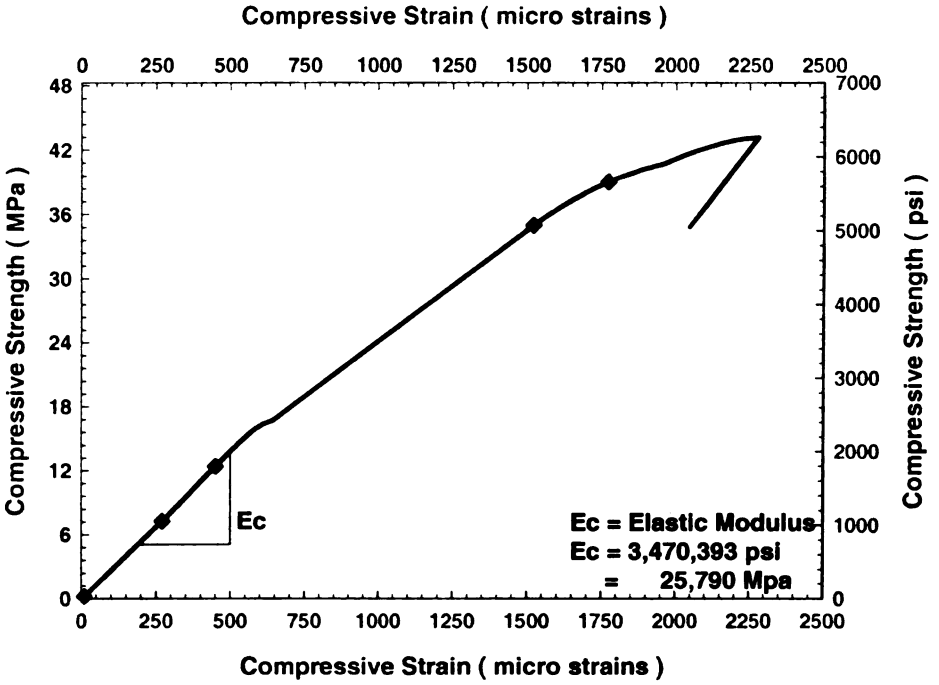

Figure A1- 5 Elastic Modulus Test – Transfer – SCC3 – Test2

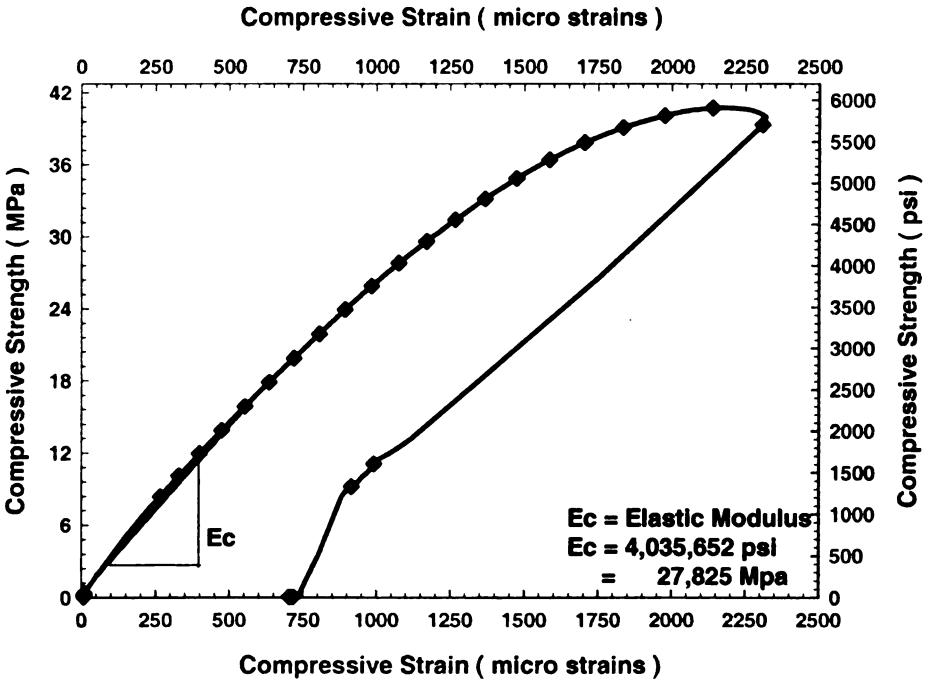

Figure A1- 6 Elastic Modulus Test – Transfer – NCCB – Test1

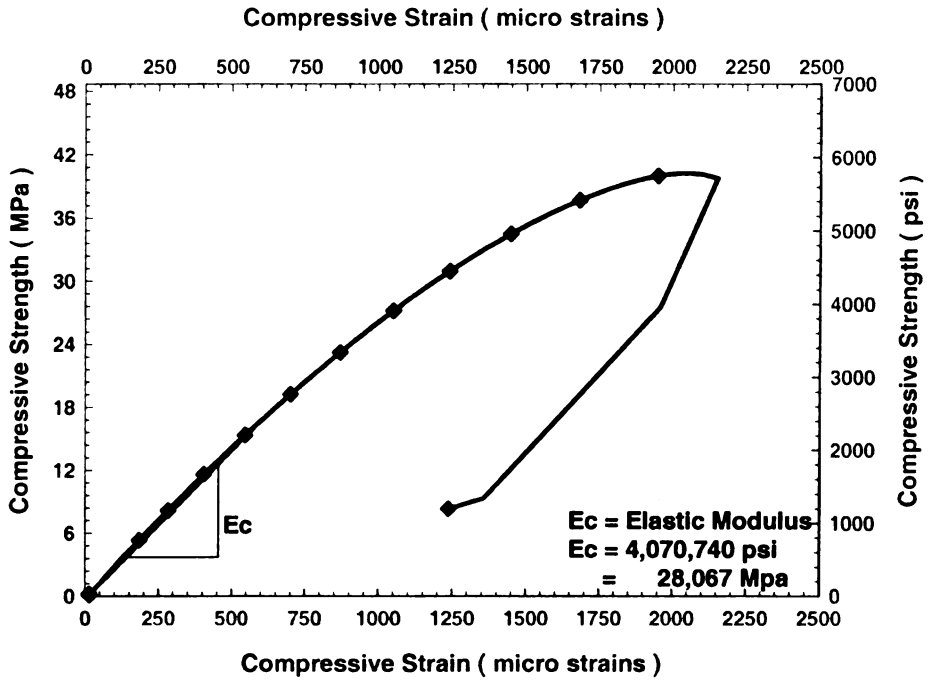

Figure A1- 7 Elastic Modulus Test – Transfer – NCCB – Test2

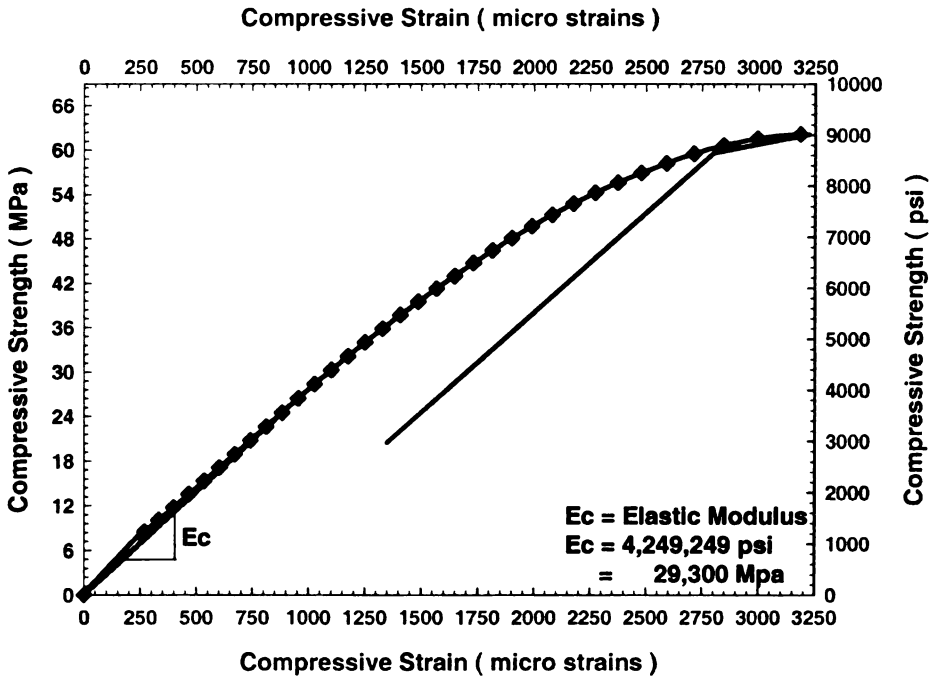

Figure A1- 8 Elastic Modulus Test – 28 Days – SCC1 – Test1

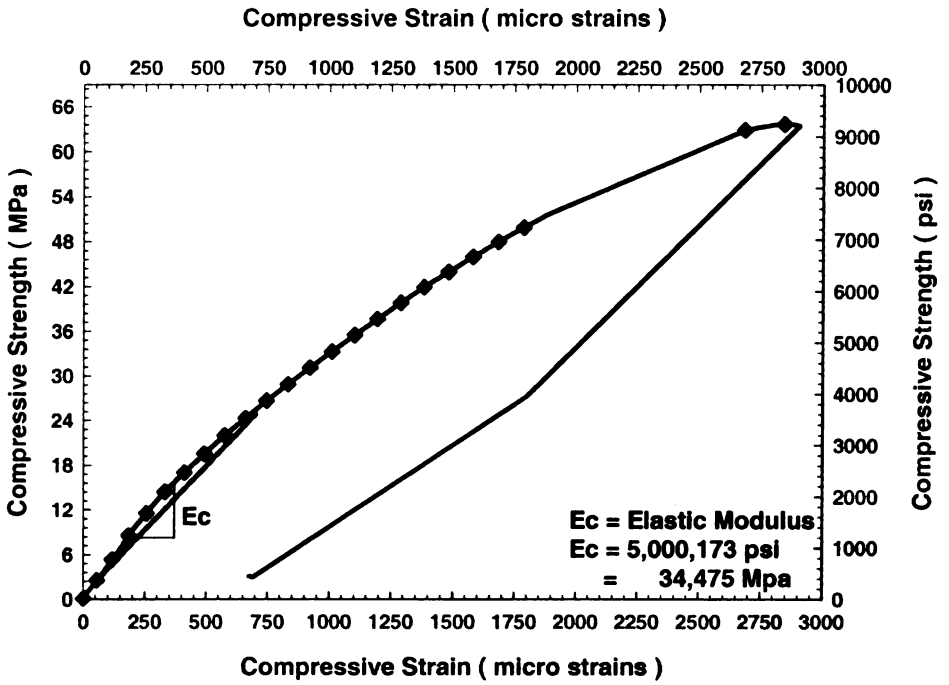

Figure A1- 9 Elastic Modulus Test – 28 Days – SCC1 – Test2

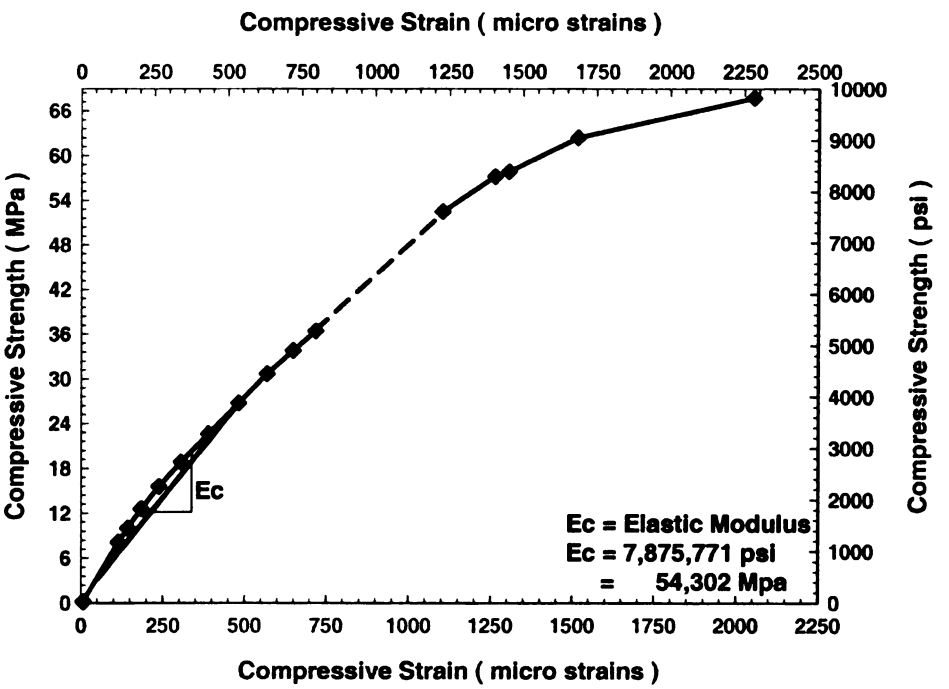

Figure A1- 10 Elastic Modulus Test – 28 Days – SCC2A – Test1

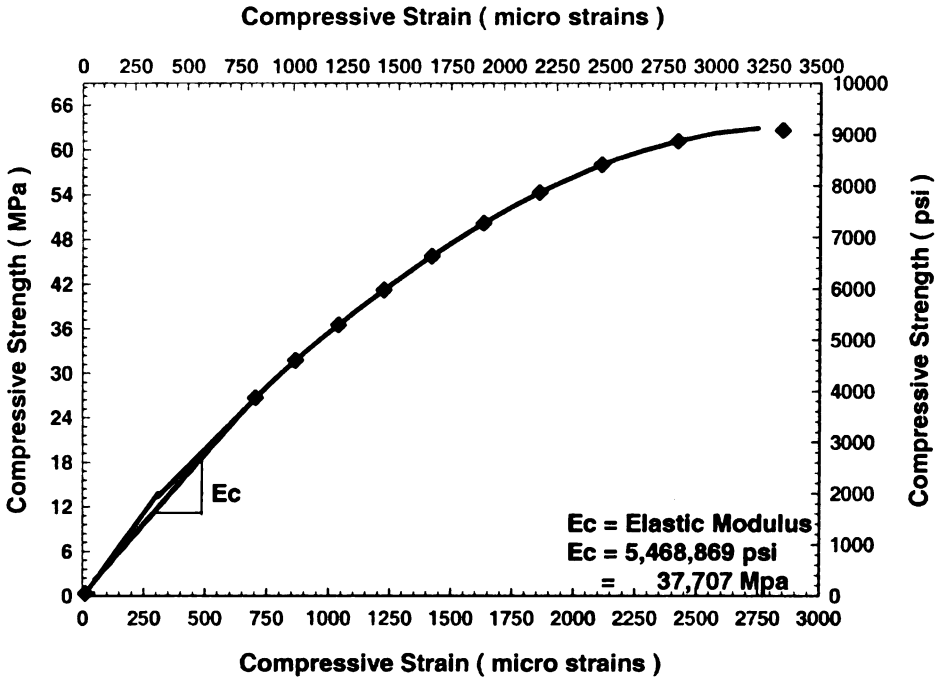

Figure A1- 11 Elastic Modulus Test – 28 Days – SCC2A – Test2

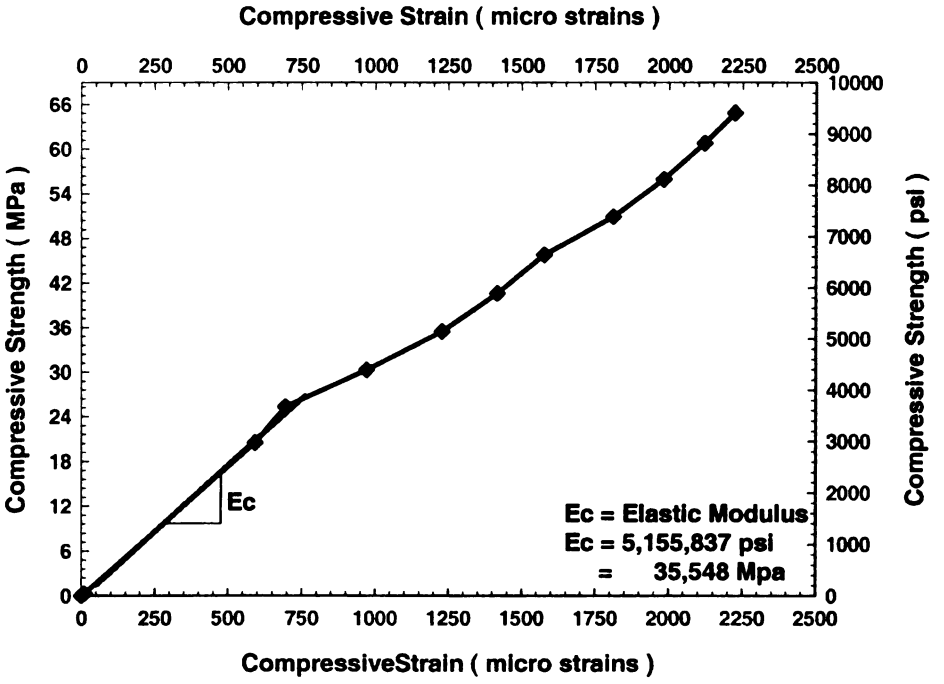

Figure A1- 12 Elastic Modulus Test – 28 Days – SCC2A – Test3

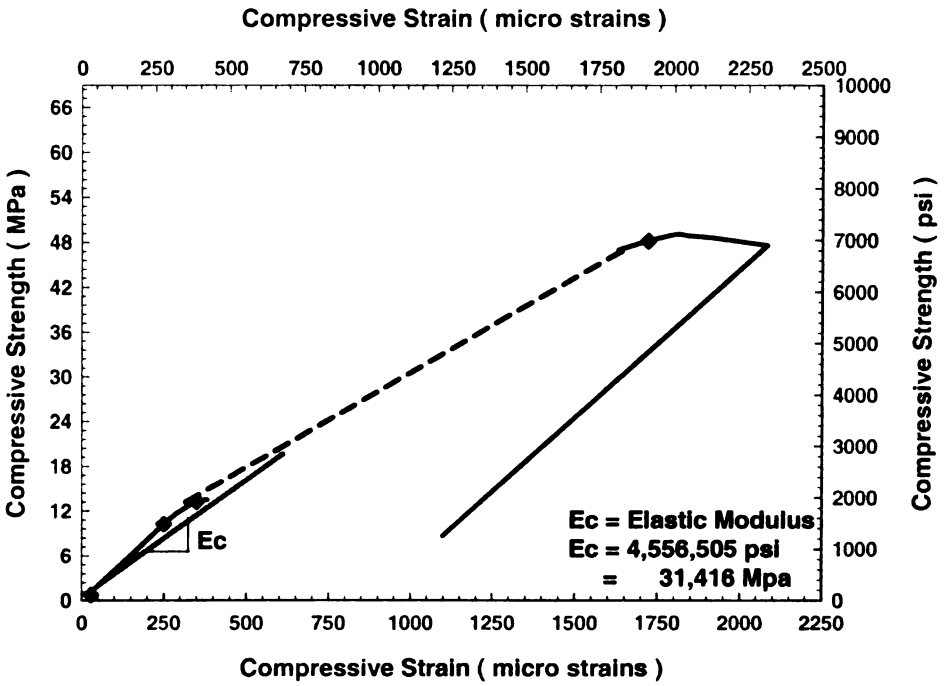

Figure A1- 13 Elastic Modulus Test – 28 Days – SCC3 – Test1

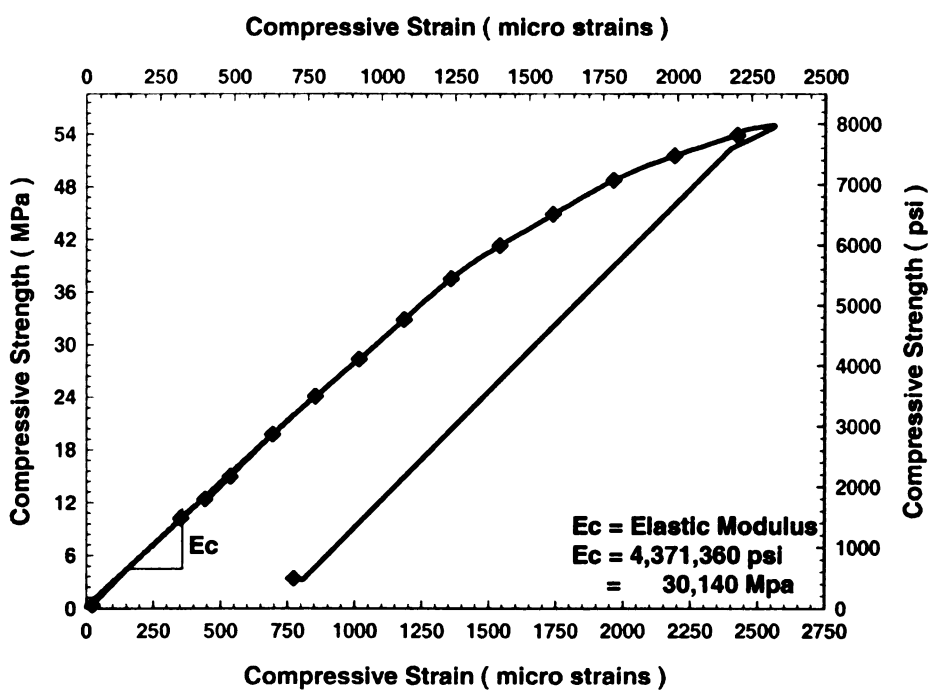

Figure A1- 14 Elastic Modulus Test – 28 Days – SCC3 – Test2

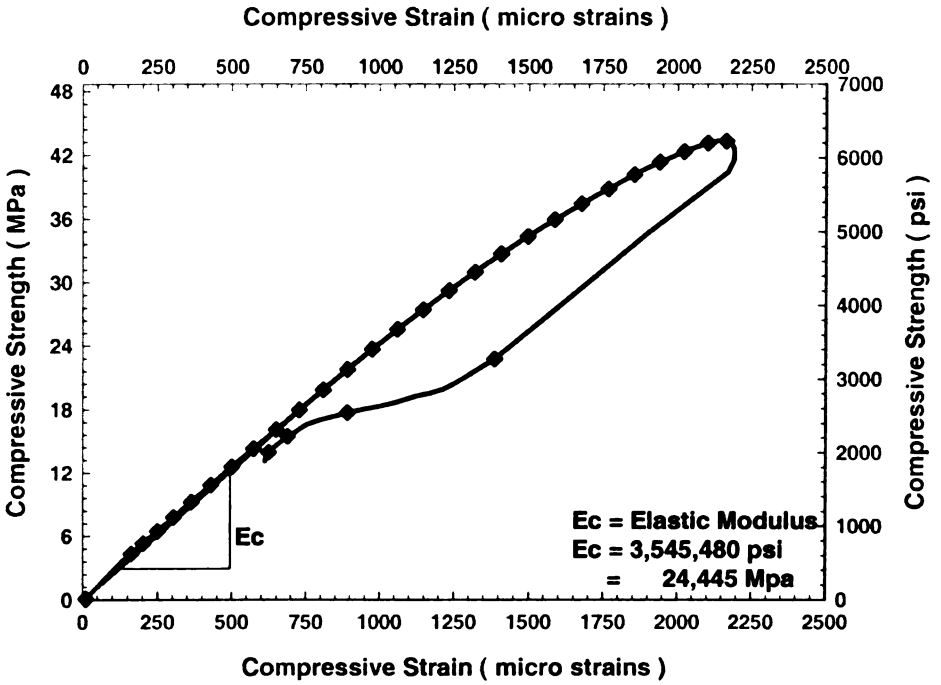

Figure A1- 15 Elastic Modulus Test – 28 Days – NCCB – Test1

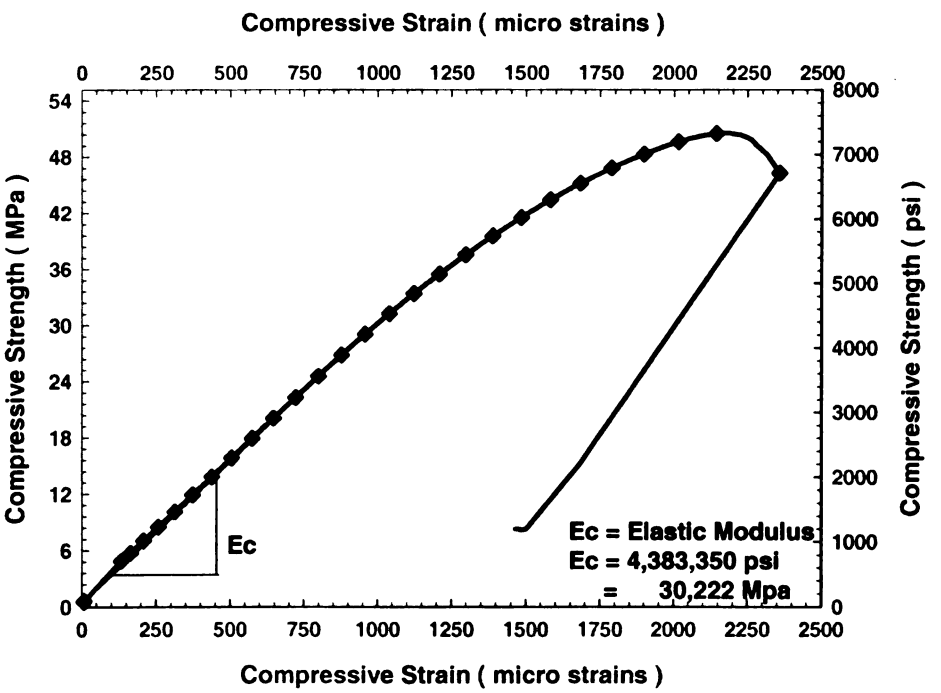

Figure A1- 16 Elastic Modulus Test – 28 Days – NCCB – Test2

Appendix 2 – Pull Out Test Response

The Pull out test was performed on the same strands used in the beam specimens. The pull out block and test procedure was similar to that proposed by Moustafa (1974) (see Chapter 6). A total of six strands were pulled out for each type of mix. Three strands were pulled out at the time of release of prestress (approximately 3 days of age) and the remaining three strands were pulled out at 7 days for all mixes.

This appendix contains the pull-out force-slip response of each of the strands of all the mix types. Firstly, the response of the pull-out test at release for all mixes is given followed by the response at 7 days. The plots are provided in the following order: SCC1, SCC2A, SCC2B, SCC3 and NCCB for both ages of concrete (release and 7 days). The combined average plots for each mix at release (3 days) and at 7 days are given at the end. Also, a combined plot of the average responses of each mix showing the peak loads at first strand slip is also given.

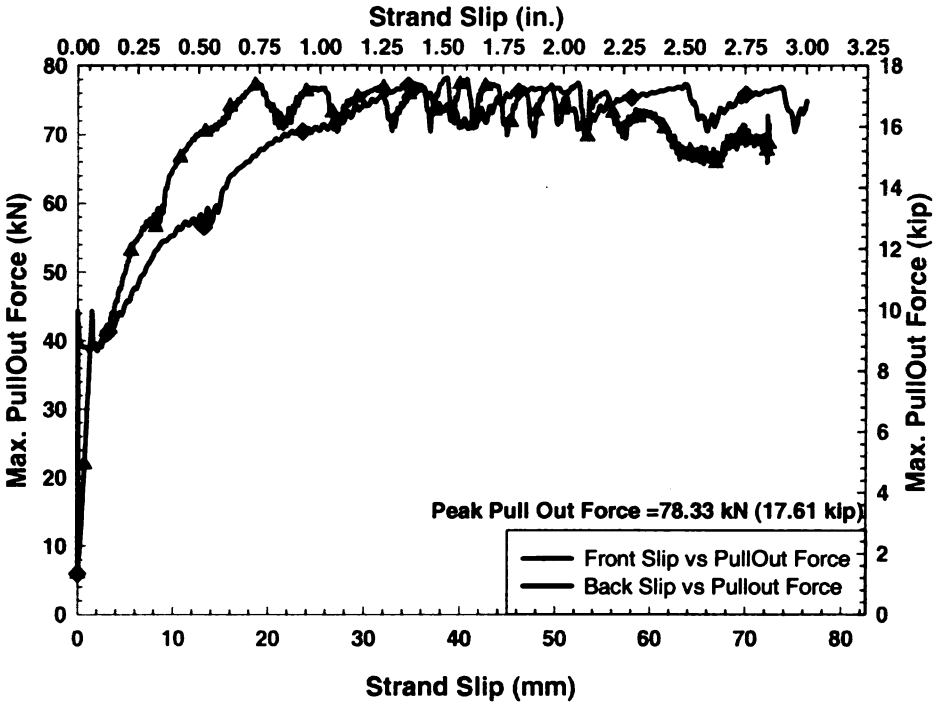

Figure A2- 1 Pull Out Test Prestress Release. – SCC1 – Strand #1

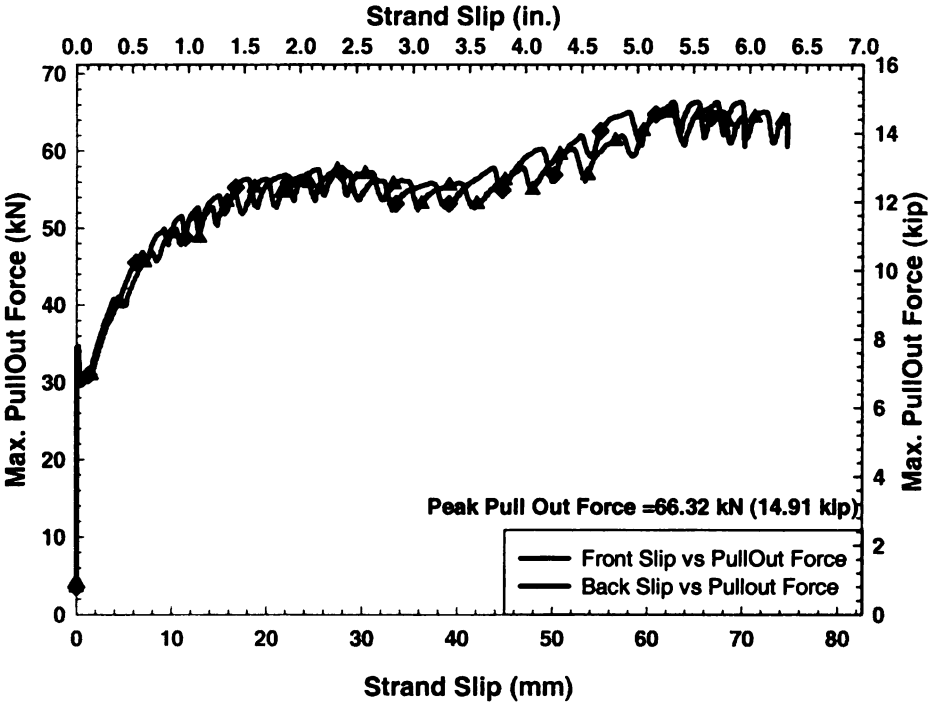

Figure A2- 2 Pull Out Test at Prestress Release. – SCC1 – Strand #2

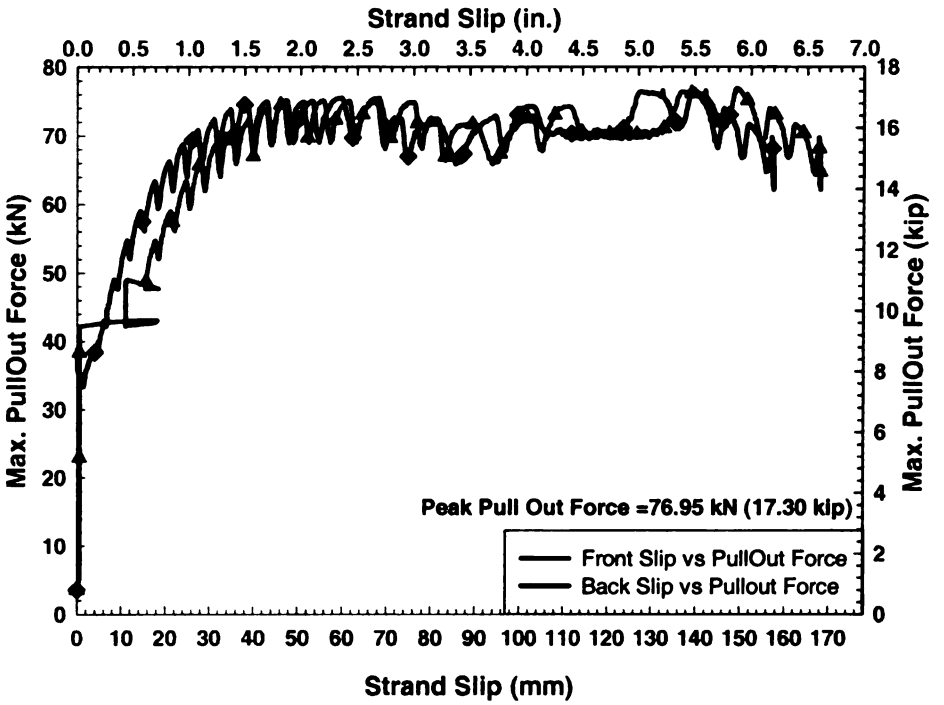

Figure A2- 3 Pull Out Test at Prestress Release. – SCC1 – Strand #3

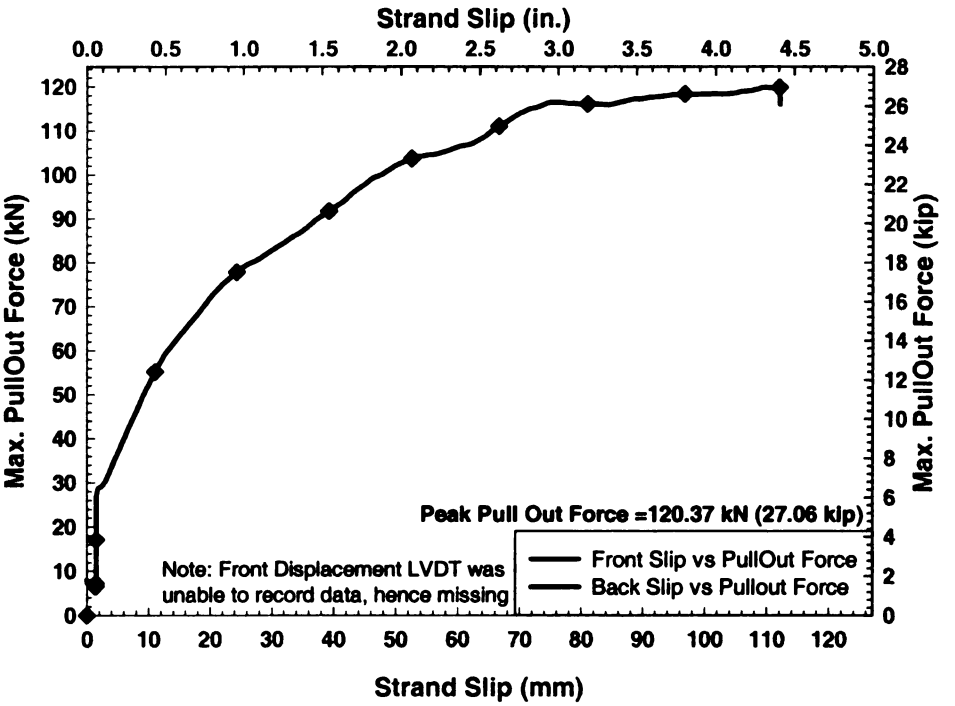

Figure A2- 4 Pull Out Test at Prestress Release – SCC2A – Strand #1

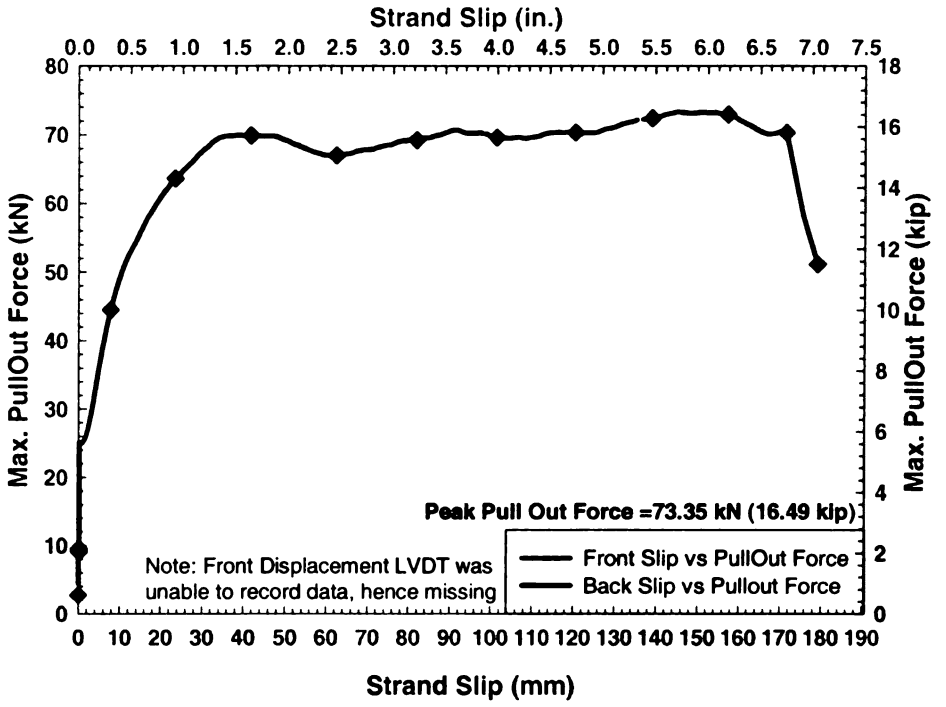

Figure A2- 5 Pull Out Test at Prestress Release. – SCC2A – Strand #2

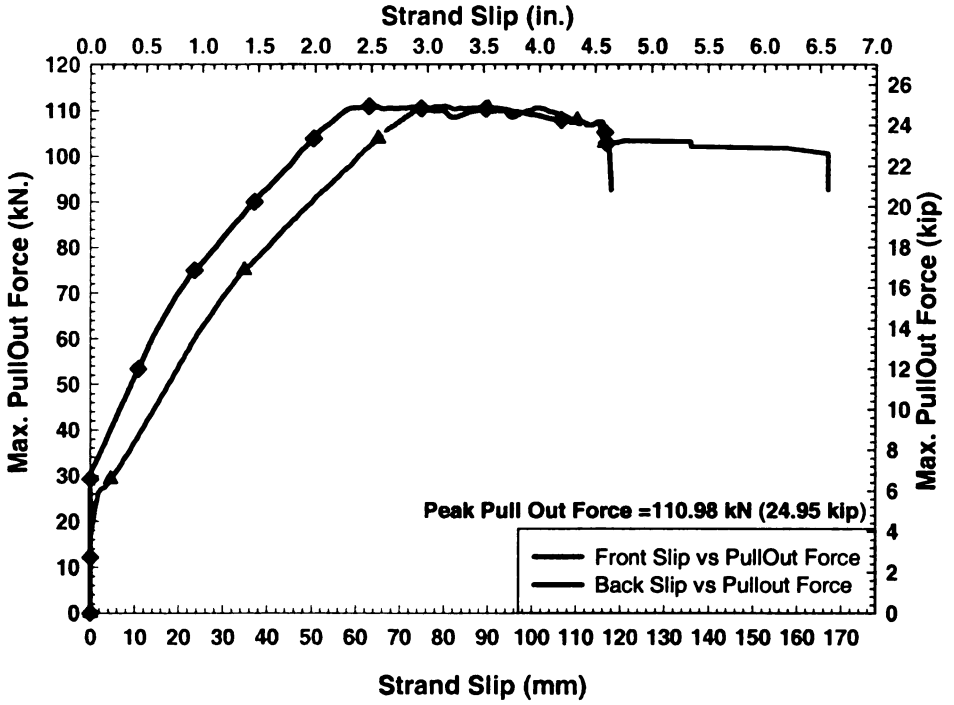

Figure A2- 6 Pull Out Test at Prestress Release – SCC2A – Strand #3

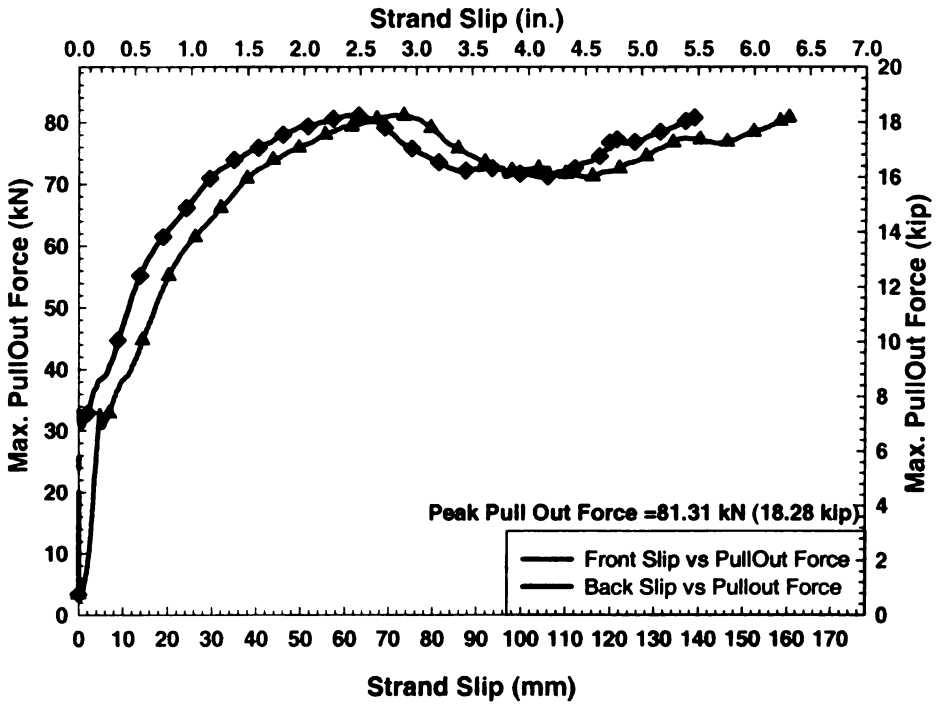

Figure A2- 7 Pull Out Test at Prestress Release. – SCC2B – Strand #1

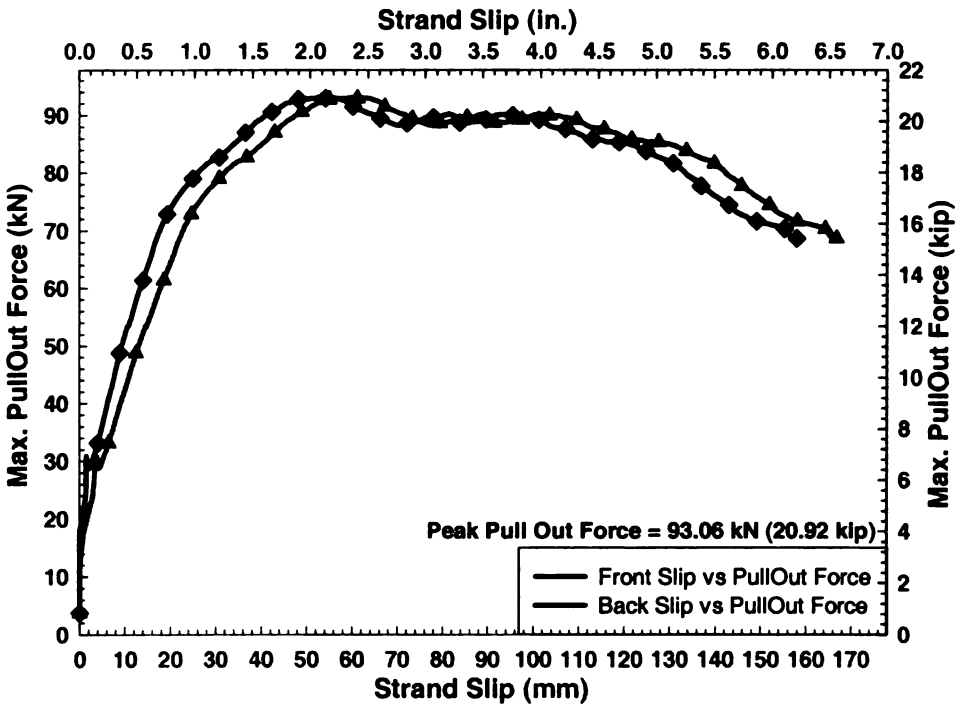

Figure A2- 8 Pull Out Test at Prestress Release. – SCC2B – Strand #2

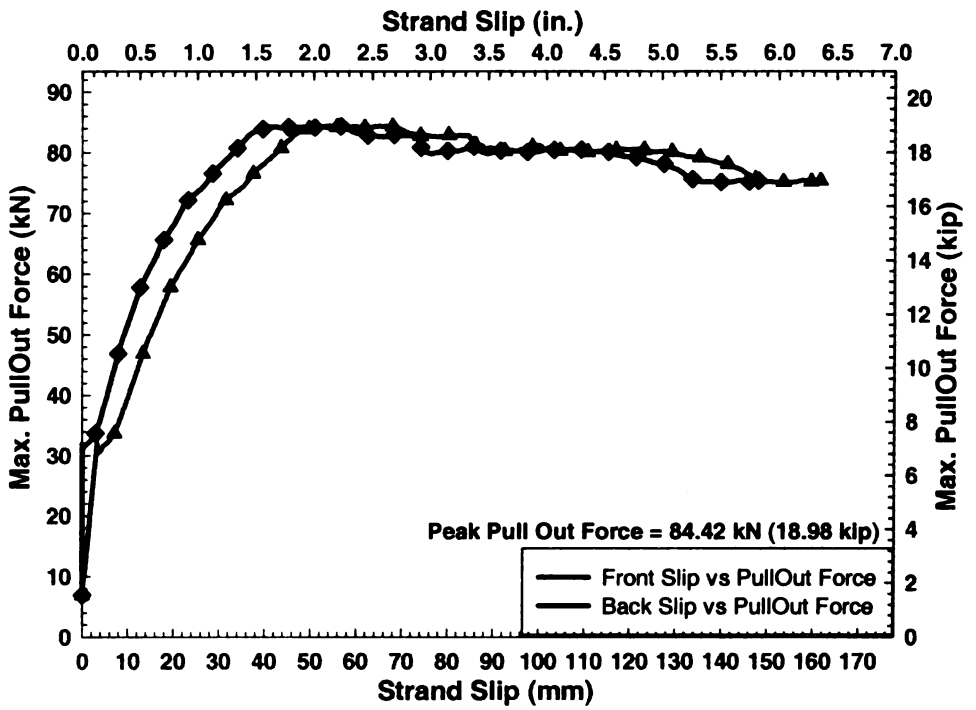

Figure A2- 9 Pull Out Test at Prestress Release. – SCC2B – Strand #3

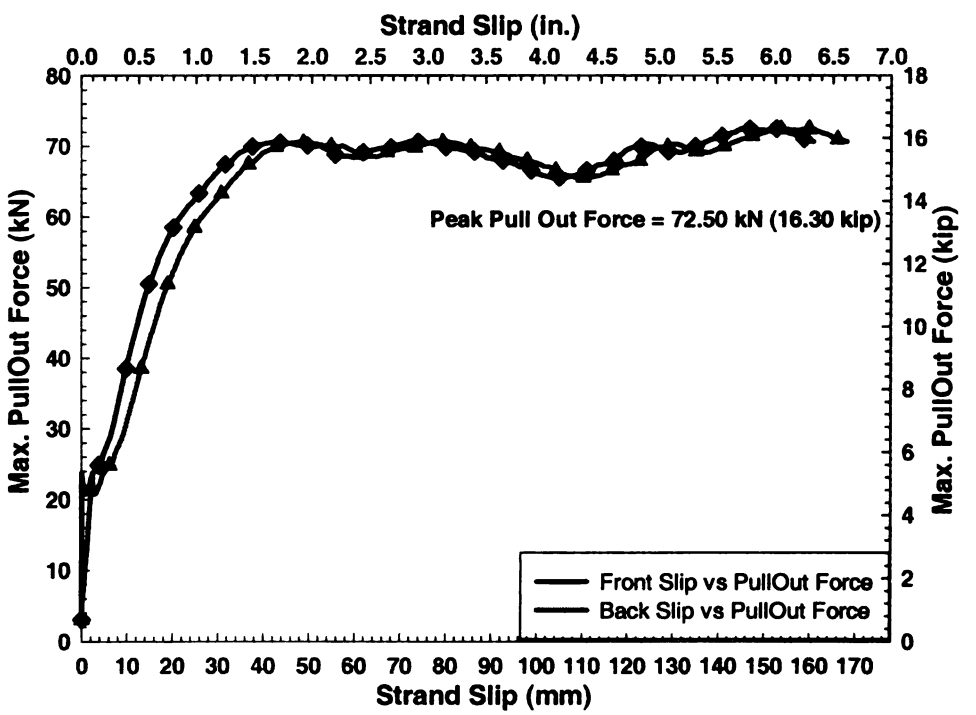

Figure A2- 10 Pull Out Test at Prestress Release.. – SCC3 – Strand #1

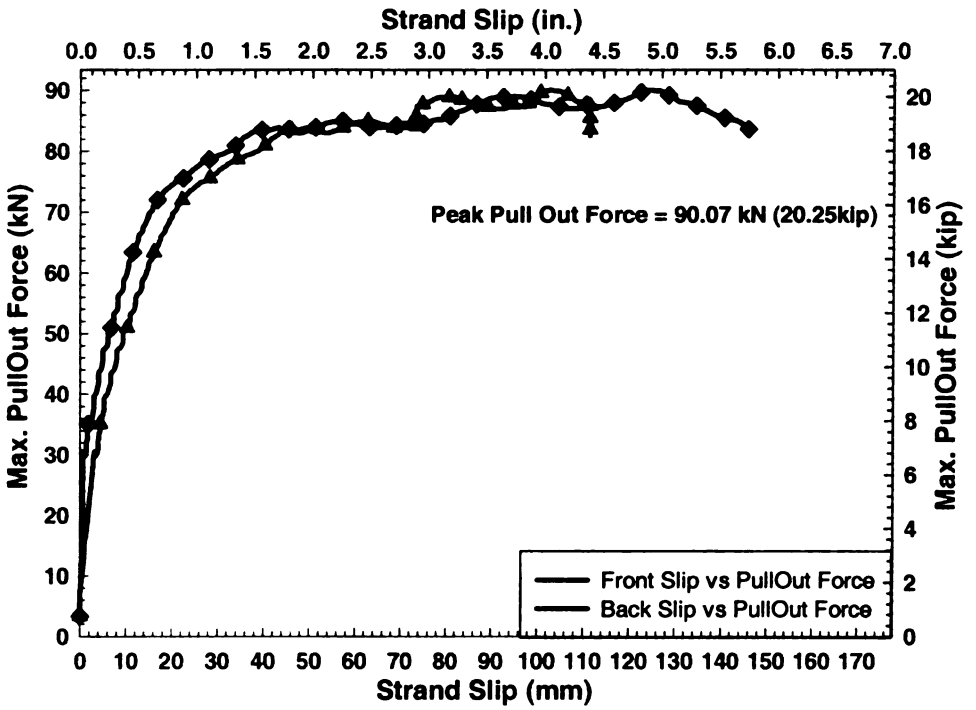

Figure A2- 11 Pull Out Test at Prestress Release. – SCC3 – Strand #2

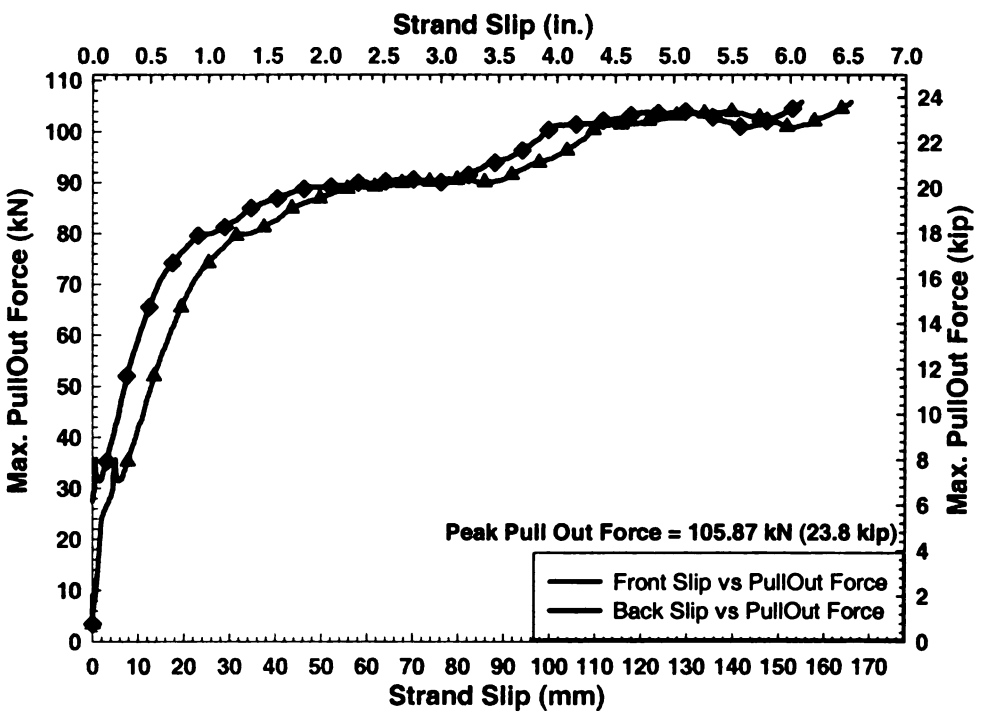

Figure A2- 12 Pull Out Test at Prestress Release. – SCC3 – Strand #3

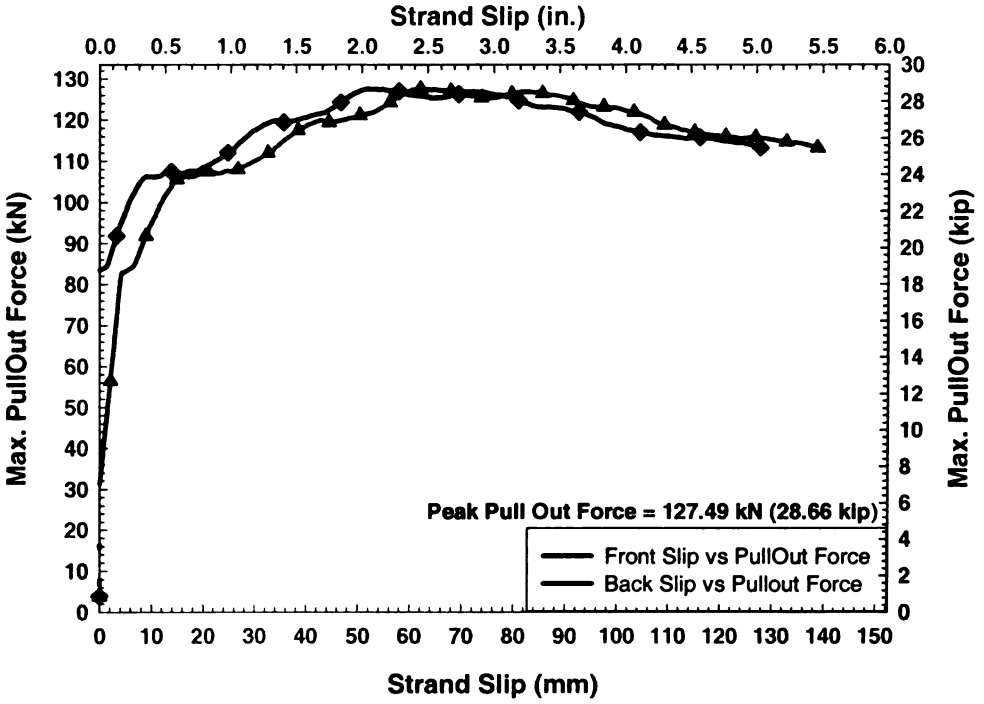

Figure A2- 13 Pull Out Test at Prestress Release. – NCCB – Strand #1

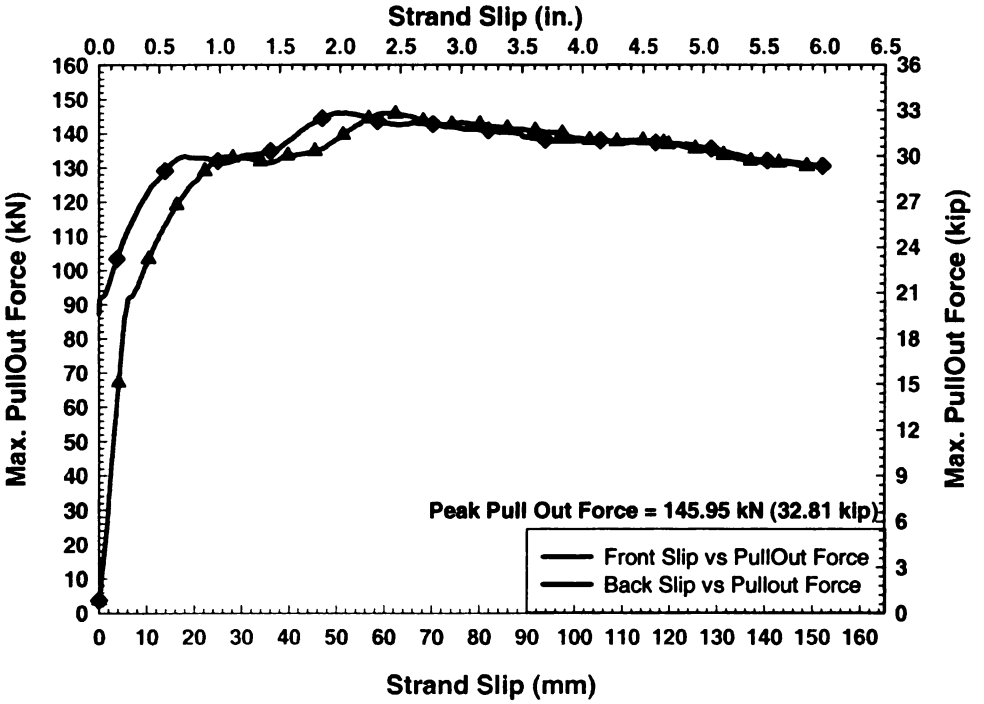

Figure A2- 14 Pull Out Test at Prestress Release. – NCCB – Strand #2

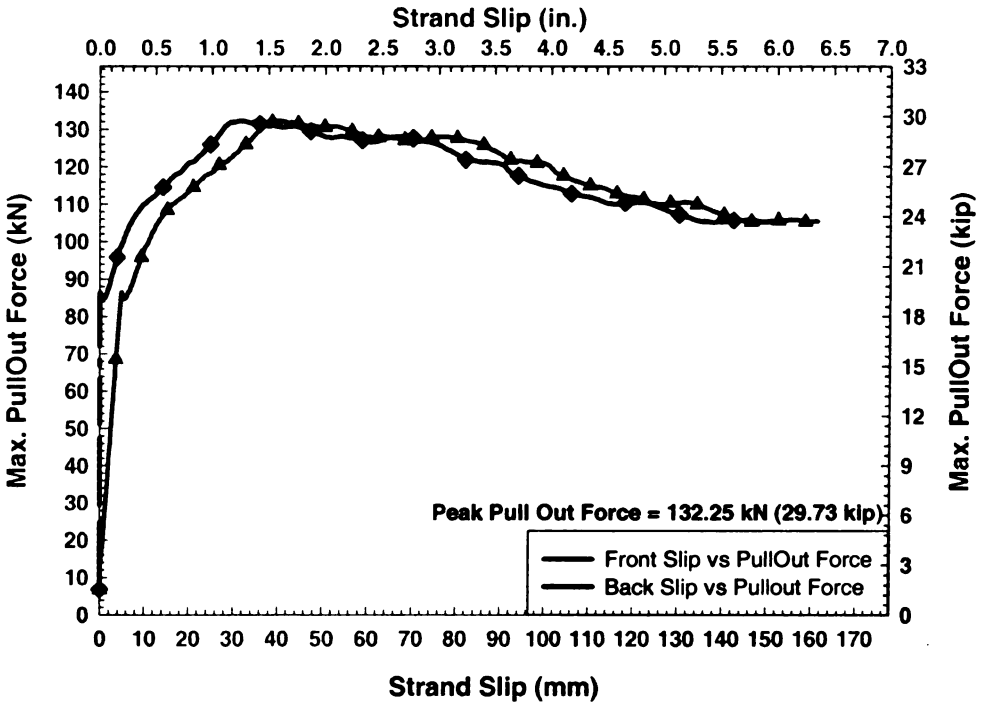

Figure A2- 15 Pull Out Test at Prestress Release. – NCCB – Strand #3

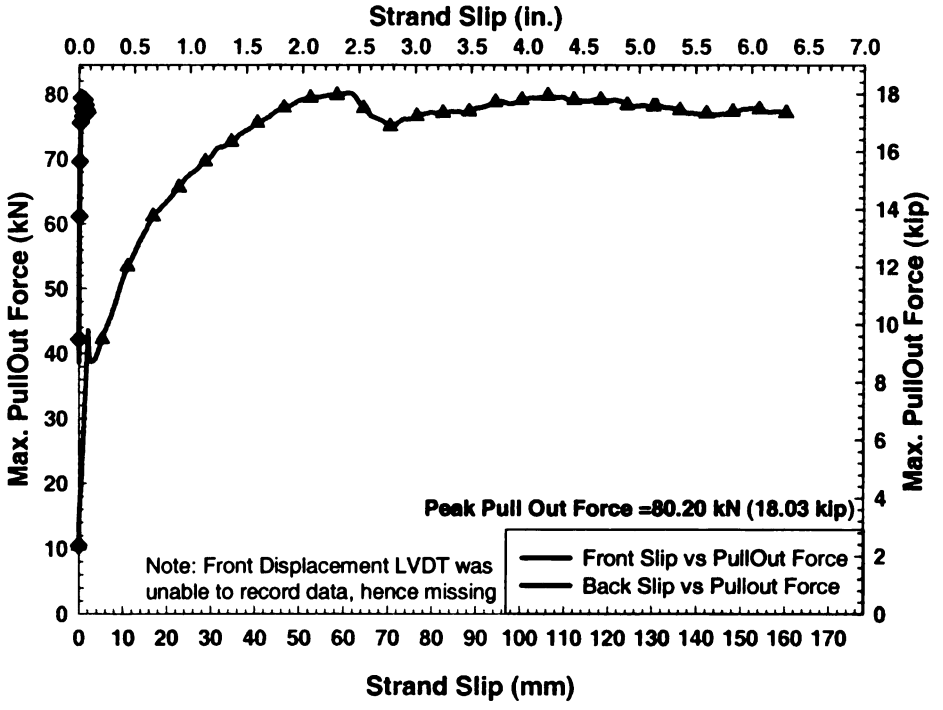

Figure A2- 16 Pull Out Test at 7 Days – SCC1 – Strand #4

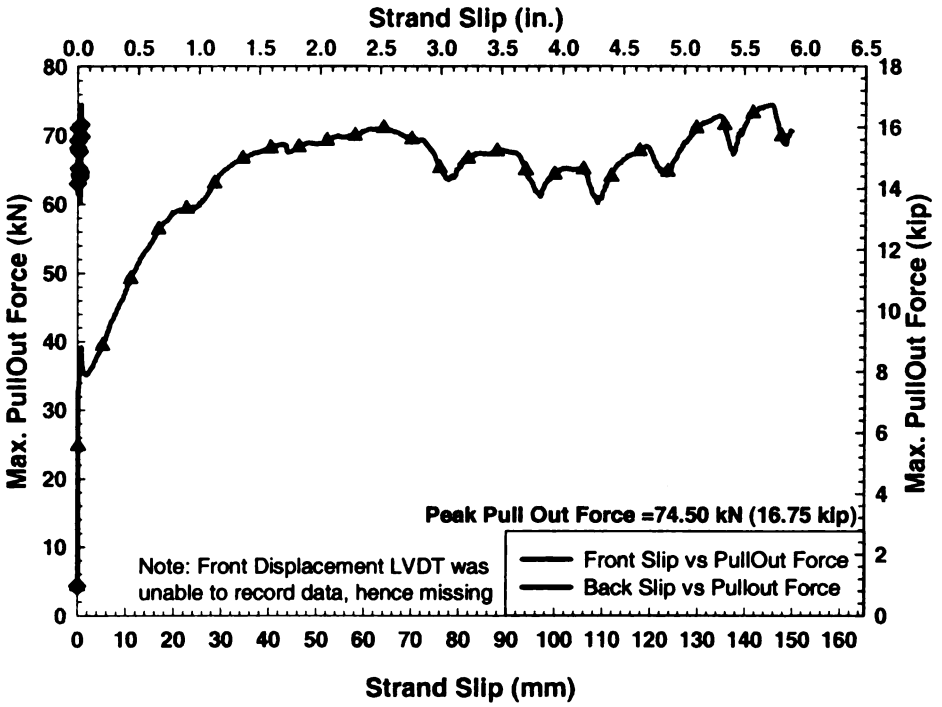

Figure A2- 17 Pull Out Test at 7 Days – SCC1 – Strand #5

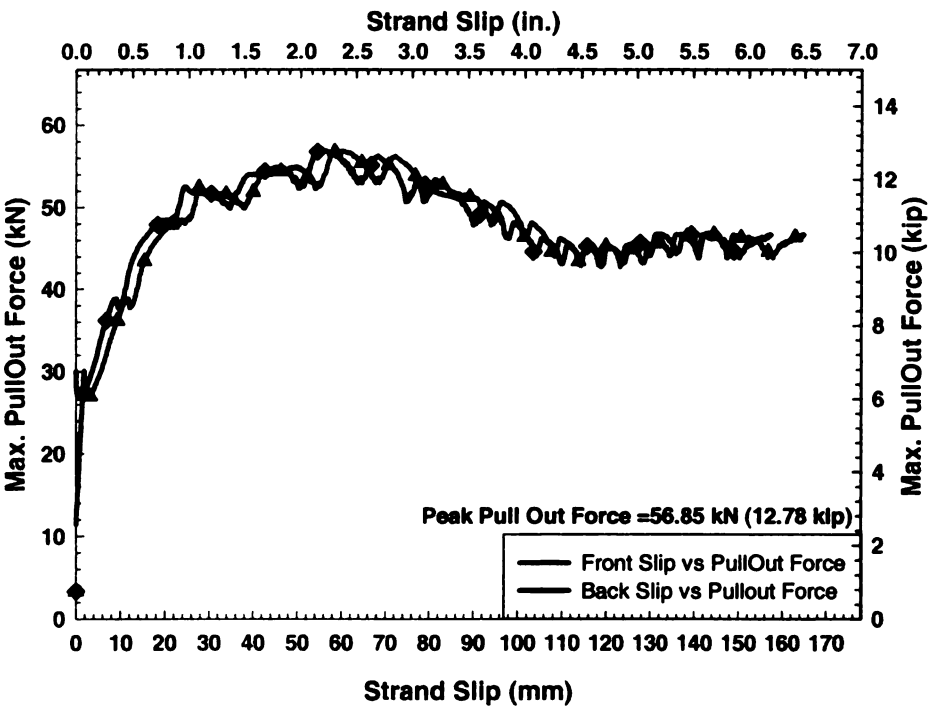

Figure A2- 18 Pull Out Test at 7 Days – SCC1 – Strand #6

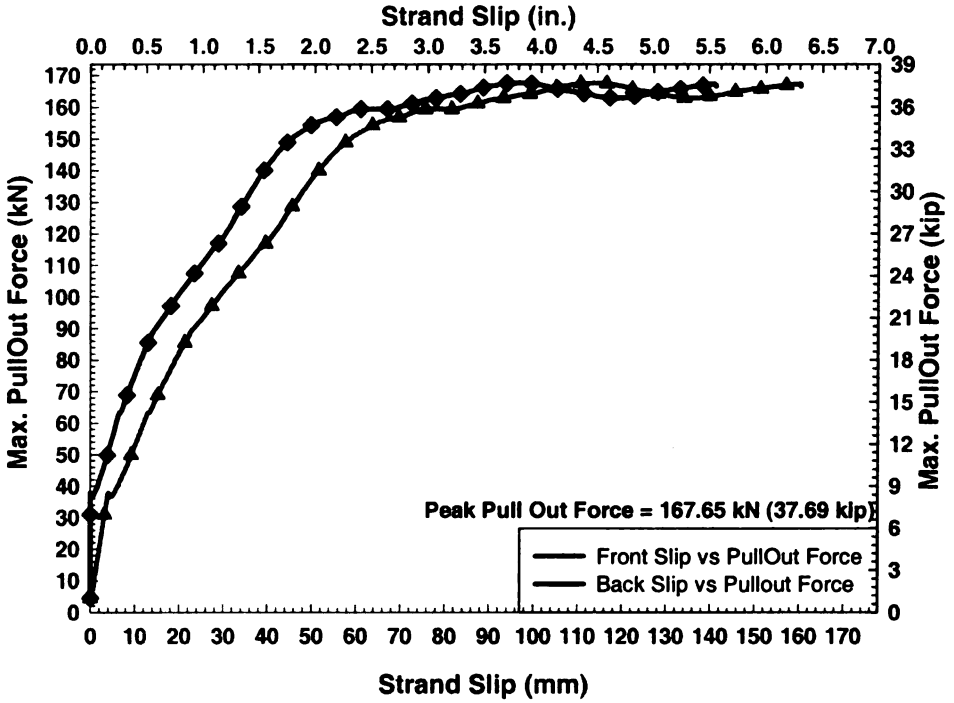

Figure A2- 19 Pull Out Test at 7 Days – SCC2A – Strand #4

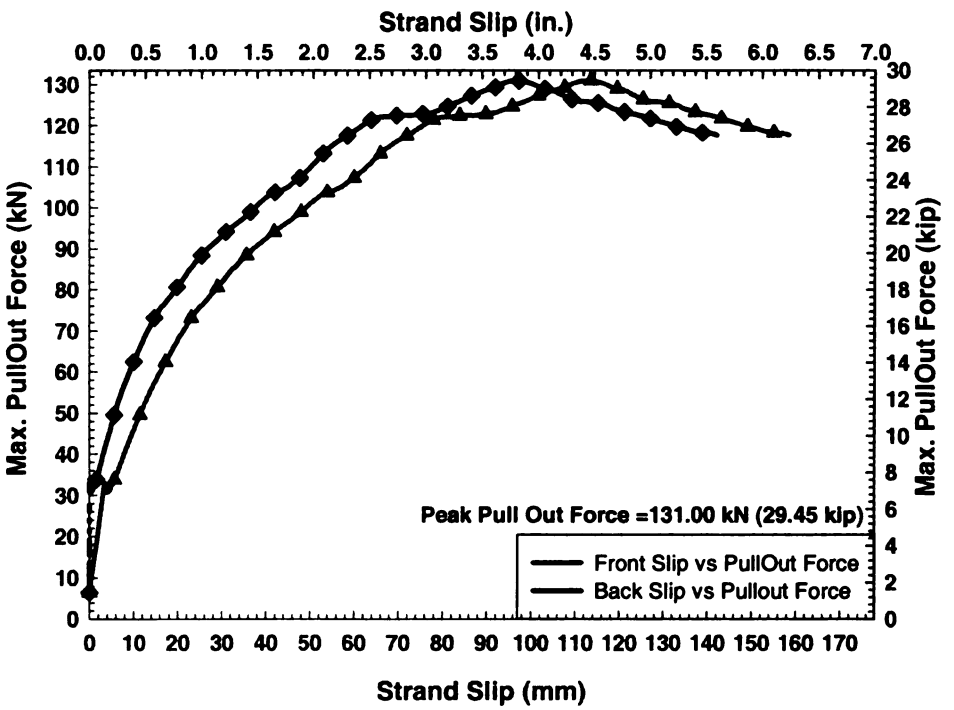

Figure A2- 20 Pull Out Test at 7 Days – SCC2A – Strand #5

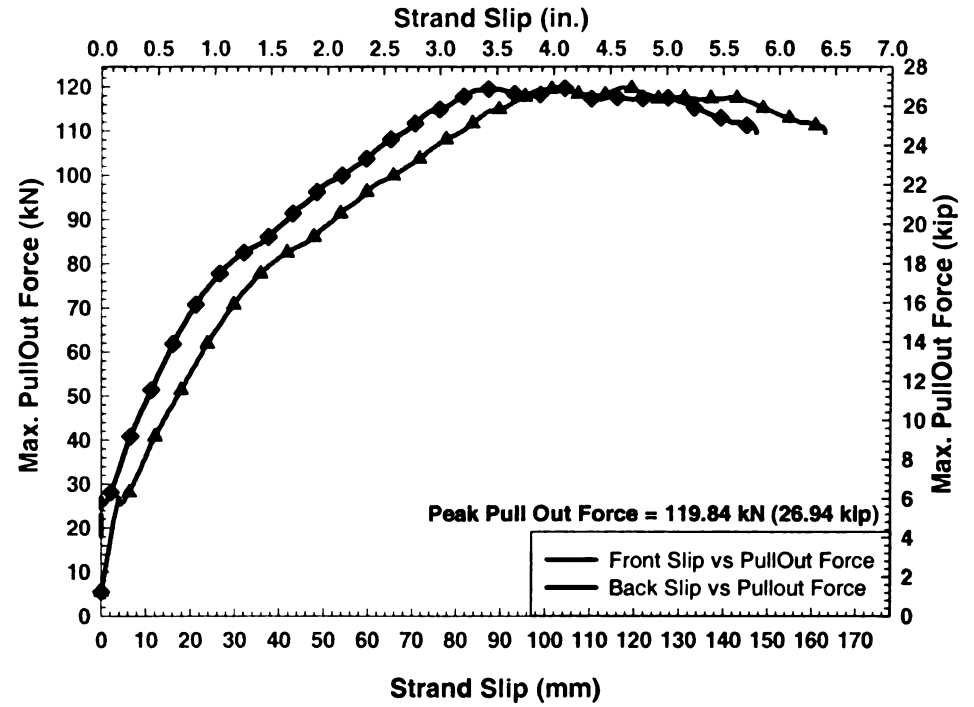

Figure A2- 21 Pull Out Test at 7 Days – SCC2A – Strand #6

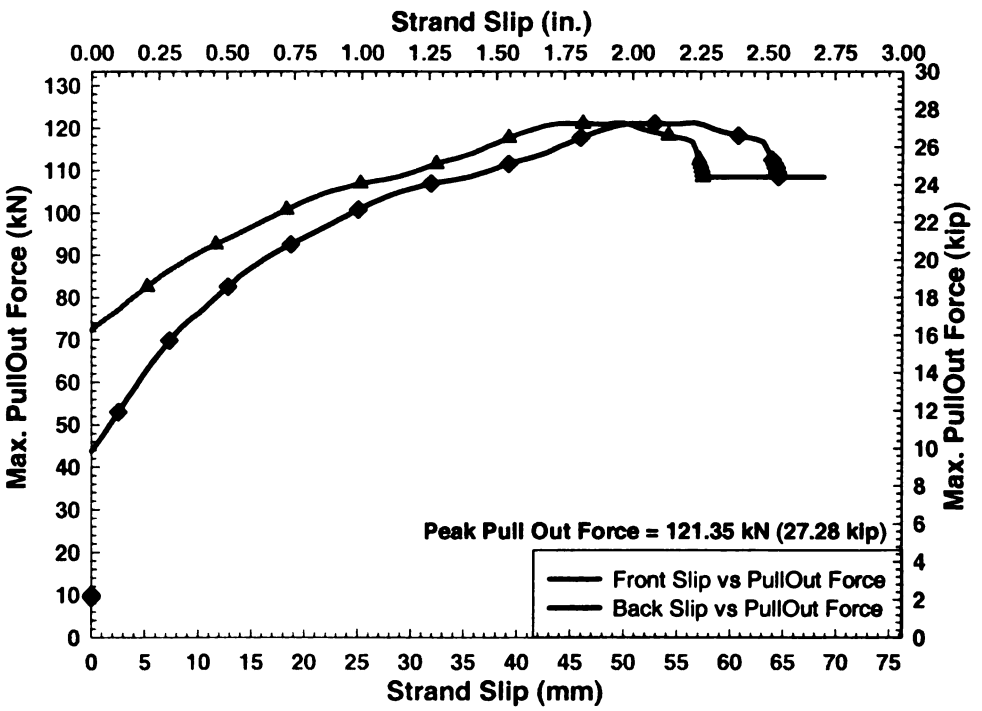

Figure A2- 22 Pull Out Test at 7 Days – SCC2B – Strand #4

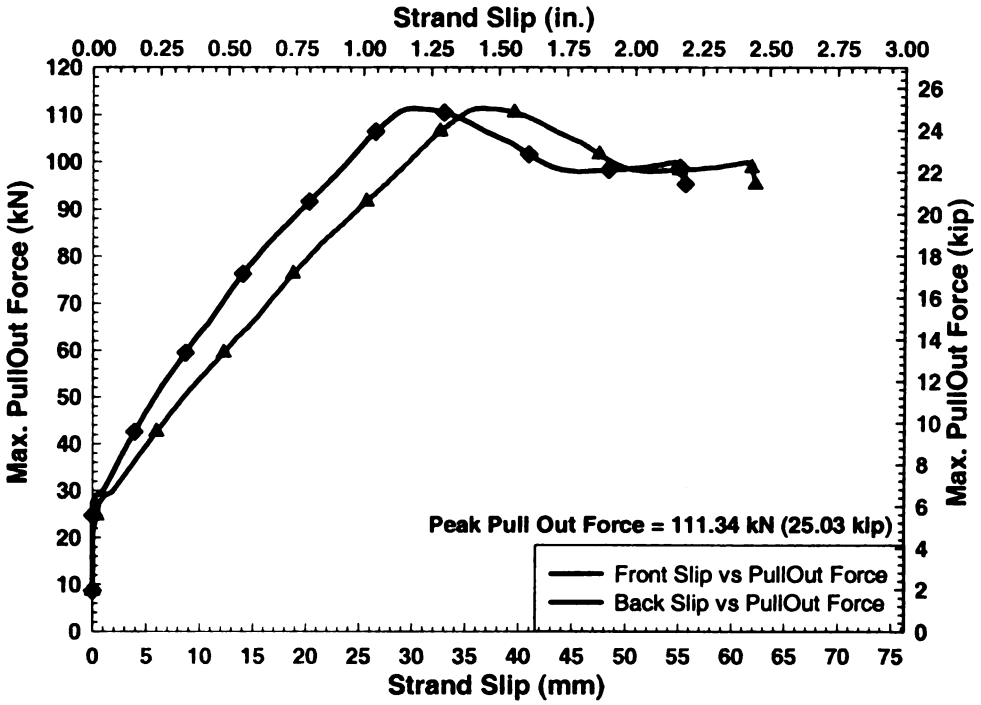

Figure A2- 23 Pull Out Test at 7 Days – SCC2B – Strand #5

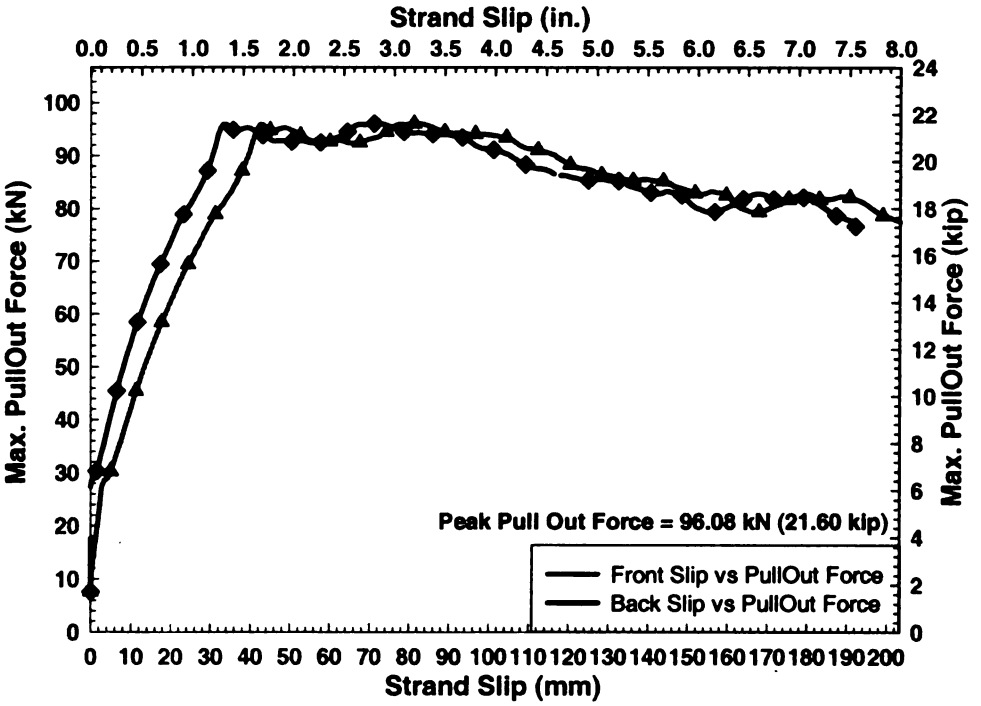

Figure A2- 24 Pull Out Test at 7 Days – SCC2B – Strand #6

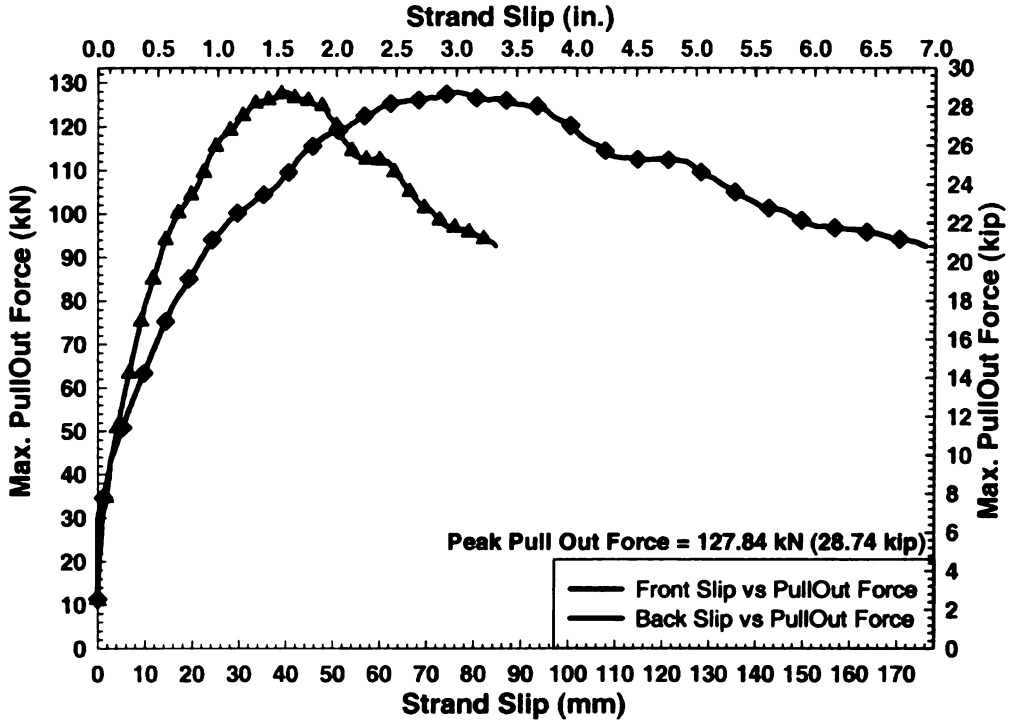

Figure A2- 25 Pull Out Test at 7 Days – SCC3 – Strand #4

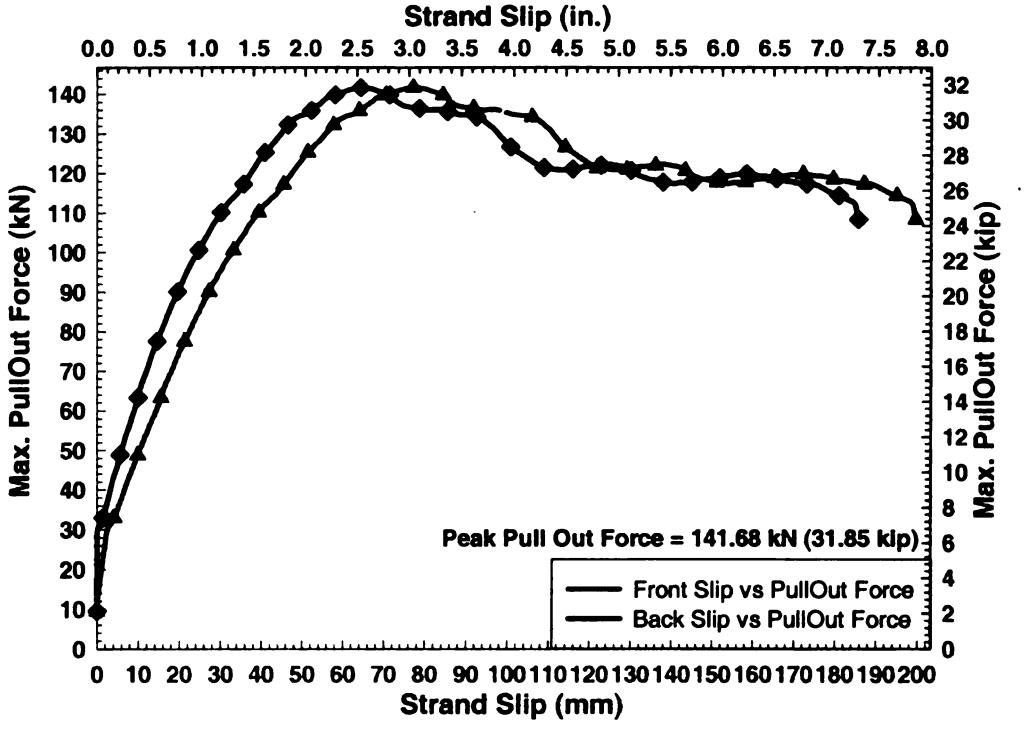

Figure A2- 26 Pull Out Test at 7 Days – SCC3 – Strand #5

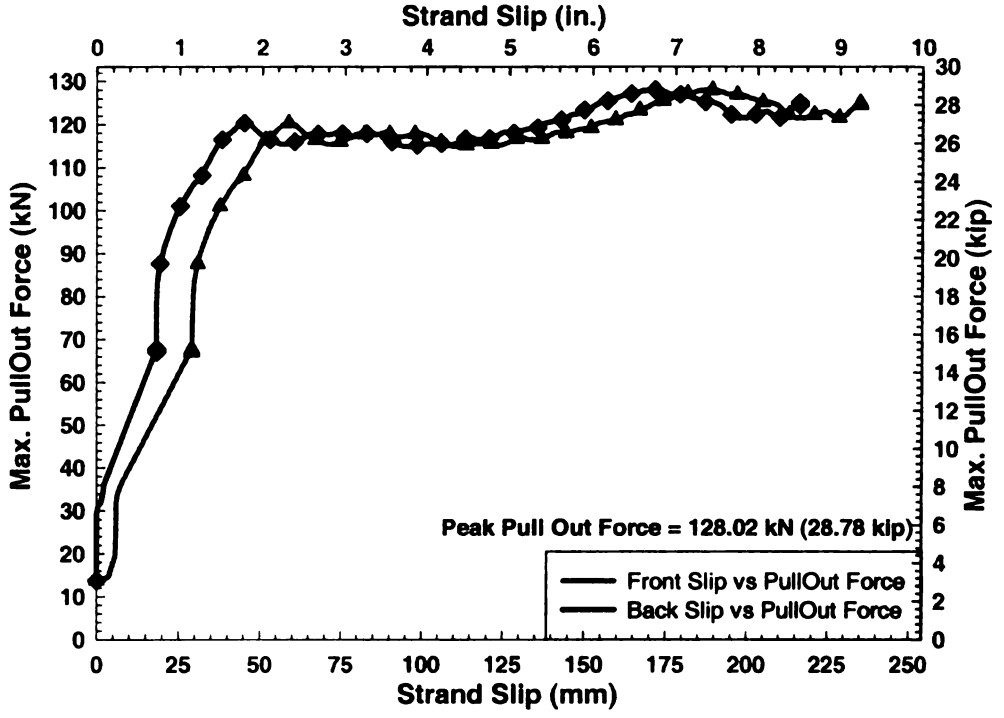

Figure A2- 27 Pull Out Test at 7 Days – SCC3 – Strand #6

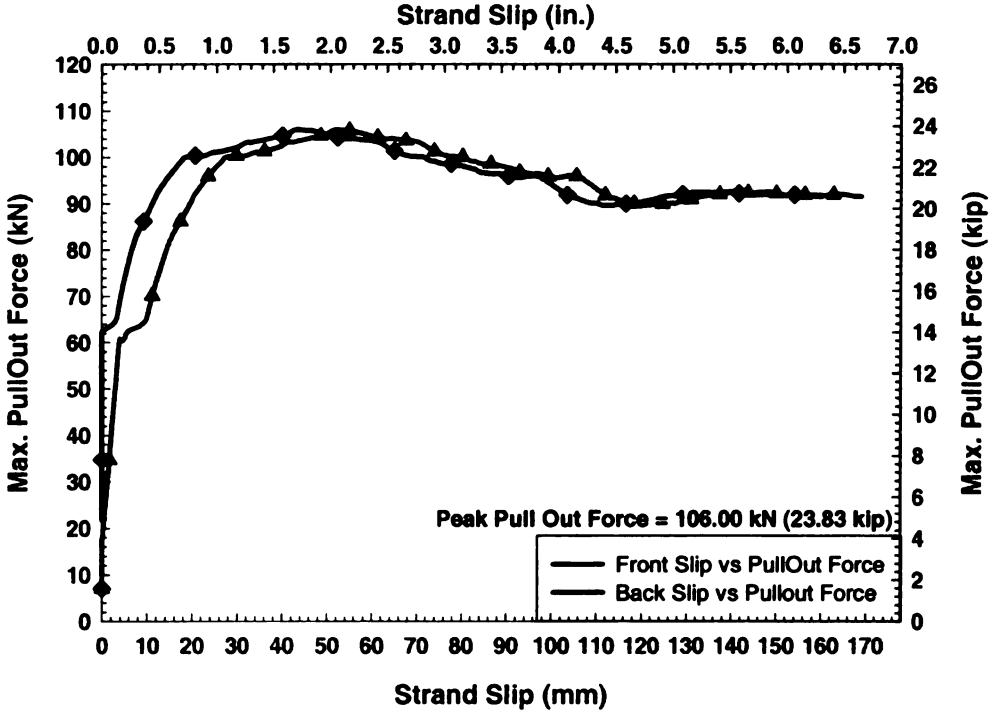

Figure A2- 28 Pull Out Test at 7 Days – NCCB – Strand #4

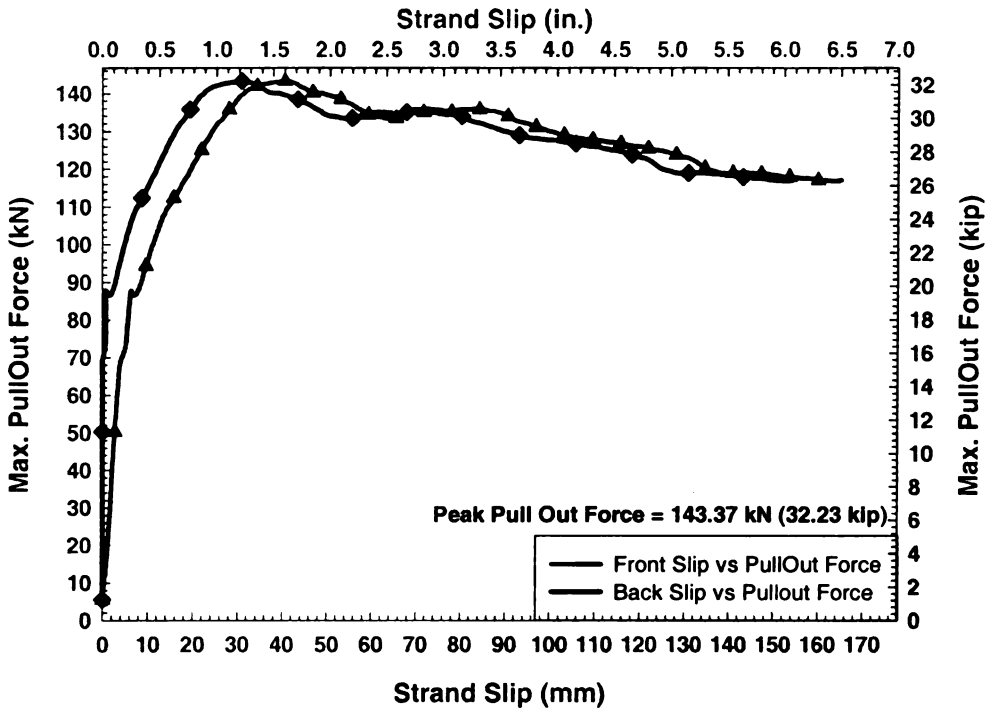

Figure A2- 29 Pull Out Test at 7 Days – NCCB – Strand #5

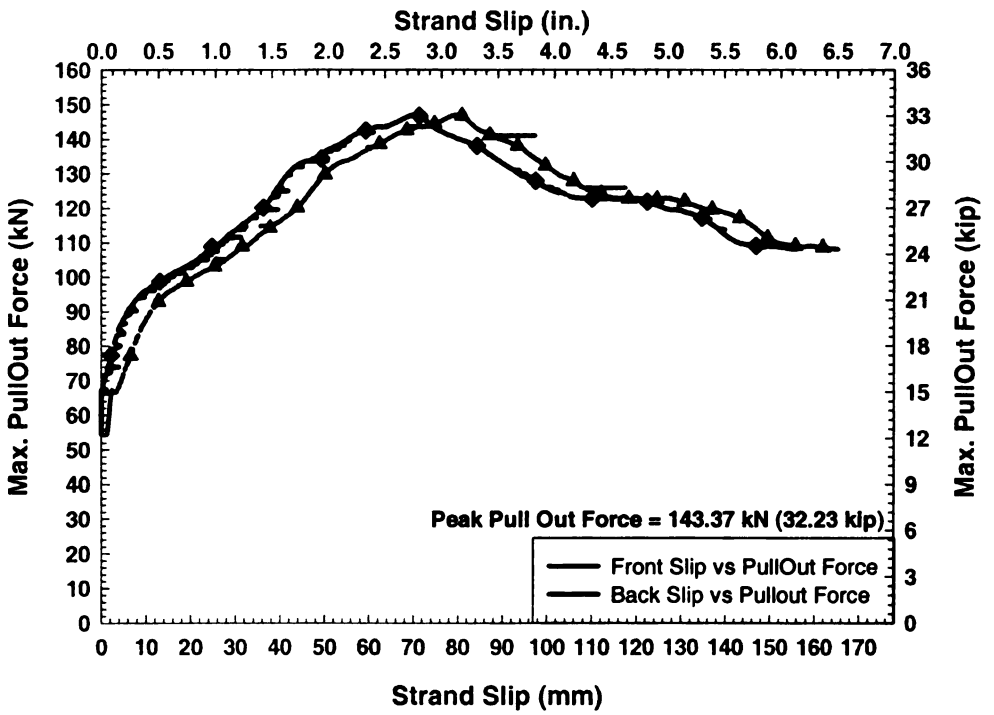

Figure A2- 30 Pull Out Test at 7 Days – NCCB – Strand #6

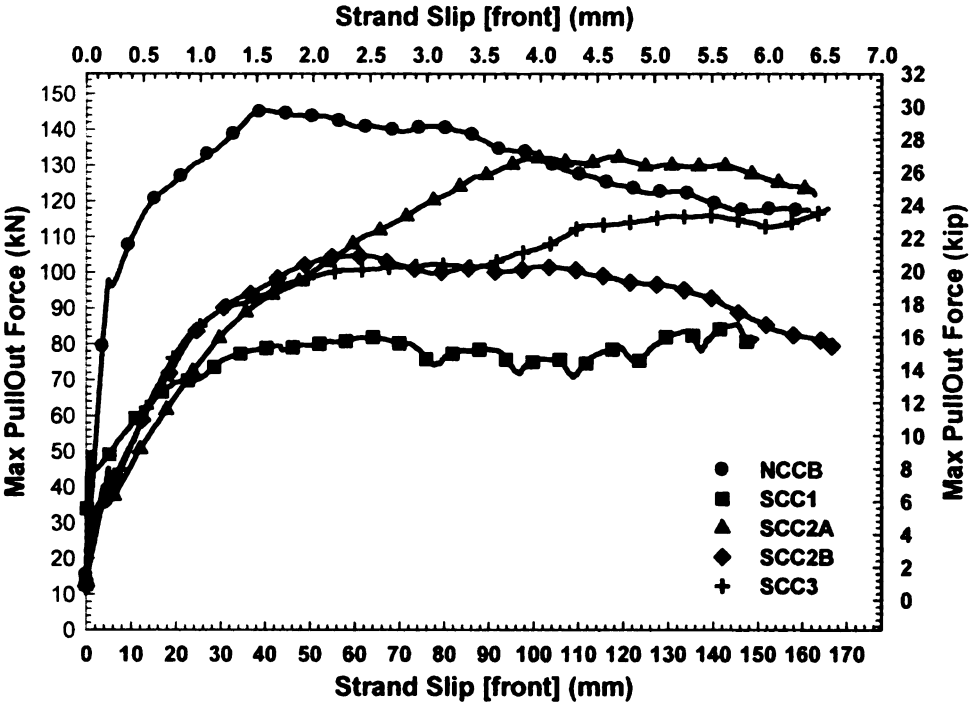

Figure A2- 31 Combined Average Pull-out Test response – At 3 Days

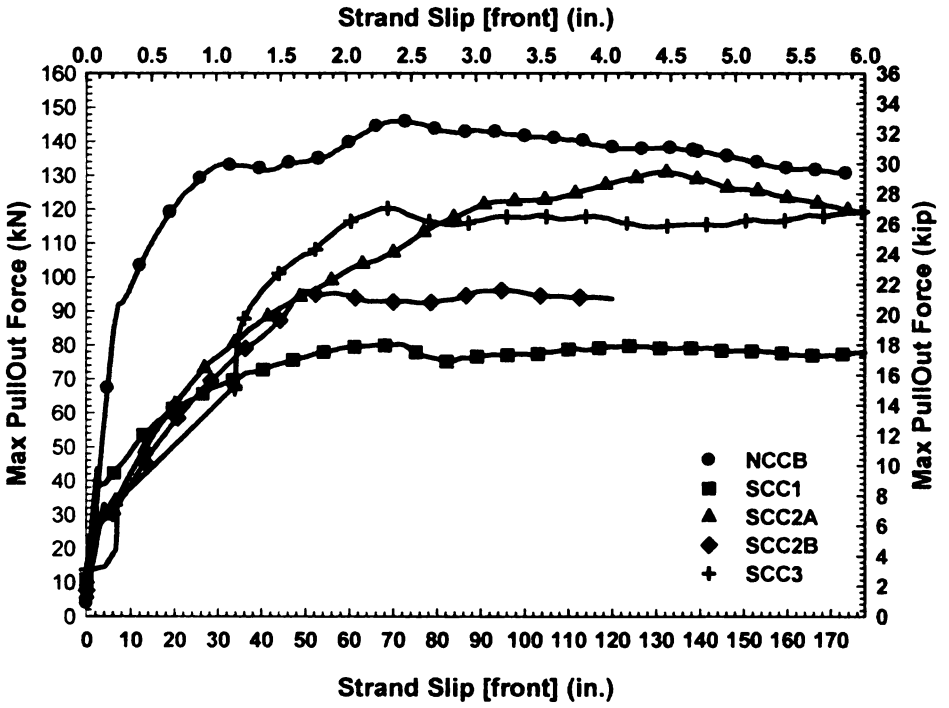

Figure A2- 32 Combined Average Pull-out Test response – At 7 Days

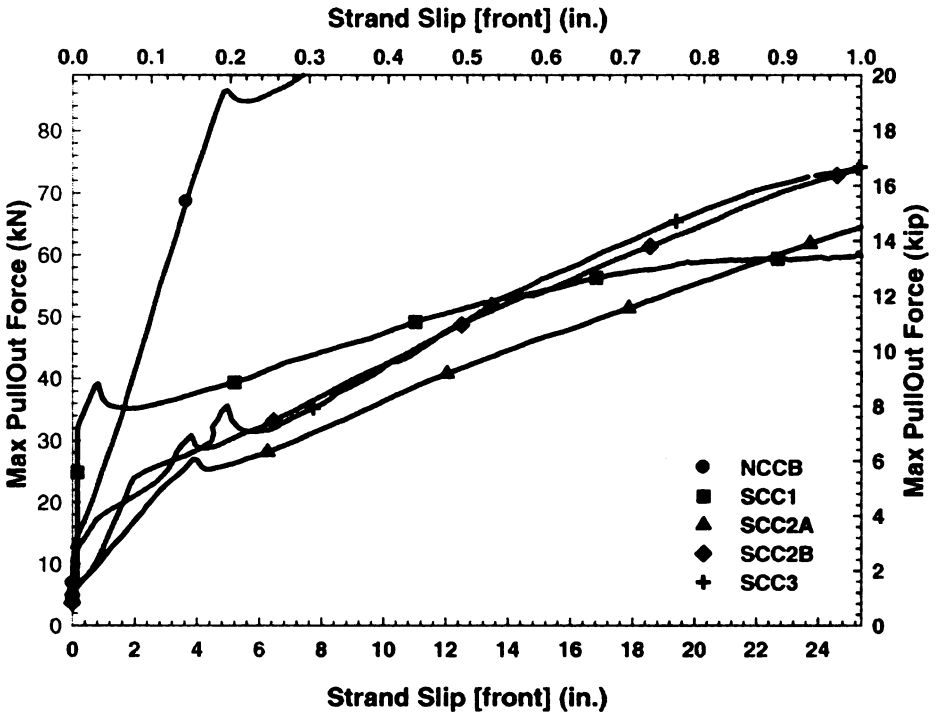

Figure A2- 33 Combined Average First Slip - Pull-out Test Response – At 3 Days

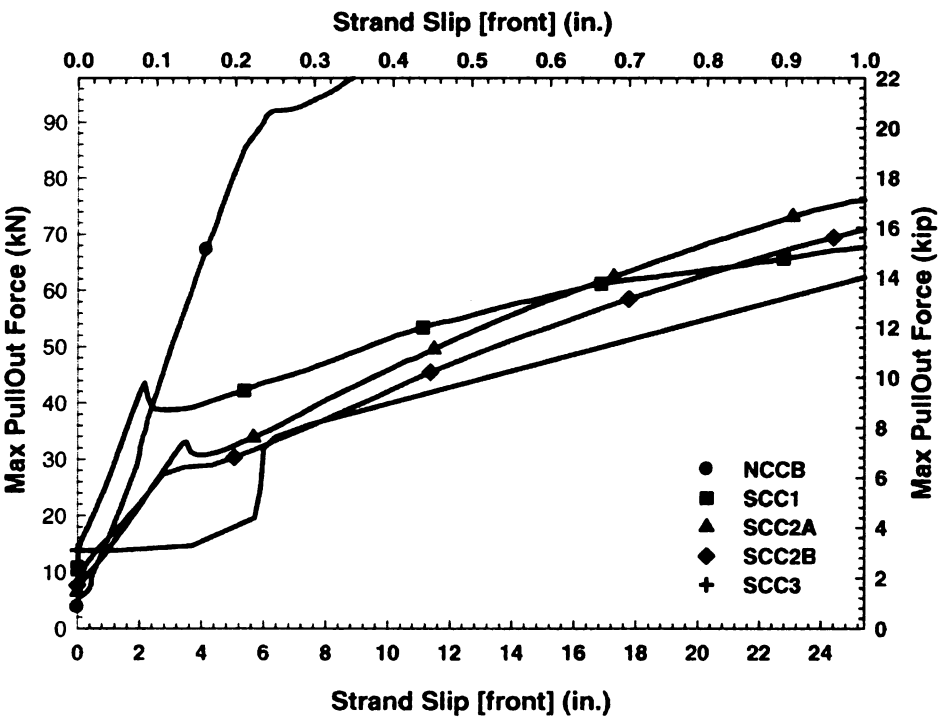

Figure A2- 34 Combined Average First Slip - Pull-out Test Response – At 7 Days

Appendix 3 - Transfer Length – Concrete Strain Profiles

The transfer length measurement was done using two methods: a) concrete strain profiles (95% average maximum strain method) and b) draw-in measurements. This section includes the plots for concrete strain profiles for each test specimen. The concrete strain profiles were measured on both the sides of the test specimen. Two trials of readings were taken on each side. A total of 8 plots were obtained for each test specimen. Only the average of the eight plots (each test specimen) are provided here. Two specimens per mix type were cast. The average of the concrete strain profiles for both of the beams cast per mix (average of 16 profiles, each mix type) were given in Chapter 6. The concrete strain profiles for each beam (average of 8) for various mix types are given in this section in the following order: SCC1, SCC2A, SCC2B, SCC3 and NCCB.

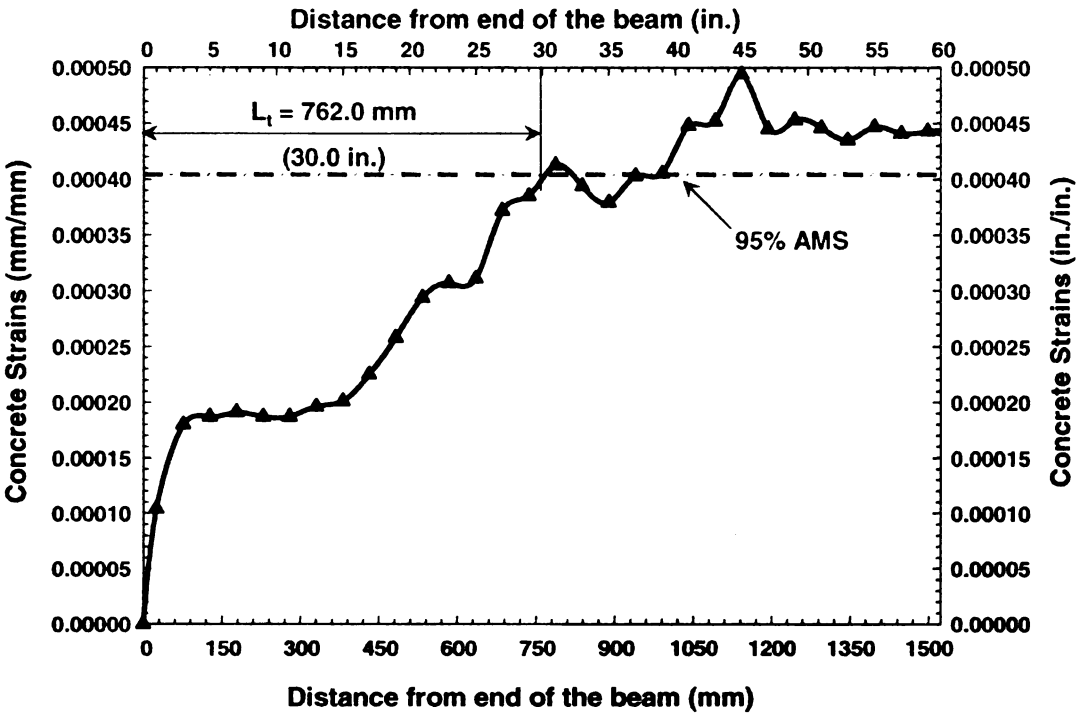

Figure A3 - 1 Concrete Strain Profile – SCC1 – Beam1

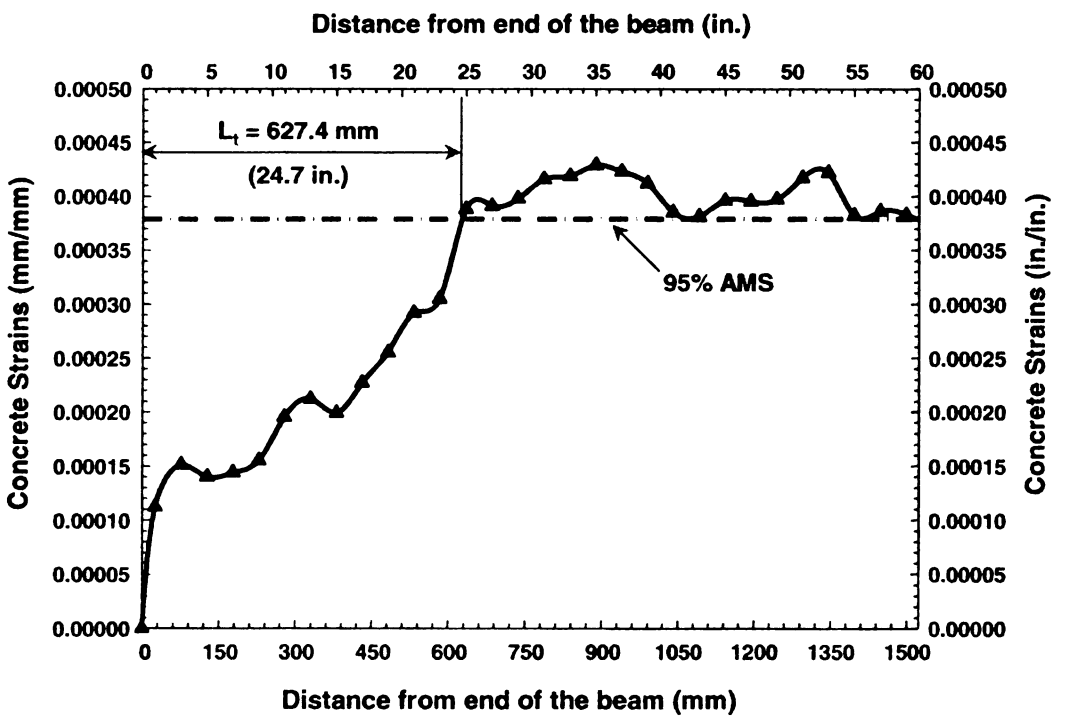

Figure A3 - 2 Concrete Strain Profile – SCC1 – Beam2

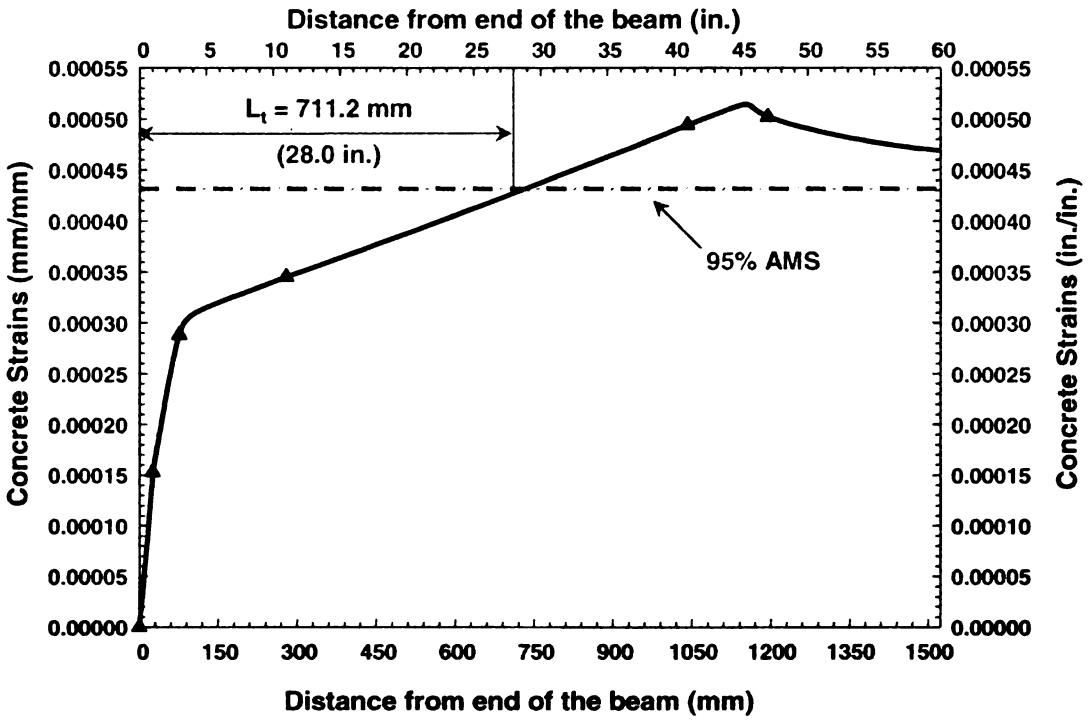

Figure A3 - 3 Concrete Strain Profile – SCC2A – Beam1

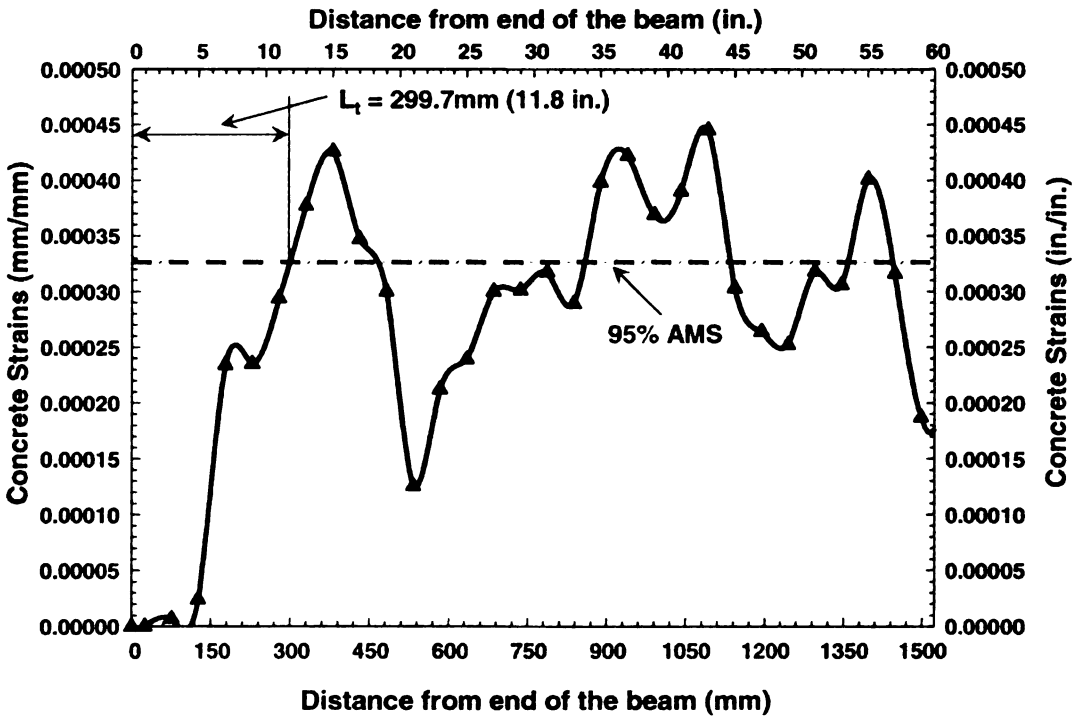

Figure A3 - 4 Concrete Strain Profile – SCC2A – Beam2

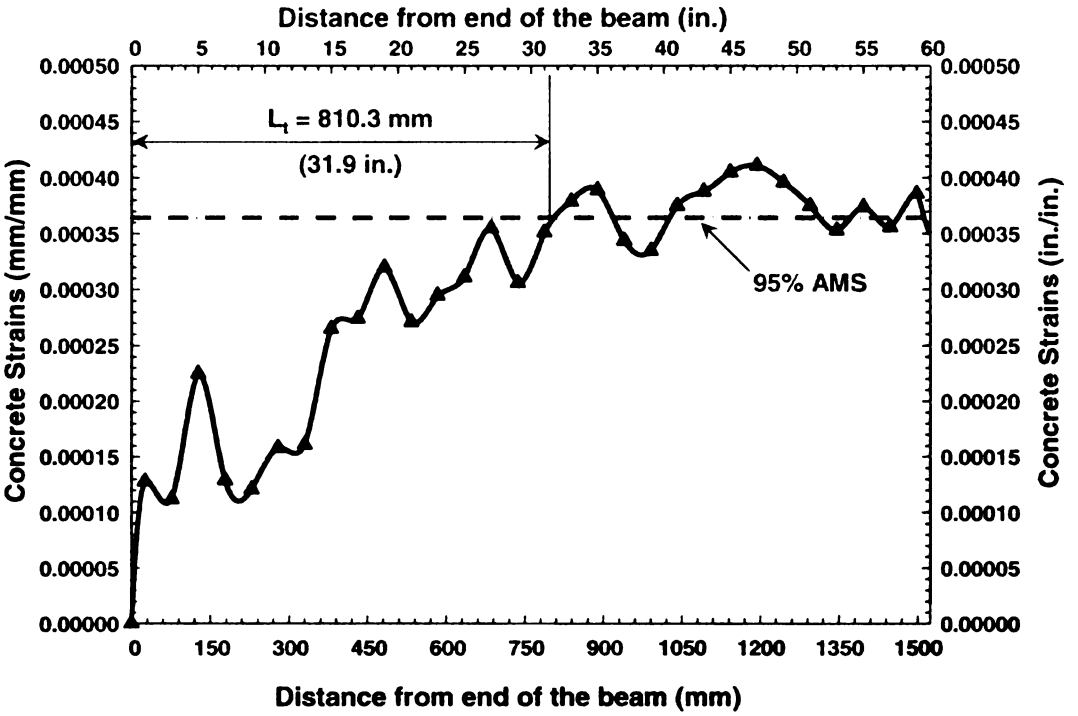

Figure A3 - 5 Concrete Strain Profile – SCC2B – Beam1

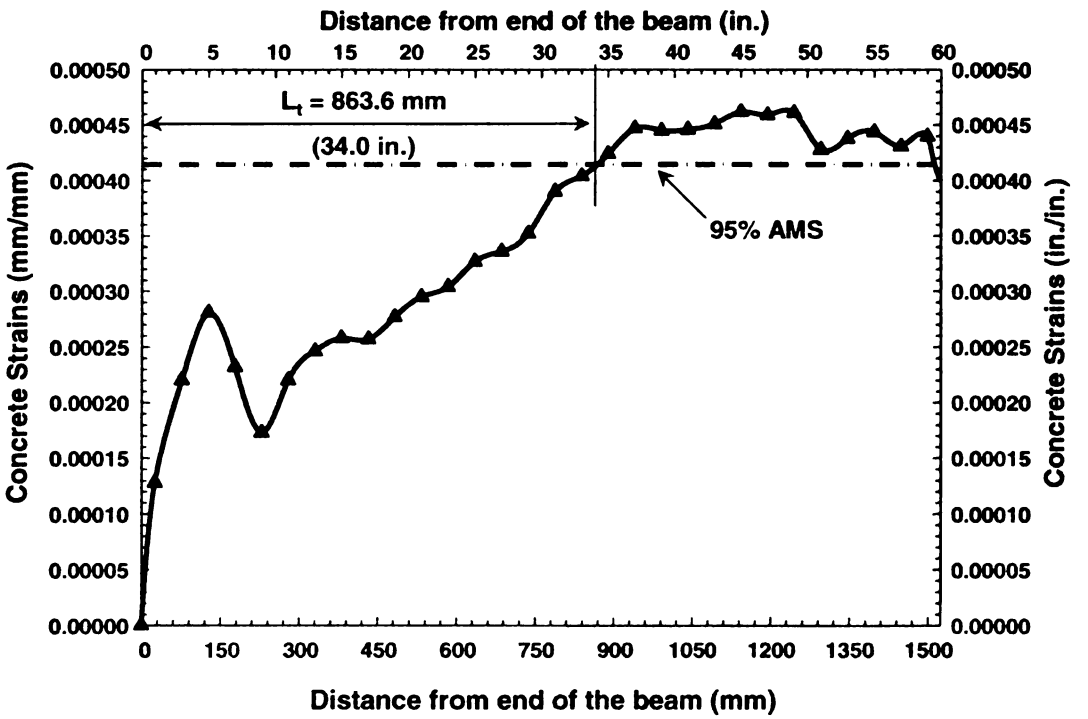

Figure A3 - 6 Concrete Strain Profile – SCC2B – Beam2

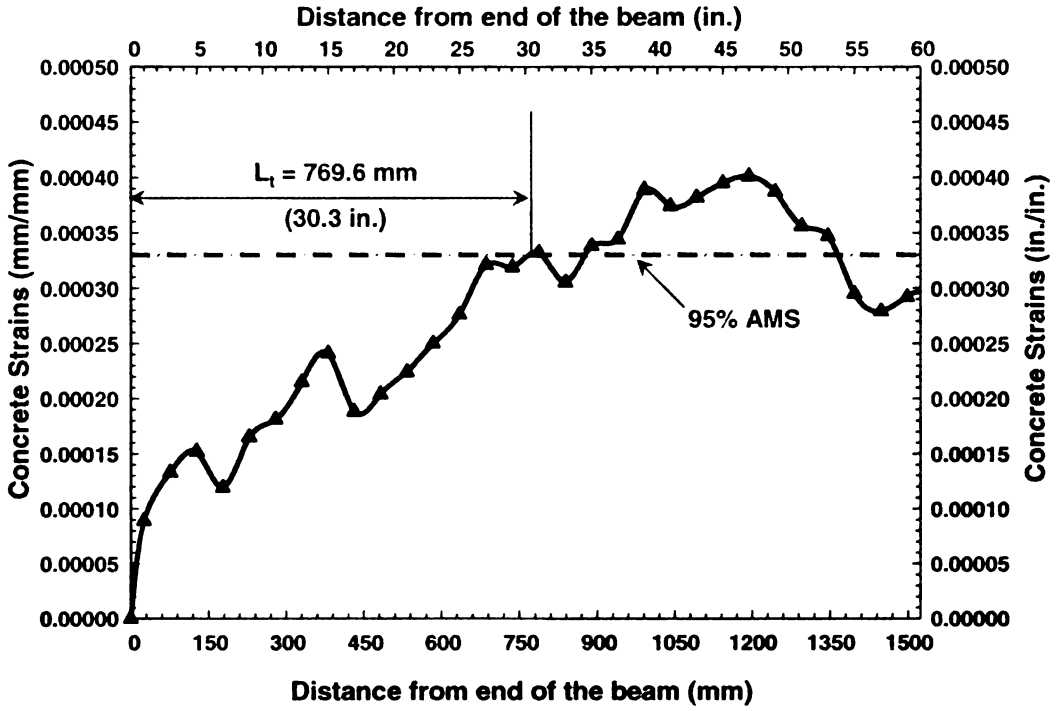

Figure A3 - 7 Concrete Strain Profile – SCC3 – Beam1

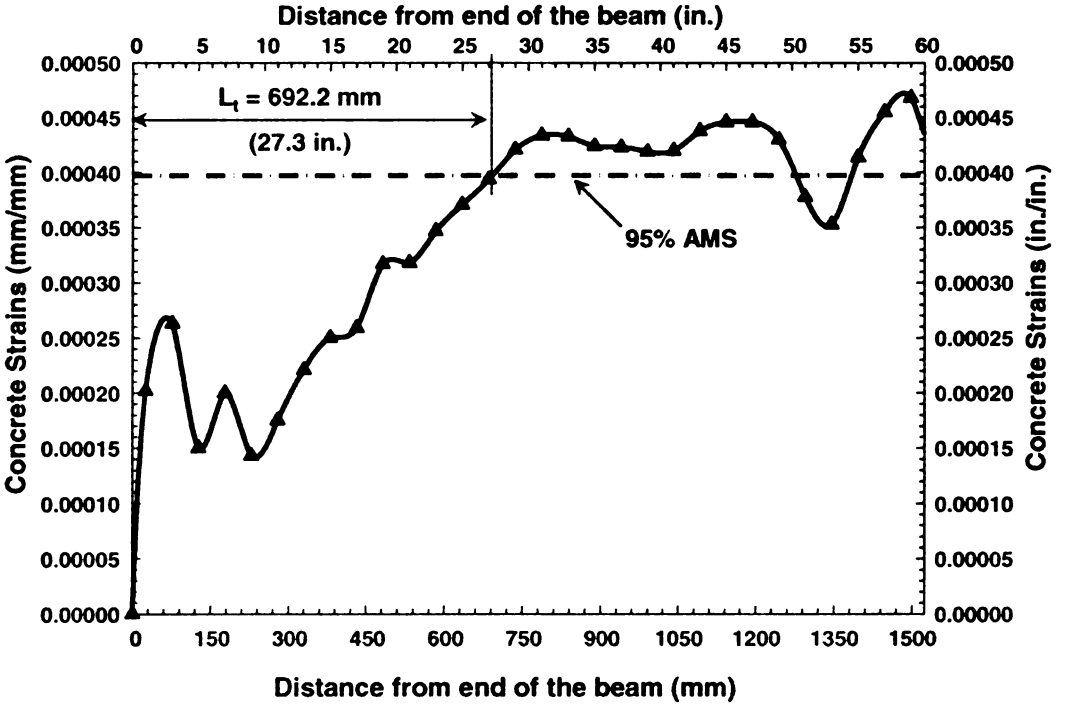

Figure A3 - 8 Concrete Strain Profile – SCC3 – Beam2

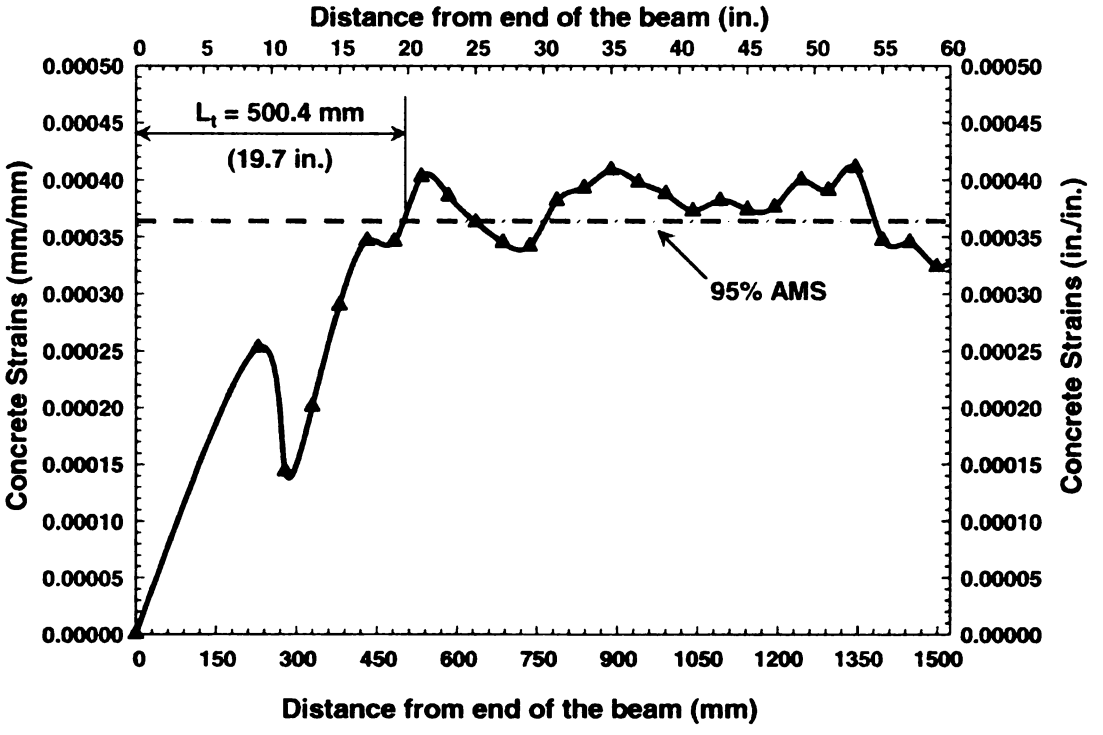

Figure A3 - 9 Concrete Strain Profile – NCCB – Beam1

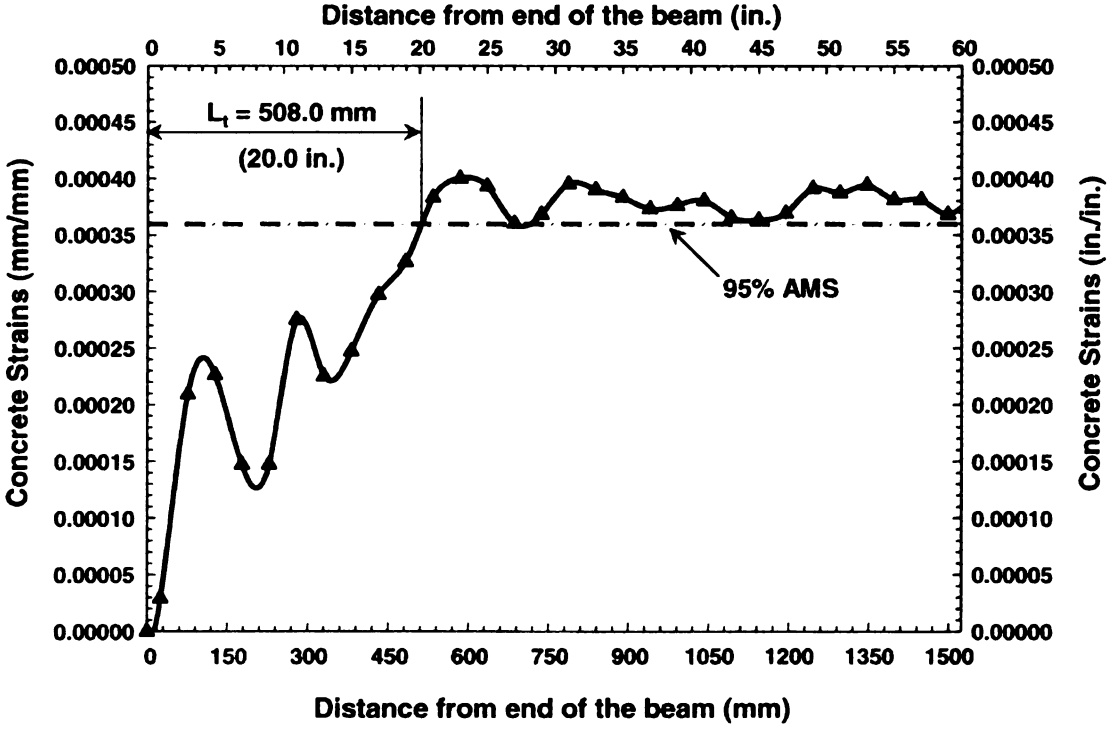

Figure A3 - 10 Concrete Strain Profile – NCCB – Beam2

Appendix 4 - Development Test Response

Development length for the prestressing strands was measured by performing flexural tests on the beam units. For each test specimen two development length tests, (one per beam end) were obtained. Thus, a total of four development length tests were performed for each concrete mix type. This section provides the moment-displacement response at the critical section obtained from these development length tests. The nominal moment (M_n) that can be developed in the cross section was calculated using the computer program Response 2000 [15], which is a research-oriented program for the analysis of concrete sections with refined concrete and steel constitutive models. In the following plots, this nominal moment is shown as a horizontal line. If the test response intersects with this line, then the moment capacity for that particular embedment length was achieved and the embedment length was considered to be a sufficient development length for that beam unit.

The development length test responses are provided in the following order of mix types: SCC1, SCC2A, SCC2B, SCC3, NCCA, and NCCB. For each mix type, the tests responses are provided in the following order: Unit1-EndA, Unit-1-EndB, Unit2-EndA and Unit2-End2.

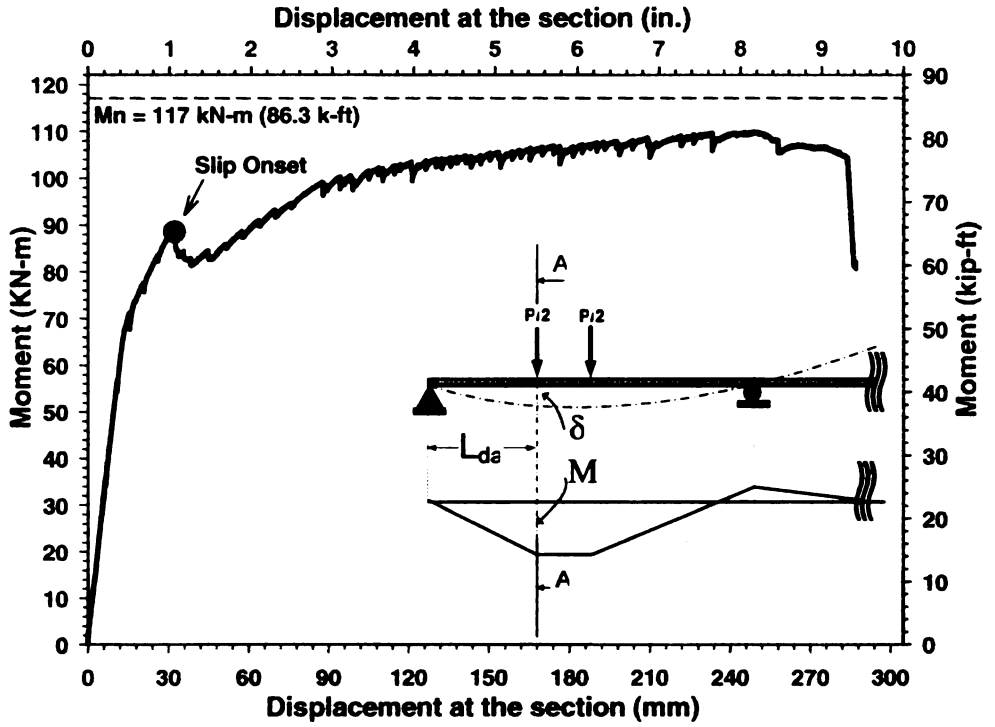

Figure A4 - 1 Moment vs. Displacement- SCC1-1-A - L_e = 72.38 in

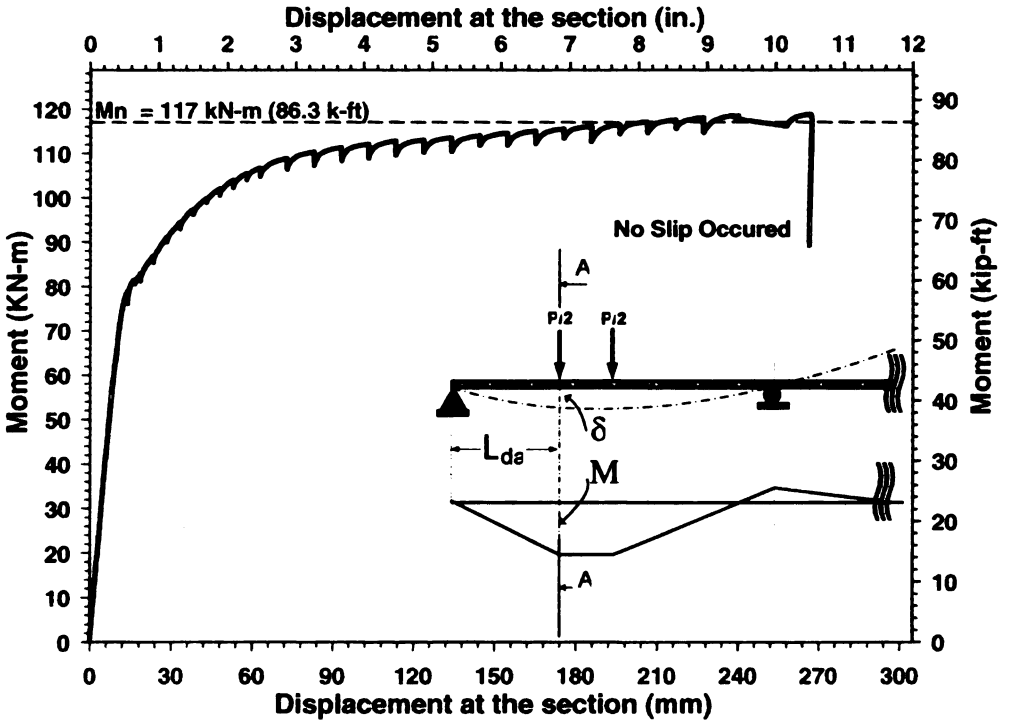

Figure A4 - 2 Moment vs. Displacement- SCC1-1-B - L_e = 137.75 in

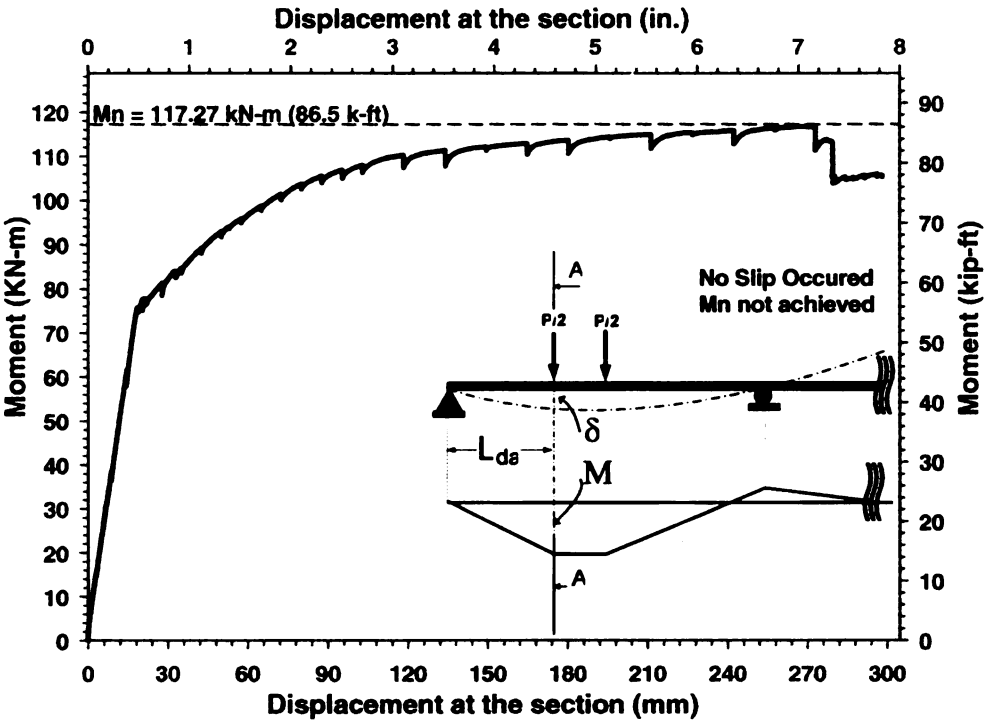

Figure A4 - 3 Moment vs. Displacement- SCC1-2-A - L_e =122.00 in

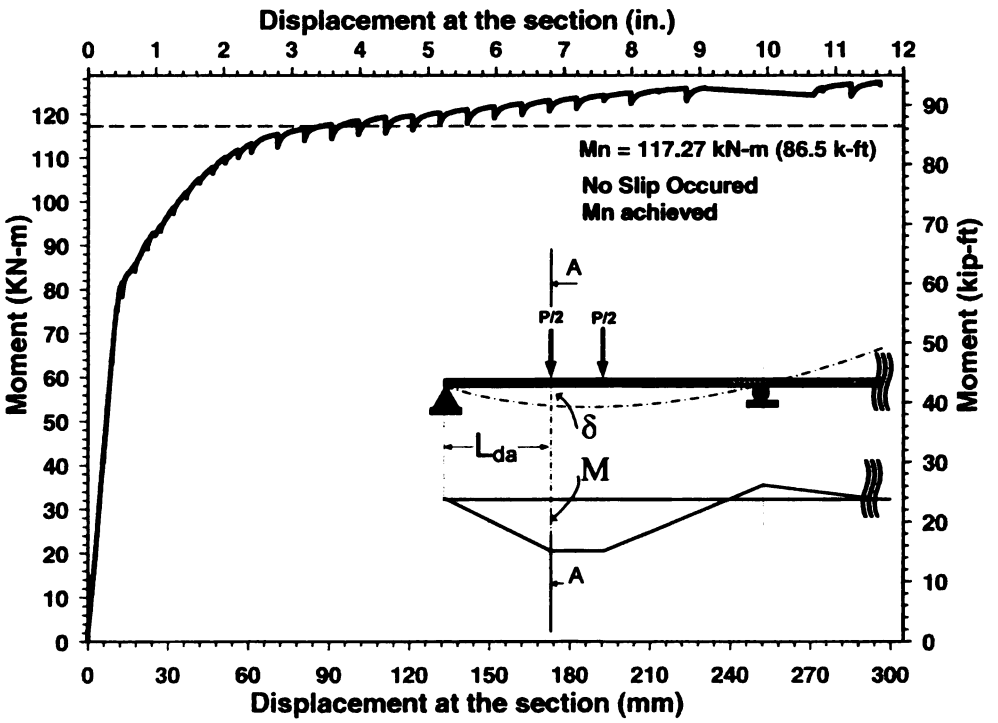

Figure A4 - 4 Moment vs. Displacement- SCC1-2-B - L_e = 118.50 in

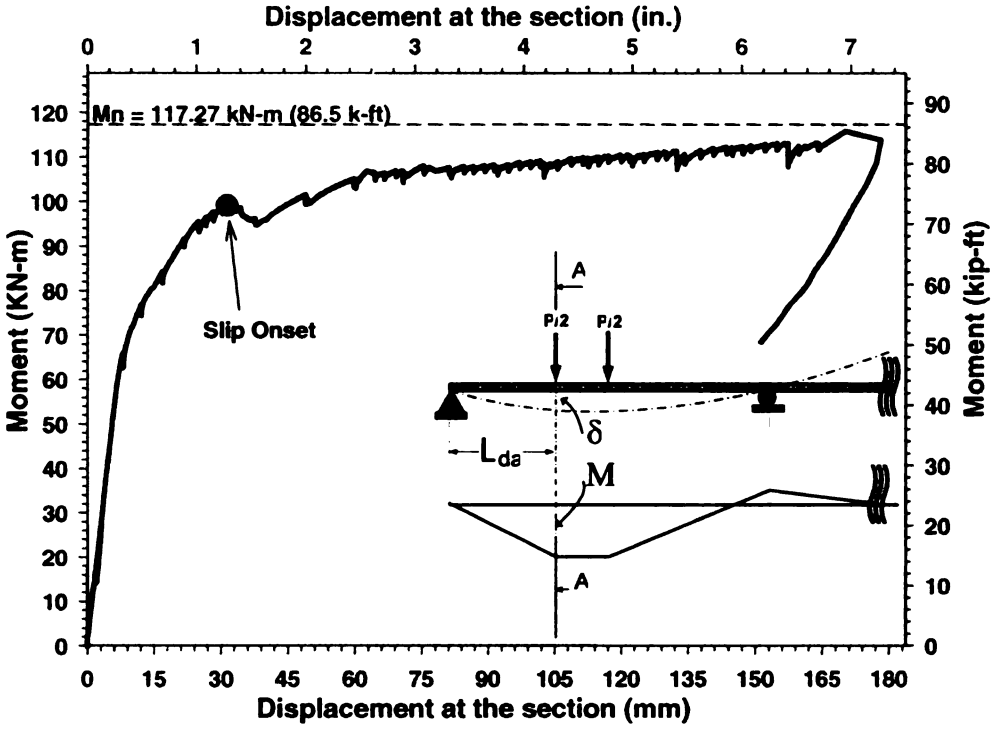

Figure A4 - 5 Moment vs. Displacement- SCC2A-1-A - L_e = 70.50 in

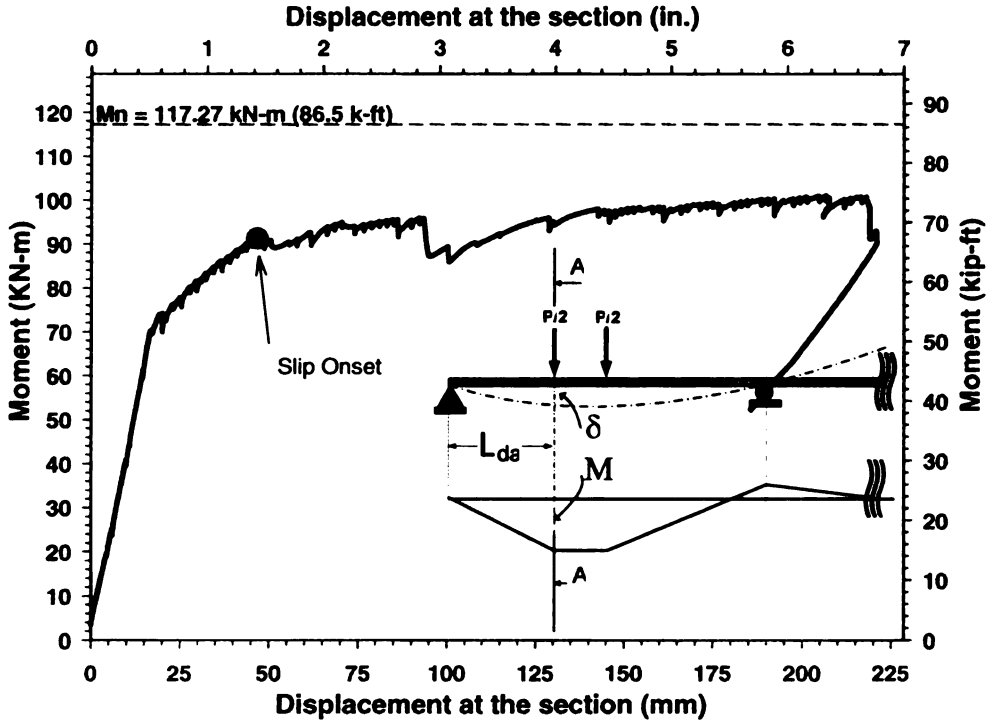

Figure A4 - 6 Moment vs. Displacement- SCC2A-1-B - L_e = 64.50 in

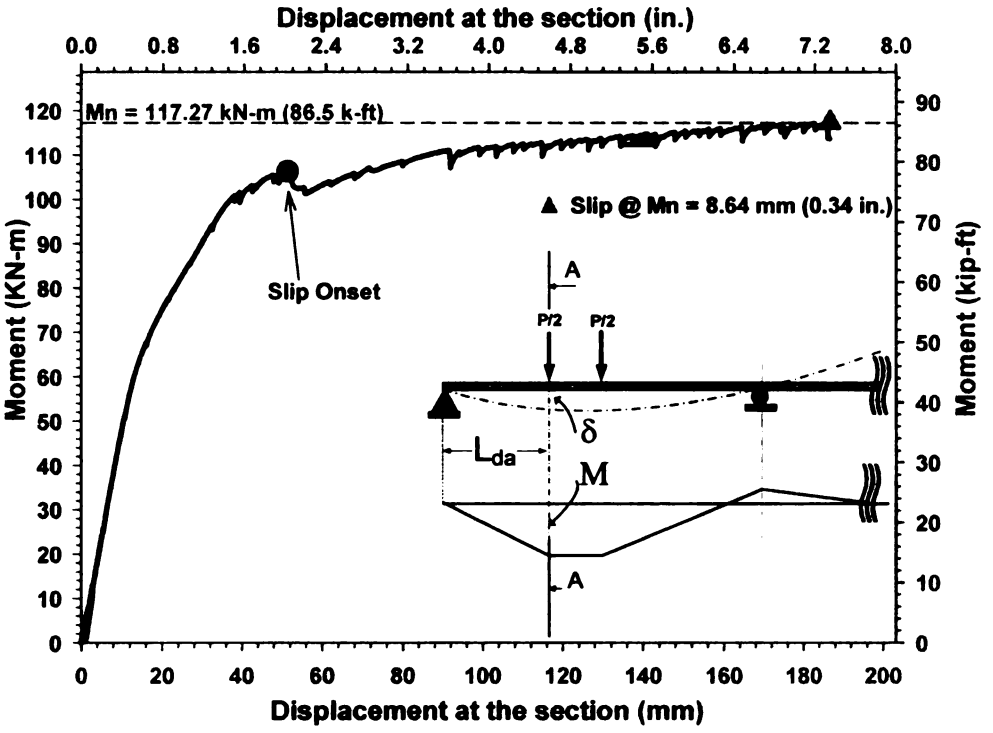

Figure A4 - 7 Moment vs. Displacement- SCC2A-2-A - L_e = 80.00 in

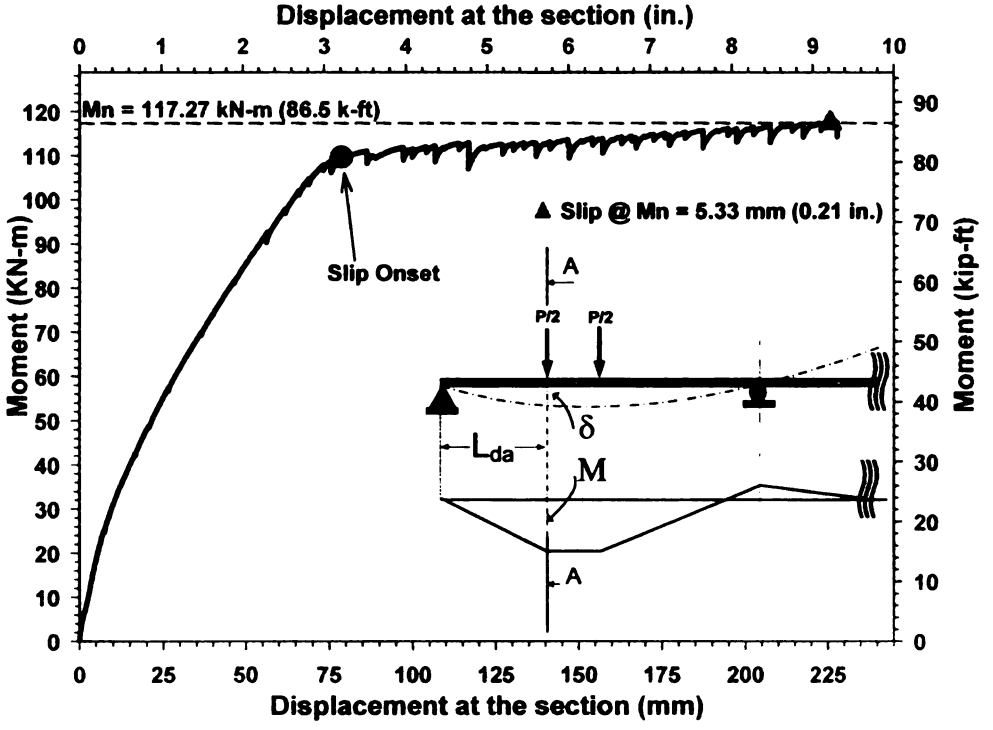

Figure A4 - 8 Moment vs. Displacement- SCC2A-2-B - L_e = 86.75 in

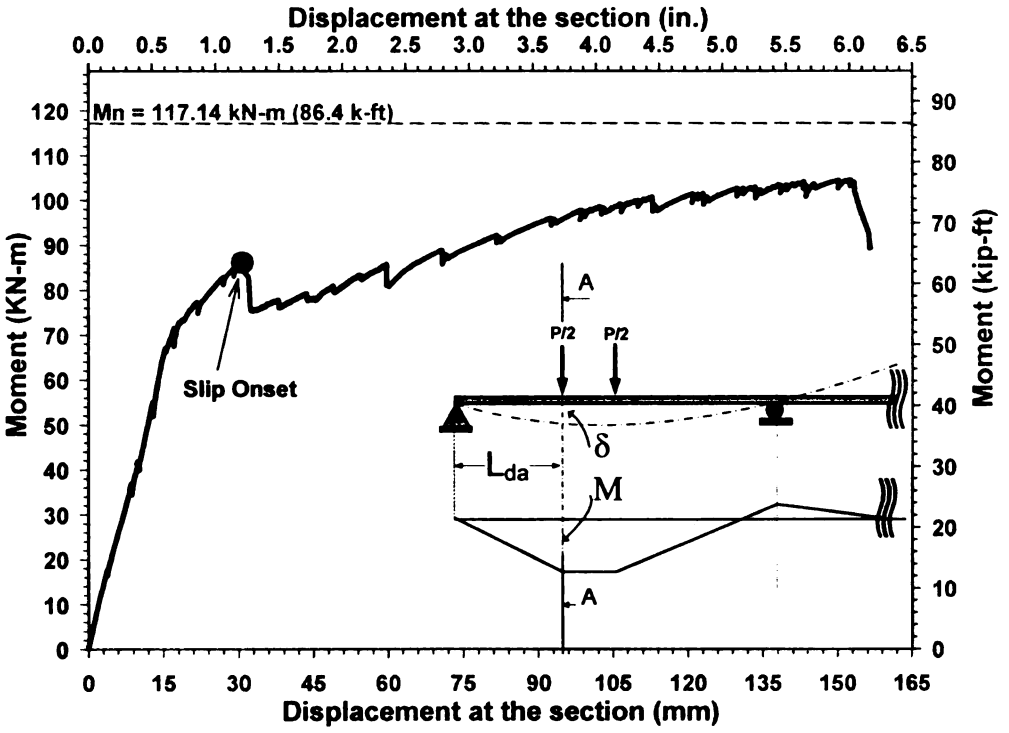

Figure A4 - 9 Moment vs. Displacement- SCC2B-1-A - L_e = 70.50 in

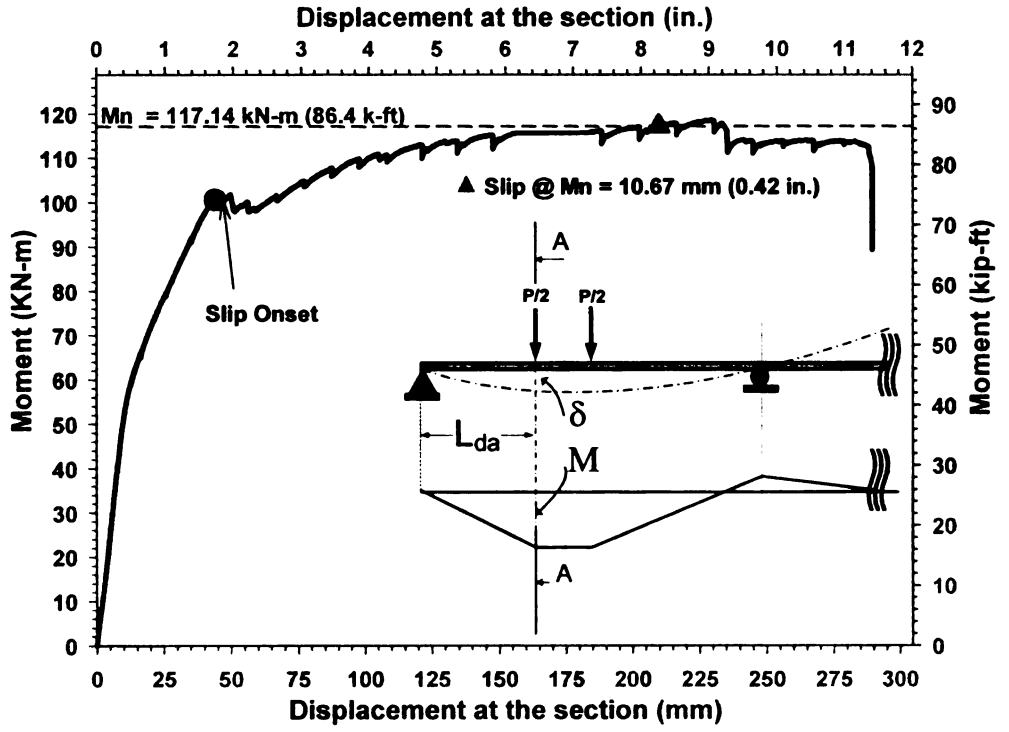

Figure A4 - 10 Moment vs. Displacement- SCC2B-1-B - L_e = 102.75 in

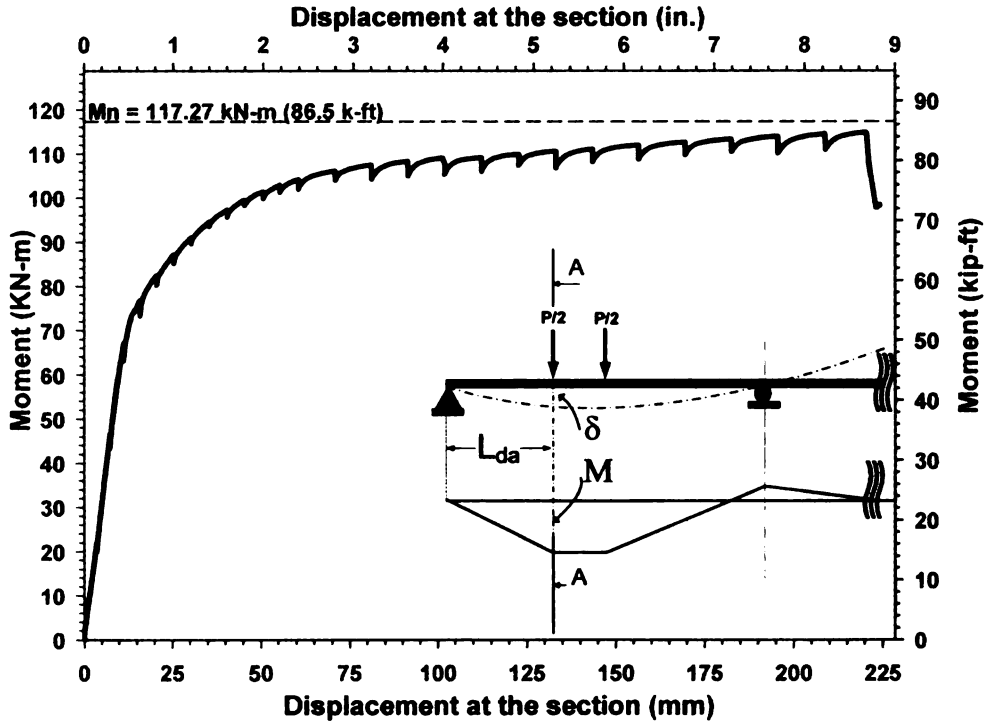

Figure A4 - 11 Moment vs. Displacement- SCC2B-2-A - L_e = 126.75 in

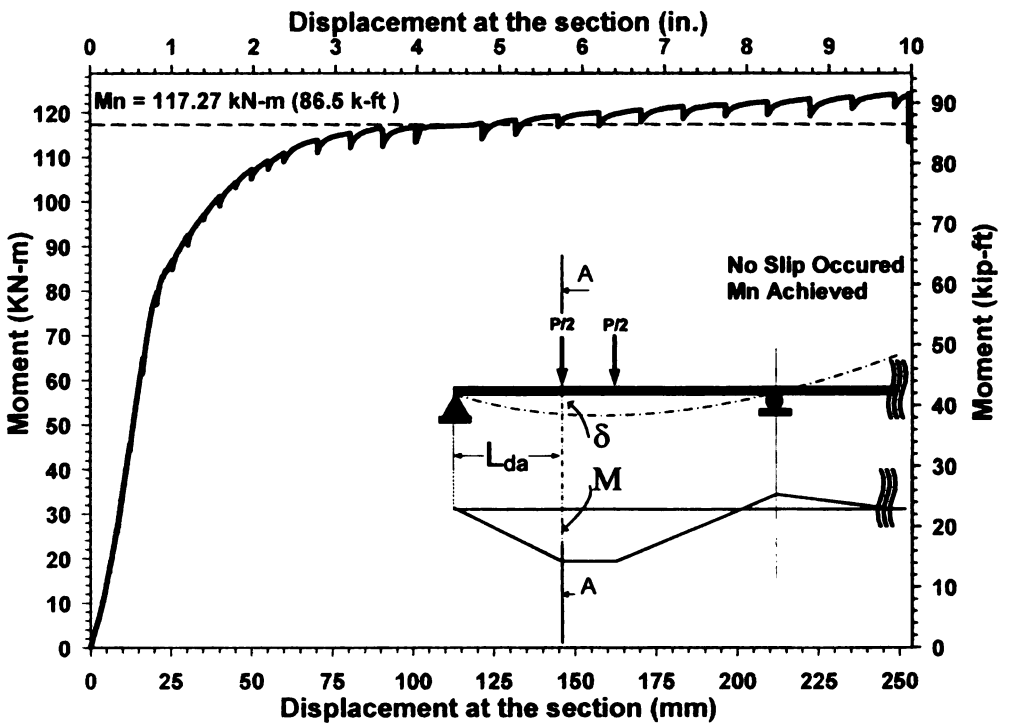

Figure A4 - 12 Moment vs. Displacement- SCC2B-2-B - L_e = 103.80 in

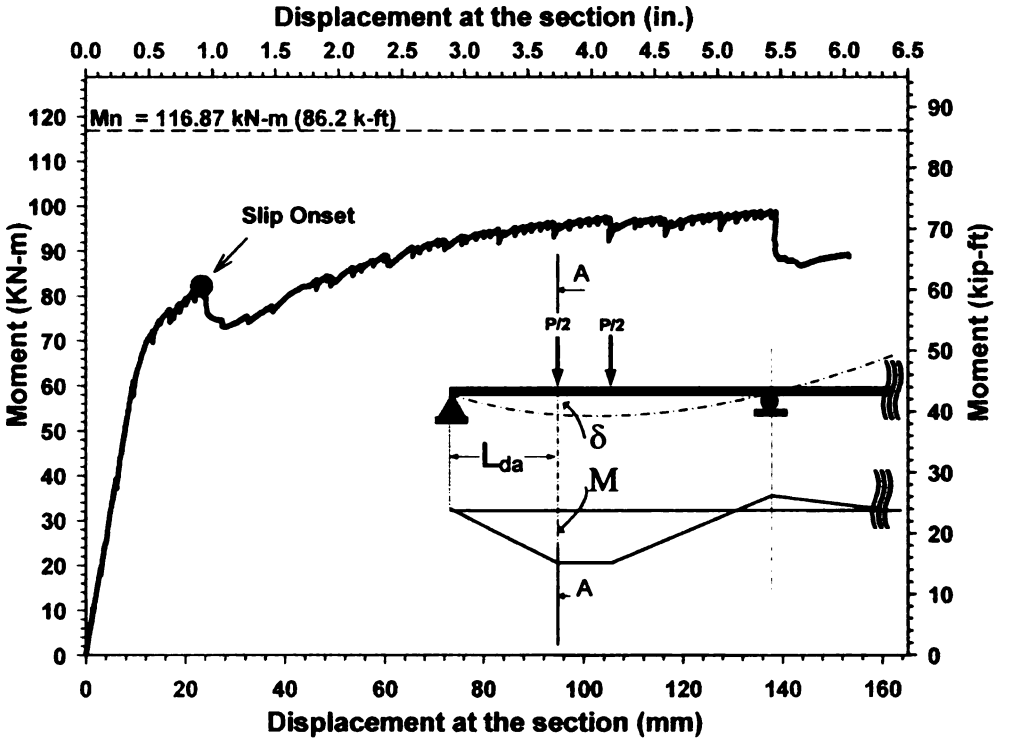

Figure A4 - 13 Moment vs. Displacement- SCC3-1-A - L_e = 58.50 in

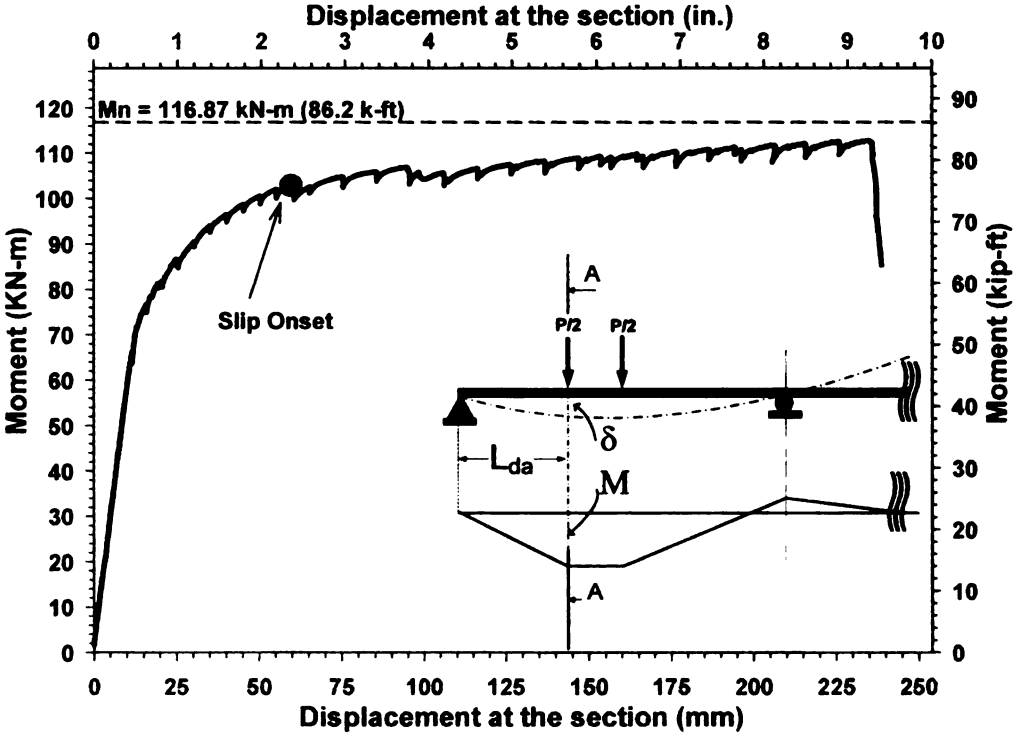

Figure A4 - 14 Moment vs. Displacement- SCC3-1-B - L_e = 97.75 in

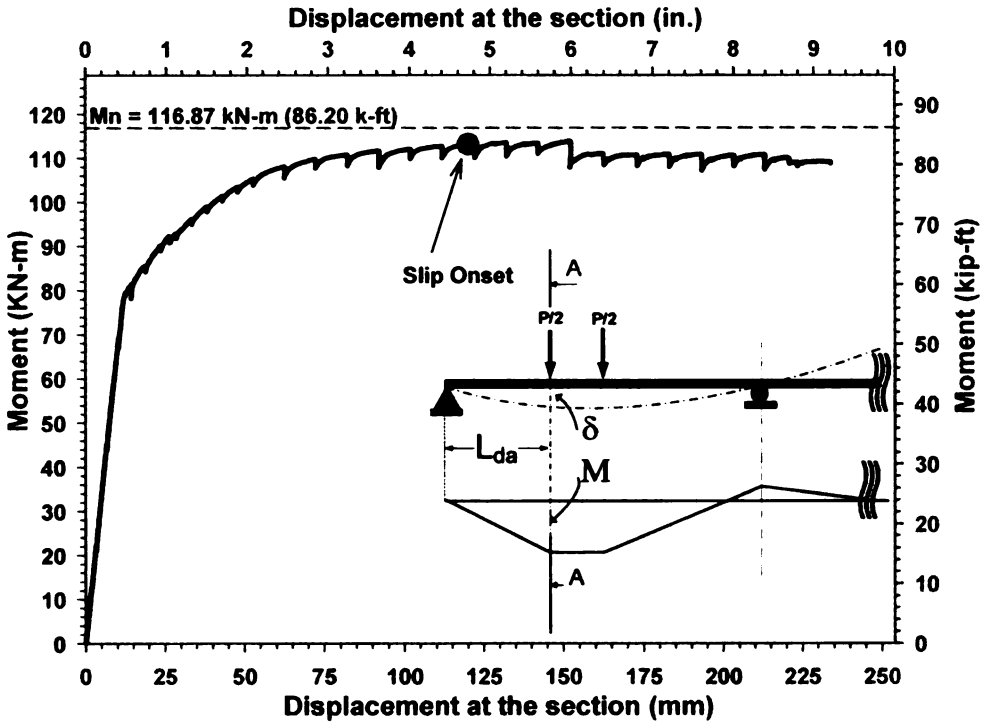

Figure A4 - 15 Moment vs. Displacement- SCC3-2-A - L_e = 106.50 in

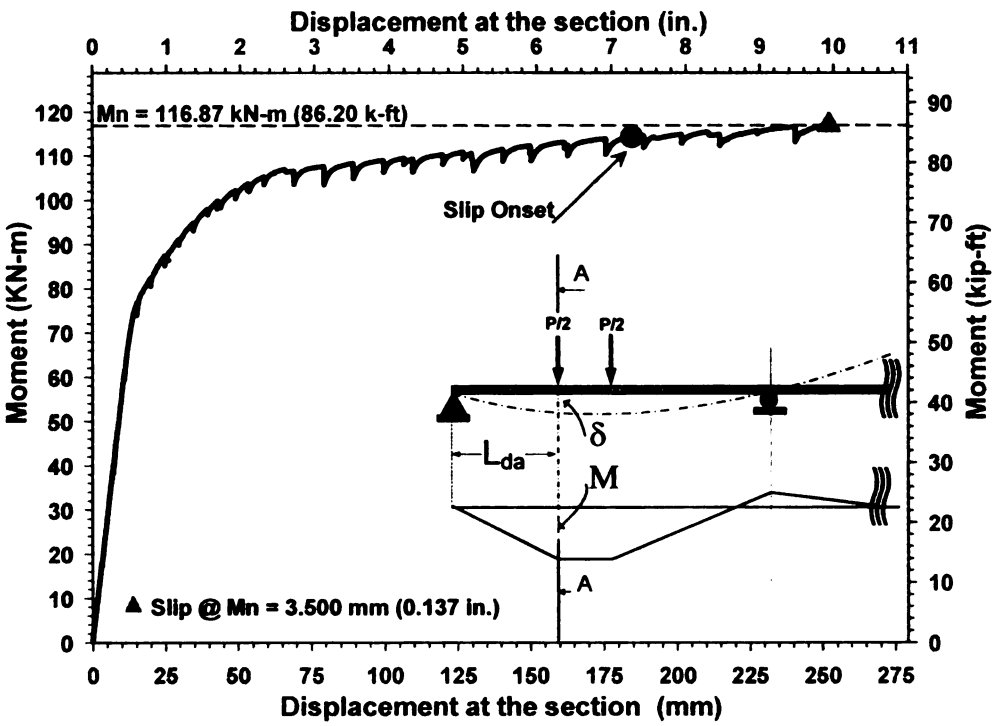

Figure A4 - 16 Moment vs. Displacement- SCC3-2-B - L_e = 103.00 in

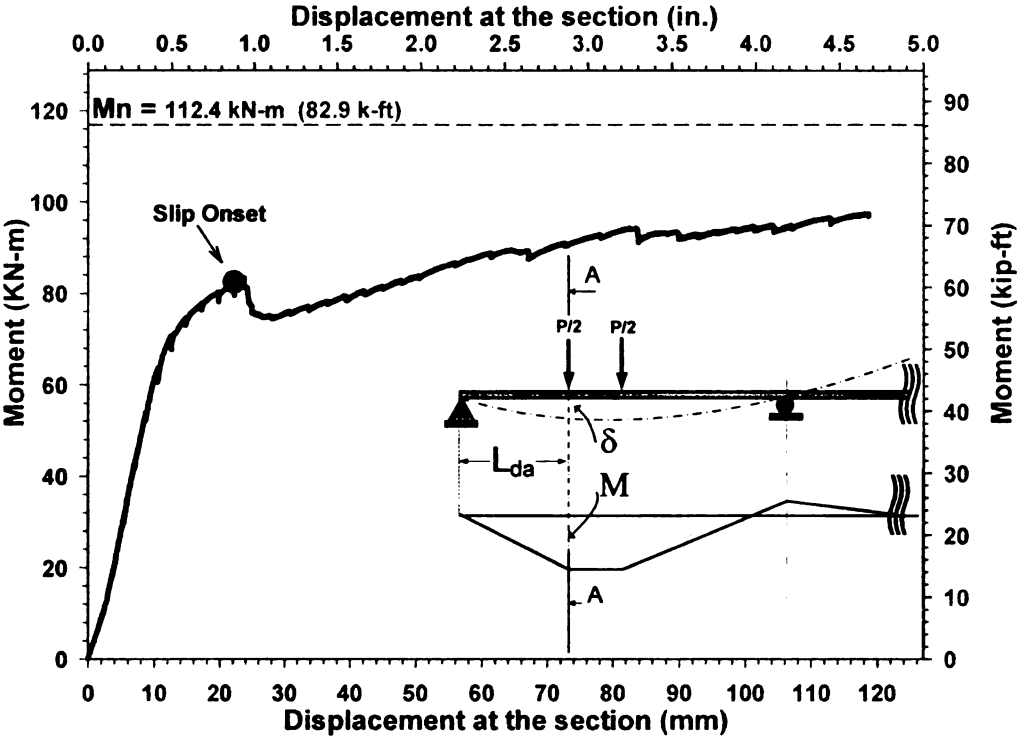

Figure A4 - 17 Moment vs. Displacement- NCCA-1-A - L_e = 76.00 in

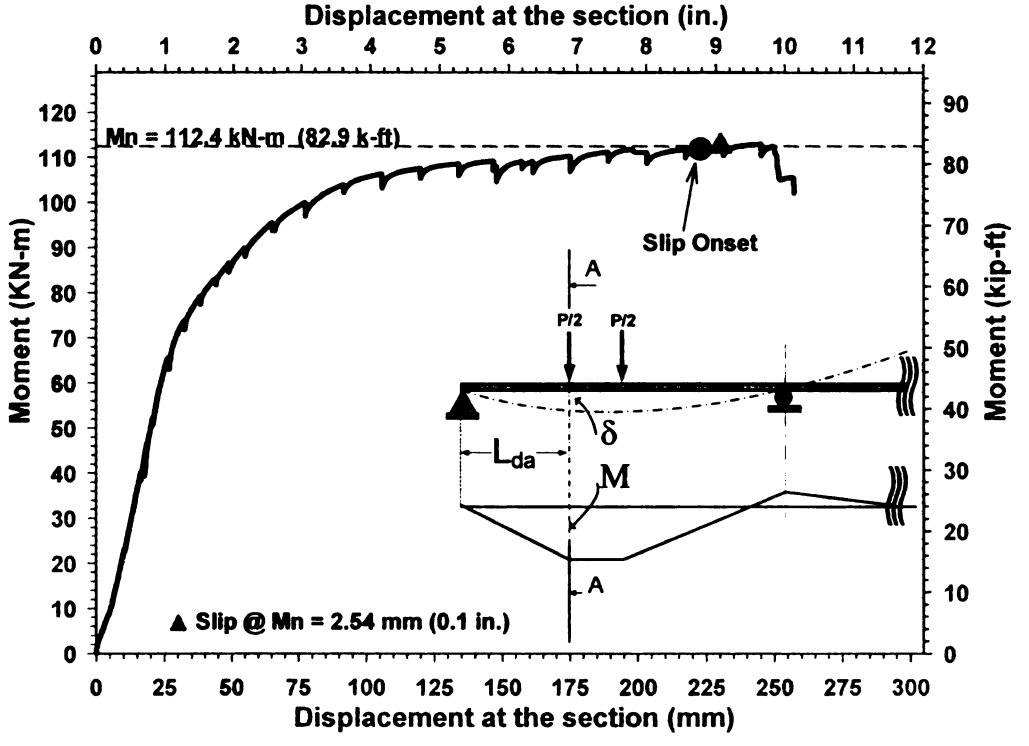

Figure A4 - 18 Moment vs. Displacement- NCCA -1-B - L_e = 122.75 in

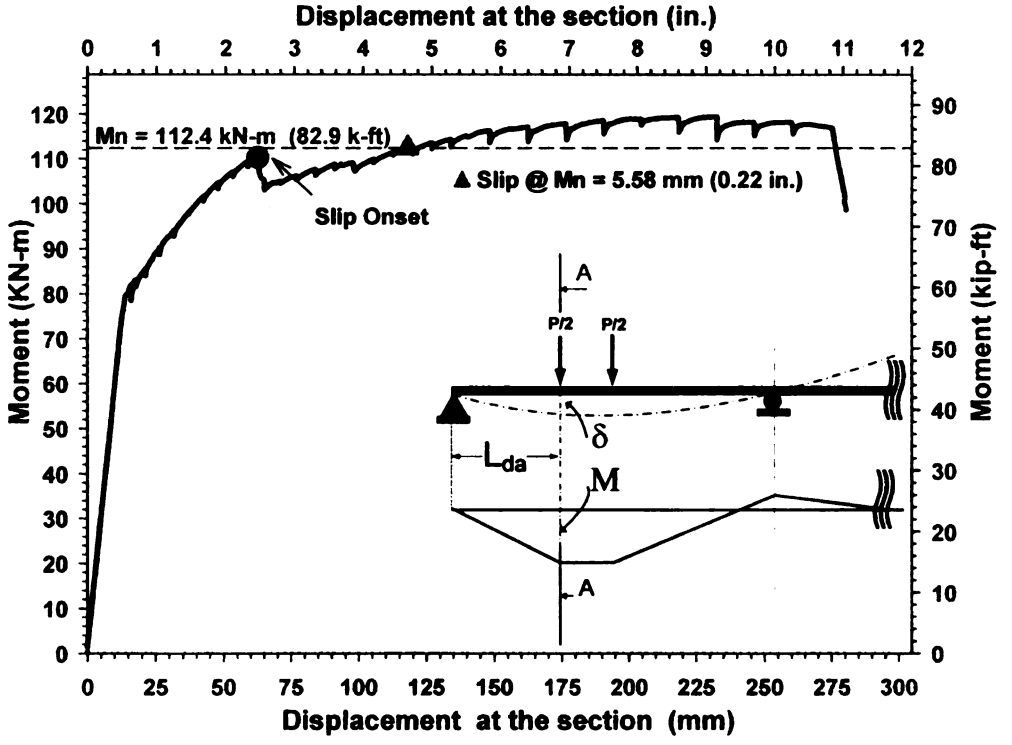

Figure A4 - 19 Moment vs. Displacement- NCCA -2-A - L_e = 111.00 in

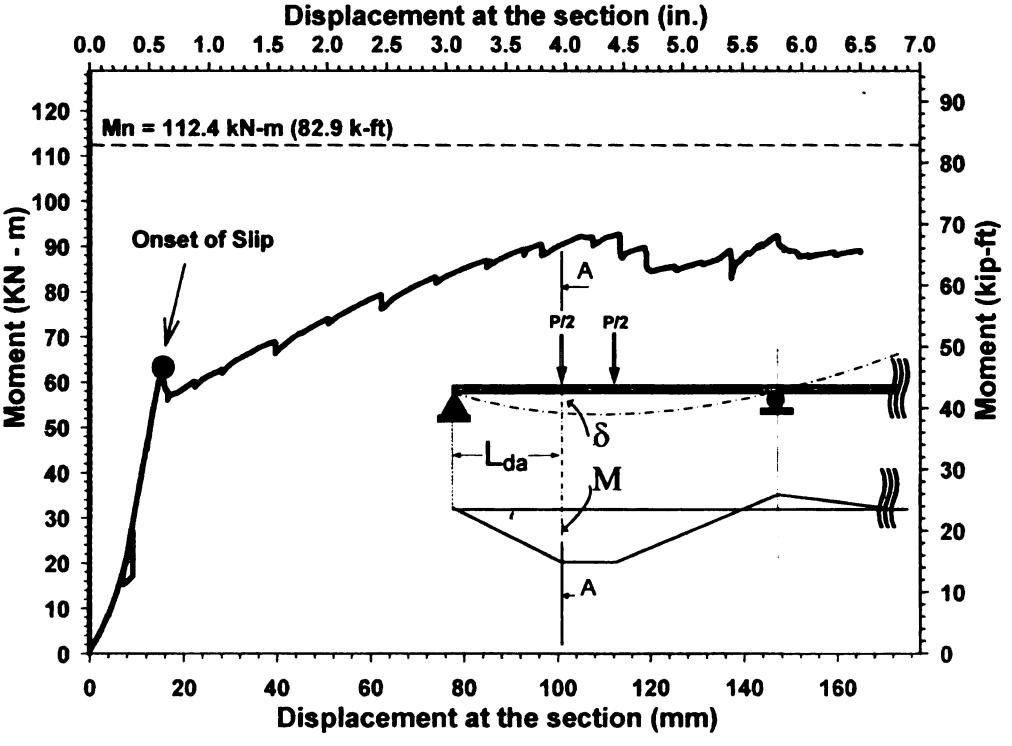

Figure A4 - 20 Moment vs. Displacement- NCCA -2-B - L_e = 60.00 in

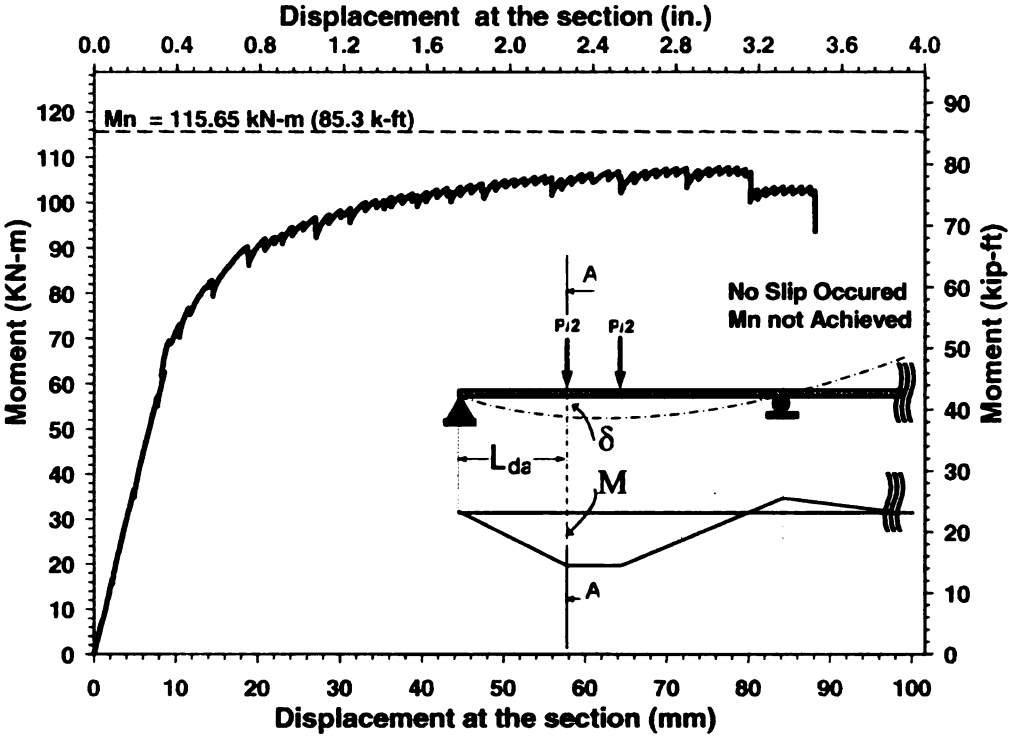

Figure A4 - 21 Moment vs. Displacement- NCCB -1-A - L_e = 63.75 in

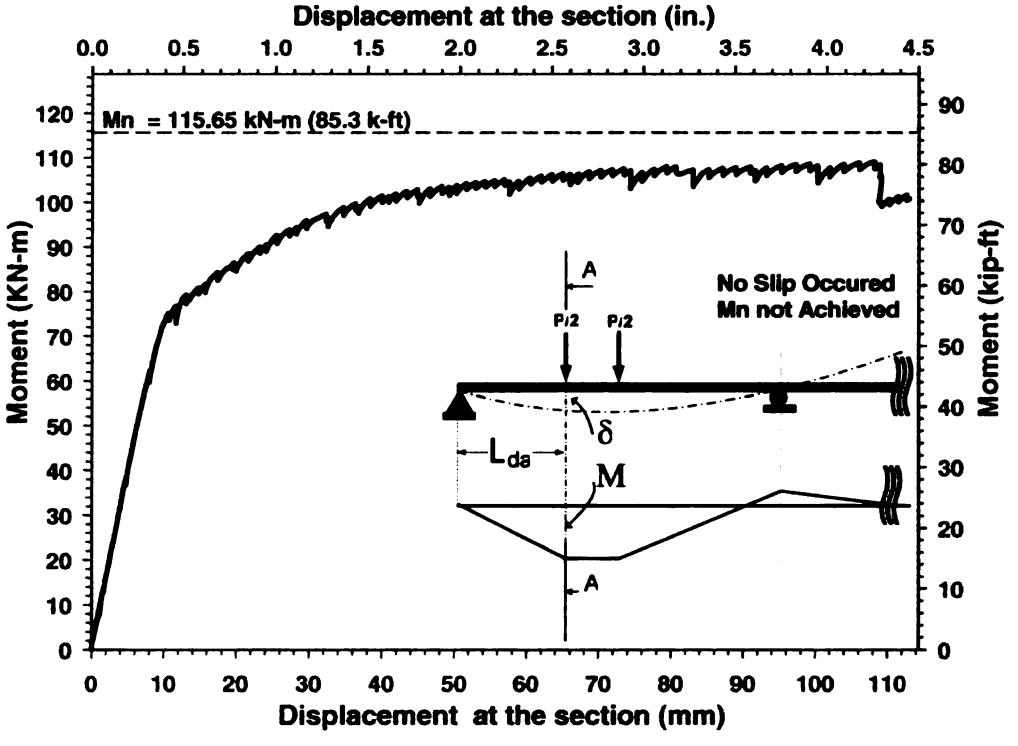

Figure A4 - 22 Moment vs. Displacement- NCCB -1-B - L_e = 64.00 in

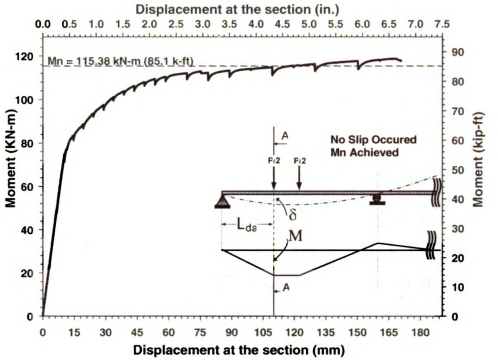

Figure A4 - 23 Moment vs. Displacement- NCCB -2-A - L_e = 100.50 in

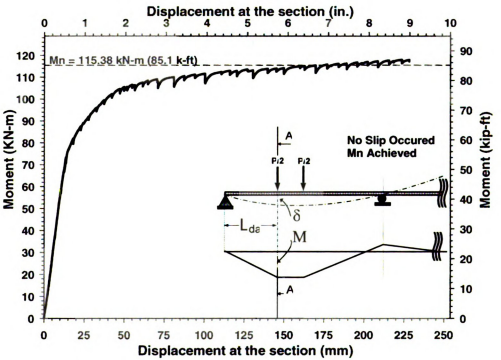

Figure A4 - 24 Moment vs. Displacement- NCCB -2-B - L_e = 93.50 in

Table A5 - 1 Prestressing Details

MIX	Beam#	End #	f'_c at transfer (psi)	f'_c at Day of flexural Testing (psi)	f_{si} (without losses) (ksi)	*f_{se} at Day of flexural Testing (ksi)	Date of Prestress	Date of Prestress Release	Date of Flexural Testing
SCC2A	1	A	7693	9182	212.08	182.02	8-Jul-04	12-Jul-04	30-Oct-04
	1	B	7693	9182	212.08	181.96	8-Jul-04	12-Jul-04	3-Nov-04
	2	A	7693	9182	216.95	186.04	8-Jul-04	12-Jul-04	9-Nov-04
	2	B	7693	9182	216.95	185.95	8-Jul-04	12-Jul-04	15-Nov-04
SCC2B	1	A	6704	9064	233.26	199.83	26-Jul-04	29-Jul-04	16-Nov-04
	1	B	6704	9064	233.26	199.80	26-Jul-04	29-Jul-04	18-Nov-04
	2	A	6704	9064	189.01	161.81	26-Jul-04	29-Jul-04	23-Nov-04
	2	B	6704	9076	189.01	161.62	26-Jul-04	29-Jul-04	30-Nov-04
SCC3	1	A	6704	7971	247.85	211.95	3-Aug-04	6-Aug-04	2-Dec-04
	1	B	6704	7971	247.85	211.92	3-Aug-04	6-Aug-04	7-Dec-04
	2	A	6704	7971	230.90	197.56	3-Aug-04	6-Aug-04	10-Dec-04
	2	B	6704	7971	230.90	196.79	3-Aug-04	6-Aug-04	21-Dec-04
NCCB	1	A	5545	6991	231.12	197.27	13-Aug-04	16-Aug-04	22-Dec-04
	1	B	5545	6991	231.12	197.50	13-Aug-04	16-Aug-04	25-Dec-04
	2	A	5545	7045	173.37	147.52	13-Aug-04	16-Aug-04	29-Dec-04
	2	B	5545	7045	173.37	147.52	13-Aug-04	16-Aug-04	30-Dec-04
SCC1	1	A	7685	8908	200.50	171.83	31-Aug-04	4-Sep-04	4-Jan-05
	1	B	7685	8908	200.50	171.82	31-Aug-04	4-Sep-04	5-Jan-05
	2	A	7685	9038	200.08	171.43	31-Aug-04	4-Sep-04	6-Jan-05
	2	B	7685	9038	200.08	171.39	31-Aug-04	4-Sep-04	9-Jan-05

* f_{se} is the effective stress, the values shown also include long term losses up to the day of test. 1Mpa =145.0377 psi

REFERENCES

[1] Abrishami, H.H., and Mitchell, D.(1993, June), "Bond Characteristics of Pretensioned Strand," *ACI Materials Journal*, 90(3), 228-235.

[2] American Association of State Highway and Transportation Officials (AASHTO), AASHTO LRFD Bridge Design Specifications, Second Edition, 1998.

[3] American Concrete Institute (ACI), Building Code Requirements for Structural Concrete and Commentary, ACI 318-02, Farmington Hills, Michigan, 2002.

[4] Antoine E Namaan. (1982) "Prestressed Concrete Analysis and Design Fundamentals."

[5] Attiogbe, E., See, H., and Daczko J., "Engineering Properties of Self-Consolidating Concrete," P*roceedings of the First North American Conference on the Design and Use of Self-Consolidating Concrete*, Evanston, IL, November 2002.

[6] Balazs,G.L.(1993). "Transfer Lengths of prestressing strands as a function of draw-in and initial prestress." *PCI Journal* 38(2) 86-93.

[7] Barnes,R.W., Burns,N.H., & Kreger, M.E. (1999, December). "Development Length of 0.6 inch prestressing strand in standard I shaped pretensioned concrete beams." *Research Report 1388-1. Center of Transportation Research, Bureau of Engineering Research*, University of Texas at Austin,

[8] Buckner, C.Dale., (1995, April) "A Review of Strand Development Length for Pretensioned Concrete Members," *PCI Journal*, 40(2), 84-105.

[9] Byung Hwan Oh., and Eui Sung Kim.,(2000, December). "Realistic Evaluation of Transfer Lengths in Pretensioned. Prestressed Concrete Members." *ACI Structural Journal*. 97(6). 821-830.

[10] Cousins, T.E., Badeaux, M.H., and Mostafa, S..(1992, February), "Proposed Test for Determining Bond Characteristics of Prestressing Strand," *PCI Journal*, 66-73

[11] Daczko, J., and Constantiner, D. (2002, November), "Not All Applications are Created Equal; Designing and Selecting the Appropriate SCC Mixture," *Proceedings of the First North American Conference on the Design and Use of Self-Consolidating Concrete*, Evanston, IL.

[12] Daczko, J., and Kurtz, M.A. (2001, October), "Development of High-Volume Coarse Aggregate Self-Compacting Concrete." *Proceedings of the Second International Symposium on Self-Compacting Concrete*, Tokyo, Japan.

[13] Dallas R. Rose., Bruce W. Russell. (1997, August). "Investigation of standardized tests to measure the bond performance of prestressing strand." *PCI Journal*, 42 (4), 56-80.

[14] Deatherage, J.H., Burdette, E.G., and Chew, C.K. (1994, February), "Development Length and Lateral Spacing Requirements of Prestressing Strand for Prestressed Concrete Bridge Girders," *PCI Journal*, 39(1), 70-83.

[15] Evan C. Bentz., Michael P.Collins, (2000). "Response-2000" *Version 1.0.5 – Reinforced Concrete sectional analysis using the modified compression field theory.*

[16] Gross, P. Shawn and Ned H.Burns. (1995, June). "Transfer and Development Length of 15.2mm (0.6 in.) diameter prestressing strand in high performance concrete: Results of Hoblitzell-Buckner Beam tests." *Research report 580 -2. Center of Transportation Research, Bureau of Engineering Research*, University of Texas at Austin.

[17] Hanson, N.W. and Kaar, P.H. (1959) *"Flexural Bond Tests of Pretensioned Prestressed Beams,"* ACI Journal, 55(7), 783-803.

[18] Kaar, P.H., LaFraugh, R.W., and Mass, M.A. (1963, October) "Influence of Concrete Strength on Strand Transfer Length," *PCI Journal*, 47-67

[19] Khayat, K.H, and Daczko, J.(2002, November) "The Holistic Approach to Self-Consolidating Concrete," *Proceedings of the First North American Conference on the Design and Use of Self-Consolidating Concrete*, Evanston, IL,

[20] Khayat, K.H. (1999, June) "Workability, Testing, and Performance of Self-Consolidating Concrete," *ACI Materials Journal*, 96(3), 346-353

[21] Khayat, K.H., K. Manai and A.Trudel.(1996, December) "In Situ Mechanical Properties of Wall Elements cast using Self Consolidating Concrete". *ACI Materials Journal.* 94(6). 491-500

[22] Khayat, K.H., Patrick Paultre., and Stephan Tremblay. (2001, October), "Structural Performance and In-Place properties of Self-Consolidating Concrete used for casting highly reinforced columns". *ACI Materials Journal.* 98(5), 371 – 378

[23] Leonhardt, F. (1964) "Prestressed Concrete – Design and Construction", Wilhem Ernst & Sohn, Berlin.

[24] Logan, D.R., (1996, April) Discussion of "A Review of Strand Development Length for Pretensioned Concrete Members." *PCI Journal*, 41(2), 112-116.

[25] Logan, D.R.. (1997, April). "Acceptance criteria for bond quality of strand for pretensioned prestressed concrete applications." *PCI Journal*, 42(2), 52-90

[26] Nan Su, Kung-Chung Hsu, His-Wen Chai.(2001) "A simple mix design method for Self Compacting Concrete". *Cement and Concrete Research*, V.31, 1799-1807

[27] Okamura, H. (1999, June), "Self-Compacting High-Performance Concrete," *ACI Materials Journal*, 96(3), 346-353.

[28] Persson, B., "A Comparison between Mechanical Properties of Self-Compacting Concrete and the Corresponding Properties of Normal Concrete," *Cement & Concrete Research*, 31 (2001) 193-198

[29] Petersson, O., Gibbs, J., and Bartos, P.(2002, November) "Testing-SCC," *Proceedings of the First North American Conference on the Design and Use of Self-Consolidating Concrete*, Evanston, IL.

[30] Precast/Prestressed Concrete Institute (PCI), *"Interim Guidelines for the use of Self-Consolidating Concrete in Precast/Prestressed Concrete Institute Member Plants,"* TR-6-03, Chicago, Illinois, April 2003.

[31] Rose, D.R., and Russel, B.W. (1997, August) "Investigation of Standardized Tests to Measure the Bond Performance of Prestressing Strand," *PCI Journal*, 42 (4), 56-80.

[32] Russell, B.W., and Burns, N.H. (1997, May) "Measurement of Transfer Lengths on Pretensioned Concrete Elements," *Journal of Structural Engineering*, 123(5), 541-549.

[33] Russell, B.W., and Burns, N.H., (1996, April) Discussion of "A Review of Strand Development Length for Pretensioned Concrete Members," *PCI Journal*, 41(2), 116-119.

[34] Russell, B.W., and Ned H.Burns. (1993, January). "Design Guidelines for Transfer, Development and Debonding of large Diameter Seven wire strands in pretensioned concrete girders." *Research Report 1210-5F. Center of Transportation Research, Bureau of Engineering Research,* University of Texas at Austin.

[35] Shahawy, M. (2001, August), "A Critical Evaluation of the AASHTO Provisions for Strand Development Length of Prestressed Concrete Members," *PCI Journal*, 46(4), 94-117.

[36] Thatcher, D.B., Heffington, J.A, Kolozs, R.T., Sylva III, G.S., Breen, J.E., and Burns,N.H. (2002, January). "Structural Lightweight concrete prestressed girgers and panels." *Research report 1852-1 Center for transportation research. Bureau of Engineering Research*, University of Texas at Austin.

[37] Transportation Research Board, "Research Problem Statements," A2C03 Committee on Concrete Bridges, Group 2 – Design and Construction of Transportation Facilities, Technical Activities Div..

[38] Vachon, M. (2002, July) "ASTM Puts Self-Consolidating Concrete to the Test," ASTM Standardization News, July 2002, url: http://astm.org/cgi-bin/SoftCart.exe/SNEWS/JULY_2002/vachon_jul02.htm

[39] Xie, Y., Liu, B., Yin, J., and Zhou, S., "Optimum Mix Parameters of High-Strength Self-Compacting Concrete with Ultrapulverized Fly Ash," *Cement & Concrete Research*, 32 (2002) 477-480.

[40] Zhu, W., Gibbs, J.C., and Bartos, P.J.M., "Uniformity of In Situ Properties of Self-Compacting Concrete in Full-Scale Structural Elements," *Cement & Concrete Composites*, 23 (2001) 57-64.

[41] Zia, P., and Mostafa, T. (1977, October) "Development Length of Prestressing Strands," *PCI Journal*, 55-65.